

Functional analysis of the von Hippel-Lindau tumour suppressor and its role in tumourigenesis

Inauguraldissertation

zur
Erlangung der Würde eines Doktors der Philosophie
vorgelegt der
Philosophisch-Naturwissenschaftlichen Fakultät
der Universität Basel
von

Robert E. Barry

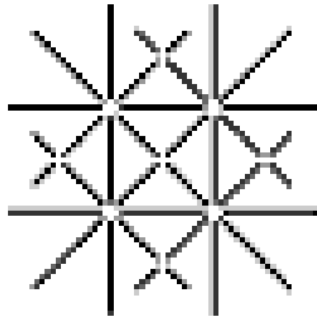
aus Dublin (Irland)

Zürich, 2004

Genehmigt von der Philosophisch-Naturwissenschaftlichen Fakultät auf Antrag von Prof.Dr.Denis Monard, Prof.Dr.Wilhelm Krek und Prof.Dr.Holger Moch.

Basel, den 29. Juli 2004

**Prof. Dr. Marcel Tanner
(Dekan)**



UNI
BASEL

UNIVERSITÄT BASEL



Robert Edward Barry

Zürich – 2004

Functional analysis of the von Hippel-Lindau tumour suppressor and its role in tumourigenesis

Dissertationsleiter:

Prof.Dr.Wilhelm Krek

Institut für Zellbiologie, ETH Zürich

Fakultätsverantwortlicher:

Prof.Dr.Denis Monard

Friedrich Miescher Institute for Biomedical Research

Korreferent:

Prof.Dr.Holger Moch

Institut für Klinische Pathologie, Universitätsspital Zürich

A thesis submitted to the faculty of Natural Sciences at the university of Basel as partial fulfilment of Doctoral studies undertaken at the Friedrich Miescher Institute for Biomedical Research, Basel, and completed at the Institute of Cell Biology, Eidgenössische Technische Hochschule, Zürich

*In loving memory of my dear grandmother, Mrs. Joan Collis,
who was diagnosed with cancer and died during
the writing of this thesis*

**Jeder, der zur wahren Erkenntnis durchringen will, muß den Berg
Schwierigkeiten allein erklimmen**

Helen Keller

Acknowledgements

I would like to take this opportunity to extend my sincere gratitude to my thesis supervisor Prof.Dr.Wilhelm Krek whose support, patience and motivation made this doctoral work not only possible, but also very enjoyable. Willy's innate sense of enthusiasm and encouragement, particularly in times of difficulty, proved a source of motivation and helped in remaining focused on the task at hand. I am particularly appreciative for his personal support and his interest in my career, support that has been instrumental in helping me to realise my future undertaking. For this I am truly grateful. It only leaves me to thank him for giving me the opportunity to have worked in his laboratory and to wish him all the very best for the future.

I would also like to thank all members of the krek laboratory, past and present – Christiane Wirbelauer, Hedwig Sütterluty, Matthias Gstaiger, Joanna Lisztwan, Georges Imbert, Anne-Isabelle Michou, Françoise Reymond, Alexander Hergovich, Pia Ballschmieter, Malte Lewerenz, François Lehembre, Peter Staller, Jitka Sulitkova, Thos Geiger, Nabil Djouder, Majid Sabil, Christine Parusel, Dimitris Anastasiou, Ayça Sayi, Yandong Shi, Armelle Yart, Ian Frew and Gudrun Christiansen. In particular I would like to express my genuine thanks to Christiane Wirbelauer, whose generous help and support particularly in the formative years of this study proved invaluable. Vielen Dank Chris! In addition, I would like to extend a big thank you to Armelle Yart for her critical analysis of this thesis and continued support throughout. Merci énormément Armelle! All members of the laboratory have helped in many ways, and if I were to start thanking each, then I'd need a second thesis. Suffice is to say I appreciate all your support.

I would also like to extend many thanks to the technical and administrative support at the *Friedrich Miescher Institute* in Basel where this work has been carried out, and more recently at the *Eidgenössische Technische Hochschule* in Zürich where the laboratory is presently based.

Sincere gratitude is expressed to Prof.Dr.Denis Monard as Fakultätsverantwortlicher, and to Prof.Dr.Holger Moch as Korreferent. I understand the inconvenience entailed in processing a doctoral thesis and defence, and would like to say how much I appreciate your time and effort.

Finally, it leaves me to thank friends who have stood by me. As there are far too many to mention, and fearing that someone would be forgotten, I have chosen not to name people. You know who you are, and what you've done. Thanks a million!

Last but most certainly not least - my parents and family. No words can express the unconditional support you have always given me. Having you there makes this all worthwhile.

Thesis structure

This thesis is divided into eight chapters. The introduction comprises chapters 1-5, and while somewhat detailed, represents work submitted as a current peer review on the functional analysis of the von Hippel-Lindau tumour suppressor and its role in tumourigenesis. It summarises the current worldwide literature concerning VHL biology.

Chapter 1 details VHL disease with respect to tumour formation, diagnosis and clinical management. Each lesion is described. This chapter, while lacking in its molecular biological content, was deemed important as it demonstrates the disease that stems from *VHL* inactivation. This is the ultimate reason why familial cancer syndromes like VHL disease are studied - so as to obtain insights into how they function and the consequence of their deregulation that may result in a pathological outcome. Chapter 2 describes the molecular aspects of the *VHL* gene, and its gene product. It summarises work related to the biochemical structure of the VCB complex, and discusses what can be learned from evolutionary conservation of the *VHL* locus. Chapter 3 details current concepts of *VHL* mutational analysis with an emphasis on the role of VHL in sporadic tumours of the same tissue origin as those seen in VHL disease. Chapter 4 discusses the role of pVHL as a component of an E3 ligase, and the consequence of Hif- α regulation. It also highlights other pVHL-protein interactions that are believed to be additional ligase substrates, or which represent novel functions of pVHL. Finally, chapter 5 discusses the role of pVHL in tumour formation and tumour progression. It describes current *in vivo* tumour models in which VHL function can be studied, and documents the evidence available for the involvement of pVHL in tumour growth, invasion and metastasis.

Chapter 7 represents the results of work undertaken as partial fulfilment of this doctoral study. It is divided into three parts. Part I describes the results obtained from a novel proteomics approach that was developed in an attempt to identify new pVHL interactions. Part II outlines work contributed to an article published in *Nature Cell Biology* corresponding to pVHL intracellular localisation and dynamics. Finally part III describes work pertaining to the targeting of endogenous pVHL by RNA interference.

Chapter 8 discusses the observations and findings related to chapters 1 through 7. It is divided into two main parts. The first is the peer review currently in press, which represents a summary and critical discussion of work outlined in chapters 1-5. The second part of the discussion is a brief discussion of the work documented in chapter 7. Particular emphasis is given to future perspectives intended to develop those results obtained from the proteomics approach.

Éist le fuaim na habhann agus gheobhaidh tú breac



Ní dhéanfaidh smaoineamh an treabhadh duit

Table of Contents

ABSTRACT.....	10
CHAPTER 1 - VHL Disease.....	12
1.1 Background and clinical features of VHL disease	12
1.2 Diagnosis, surveillance and clinical classification of VHL disease	14
1.3 Central nervous system lesions	15
1.3.1 CNS Haemangioblastoma.....	15
1.3.2 Retinal Angioma.....	17
1.3.3 Endolymphatic Sac Tumours	19
1.4 Visceral Lesions	20
1.4.1 Renal Cell Carcinoma and Renal Cysts	20
1.4.2 Pheochromocytoma	22
1.4.3 Pancreatic cysts and tumours	23
1.4.4 Epididymal cysts and cystadenoma	24
1.4.5 Adnexal papillary tumour of probable mesonephric origin (APMO).....	25
CHAPTER 2 - The VHL Gene.....	27
2.1 Introduction	27
2.2 Mapping, identification, and cloning of the VHL gene	27
2.3 VHL gene structure and sequence.....	27
2.4 Promoter Analysis	28
2.5 3' untranslated region of the VHL gene.....	30
2.6 VHL Expression	31
2.6.1 Expression pattern of VHL mRNA.....	31
2.6.2 Expression pattern of pVHL	32
2.7 The VHL protein product	34
2.8 Intracellular localisation of pVHL	35
2.9 Structure of VHL.....	38
2.9.1 Structural analysis of Elongin C- pVHL interaction.....	38
2.9.2 Structural analysis of HIF1 α - pVHL interaction	40
2.10 Sequence Homology.....	42
CHAPTER 3 - Mutational analysis of the VHL gene	47
3.1 Introduction	47
3.2 Structural analysis of pVHL highlights mutational hot-spots.....	49
3.3 Knudson's two-hit hypothesis for tumourigenesis	50
3.4 Genotype-Phenotype Correlations in VHL Disease	51
3.5 Germline Mutations	52
3.6 somatic mutations	54
3.6.1 Allelic deletions	54
3.6.2 Intragenic mutations.....	56
3.6.3 Methylation.....	57
3.7 Somatic mutations in sporadic tumours	58
3.7.1 Mutations in sporadic renal cell carcinoma	59
3.7.2 Sporadic mutations in CNS haemangioblastoma.....	61
3.7.3 Sporadic mutations in pheochromocytoma	62
CHAPTER 4 - Functional analysis of the VHL tumour suppressor.....	65
4.1 Introduction	65
4.2 pVHL and ubiquitin-mediated proteolysis.....	65

4.3	pVHL is a component of an E3 ubiquitin ligase complex.....	66
4.4	pVHL targets HIF- α for degradation.....	69
4.5	The HIF system.....	70
4.5	The HIF system.....	71
4.5.1	HIF and regulation by protein hydroxylation.....	74
4.6	Additional ubiquitination targets of pVHL.....	76
4.6.1	Hyperphosphorylated-RNA polymerase II large subunit, hsRPB1.....	76
4.6.2	RNA polymerase II subunit hsRPB7.....	77
4.6.3	VHL-interacting deubiquitinating enzymes.....	78
4.6.4	Atypical protein kinase C.....	79
4.7	Alternative pVHL interactions.....	82
4.7.1	pVHL interacts and stabilises microtubules.....	82
4.7.2	TAT-binding protein-1 (TBP1); An ATPase involved in HIF- α degradation ...	83
4.7.3	Tric/CCT; a protein chaperonin involved in VCB assembly.....	84
4.7.4	von Hippel-Lindau binding protein – VBP1.....	85
CHAPTER 5 - VHL and Tumourigenesis		86
5.1	Introduction.....	86
5.2	VHL knockout and functional inactivation studies.....	86
5.2.1	Complete Knockout: VHL-/-.....	86
5.2.2	Heterozygotic predisposition to tumourigenesis: VHL+/-.....	88
5.3	VHL involvement in tumour growth.....	92
5.3.1	Angiogenesis.....	92
5.3.2	Growth factors and enhanced cell proliferation.....	94
5.3.3	Cell survival and apoptotic evasion.....	94
5.3.4	VHL and the extracellular matrix.....	95
5.3.5	VHL and cell polarity.....	97
5.3.6	Branching morphogenesis and vasculogenesis.....	98
5.3.7	VHL and tumour cell invasion.....	99
5.3.8	VHL and tumour metastasis.....	99
CHAPTER 6 - Materials and Methods.....		102
6.1	Materials.....	102
6.1.1	General Chemicals.....	102
6.1.2	Drugs and tissue culture reagents.....	104
6.1.3	Antibodies.....	105
6.1.4	Radiochemicals.....	107
6.1.5	Restriction Enzymes.....	107
6.1.6	Bacterial strains and media.....	107
6.1.7	Oligonucleotides.....	108
6.2	DNA and RNA manipulation.....	111
6.2.1	Isolation of plasmid DNA.....	111
6.2.2	Isolation of DNA from agarose gels.....	112
6.2.3	Isolation of total RNA.....	112
6.2.4	Northern Blot Analysis.....	112
6.2.5	Construction of plasmids.....	113
6.2.6	Standard recombinant DNA reactions.....	114
6.2.7	Polymerase chain reaction.....	114
6.2.8	Reverse transcriptase-PCR.....	114
6.2.9	DNA sequencing.....	114
6.3	Cell culture.....	114
6.3.1	Culture of immortalised cell lines.....	114
6.3.2	Transfection of cells.....	115

6.3.3	siRNA transfection of cells	115
6.3.4	Retroviral transduction of cells	115
6.4	Cell cycle analysis	115
6.4.1	Fluorescent activated cell sorting (FACS)	115
6.4.2	Arresting cells	116
6.5	Protein manipulation	116
6.5.1	Immunoprecipitation and Western blotting	116
6.5.2	Cell fractionation	117
6.5.3	Glycerol gradient	118
6.5.4	Far Western	118
6.5.5	Metabolic labelling of cells	119
6.5.6	<i>In vitro</i> transcription/translation reactions	119
6.5.7	Generation and affinity-purification of antibodies	119
6.5.8	Bacterial expression and purification of GST-fusion proteins	119
6.5.9	Covalent coupling of antibody to protein A sepharose	120
6.5.10	Baculoviral expression of proteins	120
6.6	Cellular and biochemical assays	121
6.6.1	Cell Proliferation Assay	121
6.6.2	Reporter gene assay	121
6.6.3	<i>In vitro</i> ubiquitination assay	121
6.6.4	Microtubule co-sedimentation assay	122
6.6.5	Microtubule stability assay	122
6.6.6	<i>In vitro</i> phosphorylation of pVHL	123
6.7	Imaging	123
6.7.1	Immunofluorescence microscopy	123
6.7.2	Time-lapse video microscopy	123
6.8	Proteomics	124
6.8.1	2D-gel electrophoresis	124
6.8.2	Peptide Identification	124

CHAPTER 7 - RESULTS..... 126

PART I - Identification of novel VHL interacting proteins 126

7.1	Introduction	126
7.2	Towards defining an experimental approach	127
7.3	Endogenous pVHL IP and analysis by mass spectrometry	130
7.4	pVHL interacts with the AAA-ATPase family member, p97	135
7.4.1	Introduction	135
7.4.2	pVHL interacts with p97	138
7.4.3	Verification of a pVHL – p97 interaction	139
7.4.4	Towards a functional significance for a p97-VHL interaction	140
7.4.4.1	Sequence analysis	140
7.4.4.2	VHL RNAi does not effect p97 levels	141
7.4.4.3	p97 involvement in proteolytic control of HIF α	142
7.4.4.4	Role of p97 in microtubule stability	145
7.4.4.5	pVHL interacts with HDAC6	147
7.5	pVHL precipitates human homologues of Gcd10p/Gcd14p	150
7.5.1	Introduction	150
7.5.2	Towards defining a function for a pVHL-protein A/B interaction	153

PART II - Investigating pVHL intracellular dynamics..... 155

7.6	Introduction	155
7.6.1	Intracellular localisation of ectopically expressed pVHL ₁₉ and pVHL ₃₀	157

7.6.2	Intracellular localisation of endogenous pVHL ₃₀	157
7.6.3	The importance of microtubule stability in pVHL ₃₀ intracellular localisation	158
7.6.4	The effect of MT stab/destab drugs on pVHL ₃₀ intracellular localisation	159
7.6.5	Recomb. VHL ₃₀ and VHL ₁₉ can exhibit both nuc. and cytopl. ubn activity...	161
PART III - Investigating VHL RNA Interference		164
7.1	Introduction	164
7.2	VHL RNA interference.....	165
7.3	VHL RNAi does not up-regulate HIF- α protein levels nor HIF transcrip. activity	167
7.4	VHL RNAi confirms pVHL regulation of phosphorylated cofilin	170
CHAPTER 8 - Discussion and Future Perspectives		174
Part I – Peer Review		175
Part II - Discussion and Future Perspectives		189
8.1	p97 in HIF regulation.....	189
8.2	p97 and the malformed protein response	191
8.3	A potential role for pVHL in the critical methylation of tRNA _i ^{met}	192
8.4	pVHL intracellular dynamics.....	196
8.5	VHL RNA interference.....	197
8.6	Therapeutic intervention in VHL disease.....	197
References		200

ABSTRACT

Complex genotype-phenotype relations are a hallmark of VHL disease. Patients develop a wide range of tumours depending on how and where pVHL malfunctions. Thus it appears that the VHL tumour suppressor gene product must have multiple and tissue specific functions.

pVHL interacts with the proteins Elongin C, Elongin B, and Cullin 2 in a complex referred to as the VCB-Cul2 complex. This complex displays structural analogy to the Skp1-Cdc53/Cul1-F-box protein (SCF) complex. As with its SCF counterparts, the VCB-Cul2 complex has been shown to constitute an E3 ligase, which serves to recruit protein substrates for degradation by the 26S proteasome. To date, only one such target has been firmly established, the transcription factor Hif- α (hypoxia inducible factor). Proteolytic degradation of Hif- α reflects a key cellular mechanism in the control of adaptive gene expression in response to changes in oxygen levels. While identification of Hif- α as a substrate for the VCB-Cul2 complex proves to be a crucial milestone in VHL biology, isolation of other proteins that are targeted for ubiquitination by VHL represent a major challenge.

A proteomics approach was developed in an effort to expose unknown pVHL protein interactions, and thereby highlighting novel functions of the VHL tumour suppressor. One candidate protein is a 97-kDa ATPase called p97. p97 is a member of the AAA family of ATPase's and is involved in a myriad of distinct cellular functions, interestingly among which include binding to poly-ubiquitin chains and facilitating substrate presentation to the proteasome. We show that p97 binds pVHL both *in vitro* and *in vivo*, and propose a model whereby p97 may facilitate presentation of ubiquitinated Hif- α to the 26S proteasome for subsequent degradation. We also demonstrate that, similar to pVHL, p97 can promote microtubule stability, and propose a model through binding to HDAC6, a histone deacetylase known to bind p97 and shown here to bind pVHL *in vitro*, that these proteins might be involved in the malformed protein response, and that this potential function could be microtubule dependent.

The proteomics approach also uncovered additional protein interactions, namely two uncharacterised proteins with homologues in *S.Cerevisiae* known to complex and constitute a critical RNA methyltransferase. We suggest that this co-precipitating complex is the mammalian orthologue and we provide preliminary data showing, in addition to the endogenous interaction, *in vitro* binding to pVHL. Finally we propose a model where, by means of its ability to negatively regulate the activity of this complex,

pVHL could be involved in the mammalian stress-responsive pathway, thereby helping to explain, in part, the observation that the inability of renal cell carcinoma cells lacking VHL to exit the cell cycle upon serum withdrawal can be restored upon reintroduction of pVHL into these cells.

In a second part to this thesis, pVHL intracellular dynamics have been studied. We demonstrate that pVHL₁₉ and pVHL₃₀ exhibit different localisation patterns, with pVHL₃₀ residing primarily in the cytoplasm, and pVHL₁₉ in the nucleus. We show that when pVHL₃₀ is in the cytoplasm, it co-localises with microtubules, and that this localisation is altered upon microtubule destabilisation, which renders a strong nuclear signal for pVHL₃₀. We conclude that pVHL intracellular dynamics are reflective, in part, by the stability of the microtubule network. This work contributed to an article in *Nature Cell Biology*.

The third part of the results outlines the targeting of endogenous pVHL by RNA interference. Optimal conditions for VHL RNAi and a study on the cellular effects are presented. Hif- α regulation is investigated in the presence of VHL siRNA oligos, and the lack of Hif- α up-regulation discussed. Finally, positive regulation of phospho-cofilin, an important component in actin cytoskeleton rearrangements, is demonstrated as the only positive read-out for VHL RNAi to date, and the implications this regulation by pVHL might have on cell shape changes and movement is briefly discussed.

CHAPTER 1

VHL Disease

1.1 Background and clinical features of VHL disease

Von Hippel-Lindau disease is an autosomal dominantly inherited, multi-system, family cancer syndrome predisposing individuals to a defined pattern of tumours. It has been estimated that the birth incidence of VHL disease is between 1 in 36,000 - 45,500 live births [10]. The tumours are of specific histological types: retinal, cerebellar, and spinal haemangioblastomas, clear-cell type (non-papillary) renal cell carcinoma (RCC), pheochromocytoma, pancreatic islet tumours and endolymphatic sac tumours of the inner ear. In addition, multiple renal, pancreatic, epididymal and broad ligament cysts occur. In this chapter a concise overview will be outlined defining each malignancy associated with VHL disease, their means of detection and available treatment. While this chapter does not contain molecular detail, it was considered important in order to gain a comprehensive understanding of VHL biology, and represents the justification for studying this disease, and for studying familial cancer syndromes in general.

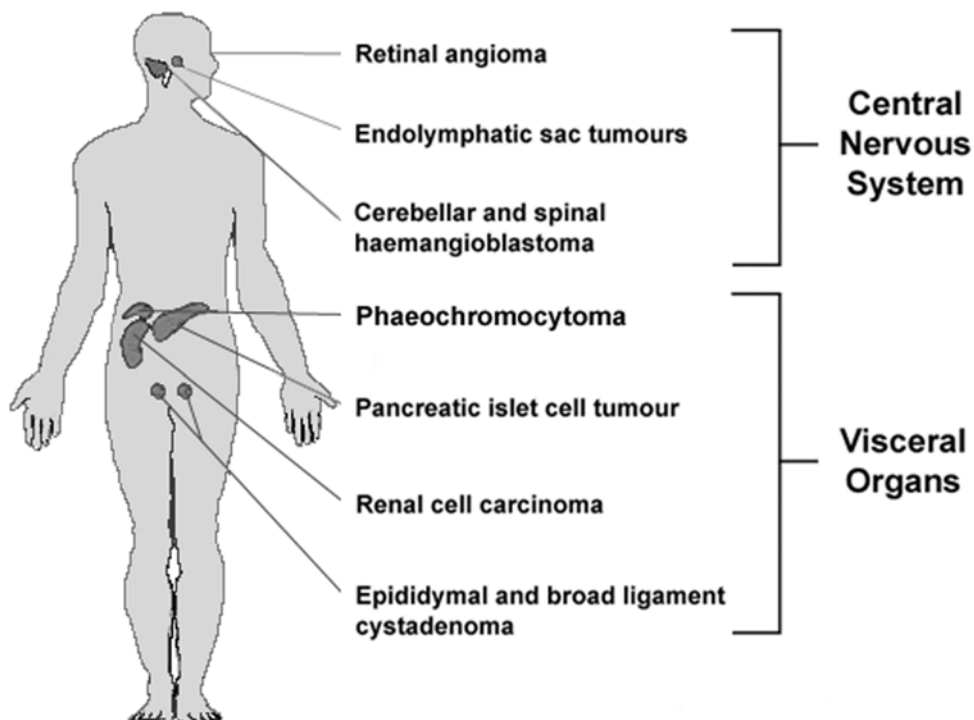


Figure 1. Location of principal neoplasma associated with von Hippel-Lindau disease.

Von Hippel-Lindau (VHL) disease is named after the German ophthalmologist Eugene von Hippel, who described retinal haemangioblastoma in 1904, and the Swedish pathologist Arvid Lindau who associated retinal and central nervous system (CNS) haemangioblastoma with cysts of the kidneys, pancreas and epididymis in 1926 [14] [15]. The first report on pheochromocytoma in VHL disease appeared in 1953 [16]. The most recently discovered VHL-related tumours are the endolymphatic sac tumours of the inner ear and the adnexal papillary tumour of probable mesonephric origin (AMPO), otherwise known as lesions of the broad ligament [18].

The mean age at symptomatic diagnosis varies: 24.5 years for retinal angioma, 29 years for haemangioblastoma, and 44 years in renal cell carcinoma (RCC). Due to the early onset of retinal angioma and cerebellar haemangioblastoma, these complications appear more frequent than RCC in cross-sectional studies and are the most common first manifestations of the disease. VHL disease may manifest in childhood or old age, but most patients present in the second and third decade, and penetrance is almost complete by age 60 years [21, 22]. These results are summarised in tables 1 and 2, which compare clinical data from several large independent studies.

Table 1. Cause of death in VHL disease

Adapted from Richard et al. 2000

Author	Lamiell et al.	Maher et al.	Maddock et al.	Richard et al.
Deceased patients	182	51	44	13
Age at death^(years)	36.9±14 (13-67)	41±14 (13-67)	40.9±14.6 (12-65)	47±16 (24-81)
Cause of death				
CNS Haemangioblastoma	55%	41%	52.30%	61.50%
Renal cell carcinoma	13%	47%	27.30%	30.80%
Others	32%	12%	28.40%	7.70%

Table 2. Clinical data from three large series of VHL patients

ND not detailed. Adapted from Richard et al 2000

Author	Maher et al.	Maddock et al.	Richard et al.
Patients (n)	152	83	215
CNS Haemangioblastoma			
Frequency	72%	63.80%	72%
Multipe tumours	38%	ND	43%
Age at diagnosis in yrs (range)	29±10 (11-61)	30±12 (4-76)	30±11.5 (13-70)
Other Manifestations of VHL			
Retinal Haemangioblastoma	59%	41%	44%
Renal cell carcinoma	28%	14.50%	36.70%
Pheochromocytoma	7%	14.50%	17.20%
Pancreatic lesions	ND	22%	53%
Presenting manifestations			
CNS Haemangioblastoma	41%	38.50%	38.80%
Retinal Haemangioblastoma	43%	25.30%	23.70%
Others	13%	36.20%	37.50%

1.2 Diagnosis, surveillance and clinical classification of VHL disease

Metastases from renal cell carcinoma and neurological complications from cerebellar haemangioblastoma (Hb) are the most common causes of death in VHL disease. However, improved surveillance through early detection of tumours by intensive radiological and clinical screening, together with advanced operation techniques are helping to reduce both morbidity and mortality in VHL disease [24-26].

Diagnosis of von Hippel-Lindau disease is often based on clinical criteria. Patients with a family history, and a CNS Haemangioblastoma, including retinal angioma, phaeochromocytoma (Phaeo), or RCC are diagnosed with the disease. To meet the diagnostic criteria, those with no relevant family history must have two or more CNS Hb's, or one CNS Hb and a visceral tumour, with the exception of epididymal and renal cysts, which are frequent in the general population [29-31]. Table 3 summarises standard screening procedures for at-risk individuals.

Table 3. Recommended intervals for screening in at-risk individuals

Adapted from Choyke et al. 1995

Test	Start age (frequency)
Ophthalmoscopy	Infancy (early)
Plasma or 24 h urinary catecholamines and metanephrines	2 years of age (yearly and when blood pressure is raised)
MRI of cranio-spinal axis	11 years of age (yearly)
CT and MRI of internal auditory canals	Onset of symptoms (hearing, loss, tinnitus, vertigo, or unexplained difficulties of balance)
Ultrasound of abdomen	18 years of age or earlier if clinically indicated (yearly)
Audiological function tests	When clinically indicated

Specific correlations of genotype and phenotype have emerged in affected families. As outlined in table 4, several familial phenotypes of von Hippel-Lindau disease are now recognised, providing useful information to screen and counsel affected individuals [32]. Clinically, VHL disease can be subdivided into two main classes. Type 1 families have a greatly reduced risk of phaeochromocytoma's, but can develop all the other tumour types generally associated with the disease. Type 2 families have phaeochromocytoma's, but have either a low-risk (type 2A) or high-risk (type 2B) for renal cell carcinomas. Type 2C families have phaeochromocytoma's only, with no other neoplastic findings characteristic of VHL disease [33].

Table 4. Clinical sub-divisions in VHL disease

Class	Tumour types observed in families		
	Haem.	RCC	Phaeochr.
Type 1	+	+	–
Type 2A	+	–	+
Type 2B	+	+	+
Type 2C	–	–	+

Advances in genetic testing for the disease include qualitative and quantitative Southern blotting, which has been added to DNA sequence analysis. This improved testing has increased the detection rate of DNA mutations in peripheral blood leucocytes from 75% to nearly 100% [34]. In 1996, there were more than 137 distinct intragenic germ-line mutations reported in affected families in North America, Europe, and Japan [35]. Mutation types included missense, non-sense, micro-deletion, insertion, deletion, and splice site [35]. Known mutations of von Hippel-Lindau disease are now stored online (www.umd.be), where some 834 somatic mutations have been collected. Since genetic testing detects mutations in nearly 100% of documented affected families, serial clinical surveillance studies are recommended for family members with mutations. A more detailed mutational analysis of the VHL locus will be discussed in chapter 3.

A diagnostic challenge arises in *de novo* cases (i.e. the first affected member of a family) of von Hippel-Lindau disease. These cases arise in as many as 20% of kindred's [36]. The initial mutation in a *de novo* case might result in disease mosaicism. This means that some, but not all, tissues could carry the new disease mutation. Thus, such patients might have clinical signs of the disease, but test negative genetically, because the VHL mutation is not carried in all peripheral leucocytes. The earlier the new mutation arises in embryogenesis, the more numerous and varied the types of cells that will carry the mutation.

1.3 Central nervous system lesions

1.3.1 CNS Haemangioblastoma

Haemangioblastoma manifests in early adulthood and is the most common presenting manifestation of VHL, revealing the disease in 30-50% of cases (Table 1). CNS haemangioblastoma arise preferentially in the cerebellum (~37%), brain stem (~10%) and spinal cord (~50%), but are rare in the cerebrum (~1%) [37]. Haemangioblastoma are benign tumours mainly found in the brain stem, with a heterogeneous histology comprising endothelial cells, pericytes and interstitial stromal cells. About 60% are cystic and 40% are solid. They are the most common brain stem tumour in the adult, comprising about 7% of all brain stem tumours. Haemangioblastoma may be multiple, particularly in VHL disease and when located in the spinal cord. On gross pathology, they

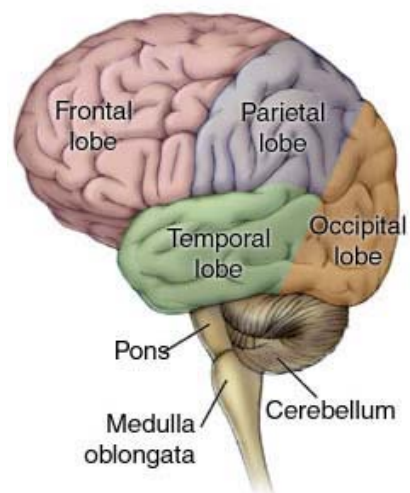


Figure 2. Basic anatomy of the brain. The image illustrates the brain, viewed from the side, showing the major lobes (frontal, parietal, temporal and occipital) and the brain stem structures. The brainstem is the portion of the brain connecting the cerebral hemispheres with the spinal cord. It contains the midbrain, pons, and medulla oblongata.

are well demarcated, highly vascularised nodules frequently associated with a cyst whose walls are usually composed of gliotic tissue (see Fig.3A). Although they can be easily diagnosed by CT (computed tomography), MRI (magnetic resonance imaging) is the most effective non-invasive modality to diagnose haemangioblastoma's (Figs. 3, 4).

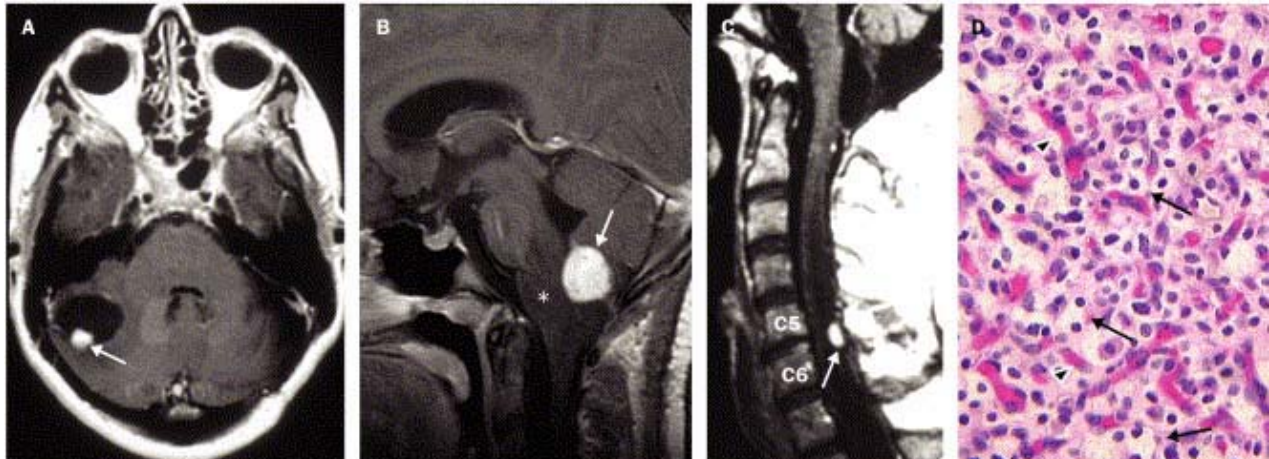


Figure 3. MRI and histological features of CNS haemangioblastoma

(A). MRI of a cerebellar haemangioblastoma (arrow) with an associated cyst (homogenous associated dark region) in a 40-year old woman. (B). MRI of medullary haemangioblastoma (arrow) in a 12-year old girl. (C). MRI of the spinal cord of a 50-year old man. The haemangioblastoma is located in the posterior portion of the spinal cord at C5 and C6 (arrow). (D). Haematoxylin and eosin staining of a haemangioblastoma showing the stromal cells (arrows) distributed within a capillary network (arrowheads).

Adapted from Lonser et al. 2003

The three specific elements that allow an almost certain diagnosis of haemangioblastoma are, however, the brain stem location, the cystic nature, a peripheral enhancing nodule and the presence of large vessels at the periphery or within the mass. Angiography is, however, necessary not only to definitely depict the lesion which clearly appears as a highly vascular nodule with a prolonged stain and a draining vein, but also to identify small nodules that can be missed on MRI.

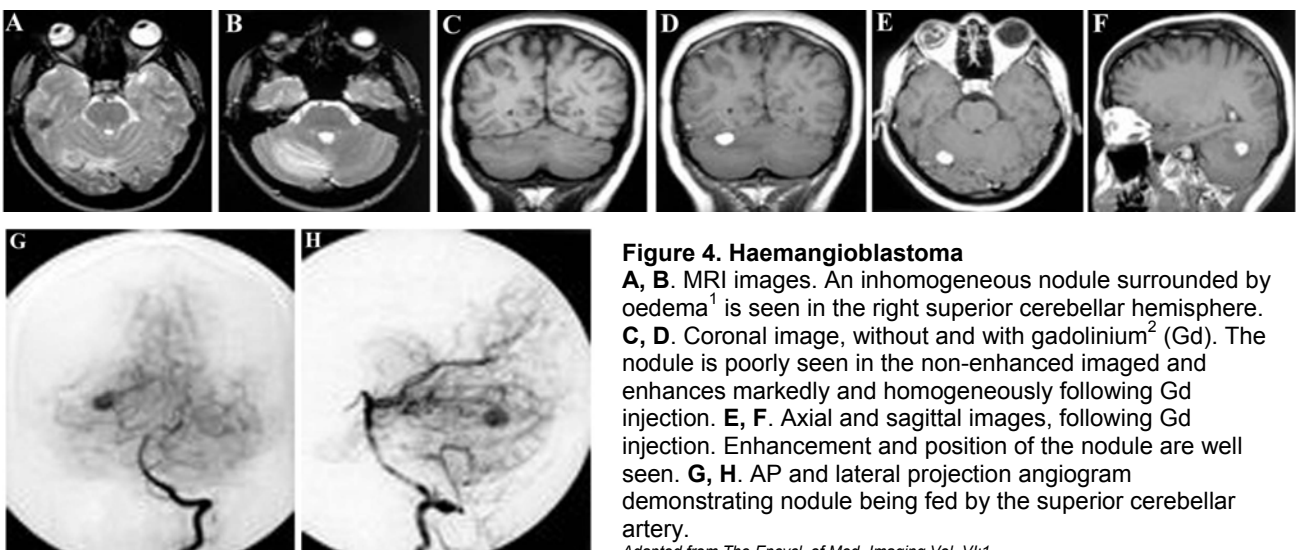


Figure 4. Haemangioblastoma

A, B. MRI images. An inhomogeneous nodule surrounded by oedema¹ is seen in the right superior cerebellar hemisphere. **C, D.** Coronal image, without and with gadolinium² (Gd). The nodule is poorly seen in the non-enhanced image and enhances markedly and homogeneously following Gd injection. **E, F.** Axial and sagittal images, following Gd injection. Enhancement and position of the nodule are well seen. **G, H.** AP and lateral projection angiogram demonstrating nodule being fed by the superior cerebellar artery.

Adapted from The Encycl. of Med. Imaging Vol. VI:1

¹ Oedema is an abnormal excess accumulation of serous fluid in connective tissue or in a serous cavity

² Gadolinium is a magnetic metallic element of the rare-earth group used for contrast medium in imaging procedures like MRI

Patient outcome has been greatly ameliorated by microsurgery and progress in intensive care, but the possibility of other tumours developing is still a major problem. Postoperative mortality is 7-10% and is higher in brainstem-associated lesions [38].

1.3.2 Retinal Angioma

Retinal angioma is a benign vascular tumour of the retina, which in VHL disease usually occurs as a clinically observable fundus³ lesion in the 20 to 40-year old age group. They may be present at birth but are frequently not detected until this time because of the usual small size and peripheral location of the tumours. Although they may develop anywhere in the retina, they tend to be most prevalent in the temporal mid-periphery of the eye.

Retinal angioma begin as a proliferation of endothelial cells between arterioles and venules in the capillary bed [39]. The angioma gradually enlarges and the surrounding capillary network develops into a large fistular single arteriolar and venous channel, which serves to feed and drain the tumour [40] (Figure 6). Micro-vasculopathy⁴ occurs in the capillary bed, as blood is shunted to the tumour from the surrounding retina. The non-perfused area may then develop intra-retinal oedema through leakage of plasma and other blood constituents into the retinal tissue, which leads to hard exudates and eventual involvement of the macula via cystoid maculopathy (Figure 4). Macular oedema represents the major cause of vision loss in VHL disease. The maculopathy first presents as early oedema or discrete exudates in a star-shaped pattern and can occur with peripheral angioma in the presence of normal intervening retina [41]. If unrecognised and untreated at this early stage, the majority of these angioma will eventually haemorrhage, resulting in massive exudation, retinal detachment and ultimately, neo-vascular glaucoma and blindness.

Treatment of retinal angioma is dependent on the presence of tumour exudation and macular involvement. Angioma's that are small, stable and asymptomatic may be followed by photo-documentation. Treatment becomes necessary when there is a threat

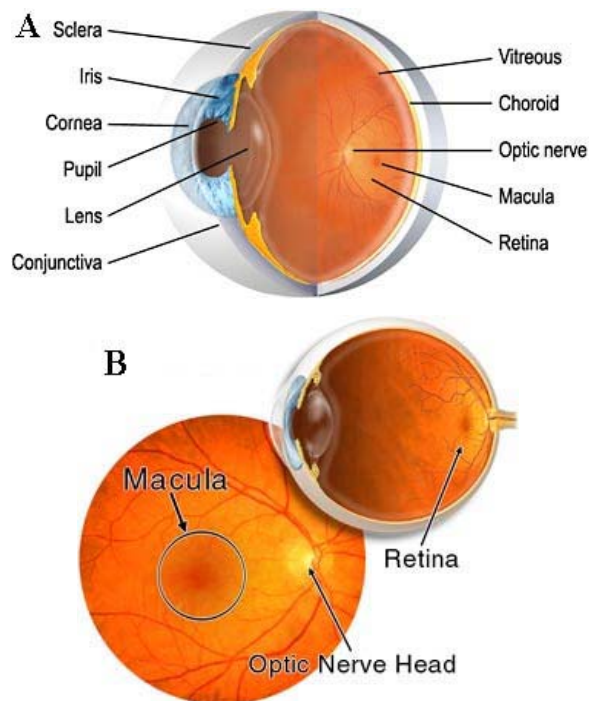


Figure 5. (A) Basic anatomy of the eye. This graphic lists many of the essential components of the eye's optical system in an aid to help understand the text. (B). The *macula* is the highly sensitive area of the retina. It is responsible for critical focusing vision. It is the part of the retina most used. We use our macula to read or to stare intently at an object.
Adapted from www.stlukeseye.com

³ Fundus refers to the bottom of or part opposite the aperture of the internal surface of a hollow organ, in this case the part of the eye opposite the pupil

⁴ Vasculopathy refers to any pathological condition regarding vasculature

to macular function by exudation. Argon laser photocoagulation is the treatment of choice in tumours less than 2.5 disc diameters in size [41]. Laser is applied to the tumour itself, leaving a pigmented scar and involuted feeder vessels. Tumours larger than 2.5 disc diameters and those with sub-retinal fluid are more effectively treated with cryotherapy⁵ [42]. Eye wall resection, which involves the surgical removal of the tumour through a cut in the sclera, has been successful for treating larger tumours (greater than 4.5mm) where photocoagulation and cyrotherapy modalities are not an option, however, this procedure is not without significant risk [41].

There are several treatment strategies on the horizon that show promise for the ocular management of this disease and include the use of radiotherapy, such as brachytherapy⁶ or linear-accelerated based radio-surgery [43, 44]. Molecular biological and pharmaceutical advances also offer interesting therapeutic potential. Active research is ongoing to devise drugs designed to target specific bio-molecules. In the case of VHL disease, it is known that mutations in the VHL tumour suppressor gene result in changes in the oxygen-regulation factor, hypoxia inducible factor, HIF. This factor subsequently binds to specific enhancer elements of the VEGF gene and stimulate angiogenesis⁷ (regulation of these

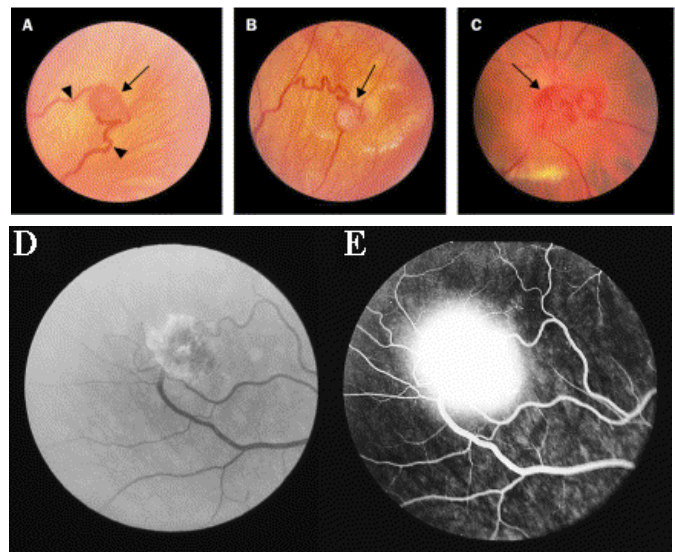


Figure 6. Ophthalmoscopic view of retinal angioma. (A) Peripheral retinal angioma (arrow) with an enlarged vessel in a 22-year-old woman. (B) Peripheral retinal angioma (arrow) with fibrous changes, hard exudates and retinal oedema in the surrounding region in a 24-year-old man. (C) Retinal angioma (arrow) on the optic nerve head with yellow retinal hard exudates below it in a 32-year-old man. (D) The vascular tumour is seen as a mass of blood vessels. (E) After injection of fluorescein dye to identify the blood vessels, the highly vascular nature of the tumour is apparent.

Adapted from references Kaelin et al. 1998 and Lonser et al. 2003

factors by VHL and it's consequence will be dealt with in more detail at a later stage). This increase in angiogenesis under normoxic (normal oxygen levels) conditions in key target organs such as the brain, kidney and eye leads to high morbidity and reduced life expectancy. Interestingly, *Aiello et al.* [45] reported a case of rapid and durable recovery of visual function in a patient with VHL disease and optic nerve head angioma after systemic administration of a VEGF receptor inhibitor SU5416. VEGF is a homo-dimeric cytokine that was originally identified for its effects on endothelial cell proliferation and vascular permeability. Since it's discovery, VEGF has been shown to bind on the surface of epithelial cells to tyrosine kinase receptors, Flt-1 and KDR (or VEGFR-1 and -2 respectively), which regulate VEGF-induced physiologic and patho-physiologic

⁵ Cryotherapy, also known as cryosurgery, is a commonly used procedure for the treatment of a variety of benign and malignant lesions. The mechanism of destruction is necrosis, which results from the freezing and thawing of cells. Treated areas re-epithelialise. Adverse effects are usually minor and short-lived

⁶ Brachytherapy is radiotherapy in which the source of radiation is placed (as by implantation) in or close to the area being treated

⁷ Angiogenesis is the formation and differentiation of blood vessels

angiogenesis. Overproduction of VEGF in the mouse brain causes lesions that are reminiscent of haemangioblastoma. Therefore, increased expression of VEGF could explain the highly vascular nature of VHL-related tumours, and hence represent a target for systemic therapy. In recent years, a number of VEGF-targeted strategies have been tested in clinical trials, including anti-VEGF antibodies and small molecule inhibitors of VEGFR-1 and -2. Among these is SU5416. Although caution is warranted in drawing conclusions from an isolated case report, the clear association between the initiation of treatment and marked improvement in numerous visual function parameters in a condition where spontaneous resolution is extremely rare, coupled with a plausible mechanism of action, suggests that systemic inhibition of VEGF should be considered as a potential therapeutic method for VHL disease.

1.3.3 Endolymphatic Sac Tumours

Endolymphatic sac tumour (ELST) [46] is a rare neoplasm arising from the temporal petrous region⁸. The origin of this tumour is thought to be the endolymphatic sac [46, 47]. ELST histologically shows epithelial features, such as papillary architecture, glandular formation and a colloid-like structure. The tumour is believed to be an epithelial tumour [47, 48]. These tumours, while rare, are frequently associated with von Hippel-Lindau disease [18]. MRI revealed evidence of these tumours, as demonstrated by systematic radiological study of 121 patients with VHL, and showed an incidence of 11% [18]. ELST are highly vascular, and often erode or expand the surrounding temporal bone. Histologically, ELST's form papillary cystic regions filled with proteinaceous material (Fig.8D) characterised by a simple cuboidal epithelium covering highly vascularised stroma with blood capillaries in close contact with the surrounding epithelium.

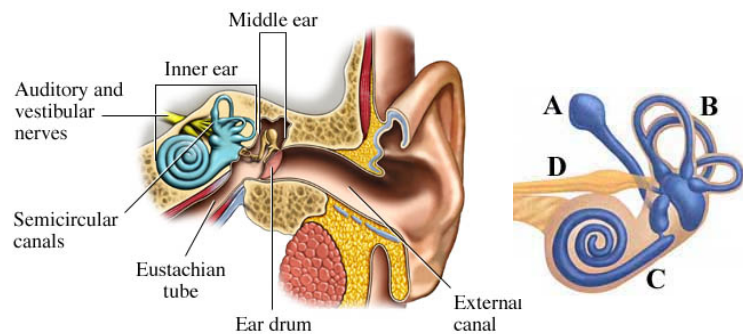


Figure 7. The basic anatomy of the external, middle and inner ear. The inner ear consists of (A) the endolymphatic sac, (B) the semicircular canals, (C) the cochlea and (D) the auditory nerve. The endolymphatic duct originates from the connecting duct between saccule and utricle. It consists of three parts: the shorter inner portion, the highly convoluted intermediate (or 'rugose') portion and the distal portion that is ensheathed by two layers of the dura. The intermediate part supposedly is the origin of ELST.

Diagnosis is easily made by CT scan and MRI (fig.6). On CT scan, ELST is seen as a destructive lesion lysing temporal bone, medial mastoid⁹ and auditory canal (Fig. 6B). With MRI, ELST appears as a heterogeneous lesion and is markedly enhanced after contrast medium injection, e.g. gadolinium (Fig. 8A). Early radiological detection is

⁸ Petrous region is of, relates to, or constitutes the exceptionally hard and dense portion of the human temporal bone that contains the internal auditory organs

⁹ Mastoid refers to part of the temporal bone behind the ear

crucial because timely therapy will prevent hearing deficits from progressing. Surgery is curative for completely excised tumours, and the preoperative level of hearing is usually preserved. The importance of adjunctive radiation remains unclear, but inoperable tumours have been radiated [49]. ELST are not known to metastasise [50].

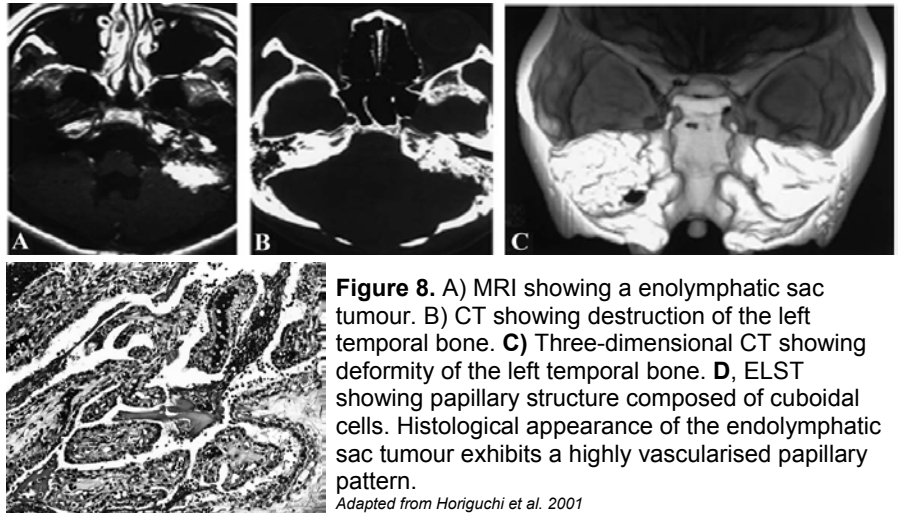


Figure 8. A) MRI showing an endolymphatic sac tumour. B) CT showing destruction of the left temporal bone. C) Three-dimensional CT showing deformity of the left temporal bone. D, ELST showing papillary structure composed of cuboidal cells. Histological appearance of the endolymphatic sac tumour exhibits a highly vascularised papillary pattern.

Adapted from Horiguchi et al. 2001

1.4 Visceral Lesions

1.4.1 Renal Cell Carcinoma and Renal Cysts

Renal cell carcinomas (RCC) account for 80-85% of all primary renal neoplasms. RCC is the major malignant neoplasm in the von Hippel-Lindau disease and the primary cause of inherited renal cancer. Almost half the number of patients diagnosed with RCC have metastatic disease on presentation [51]. Metastatic RCC has an extremely poor prognosis, with a median survival of less than 1 year. The classification of RCCs reflects the morphology, cell of origin, and molecular basis of the different types of renal carcinomas [52]. Table 5 outlines the five distinct types.

Similar to the colon and breast cancer fields, studies in the renal cancer area have identified several tumour suppressor genes and oncogenes involved in the pathogenesis of hereditary renal cancer syndromes. These same genes have been implicated in the pathogenesis of the majority of

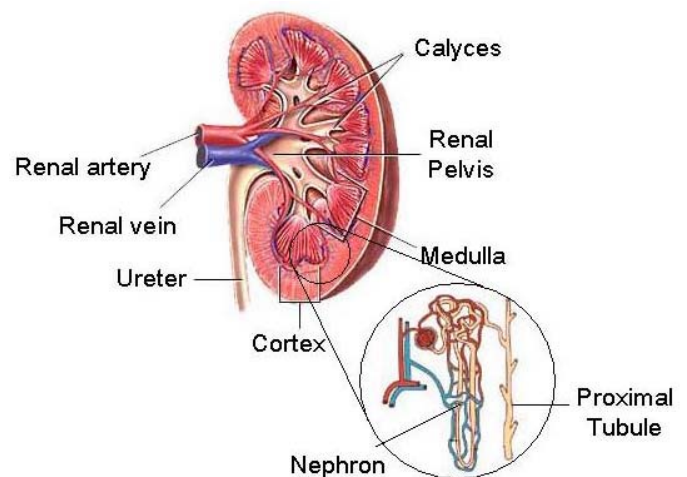


Figure 9. Gross anatomy of the kidney.

Pathologically, renal cell carcinoma is a malignant epithelial tumour of the renal parenchyma and is often found in the renal cortex. The most common cellular pattern is clear cell carcinoma, arising from cells of the proximal tubuli [1].

Table 5. Renal Cell Carcinoma Classification

Type	Frequency
1. Clear cell renal carcinomas	80%
2. Papillary or chromophilic	15%
3. Chromophobic	5%
4. Oncocytic	<1%
5. Collecting duct carcinomas	Very rare

sporadic renal cancers and have helped define new targets for therapy. Among those genes identified is the VHL tumour suppressor gene. VHL syndrome is the most common familial syndrome with clear cell renal carcinoma as one of its features. Proximal tubular epithelium is thought to be the cell of origin for clear cell RCC (fig.7).

Contrast-enhanced abdominal CT is the standard for detection of renal involvement in the disease (fig.8). CT allows detection and quantification by size and number of renal cell carcinomas and cysts, allowing serial monitoring of individual lesions. MRI is an alternative method of detection for patients who have reduced renal function. Histologically, they are always of the clear-cell subtype (fig.10), and small carcinomas tend to be low grade [53]. Treatment recommendations can depend on tumour size.

Options for treatment range from bilateral nephrectomy, nephron-sparing surgery¹⁰ to follow-up investigations only [54]. If both kidneys are affected with multiple cysts and tumours, a difficult decision has to be made between radical nephrectomy or nephron-sparing surgery. This decision depends on risk factors for

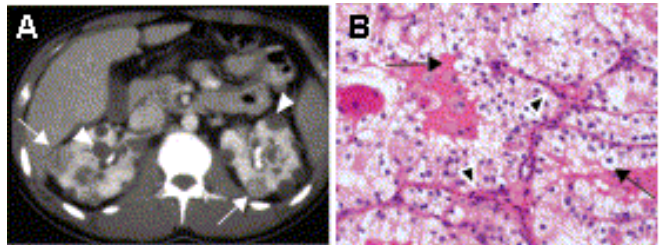


Figure 10. (A) CT image and (B) Histology of RCC and renal cysts. Bilateral multifocal RCC with both solid (arrows) and cystic (arrowheads) disease in a 22-year-old man.

Adapted from Lonser et al 2003

metastatic spread (size, progression, capsule involvement and whether the tumour is symptomatic). Management of metastatic lesions is a difficult problem, since their response to chemotherapy and radiotherapy is poor. A prospective analysis on treatment of renal cell carcinoma in VHL patients demonstrated that, using a 3 cm renal tumour diameter as an indication for renal surgery, no patient with renal cancer and VHL disease has metastatic disease regardless of the number of tumours [55]. At the third International meeting on VHL disease a consensus was reached to use a 3 cm threshold as the lower limit to perform renal surgery and whenever feasible preferably using nephron-sparing surgery [56]. This approach may help to prevent metastases, and avoid unnecessary renal damage due to frequent surgery, necessitating renal dialysis or transplantation.

Percutaneous¹¹ radio-frequency ablation or cryoablation of small carcinomas are experimental treatments and hold promise of being less invasive than other treatments. Pavlovich and colleagues [57] have reported early results of an ongoing trial of percutaneous radio-frequency ablation for small renal tumours, but it remains experimental until procedural and imaging parameters that correlate with tumour destruction are validated.

¹⁰ Nephron-sparing surgery refers to partial nephrectomy

¹¹ Percutaneous approaches are those effected or performed through the skin

1.4.2 Pheochromocytoma

Pheochromocytoma and paraganglioma are terms describing a neoplasm of chromaffin cells¹² found in the adrenal medulla or elsewhere within the sympathetic paraganglionic axis. The adrenal tumours are usually referred to as pheochromocytoma's, whereas an extra-adrenal tumour is often termed extra-adrenal pheochromocytoma or paraganglioma, the latter usually reserved for a non-functional (i.e. non-catecholamine secreting) neoplasm. This terminology is based on historical histopathological techniques, and since these neoplasms are otherwise indistinguishable, the terminology may be confusing. Furthermore, extra-paraganglioma may also arise from special structures in the neck, referred to as chemodectomas, glomus jugulare, or carotid body tumours. While pheochromocytoma is

the tumour type of discussion here, it is important to note that in contrast to other familial pheochromocytoma syndromes such as multiple endocrine neoplasia type II (MEN 2) and neurofibromatosis type I (NF 1), it has been reported that up to 12% of VHL patients present extra-adrenal paraganglioma [58-61]. Pheochromocytoma's can be benign or malignant, sporadic or familial tumours. In one study performed by Walther and colleagues [61], a series of 246 patients with VHL syndrome were studied. 64 patients were found to have a pheochromocytoma, the mean age at diagnosis being 29 years with a range from age 6 to age 54. Bilateral tumours in this group were found in 39% of patients.

As already mentioned, and a topic that will be discussed in more detail in chapter 3, genotype-phenotype correlations have emerged in VHL disease. Clinical classification of VHL disease groups families which manifest low-risk (Type 1) or high-risk (Type 2) of pheochromocytoma, and some VHL families (Type 2C) present as familial pheochromocytoma without haemangioblastoma or renal carcinoma [62-66]. These studies show strong evidence that the presence or absence of pheochromocytoma is correlated with the type of VHL germ-line mutation.

The first diagnostic step is represented by the measurement of catecholamines and their metabolites (metanephrines) in urine and plasma. Localisation and staging of

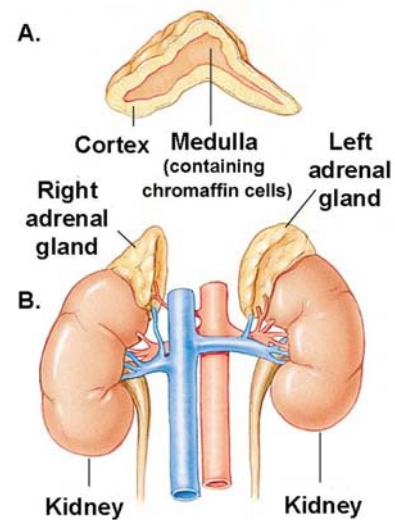


Figure 11. Anatomical location of the adrenal gland. (A). Simplified diagrammatic Cross section through an adrenal gland illustrating the chromaffin cell-containing adrenal medulla from which pheochromocytomas arise. (B). Gross anatomy of the adrenal glands with respect to the kidney.

¹² Chromaffin cells, so called due to the fact that they stain deeply with chromium salts, are characteristically located in the adrenal medulla and paraganglia (paraganglia, chromaffin) of the sympathetic nervous system. They store catecholamine secretory vesicles, e.g. adrenaline, which is released upon stimuli

phaeochromocytoma is based on MRI, and metaiodobenzylguanidine (MIBG) scintigraphy is useful to confirm the catecholamine-producing nature of the tumour and reveal extra-adrenal tumours [4, 67]. Scintigraphy after administration of radio-labelled octreotide, a somatostatin analogue, has had only limited success, depending on anatomic factors, expression of somatostatin receptors, and delivery of the radio-pharmaceutical to the tumour cells [68]. Preliminary results presented by *Pacak et al.* show that 6-[¹⁸F]-fluorodopamine PET scanning can detect and localise phaeochromocytoma, not only as a primary tumour in the adrenal gland but also as a recurrent extra-adrenal or metastatic tumour and is superior to MIBG scanning [69].

Operative treatment can be considered in symptomatic phaeochromocytoma or if a growing mass in the adrenal gland is present. Satisfactory results have been reported from laparoscopic¹³ removal of adrenal tumours in VHL patients [70, 71]. Since bilateral tumours develop in 47% of VHL patients with phaeochromocytoma, most patients become independent on steroids after bilateral adrenalectomy [70]. Enucleation¹⁴ rather than adrenalectomy is therefore recommended by an increasing number of surgeons. Adrenal-sparing surgery is safe, effective and can preserve adrenal function in VHL patients.

1.4.3 Pancreatic cysts and tumours

Pancreatic involvement is frequent in VHL disease, presenting in up to 70% of affected patients, but in most cases is limited to isolated or multiple benign cysts [72]. Serous cystadenomas are benign multi-cystic calcified tumours and less frequently encountered. Cystic manifestations commonly have no clinical implications but abdominal pain and cholestatic jaundice¹⁵ can result from compression by enlarged cysts. Neuroendocrine tumours, islet

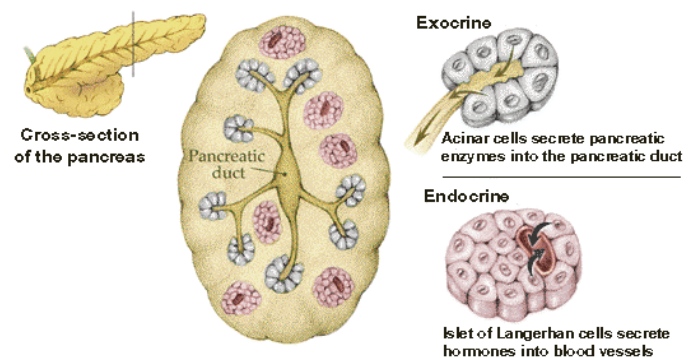


Figure 13. The pancreas has endocrine and exocrine functional components. Islet of Langerhans cells are components of the endocrine system. These are cells of the pancreas that produce and secrete hormones into the bloodstream.

Adapted from John Hopkins Pathology Homepage

cell tumours, frequently multi-focal, are observed in 10-15% of VHL patients. These tumours tend to be slow growing but have the potential of a truly malignant course.

Endocrine tumours of the pancreas are very rare, accounting for only 5% of all pancreatic cancers. There are several types of islet cells and each produces its own hormone.

¹³ Laparoscopy refers to a fiber-optic instrument that is inserted through an incision in the abdominal wall and is used to examine visually the interior of the abdomen cavity

¹⁴ Enucleation refers to removing, in this case the tumour, but without cutting into the vital organ, in this case the adrenal gland

¹⁵ Cholestatic jaundice, or cholestasis, refers to impairment of bile flow due to obstruction in small bile ducts (intrahepatic cholestasis) or obstruction in large bile ducts (extrahepatic cholestasis)

Functional endocrine tumours are named after the hormone they secrete, e.g. insulinoma is the most common tumour of the endocrine pancreas. 10-15% of VHL patients will develop islet cell cancer. Symptoms vary among the different islet cell cancer types.

Surgery and chemotherapy have been shown to improve the outcome of patients even if they have metastatic disease. Most patients with metastasis do not survive five years. Islet cell cancer tends to spread to the surrounding lymph nodes, stomach, small intestine, and liver. There are no known risk factors associated with sporadic islet cell cancer. Therefore, it is not clear how to prevent its occurrence. Individuals with VHL disease or MEN syndrome, however, have a genetic predisposition to developing islet cell cancer and should be screened regularly in an effort to catch the disease early.

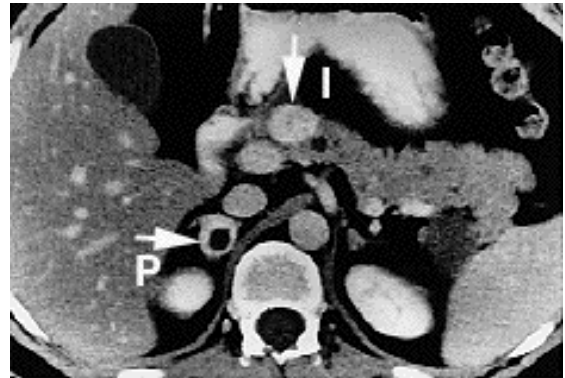


Figure 14. Patient with phaeochromocytoma and islet cell tumour of the pancreas. (P) phaeochromocytoma with a necrotic center. (I) islet cell tumour present in the neck of the pancreas. Two small pancreatic cysts are also observed.

Adapted from Choyke et al. 1995

1.4.4 Epididymal cysts and cystadenoma

Two types of lesions are encountered: simple cysts without specificity, and papillary cystadenomas with columnar clear cells lining a highly vascular stroma, a pattern sometimes confused with metastasis of renal cell carcinoma. Papillary cystadenomas of the epididymis (PCE), are seen in approximately 10-26% of men with VHL [29, 73, 74]. PCE's are rarely found as unilateral lesions in the general population but when they are bilateral they are virtually

pathognomonic of VHL disease. Epididymal cysts with no solid component are also commonly reported in VHL but are seen in 23% of the general population making epididymal cysts an unreliable diagnostic characteristic for VHL [75]. The PCE can be unilateral or bilateral and is most often found in the globus major, the head of the epididymis. PCE may involve the spermatic cord as well [76]. The lesions are typically 2-3cm. PCE's are firm and easily palpable but can contain cystic spaces with clear yellow or hemorrhagic fluid [75]. Histologically, PCE resembles endolymphatic sac cysts and renal cysts lined by clear cells containing fat and glycogen with tubular and papillary

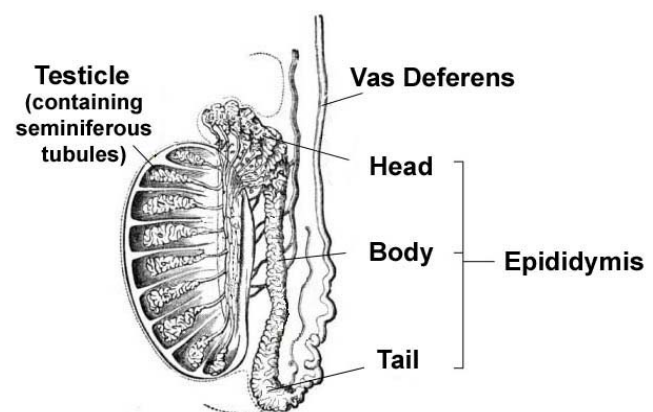


Figure 15. The epididymis is a coiled, microscopic tubule that carries sperm from the testicle into the vas deferens. This 20-foot long tubule is coiled up into the length of about one inch and is very fragile.

Adapted from: www.drpadron.com

structures, a fibrous stroma and surrounding pseudo-capsule of dense collagenous tissue [76].

The probable origin of these lesions is from epididymal duct epithelium that arises from the embryonic mesonephric duct (NB. *Mesonephric duct* is an embryological term given to a pair of long ducts — and a smaller set of tubules attached to each duct — that will, by the time we are born, form important parts of the reproductive system in both males and females) [77]. The lesions are generally asymptomatic and detected by manual examination or ultrasound (fig.16). Infertility, presumably due to obstructive azoospermia¹⁶ has been reported and atrophy of the seminiferous tubules of the testicle may be seen [29, 78]. Because these lesions are benign and typically symptomless, they are managed conservatively and treatment is reserved for the rare occurrence of symptoms. Ultrasonography can be used to monitor their growth over time.

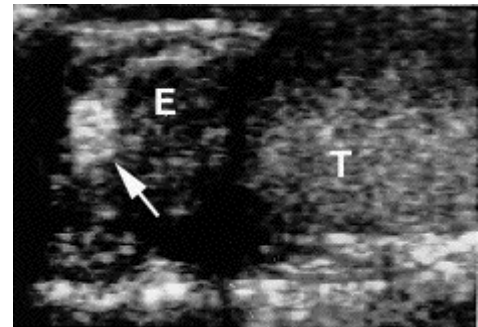


Figure 16. Ultrasonography of papillary cystadenoma of the epididymis. This lesion was palpable as a firm mass in the globus of the epididymis (arrow). E is the epididymal mass, T is the testicle.
Adapted from Choyke et al [4]

1.4.5 Adnexal papillary tumour of probable mesonephric origin (APMO)

Papillary cystadenomas in the broad ligament have rarely been reported and are unrecognised in many women with VHL disease. These lesions are regarded as the female counterpart of the cystadenoma of the epididymis. The papillary cystadenoma of mesonephric origin is commonly called the "broad ligament cyst" because most of them form in remnant mesonephric duct tissue

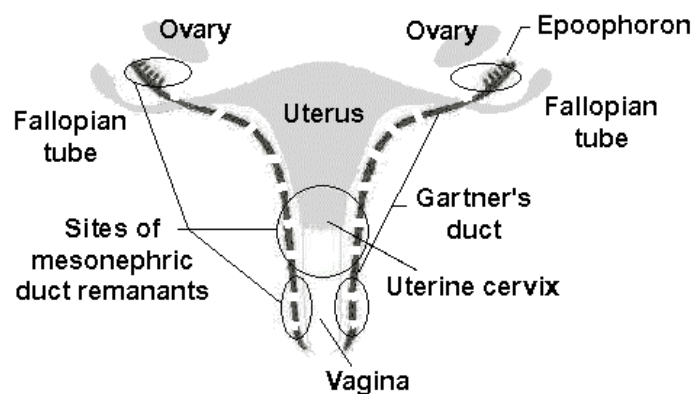


Figure 17. Sites of Mesonephric Duct Remnants in Females. It is in tissue associated with these parts of the old mesonephric duct that APMOs can be found.

that happens to be embedded in the broad ligament. However the cystadenomas that are important in VHL are not all in the broad ligament (some are below it), and they are cystadenomas, not cysts. The broad ligament is a large area of tissue that lies on top of the reproductive organs. The broad ligament lies in folds and creases on top of both ovaries and uterine tubes, connecting these structures to the larger body of the uterus. Some papillary cystadenoma of mesonephric duct origin that can help in diagnosing VHL will be found attached to adnexal (adjoining) tissue that is not part of the broad ligament.

¹⁶ Azoospermia refers to absence of spermatozoa from the seminal fluid

Gaffey *et al.* coined the more appropriate name *adnexal papillary cystadenoma of probable mesonephric origin* (APMO) [79].

Papillary cystadenoma in men are found throughout this duct system. In women, the mesonephric duct system is a remnant system. Although it is made up of the same set of tubules and ducts that are found in men, only short segments of the embryonic system, called "remnants", remain by the time a female is born. None of these segments performs any function. It is in tissue associated with these parts of the old mesonephric duct that APMOs can be found.

In 1997, a comprehensive study of the literature showed that all cases with AMPO described thus far arose in VHL patients [79]. This association indicates that the AMPO may represent a pathognomonic visceral manifestation of VHL disease. These lesions can be diagnosed by CT-imaging or ultrasonography. The tumours are grossly similar to epididymal cystadenomas. Because they are benign and typically asymptomatic, they can be managed conservatively. Treatment is reserved for the rare occurrences of symptoms and CT or ultrasonography can be used to document their size over time.

Concluding Remarks

von Hippel-Lindau disease is a hereditary cancer syndrome predisposing carriers to the development of a wide spectrum of highly vascularised tumours present in both the CNS and visceral organs. The disease is the foremost cause of inherited renal cell carcinomas (RCC), which is induced by germline mutations of the VHL tumour-suppressor gene also inactivated in most sporadic RCC. VHL disease is a potentially life-threatening disorder, however, most of the associated tumours are accessible to effective medical management on condition of an early diagnosis and the multidisciplinary concerted actions of the medical profession. Identification of the VHL gene and genotype-phenotype correlations might allow predictions of the risk of developing particular tumour types, so that personalised screening protocols can be designed for each patient once the mutation is known. A close surveillance of patients and gene carriers is imperative in order to detect manifestations early and to avoid complications. The concerted co-ordinated effort of various medical disciplines is indispensable for optimal management of patients and national medical VHL networks have been established in many countries [21, 43]. Regular surveillance includes periodic CNS gadolinium enhanced MRI, abdominal MRI, CT scan or ultrasound, urinary metanephrines measurement and ophthalmoscopy, both for early diagnosis and follow-up of different manifestations. Periodicity depends on age, number and type of manifestations in each patient.

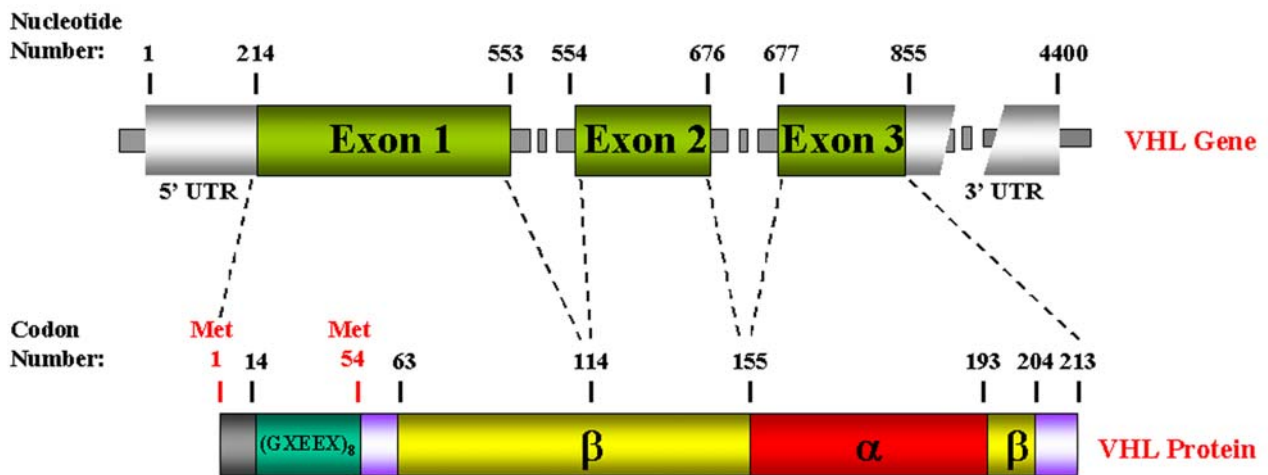


Figure 18. VHL gene structure and protein domains. The VHL protein product is encoded by three exons located on chromosome 3p25-p26. The protein product encodes a 213 amino acid poly-peptide. Internal initiation of translation at methionine 54 gives rise to a second protein product of 160 amino acids. The N-terminal region is characterised by eight acidic pentameric repeats. pVHL can be divided structurally into an α and a β domain.

2.4 Promoter Analysis

Despite the importance of VHL in oncogenesis and development, little is known about the regulation of VHL expression. To date, only three studies exist regarding the VHL promoter. Kuzmin *et al.* mapped a minimal VHL promoter by deletion analysis, but putative transcription factor binding sites were not investigated [82].

Table 6. *In silico* identification of candidate transcription factor binding sites

Conserved Region	Putative Transcription Factor
1	GATA2, GATA3, NF-1, Barbie Box
2	cRel, Nfkappa
3	Sp1 , Egr, AhR/Ar, GATA2, AP2, AP4
4	cRel, Nfkappa, Sp1 , MZF1, AP2

The VHL gene promoter has been subsequently sequenced (Genbank Accession No. AF010238). In 1999 evidence was reported for E2F1 activation of the VHL promoter, although an E2F1 binding site was not identified [83]. Finally in 2002, Zatyka *et al.* attempted to identify, *in silico*, candidate regulatory regions by defining regions of evolutionary conservation, and then proceeded to investigate these regions and specific putative transcription factor binding sites by electro-mobility shift (EMSA) and promoter activity assays (Fig.19). This latest study led to the identification of 4 regions of conservation between human, primate, and rodent sequences [84]. Sequence conservation over 100 million years of evolution suggests that these regions are of functional significance.

Analysis of specific putative transcription factor binding sites (outlined in table 6 above and figure 19 below) identified a functional Sp1 site at nucleotide position +1 to +11, which was shown to be a regulatory element. Overlapping Sp1/AP2 sites located at nucleotide position +72 to +87 were also identified. A further positive regulatory element

between nucleotide position –49 and –19 was identified. This region was specifically shown to bind as yet unidentified factors which were confirmed not to be E2F1. Upstream of the VHL minimal promoter another region, -114 to –91, was identified as being capable of binding yet another unknown factor. Although a second best candidate E2F1 site spans this region, this unknown factor was confirmed again not to be E2F1. Zaytka *et al.* refer to these unknown factors as VHL-TF1, -TF2, and –TF3, and further studies are required to characterise their identity.

actttataag cgtgatgatt ggggtgtccc gtgtgagatg cccaccctc gaaccttggt -560
aggacgtcgg cacattgctg gtctgacatg aagaaaaaaaa aattcagtta gtcca**ccagg** -500

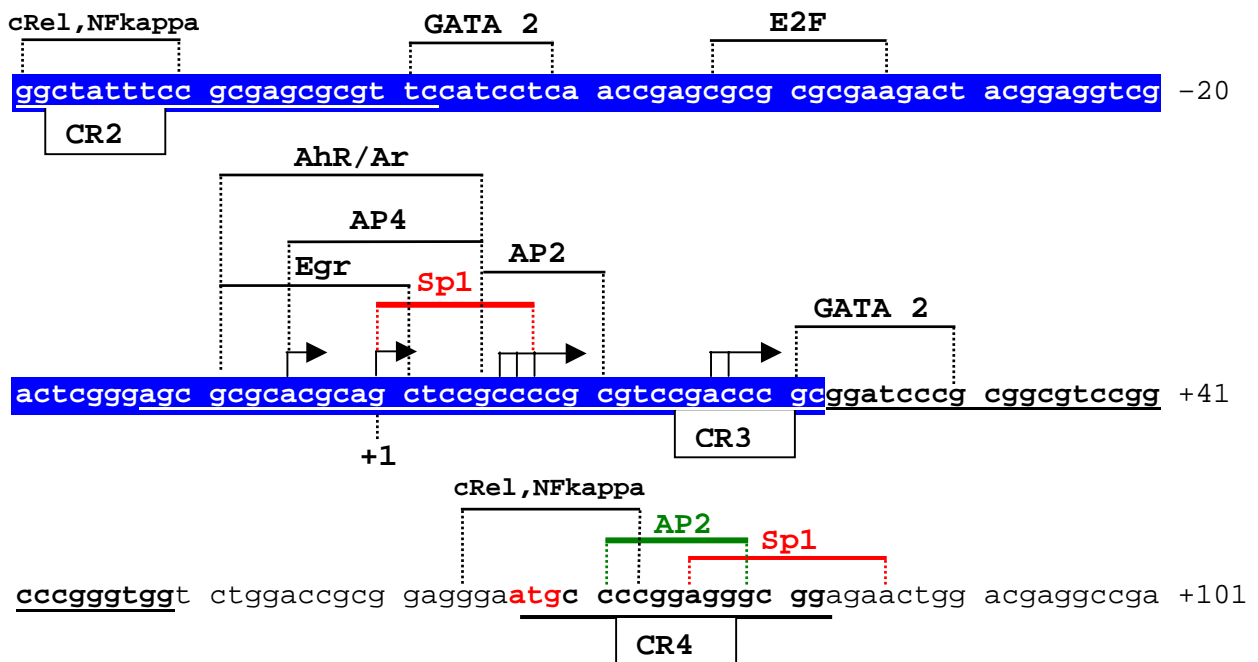
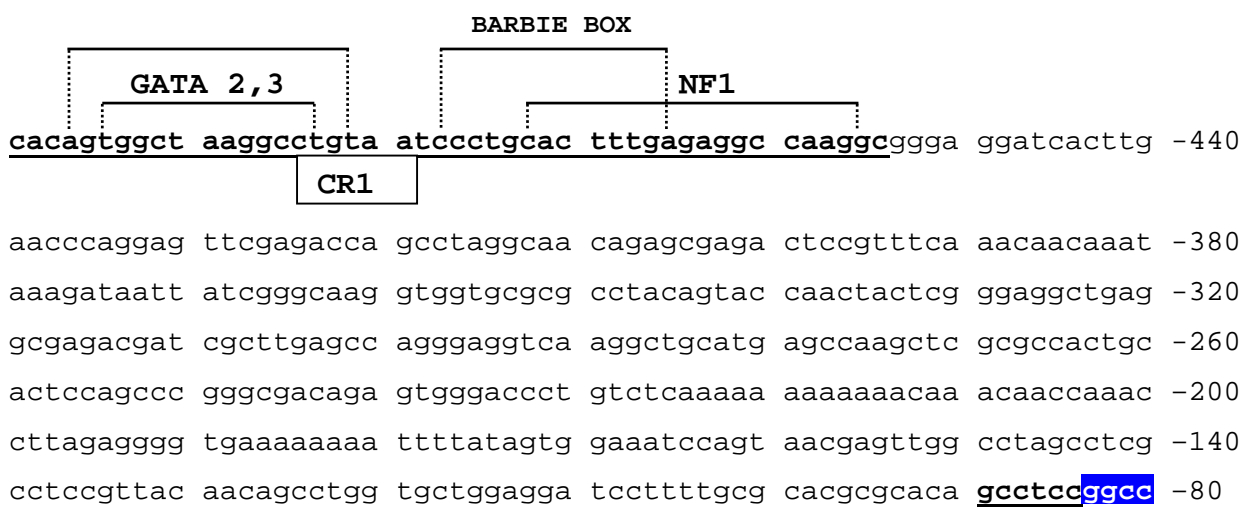


Figure 19. VHL promoter sequence. Underlined and in bold, CR1-CR4, the regions of conservation between human and rat as defined by Zatyka *et al.* 2002. Promoter sequences are the *in silico* predicted putative binding sites for transcription factors. The candidate sites are only shown in regions of conservation. Studies have shown a functional Sp1 site and overlapping Sp1/AP2 sites. Other factors remain unidentified.

Sp1 is a zinc finger transcription factor which binds to GC rich sequences known as 'GC' boxes, which have been identified in 5' regions of many genes [85]. Sp1 sites are reported often to regulate initiation of transcription in TATA-less promoters (the VHL promoter is TATA-less). Although generally considered to be ubiquitous, Sp1 has also been implicated in regulation of tissue specific gene expression [86-88]. It was reported that Sp1 is a critical regulator of the Wilms tumour suppressor gene, WT1, and that Sp1 expression is temporally and spatially regulated during nephrogenesis [89]. Thus Sp1 has been implicated in renal development. As VHL mRNA foetal expression patterns are consistent with a role in nephrogenesis, Zatyka *et al.* speculate that Sp1, WT1, and VHL may have interrelated roles in nephrogenesis [90].

2.5 3' untranslated region of the VHL gene

The 3' untranslated region (3'UTR) of the human *VHL* was isolated by *Renbaum et al.* in 1996 [91]. Several putative non-canonical (ATTTAA) poly(A) signals were identified, and the functional significance of these signals was examined. Use of VHL transgene deletion mutants indicated that an ATTTAA sequence located between nucleotide +4237 and +4379 most likely serves as an active poly(A) signal in renal carcinoma cells, yielding a 3.6-kb 3'UTR. Sequence analysis revealed a 300- to 600-bp region conserved in human, murine, and rat VHL UTRs. In addition, the human 3'UTR was extremely rich in *Alu* repetitive elements.

Interspersed repetitive sequences have traditionally been dismissed as non-functional, however, more evidence is accumulating that suggests that these sequences can play a role in gene expression and neoplastic transformation [92]. *Alu* repeat sequences are estimated to account for 5% of human genomic DNA, and are found in 5% of fully spliced cDNAs, usually in the 3'UTR [93]. The region of the VHL gene that includes the 3'UTR contains 11 *Alu* repeat elements in a 4.5-kb DNA segment. Interestingly, the Wilms' tumour gene was found to be regulated by a 460-bp transcriptional silencer that contains a full-length *Alu* repeat and an *Alu*-mediated recombination event has been implicated in a founding mutation in the MLH1¹⁷ gene of hereditary colon cancer. At present no evidence exists that suggests a VHL-related functional role for these repeats. However, the high concentration of *Alu* sequences identified in this region (1 per 400-bp) may indicate a mechanism for different types of deletions, duplication, and inversions based on *Alu*-mediated recombination, both in germ-line and somatic tissue.

¹⁷ MLH1 - Human Mut L Homologue (MLH1) is homologous to the bacterial DNA mismatch repair Mut L gene. Mutations in the hMLH1 gene are associated with hereditary non-polyposis colon cancer and various other cancers.

2.6 VHL Expression

2.6.1 Expression pattern of VHL mRNA

Latif et al. identified the VHL gene and showed Northern blot analysis of VHL gene expression in foetal and adult kidney and brain as well as in adult adrenal and prostate [81]. However the first comprehensive study addressing expression of the von Hippel-Lindau tumour suppressor gene was undertaken by *Kessler et al.* and published in 1995 [94]. Here the author's investigated expression of the VHL gene in human foetal kidney, and during mouse embryogenesis using *in situ* hybridisation with ³⁵S-labelled anti-sense VHL probes derived from human and mouse cDNAs on cryosections of human foetal kidney and paraffin sections of murine embryos. The results concluded that in human foetal kidney, the enhanced epithelial expression of the VHL gene is consistent with the role of this gene in renal cell carcinoma. Furthermore, the report showed widespread expression of the VHL gene during embryogenesis. An interesting observation apparent from the *in situ* investigation was the differential developmental VHL expression within epithelial cells derived from mesoderm (kidney and epididymis), endoderm (lung and pancreas), and ectoderm (eye). In addition, the localisation of VHL expression in human and mouse nephrogenesis was consistent with the histo-pathologic studies of the origin of the clear cell phenotype of renal cell carcinoma and their associated VHL mutations [95]. To complement this work,

Table 7. Summary of VHL mRNA expression during human embryogenesis

Germ Layer	Tissue	VHL Expression
Endoderm	Gut	-
	Pancreas	-
	Lung	++
	Pharyngeal pouches	-
Ectoderm	Dorsal root ganglia	+
	Periderm	(+)
	Brain	++
	Cranial ganglia (V, VII, VIII)	+++
	Vestibular apparatus	+++
	Eye	+
	Cephalic mesenchyme	+
Mesoderm	Heart	(+)
	Indifferent gonad	++++
	Mesonephric duct	++
	Paramesonephric duct	++
	Bowman's capsule	+
	Loop of Henle	++++
	Nephrogenic cord	+
	Metanephric collecting ducts	++
	Proximal convoluted tubule	++
	Perichondrium	(+)
	Liver (haematopoietic tissue)	+
	Adrenal	(+)
	Striated muscle	+

Adapted from Richards et al. 1996

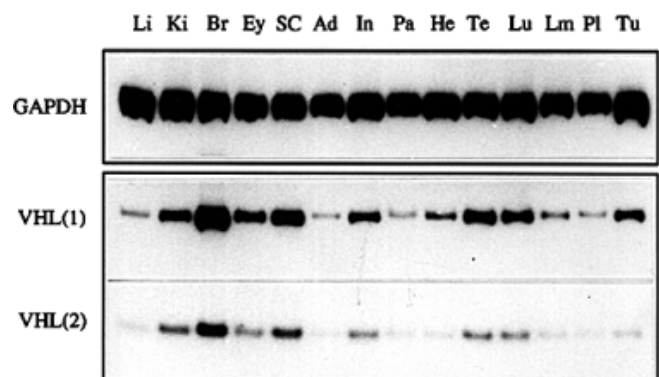


Figure 20. Quantitative RT-PCR of GAPDH and VHL mRNA in 8-10 week human foetal tissues. VHL(1) = wt-VHL; VHL(2) = Δ Exon2 VHL; Li=liver; Ki=kidney; Br=brain; Ey=eye; SC=spinal cord; Ad=adrenal; In=intestine; Pa=pancreas; He=heart; Te=testis; Lu=lung; Lm=limbs; Pl=placenta; Tu=adult proximal renal tubule cell culture.

Adapted from Richards et al. 1996

Richards et al. investigated the expression of *VHL* mRNA during human embryogenesis again by *in situ* hybridisation studies at 4, 6 and 10 weeks post conception. Although *VHL* mRNA was expressed in all three germ layers, they noted strong expression in the central nervous system, kidneys, testis and lung. Within the kidney, *VHL* mRNA was differentially expressed within renal tubules, and the authors reiterated the previous findings by suggesting that the *VHL* gene product may have a specific role in kidney development.

Moreover, two alternatively spliced *VHL* mRNAs characterised by inclusion (isoform I) or exclusion (isoform II) of exon 2 were transcribed in adult tissues. To investigate if the two isoforms were differentially expressed during embryogenesis, *VHL* mRNA was reverse transcribed from 13 foetal tissues (8-10 weeks gestation). The quantitative distribution of *VHL* mRNA within foetal tissues reflected that seen by *in situ* hybridisation and the ratio of the two *VHL* isoforms was similar between tissues (Fig.20).

2.6.2 Expression pattern of pVHL

Los et al. [96] first addressed expression of VHL protein in human tissues in 1996. The VHL protein was widely expressed in normal human tissue. The authors recorded a cellular distribution of the protein that was confined to the cytoplasm of specific cell types. Immuno-histochemistry did not facilitate the discrimination of tumours obtained from VHL patients or tumours unrelated to the VHL disease. Renal cell carcinomas, haemangioblastomas, and pheochromocytomas, either VHL-related or sporadic, demonstrated positive staining for the VHL protein, which suggests that the antibody used recognised mutated VHL protein. However, no consideration was given to alternative pVHL species, e.g. pVHL₁₉. The antibodies used were unexplained, the epitopes not described, and no proof of specificity in terms of western blot analysis or immuno-precipitation of endogenous pVHL was demonstrated. Without such pertinent data, drawing conclusions is difficult.

A year later, *Corless et al.* re-addressed the issue of pVHL expression in normal and neoplastic tissues [3]. At this time, epitope-tagged pVHL had been observed in either the nucleus or the cytoplasm of cultured cells, depending on the density of the cell culture [97-99]. In this article, the cellular localisation of pVHL in normal and neoplastic human tissues was documented using three different monoclonal antibodies, one being a commercially available antibody widely used and characterised, Ig32. This monoclonal antibody recognises both pVHL₃₀ and pVHL₁₉. The other two antibodies had epitopes mapped to a region of amino acids 72-120, hence total pVHL was being detected. Strong expression of pVHL was observed in the epithelial cells of all organs examined, particularly in renal tubules, and was exclusively cytoplasmic. Lesser degrees of staining, also cytoplasmic, were observed in other cell types.

Table 8. Summary of normal human tissues positive for pVHL immunostaining			
Epithelial Cells	Muscle Cells	Lymphoid Cells	Other
Renal tubule Renal glomerulus Colon Ileum Endometrium Bladder Prostate Thyroid follicle Bile duct	Uterine smooth muscle Intestinal smooth muscle Vascular smooth muscle Skeletal muscle	Lymphocytes	Endothelial cells Sertoli cells Leydig cells Spermatogonia / spermatocytes Peripheral nerve and ganglion cells Adrenal cortical cells

Adaped from Corless et al. 1997

A variety of carcinomas (lung, prostate, colon, breast, bladder, and thyroid) showed strong cytoplasmic staining for pVHL including four of five sporadic clear cell RCC. Of the non-epithelial neoplasms examined, only one tumour, an embryonal rhabdomyosarcoma¹⁸, failed to stain for pVHL. The findings established widespread expression of VHL at the protein level and the authors state that it provided strong evidence that most, if not all, pVHL is localised to the cytoplasm of cells *in vivo*. We now know that this is in fact not the case, and pVHL can be both nuclear and cytoplasmic (see results).

Table 9. Summary of human tumours positive for pVHL immunostaining			
Renal Tumours	Other Tumours	Other Carcinomas	Germ Cell Tumours
Clear cell carcinoma Papillary carcinoma Wilms' tumour	Phaeochromocytoma Malignant mesothelioma (pleural) Islet cell tumour Epithelioid haemangioendothelioma Leiomyoma, uterus Sex cord stromal tumour (ovary) Thymoma	Squamous cell carcinoma (lung, oral cavity) Small cell carcinoma (lung) Adenocarcinoma (lung) Adenocarcinoma (prostate) Transitional cell carcinoma (bladder) Cholangiocarcinoma (liver) Ductal carcinoma (breast) Papillary thyroid carcinoma	Seminoma (testis) Teratoma (testis) Embryonal carcinoma (testis)

Adaped from Corless et al. 1997

From these studies we can conclude that the areas of highest expression do not completely correlate with the tissues that are involved in VHL disease. The tissue specificity of VHL disease therefore cannot be entirely explained by tissue-specific expression during either foetal development or adulthood. However, the antibodies used would not distinguish between the different sized pVHL's generated by alternative translation initiation sites. It is interesting to note that subsequent studies like those mentioned have documented VHL mRNA in a wide variety of tissues in a pattern similar to the generalised expression of other tumour suppressor genes including retinoblastoma and p53 [100, 101].

¹⁸ Rhabdomyosarcome is a malignant tumor composed of striated muscle fibers

2.7 The VHL protein product

Iliopoulos *et al.* demonstrated that the product of the VHL gene is an approximately 30-kD protein [97]. In addition, they showed that the renal cell carcinoma cell line 786-O, which is known to harbour a VHL mutation,

fails to produce a wild-type VHL protein. Reintroduction of wild-type, but not mutant, VHL into these cells had no demonstrable effect on their growth *in vitro* but inhibited their ability to form tumours in nude mice.

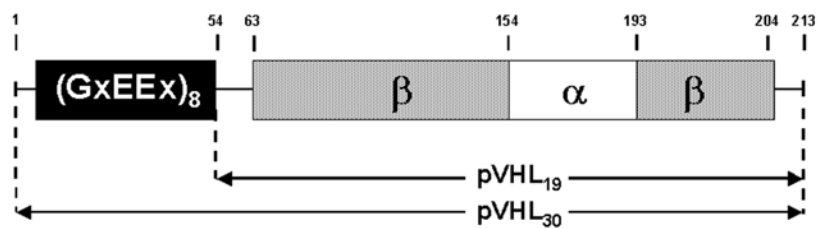


Figure 21. The VHL protein product. pVHL₃₀ has 213 amino acids, and pVHL₁₉ 160 amino acids. pVHL₁₉ results from translation at codon 54. The N-terminal region contains eight copies of an acidic pentameric repeat sequence (GxEEEx). The tertiary structure is divided into an α and a β domain. Both forms of pVHL suppress tumour formation in nude mice experiments.

To understand the mechanisms by which VHL mediates tumour suppression, biochemical analyses of VHL gene products were necessary. However, the translation start site was not evident from the initial cloning of the human VHL gene [81]. The first AUG in the human VHL open reading frame (ORF) was designated as the translation start site, i.e., amino acid 1, on the basis of homology between the mouse, rat, and human VHL sequences, and a product initiated at this start site was detected in cell lines. This site, however, contains a sub-optimal Kozak consensus sequence. A second AUG is present in the VHL ORF at codon 54. This region contains a more conserved Kozak consensus sequence, and thus serves as a second, internal, translation initiation site. The significance of a second translation start site is underscored by the lack of mutations found between the first and second methionine codons of the VHL gene in both sporadic and VHL-associated renal carcinomas. This observation suggested that mutation in this region may not lead to VHL inactivation if translation could be initiated at the second methionine codon, producing a functional VHL protein. Furthermore, both the rat and mouse contain only 19 of the 53 amino acids present in this region in the human VHL ORF. Thus, this 53-amino acid region was thought to make little or no contribution to the biologic activity of VHL protein. However, as will be outlined throughout this thesis, subtle differences in these two protein products are beginning to emerge, most notably in their intra-cellular localisation, the topic of discussion in the following section.

The two distinct native products of the human VHL gene exist with apparent molecular weights of 19- and 30-kDa. These protein products are referred to as pVHL₁₉ and pVHL₃₀ respectively. *Schoenfeld et al.* were the first to report what at the time they termed 18-kDa VHL [102]. They reported the relative abundance of both VHL protein species, and demonstrated that the shorter species was far more abundant in all cell lines tested as compared to its full-length counterpart. Importantly, they also

demonstrated that reintroduction of pVHL₁₉ into renal cell carcinoma cells lacking functional pVHL (786-0) down-regulated vascular endothelial growth factor (VEGF) and glucose transporter 1 (GLUT1), two genes regulated by hypoxia inducible factor (HIF), a transcription factor itself regulated by pVHL (see chapter 4). This result suggested that pVHL₁₉ may exhibit tumour suppressor activity, a suggestion confirmed by reintroducing this species into nude mice which resulted in the suppression of tumour formation. In addition, they demonstrated that pVHL₁₉ bound Elongins B and C, previously established pVHL₃₀ binding partners.

2.8 Intracellular localisation of pVHL

pVHL sub-cellular localisation has been represented somewhat confusingly in the literature. Several reports demonstrated both nuclear and cytoplasmic signals. pVHL has also been mapped to endoplasmic reticulum and mitochondria. Localisation patterns may be effected by changes in the cell cycle, cell density, and mutations in pVHL [98, 99, 103-105]. Localisation studies began in 1995 when Duan *et al.* reported FLAG-tagged pVHL₃₀ over-expressed in COS-7 cells exhibit a nuclear, nuclear/cytoplasmic or cytoplasmic signal in immunofluorescence. A follow up paper by

Lee et al. a year later supported this observation and developed it further by stating that the localisation pattern of rat pVHL is cell density dependent. They observed that in cells that are confluent, pVHL localises uniquely to the nucleus of NRK cells when stably over-expressed, whereas in cells that are sparse, the localisation is rendered cytoplasmic. They also identified a domain that represents a putative bipartite nuclear localisation signal (NLS) they mapped to a region within the first 60 amino acids of human VHL sequence and the first 28 in rat VHL (PR[R/K]...RPRPV). This sequence is in good agreement with known NLS consensus sequences, i.e. hepta-peptide rich in lysine and arginine (fig.22) [105, 106]. However, the functional significance of this NLS remains unclear because no thorough mutational inactivation of this sequence has been analysed. Nonetheless, these data provided the initial indication of a cell density-dependent pathway that could in part be responsible for the regulation of pVHL cellular

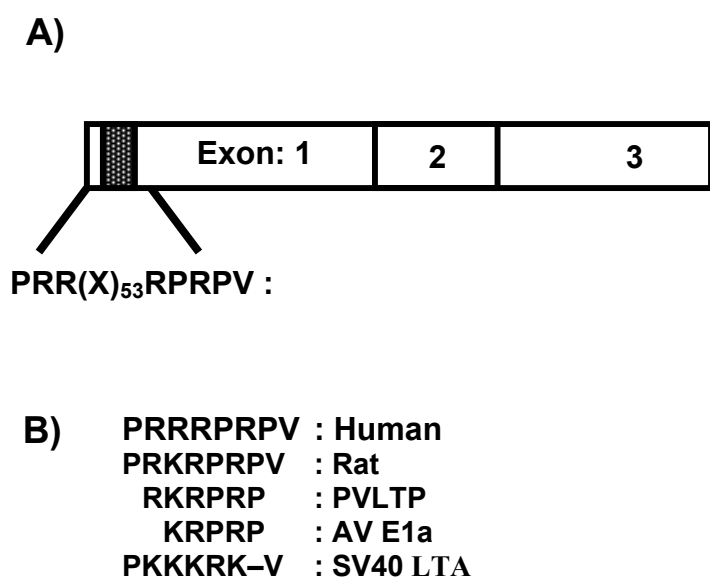


Figure 22. A) Putative bipartite nuclear localization signal in the first 60 amino acids in human VHL. Shaded box represent the acidic N-terminal repeats. B) Comparison of the bipartite NLS of human, rat, polyomavirus large tumour antigen (PVLTP), adenovirus E1a protein (AVE1a), and a simian virus 40 large tumour antigen (SV40 LTA).

Adapted from Lee et al. 1996

localisation. Understanding the molecular signalling generated upon cell contact that culminates in a localisation shift of pVHL is needed.

Studies by Ye *et al.* demonstrated that sub-cellular localisation of pVHL is regulated in a cell cycle dependent manner [103]. They illustrated exclusive VHL nuclear accumulation in cells that are in the G₁/G₀ phase of the cell cycle, whereas the majority of cells in S-phase also showed a diffuse cytoplasmic staining. This study was the first to examine endogenously expressed pVHL. However antibodies used were raised against the N-terminus and C-terminal regions, but no attempts were made to differentiate between pVHL₃₀ and pVHL₁₉. While differences in localisation were observed, they may have reflected changes in one or other species, and not shifts in total pVHL. Subsequent work presented in this thesis shows a strong nuclear localisation with some cytoplasmic staining for pVHL₁₉, while pVHL₃₀ localises predominantly to the cytoplasm of logarithmically growing cells (Fig.23).

Other reports have localised pVHL to cellular organelles including mitochondria and endoplasmic reticulum. Shiao *et al.* demonstrated that immuno-gold electron microscopy localised GFP-tagged pVHL₃₀ to the mitochondrion [104]. VEGF, TGF- β 1 and ubiquitination-associated enzymes have all been localised to the mitochondrion. In addition the mitochondrion plays a key role in glucose and lipid metabolism, and alteration in these processes as a result of abnormal VHL could lead to accumulation of glycogen and lipid in the cytosol, as seen in clear cell renal carcinoma [1]. For these reasons, the authors justify a mitochondrial localisation. Despite the tempting assumption, no endogenous data is shown, and no biochemical evidence is given in support of the above statement. Furthermore, attempts to reproduce similar findings with endogenous pVHL cast doubt on this finding (Barry and Krek; data not shown).

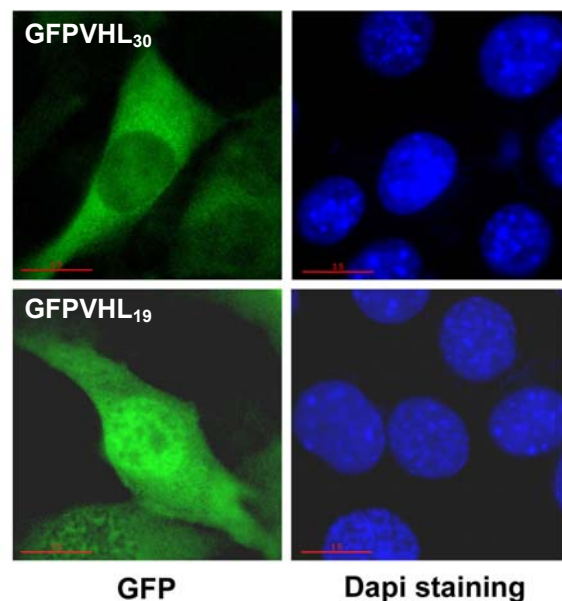


Figure 23. Mouse NIH3T3 fibroblasts stably expressing GFP-VHL₃₀ and GFP-VHL₁₉ following retro-viral transduction. Dapi represents nuclear staining; GFP represents VHL localisation with respect to alternative translation products, pVHL₃₀ and pVHL₁₉.
Adapted from chapter 7, Results.

In 2001, Schoenfeld *et al.* claimed to have mapped a 64 amino acid region in VHL responsible for its association with the endoplasmic reticulum (ER) [105]. They report that native and exogenous VHL products co-localise with markers of the ER in renal cell lines, and that sub-cellular fractionation of both native and exogenously expressed pVHL are found predominantly in the cytosolic compartment. Schoenfeld and colleagues

mapped the region 114-177 as the site necessary for pVHL cytosolic sub-cellular localisation as well as ER association. The authors attempted to reinforce their findings by analysing this region for mutational events. It is true that this region is a region of frequent mutation, and the author's use this to suggest that proper pVHL sub-cellular localisation with respect to the ER may be necessary for pVHL-mediated tumour suppression. This group originally published the finding of a second native pVHL product, pVHL₁₉. Surprisingly there is no mention of differences between the localisation patterns of alternative translation products.

Work published by our laboratory, some of which will be detailed in the results section of this thesis, demonstrates that pVHL₃₀ and pVHL₁₉ show different localisation patterns (fig.22) [107]. Moreover, while pVHL₁₉ is predominantly nuclear, pVHL₃₀ may reside in both the nucleus and cytosol, and when in the cytosol it can associate with the microtubule network. The microtubule-binding domain has been mapped and lies between residues 95-123, a mutational hot spot in VHL disease. The consequence of pVHL binding to microtubules is to stabilise them. Interestingly, mutations associated with type 2C disease fail to stabilise the microtubule array, while mutations associated with other VHL clinical types do. This data has identified a role for pVHL in the regulation of microtubule dynamics, and provides insights into the function of pVHL in the pathogenesis of type 2C malignancies, namely haemangioblastoma and pheochromocytoma.

To summarise, pVHL has been shown to exhibit intra-cellular dynamics by shuttling in and out of the nucleus, for as yet, unexplained reasons. pVHL₃₀ and pVHL₁₉ exhibit different localisation patterns, with pVHL₃₀ residing predominantly in the cytoplasm of logarithmically growing cells, and pVHL₁₉ in the nucleus. pVHL can partially localise to the ER mediated by a region in pVHL corresponding to Δ 114-177. It has also been shown to bind microtubules *in vivo*, and that the region of pVHL responsible for this interaction is Δ 95-123. Evidence exists that pVHL localisation can be affected by stimuli including cell cycle changes, cell density and stress signalling including serum deprivation, hypoxia, UV radiation and microtubule destabilising drug treatment.

2.9 Structure of VHL

Biochemical studies revealed that VHL forms a ternary complex with the Elongin C and Elongin B proteins [98, 108]. The VHL-Elongin C-Elongin B complex (henceforth VCB complex) has a central role in VHL function because most of the tumour-derived mutations destabilise this complex [98, 108, 109]. Furthermore, peptide mapping studies showed that a 12-amino acid region of VHL that contains nearly a quarter of the tumour-derived mutations makes key interactions with Elongin C [109], tightly linking the Elongin C binding and tumour suppression functions of VHL. The following section outlines the biochemical structural analysis of a pVHL–Elongin C and pVHL-HIF1 α interaction.

2.9.1 Structural analysis of Elongin C- pVHL interaction

Stebbins et al. first solved the crystal structure of pVHL in 1999. They showed that VHL has two domains: a roughly 100-residue NH₂-terminal domain rich in β sheet (β domain) and a smaller α -helical domain (α -domain), held together by two linkers and a polar interface (Fig.24). A large portion of the α -domain surface, and a small portion of the β domain, interacts with Elongin C. About half of the tumorigenic mutations map to the α domain and its residues that contact Elongin C [2]. The remaining mutations map to the β domain, and significantly, the author's noted to a β domain surface patch uninvolved in Elongin C binding. This suggested that two macromolecular binding sites might be required for the tumour suppressor effects of VHL. At this time HIF had not yet been identified as a VHL binding protein.

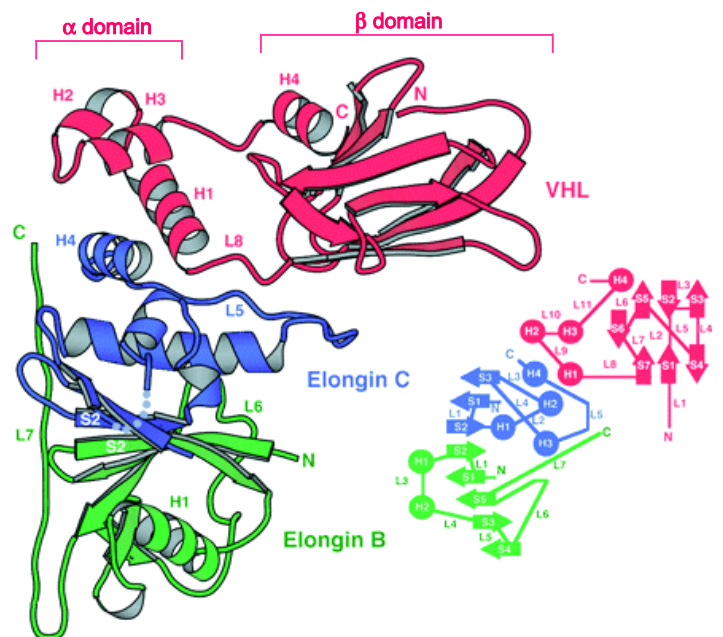


Figure 24. The VCB ternary complex. On the left is a ribbon diagram illustrating the secondary structure of the VCB complex. On the right is a topology diagram in which circles indicate helices and wide arrows indicate strands. C, COOH-terminus; N, NH₂-terminus.

Adapted from Stebbins et al. 1999

The β domain of VHL consists of a seven-stranded β sandwich (residues 63 to 154) and an α helix (H4; residues 193 to 204) that packs against one of the β sheets through hydrophobic interactions (Figs. 24 and 25). The α domain of VHL (residues 155 to 192) consists of three α helices (H1, H2, and H3). A helix from ElonginC (H4) completes the four-helix cluster arrangement, giving two pairs of helices packing at a perpendicular angle (Fig.24). The α and β domains are connected by two short

polypeptide linkers (residues 154 to 156 and 189 to 194) and by a polar interface that is stabilised by hydrogen-bond networks from the H1 helix, the β sandwich, and Elongin C. Several of the residues at the inter-domain interface have been found mutated in tumours.

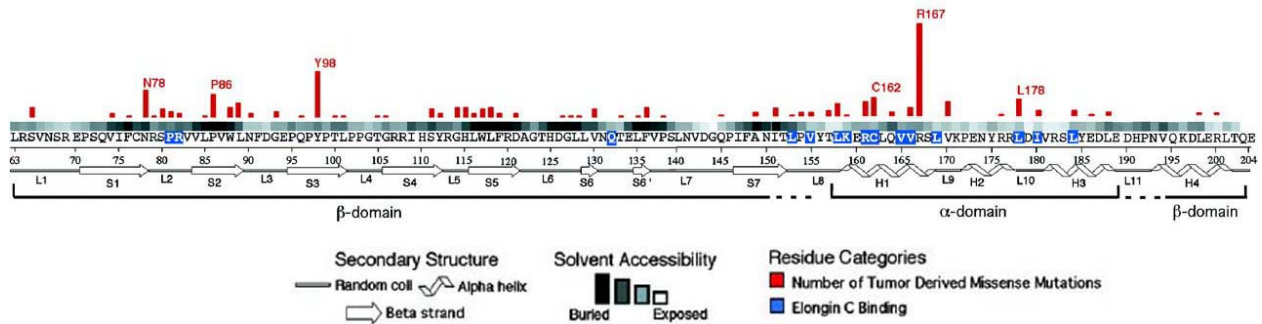


Figure 25. Sequence of VHL demonstrating that tumour-derived missense mutations are divided between the α and β domains of VHL, whereas residues contacting ElonginC cluster in the α domain. The histogram represents 279 mis-sense mutations in the database (Beraud *et al.* 1998). The six most frequently mutated amino acids are labelled. Shaded squares above each residue describe the relative solvent exposure of a residue in a hypothetical VHL monomer. Blue boxes indicate residues that make hydrogen bonds or van der Waals contacts with Elongin C.

Adapted from Stebbins et al. 1999

The H1 helix of the VHL α domain coincides with the 12-amino acid segment shown to be important for Elongin C binding, and the structure reveals that it makes extensive contacts to Elongin C. The most significant van der Waals contacts are made by Leu¹⁵⁸, which protrudes from the H1 helix and fits into an Elongin C pocket, and by Cys¹⁶² and Arg¹⁶¹ (Fig.26). These are augmented by contacts from the Lys¹⁵⁹, Val¹⁶⁵, Val¹⁶⁶, and Leu¹⁶⁹ side chains of VHL. The other two helices of the α -domain also contribute contacts (Leu¹⁷⁸, Ile¹⁸⁰, and Leu¹⁸⁴), with Leu¹⁸⁴ making the most extensive ones in this region. Additional contacts are made by residues in the first α - β linker (Leu¹⁵³ and Val¹⁵⁵) and by Arg⁸² from the β domain. The hydrogen bonds made by Arg⁸², together with those made by Lys¹⁵⁹ and Arg¹⁶¹ from the H1 helix, represent the few significant hydrogen-bond contacts made at the VHL-Elongin C interface. The arginine side chains are also anchored in the hydrogen-bond networks of the VHL α - β domain interface.

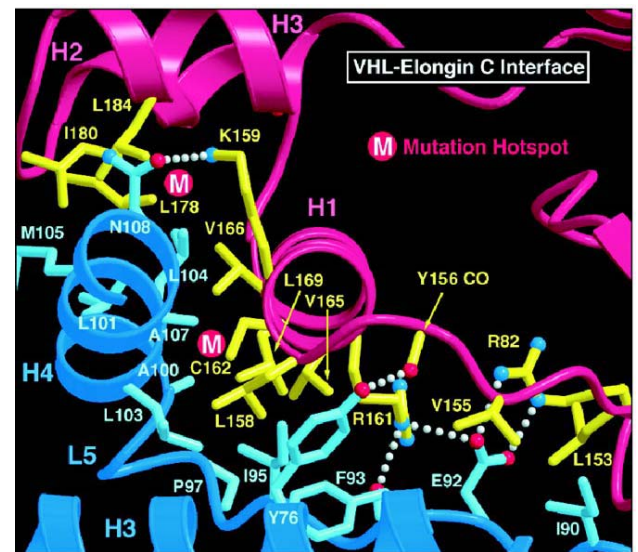


Figure 26. The VHL-Elongin C interface consists of an intermolecular hydrophobic four-helix cluster augmented by additional contacts. VHL and Elongin C secondary structural elements are shown in red and blue, respectively. VHL amino acids are in yellow and those of Elongin C are in cyan. Hydrogen bonds are indicated by white dashed lines. Red atoms indicate oxygen and blue, nitrogen. A red circle with the letter "M" indicates a residue that is one of the six most frequently mutated in cancer. The Elongin C pocket where the VHL Leu¹⁵⁸ binds is made up of Tyr⁷⁶, Phe⁹³, Leu¹⁰³, and Ala¹⁰⁷, and Cys¹¹².

Adapted from Stebbins et al. 1999

In addition the 40-amino acid SOCS (suppressor of cytokine signalling) -box sequence motif was shown to bind Elongin C and to contain sequence homology with the H1 helix of VHL. When the sequence of the SOCS1 SOCS box was compared to a library of 1,925 structures, the VHL α -domain ranked first [110, 111]. In this alignment, the pattern of hydrophobic residues in SOCS-1 and the SOCS-box consensus matches that of the entire VHL α -domain (Fig.27). These findings, in conjunction with the reported SOCS box-Elongin C binding data [110], indicate that the SOCS box and VHL α -domain represent a common structural and functional motif. Growing evidence suggests that the SOCS box, similar to the F-box of the SCF (Skp1-Cul1-F-box protein) complex, acts as a bridge between specific substrate-binding domains and the more generic proteins comprise a large family of E3 ubiquitin protein ligases [112]. As discussed again in chapter 4, this sequence and structural homology helped unveil the first known function of pVHL as a component of an E3 ubiquitin ligase complex.

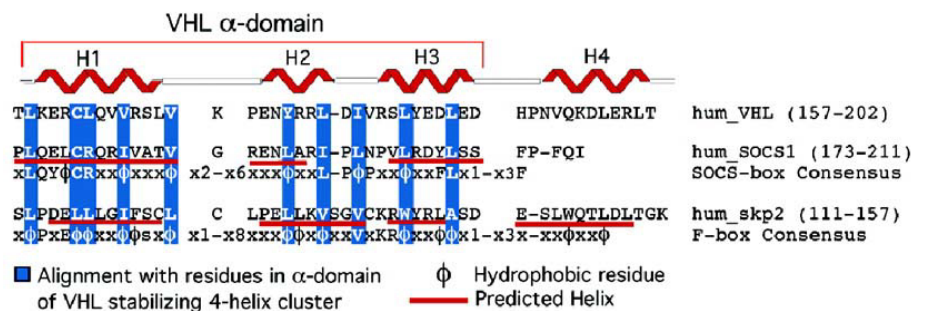


Figure 27. Alignment of the VHL α -domain, the SOCS1 and SOCS-box consensus, and the Skp2 and F-box consensus sequence. The VHL secondary structure is shown above the alignment and the α -domain is indicated. Residues that stabilise the four-helix cluster are indicated in blue. Regions predicted to be α -helical are underlined in red.
 Adapted from Stebbins *et al* 1999

2.9.2 Structural analysis of HIF1 α - pVHL interaction

The proposed model by Stebbins *et al.* that residues located within the β domain, a domain to which many mutations have been attributed, is an alternative macromolecular binding site required for tumour suppressor effects by VHL was confirmed structurally in a follow up paper by the Pavletich group in 2002 [113]. In this paper, Min *et al.* demonstrated that pVHL binds Hypoxia Inducible factor-1 α (HIF-1 α), and that this interaction is dependent on a modification involving molecular oxygen which results in the hydroxylation of a conserved Proline residue at position 564 within the HIF1 α sequence [113, 114]. The consequence of this interaction is targeting of HIF-1 α for ubiquitin-mediated proteasomal degradation [114]. It is now also appreciated that a second proline hydroxylation event occurs at Pro-402 of HIF-1 α . These sites contain a conserved LxxLAP motif and are targeted by a newly defined prolyl hydroxylase activity that in mammalian cells is provided by three isoforms termed PHD (prolyl hydroxylase domain) 1–3 (see chapter 4).

The structure illustrated in figure 28 shows that a 15-amino acid portion of HIF-1 α (residues 561 to 575) adopts an extended, β strand-like conformation. It binds pVHL in a bipartite manner, with two discontinuous HIF-1 α segments interacting with a continuous

site on pVHL. A six-residue N-terminal segment (residues 561 to 566) that is centred on Hyp⁵⁶⁴ (Hyp is the three-letter code for hydroxyproline), and a four-residue C-terminal segment (residues 571 to 574) are separated by a four-amino acid bulge that does not contact pVHL (Fig.28.B). HIF-1 α interacts exclusively with the β domain of pVHL. It binds alongside the β sandwich, making five backbone-backbone hydrogen bonds. The side of the pVHL β sandwich where HIF-1 α binds has the hydrophobic core partially exposed. This exposed hydrophobic patch, together with several partially buried polar residues, makes up the binding site of the hydroxyproline. The hydroxyproline has a central role in complex formation. It is nearly entirely buried, with 96% of its accessible surface area in a hypothetical free peptide covered by pVHL. The pyrrolidine ring inserts toward the partially exposed hydrophobic core of the pVHL β domain, making multiple van der Waals contacts with Trp⁸⁸, Tyr⁹⁸, and Trp¹¹⁷ of pVHL (Fig.29). The 4-hydroxyl group inserts farthest into pVHL and forms hydrogen bonds with the N δ of His¹¹⁵ and the OH group of Ser¹¹¹, both of which also form hydrogen bonds with other pVHL groups. The pVHL residues that interact with Hyp⁵⁶⁴ are highly conserved in the human, mouse, frog, fly, and worm pVHL orthologues (Fig.28.B). Trp⁸⁸, Tyr⁹⁸, His¹¹⁵, and Trp¹¹⁷ are among the 11 β domain residues that are invariant in the five orthologues, and Ser¹¹¹ is replaced with a threonine in the frog, fly, and worm. Mutations of Tyr⁹⁸, Ser¹¹¹, and Trp¹¹⁷ of pVHL have been shown to abolish HIF1 α binding [115]. Compared with Hyp⁵⁶⁴, the other N-segment residues make significantly fewer contacts. Among them, Ile⁵⁶⁶ makes the most contacts,

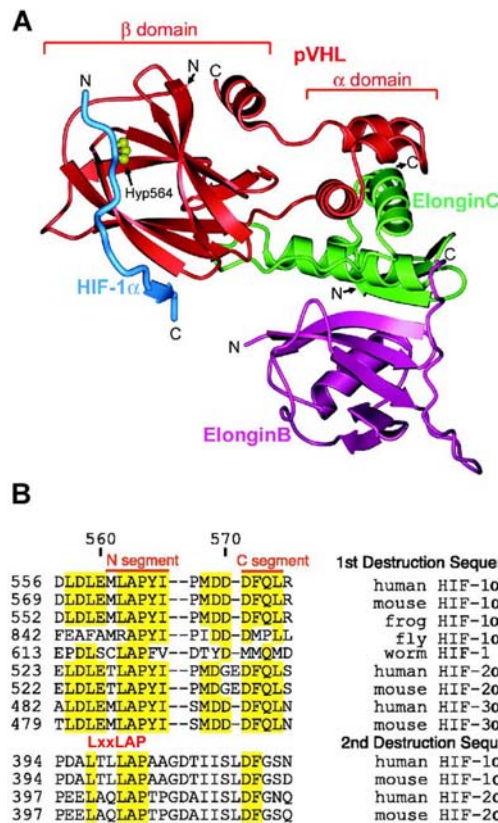


Figure 28. The HIF1 α destruction sequence binds the β domain of pVHL. (A) Schematic representation of the 15-residue portion of the HIF-1 α destruction sequence bound to the β domain of pVHL in the pVHL-ElonginB-ElonginC complex. HIF1 α is in blue, Hyp⁵⁶⁴ in yellow, pVHL in red, ElonginB in magenta, and ElonginC in green. (B) Alignment of the first destruction sequence (containing Hyp⁵⁶⁴) in the ODDs of HIF1 α orthologues and HIF2 α and HIF3 α paralogues, highlighting residues identical in seven of the nine sequences. The putative N and C segments of the second destruction sequence (containing Hyp⁴⁰²) of HIF1 α and HIF2 α orthologues are aligned below. The reported second destruction sequence is 38 residues long, and only a 23-residue region containing the conserved LxxLAP motif that aligns with the first destruction sequence is shown.

Adapted from Min et al. 2002

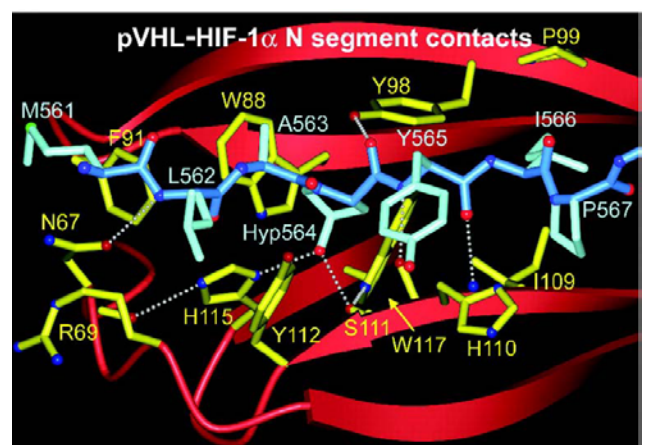


Figure 29. The contacts made by the N segment, and in particular by Hyp⁵⁶⁴, are central to the binding of HIF1 α to pVHL. The side chains of HIF1 α and pVHL are coloured in light blue and yellow, respectively. The backbones of HIF1 α and pVHL are in medium blue and red, respectively. The dotted lines indicate hydrogen bonds between the Gln⁶⁷ O δ 1, Tyr⁹⁸ O η , His¹¹⁰ NH₂, and His¹¹⁰ CO groups of pVHL, and the Leu⁵⁶² NH, Hyp⁵⁶⁴ CO, Tyr⁵⁶⁵ NH, and Tyr⁵⁶⁵ CO groups of HIF1 α .

Adapted Min et al.2002

interacting with Pro⁹⁹ and Ile¹⁰⁹ of pVHL. Met⁵⁶¹ packs with Phe⁹¹ of pVHL, Leu⁵⁶² with Tyr¹¹² and Arg⁶⁹, Ala⁵⁶³ with Trp⁸⁸, and Tyr⁵⁶⁵ with His¹¹⁰ (Fig.29). These side-chain contacts occur on the surface of the complex, however, and are unlikely to make a major contribution to specificity and affinity compared with Hyp⁵⁶⁴.

A second, independent destruction sequence containing Hyp⁴⁰² within the HIF-1 α ODD interacts with pVHL in a similar mode assuming seven instead of four residues in the bulge between its putative hydroxyproline-containing N-segment- and C-segment-like sequences (Fig.28.B) [7]. This awaits further structural determination.

2.10 Sequence Homology

Comparative genome analysis can provide novel insights into gene evolution and function. The VHL gene is highly conserved in primates, rodents, flies and worms [116]. In the fly, *Drosophila Melanogaster*, an overall 50% similarity between fly and human was calculated, and 76% similarity in the elongin C binding site [117, 118]. Figure 30 illustrates the nucleotide sequence alignment of the VHL open reading frame for human, rat and mouse.

H.Sapiens	ATGCCCGGAGGGCGGAGAACTGGGACGAGGCCGAGGTAGGCGCGGAGGAGGCAGGCGTC
R.Norvegicas	ATGCCCGGAAGGC-----AGCTAGTC-CAGAGGAGGCAG-----
M.Musculus	ATGCCCGGAAGGC-----AGCCAGTC-CAGAGGAGGCGG-----
	***** ** ** * * ***** *
H.Sapiens	GAAGAGTACGGCCCTGAAGAAGACGGCGGGGAGGAGTCGGGCGCCGAGGAGTCCGGCCCC
R.Norvegicas	--AAAG-----GATGCCG-----GGCTCT
M.Musculus	--CGGG-----GGAGCCC-----GGTCTT
	* * *** ** *
H.Sapiens	GAAGAGTCCGGCCCGGAGGAACTGGGCGCCGAGGAGGAGATGGAGGCCGGGCGGCCGCGG
R.Norvegicas	GAAGAG-----ATAGAGGCTGGGCGGCCGCGG
M.Musculus	GAGGAG-----ATGGAGGCTGGGCGGCCGCGG
	** *** ** ***** *****
H.Sapiens	CCCGTGCTGCGCTCGGTGAACTCGCGCGAGCCCTCCCAGGTCATCTTCTGCAATCGCAGT
R.Norvegicas	CCGGTTTTACGCTCTGTGAACTCGCGCGAACCCCTCTCAGGTCATCTTCTGCAACCGCAGC
M.Musculus	CCGGTGCTGCGCTCGGTGAACTCGCGCGAGCCCTCTCAGGTCATCTTCTGCAACCGCAGC
	** * * ***** ***** ***** ***** *****
H.Sapiens	CCGCGCGTCGTGCTGCCCGTATGGCTCAACTTCGACGGCGAGCCGAGCCCTACCCAACG
R.Norvegicas	CCGCGCGTCGTGCTGCCTTTGTGGCTCAACTTTGATGGTGAGCCTCAGCCCTACCCGACC

```

M. Musculus      CCGCGCGTCGTGCTGCCTTTGTGGCTCAACTTCGACGGCGAGCCTCAGCCCTACCCGATC
                    ***** * ***** ** ** ***** ***** *
H. Sapiens      CTGCCGCCTGGCACGGGCCGCCGCATCCACAGCTACCGAGGTCACCTTTGGCTCTTCAGA
R. Norvegicus   TTACCACCGGGCACCGGCCGCCGCATCCACAGCTACCGAGGTCACCTTTGGCTCTTCAGG
M. Musculus     TTACCACCGGGCACCGGCCGCCGCATCCACAGCTACCGAGGTCATCTTTGGCTCTTCAGG
                    * ** * ***** ***** ***** *****
H. Sapiens      GATGCAGGGACACACGATGGGCTTCTGGTTAACCAAACTGAATTATTTGTGCCATCTCTC
R. Norvegicus   GATGCGGGGACCCATGATGGACTTCTGGTTAACCAAACGGAAGTGTGGTGTGCCATCCCTC
M. Musculus     GATGCGGGGACCCATGATGGACTTCTGGTTAACCAAACGGAGCTGTTTGTGCCATCCCTC
                    ***** ***** ** ***** ***** ***** ** * ***** ***
H. Sapiens      AATGTTGACGGACAGCCTATTTTTGCCAATATCACACTGCCAGTGTATACTCTGAAAGAG
R. Norvegicus   AATGTTGATGGACAGCCTATTTTTGCCAACATCACATTGCCAGTGTATAACCCTGAAAGAG
M. Musculus     AATGTGCGATGGACAGCCTATTTTTGCCAACATCACATTGCCAGTGTATAACCCTGAAAGAG
                    ***** ** ***** ***** ***** ***** *****
H. Sapiens      CGATGCCTCCAGGTTGTCCGGAGCCTAGTCAAGCCTGAGAATTACAGGAGACTGGACATC
R. Norvegicus   CGGTGCCTTCAGGTTGTACGGAGCCTGGTCAAGCCTGAGAACTACAGGAGGCTGGACATC
M. Musculus     CGGTGCCTTCAGGTTGTGCGGAGCCTGGTCAAGCCTGAGAACTACAGGAGACTGGACATC
                    ** ***** ***** ***** ***** ***** *****
H. Sapiens      GTCAGGTCGCTCTACGAAGATCTGGAAGACCACCCAAATGTGCAGAAAGACCTGGAGCGG
R. Norvegicus   GTCAGGTCGCTCTATGAAGACTTGAAGACCACCCAAATGTGCGGAAAGACATAACAGCGG
M. Musculus     GTCAGGTCACTCTATGAGGATTTGGAGGACTACCCAAAGTGTGCGGAAAGACATAACAGCGA
                    ***** ***** ** ** ***** ** ***** ***** ** ** * *****
H. Sapiens      CTGACACAGGAGCGCATTGCACATCAACGGATGGGAGA-----T-----TGA
R. Norvegicus   CTGACCCAAGAGCACCTCGAGAATCAGGCCCTGGGAGAGGAGCCTGAAGGAGTCCACTGA
M. Musculus     CTGAGCCAAGAGCACCTTGAGAGTCAGCACCTGGAAGAGGAGCCT-----TGA
                    ****  ** ***** * * *      ***      *** **      *      ***

```

Figure 30. Nucleotide sequence alignment of predicted VHL open reading frames in human (*H.Sapiens*), rat (*R.Norvegicus*) and mouse (*M.Musculus*). Evolutionary analysis would suggest that the N-terminal repetitive sequence in pVHL₃₀ (red) is of less functional importance than those regions present in both pVHL₃₀ and pVHL₁₉ due to lack of conservation. Identity with human: Mouse: 81.8%; Rat: 80.7%.

As already discussed, the N-terminal sequence of pVHL₃₀ contains eight copies of a GxEx acidic repeat motif in human and higher primates, but only three copies were present in the marmoset, and only one copy was present in rodent VHL genes [116, 119]. Due to lack of conservation, evolutionary analysis would suggest that the N-terminal repetitive sequence in pVHL₃₀ is of less functional importance than those regions present in both pVHL₃₀ and pVHL₁₉. Importantly however, there is good

correlation between the pVHL domains that demonstrate most evolutionary conservation and those that were most frequently mutated in tumours.

Comparative analysis like that illustrated in Figure 30 has demonstrated conservation of the VHL gene product across many millions of years during evolution. Studies undertaken by *Woodward et al.* have highlighted not only this conservation throughout primates, but also as far back as to *C.Elegans*, demonstrating a much older evolutionary lineage dating from the beginnings of metazoan evolution [119]. The identification of a *C.Elegans* homologue is important for several reasons. First, conservation of amino acid sequence across such an evolutionary distance suggests the presence of a protein of significant functional importance. Second, *C.Elegans* provides an excellent experimental model organism in which to study the basic processes that are altered in human disease, and as we will see in chapter 4, the system from which the proline hydroxylases, proteins essential for HIF α regulation by pVHL, were isolated.

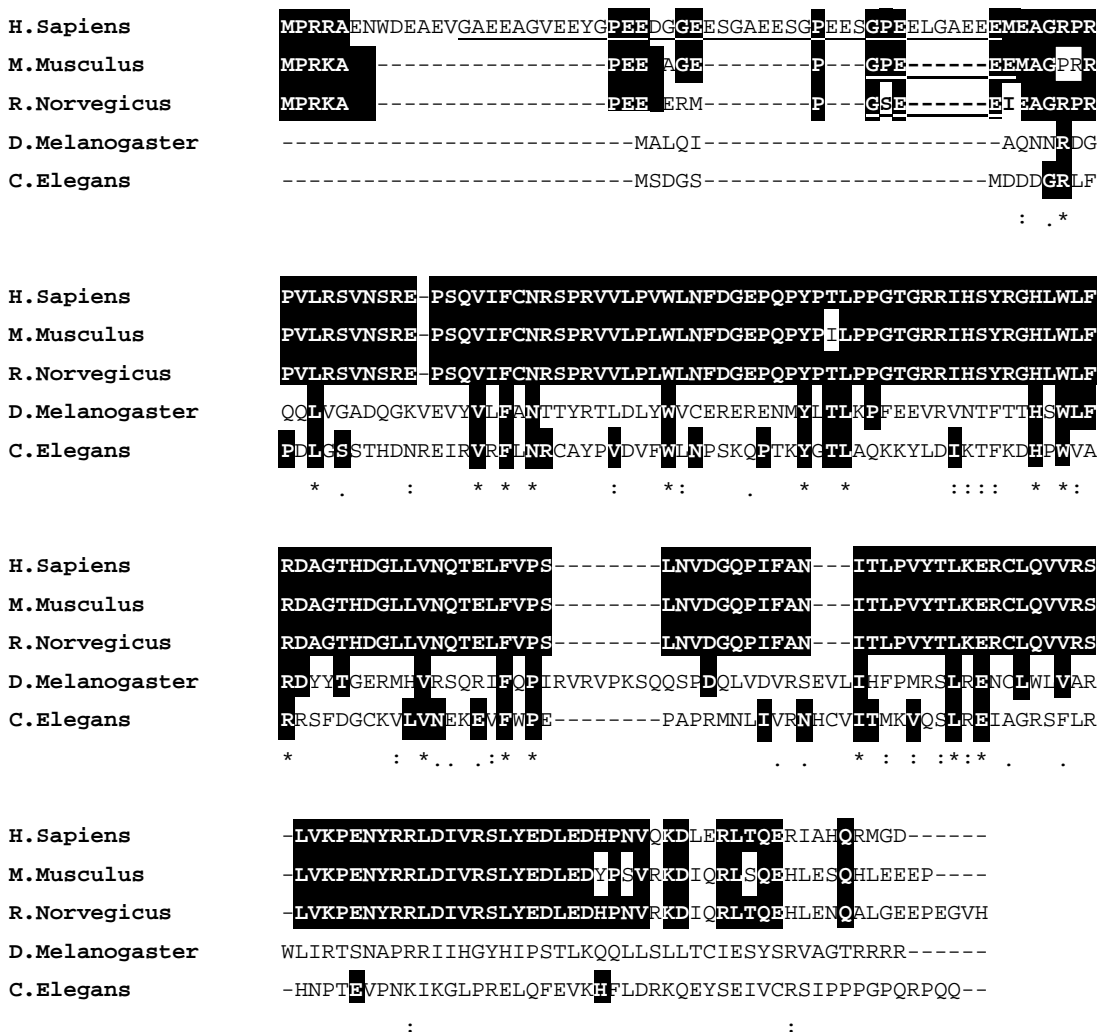


Figure 31. Amino acid sequence alignment of pVHL in human (*H.Sapiens*), mouse (*M.Musculus*), rat (*R.Norvegicus*), fly (*D.Melanogaster*) and worm (*C.Elegans*). Alignment according to ClustalW ch.EMBNet.org. Underlined are GXEEX acidic repeats.

As already mentioned, doubt has been cast on the importance of a second translational start site due to the lack of mutations found between the first and second methionine codons of the VHL gene in both sporadic and VHL-associated tumours. This observation suggests that mutation in this region might not lead to VHL inactivation if translation could be initiated at the second methionine codon, producing a functional VHL protein. Furthermore, both rat and mouse contain only 19 of the 53 amino acids present in this region of the human VHL ORF.



Figure 32. Amino acids 1-54 of human VHL. Eight acidic pentameric repeat sequences are present (GxEEEx). Only one repeat is present in rat and mouse, while all are conserved in primates.

Interestingly, the acidic motif Gly-X-Glu-Glu-X, which is repeated eight times in the N-terminal 53-amino acid region of the human sequence (fig.31), is repeated only once in the rodents and not at all in the fly or worm [119]. However, according to *Woodward et al.*, all primates with available sequences contained eight acidic repeats, with the exception of the marmoset, which only had three. The marmoset reflects evolutionarily, the oldest of the primates in this study. Therefore it is likely that this motif arose in progressively higher species by a series of duplications. Ironically, when the VHL gene was identified, the only significant homology between the predicted VHL gene product and other known proteins was the G-X-E-E-X repeat, showing similarity to a pro-cyclic surface membrane protein of *Trypanosoma brucei*. However, as already mentioned, subsequent investigations have cast doubt on the significance of this acidic repeat domain. Nonetheless, one study reports a significant pathogenic VHL mutation in the first 53 amino acids [5]. Here, 102 Swedish renal cell carcinomas were analysed for VHL mutations. In 47 patients, 70 new mutations were found, and most of them represented novel variations of the VHL gene.

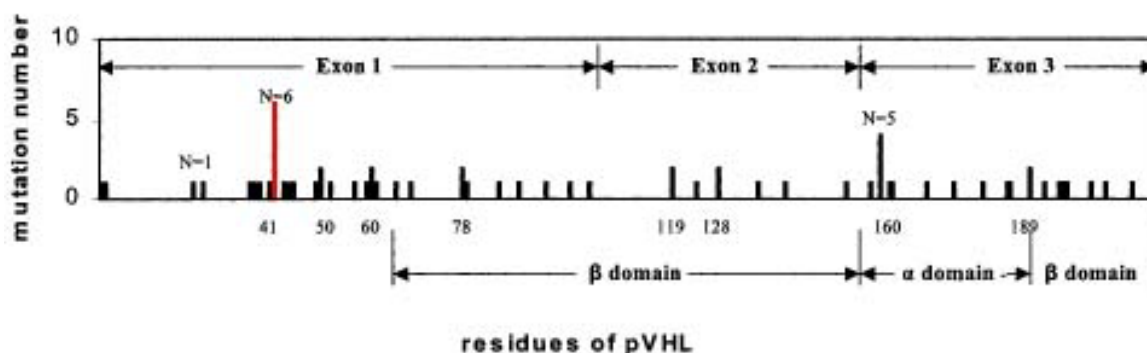


Fig 33. Distributions of the detected VHL mutations according to Ma et al. [5]. The X-axis indicates the number of the residue affected by mutations. The Y-axis indicates the number of renal cell carcinomas carrying mutations at designated residues. In red is the novel hotspot region located between residues 1-53.

Three novel hotspots were detected in the study, among them, an interesting mutation located in the N-terminal sequence of VHL. Five clear cell renal cell carcinomas and one chromophilic renal cell carcinoma harboured a 15-nucleotide in-frame deletion (codons 41-45) at a duplex tandem repeat sequence site. In 5 out of 6 patients the wild-type allele was lost in the tumour samples, suggesting a causal role for the mutations in renal cell carcinoma. However, five patients with this deletion reside in the same hospital district. Unfortunately, the authors were unable to determine if the deletion was an inherited polymorphism or a sporadic mutation, because no other normal tissue was available from these patients or their biological relatives.

This study indicates a potentially significant role for the N-terminal region. Furthermore, the fact that several groups have shown that both translational initiation sites are utilised *in vivo*, and that two protein products, despite the acidic repeat discrepancies, are conserved from rodents through to humans, and that pVHL₁₉ exhibits functional activity as well as an alternative cellular localisation pattern suggests distinct functions for both protein products, pVHL₃₀ and pVHL₁₉ [102, 107, 120]. It could also be suggested that mutations within the pVHL₃₀ N-terminal region may not be tolerated, thereby reflecting a critical role for this region in VHL biology in higher species.

Concluding Remarks

The comparative analysis of genomes is an important strategy in the molecular study of gene function. Such studies enable the reconstruction and understanding of functions that have been acquired, those that have been lost, and those that have a common heritage. The identification of specific mutations associated with human disease phenotypes complements the definition of regions of conserved homology across different animal species, and together these approaches provide a powerful molecular genetic tool toward the understanding of structure-function relationships in genes and proteins. Before looking at the functional implications of the VHL protein product, it is important to understand the fundamentals of VHL gene alterations, a topic which strikes at the core of VHL disease and the subject of consideration in the following chapter.

CHAPTER 3

Mutational analysis of the VHL gene

3.1 Introduction

Von Hippel-Lindau disease is caused by germline mutation of the VHL tumour suppressor gene followed by somatic inactivation of the remaining wild-type allele. Somatic biallelic VHL inactivation can also give rise to tumours, and requires inactivation of both VHL alleles after birth. In the following section, an introduction to the concept of tumour suppressor gene inactivation is discussed, followed by an outline of the types of mutations that occur in the VHL gene. While mutational analysis in VHL disease is somewhat complicated, an attempt to simplify this has been based on the following general criteria:

- A. Genotype-phenotype correlations
- B. Germline mutations
- C. Somatic mutations
 - Allelic deletions
 - Intragenic mutations
 - Methylation
- D. Somatic mutations in sporadic tumours

There have been conflicting reports as to whether the spectrum of *VHL* mutations observed in VHL disease differs with respect to the mutations observed in sporadic tumors [121, 122]. It is possible that some sporadic *VHL* mutations would not be tolerated in the germ line (e.g., if associated with certain "gain-of-function" effects) and that some sporadic *VHL* mutations are non-random because of exposure to specific environmental carcinogens. This chapter is aimed at summarising the available information regarding germ-line and sporadic mutations found in the VHL gene. The mutations identified are and will be useful in pre-symptomatic diagnosis. Such analyses that identify mutations associated with phenotypes contribute to the understanding of fundamental genetic mechanisms of VHL disease.

Molecular analyses reveal a broad spectrum of somatic VHL defects. Almost any nucleotide of the coding sequence may be affected by substitutions, deletions, or insertions (table 10) [122-126], and other changes may involve methylation [95]. Although most of these alterations seem distributed at random, some occur more frequently. For example, somatic mutations in RCCs cluster within VHL exon 2 [123]. Although many reports have added a lot of knowledge about VHL, it must be recognised that many patients with VHL disease still experience insufficient counselling [127]. Databases like that established by Beroud *et al* where to date some 823 VHL mutations are documented, help greatly to clinically characterise mutations in VHL [2]. However, for most mutations the number of known carriers is very low. To get a rough idea of a mutation-based VHL type, more than 10 carriers (though preferably 30-50) should be analysed. Table 11 outlines mutations in which 10 or more carriers have been analysed. It is also important to characterise for each lesion the percentage of symptomatic and asymptomatic carriers, sex distribution, age of onset of symptoms or detection as an asymptomatic lesion. For many mutations, this information is unavailable, but efforts, like those by Beroud *et al*. are helping to centralise this information and process the overwhelming abundance of information generated by such mutational studies. Figure 34 illustrates the mutational profile across the VHL poly-peptide. These studies have highlighted mutational hotspots in pVHL, which in turn have helped in the identification of protein interface regions important in pVHL tumour suppression, namely Elongin C and Hif α .

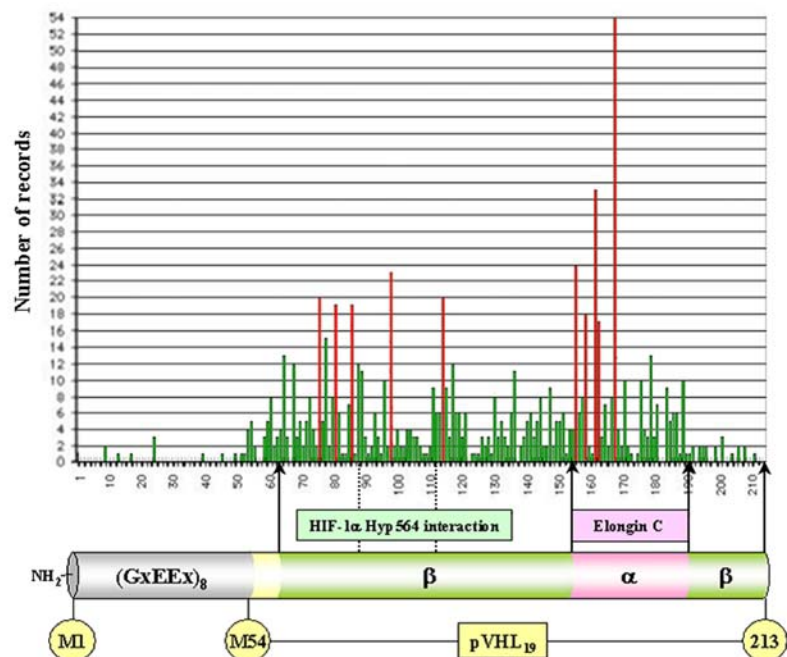
Table 10. Spectrum of mutations in the VHL gene

Mutation	VHL
Total	795
Frameshifts	297 (36,08%)
Deletions	235 (28,55%)
Insertions	62 (7,53%)
Point mutations	496 (63,68%)
Missense	399 (48,48%)
Nonsense	97 (15,2%)

Table 11. Top 20 mutated residues in pVHL

Position	Number of records	Frequency
1. 167	54	6,56 %
2. 161	33	4,01 %
3. 155	24	2,92 %
4. 98	23	2,79 %
5. 114	20	2,43 %
6. 76	20	2,43 %
7. 86	19	2,31 %
8. 81	19	2,31 %
9. 158	18	2,19 %
10. 162	17	2,07 %
11. 78	15	1,82 %
12. 178	13	1,58 %
13. 65	13	1,58 %
14. 68	12	1,46 %
15. 117	12	1,46 %
16. 88	12	1,46 %
17. 136	11	1,34 %
18. 89	11	1,34 %
19. 175	10	1,22 %
20. 96	10	1,22 %

Figure 34. Distribution of VHL-mutations are concentrated in the HIF α and Elongin C binding domains. Red bars highlight the ten most frequent mutations as outlined in box 2. Below the histogram is the VHL protein. Noteworthy, residues 88-111 constitute the pVHL-Hyp564 interacting interface which harbours the frequently mutated residue Y98, the 'black forest' founder mutation. Some 823 germ-line and somatic mutations have been collected so far (www.umd.be) - Beroud *et al*. 1998; Maddock *et al*. 1996; Maher *et al*. 1999.



3.2 Structural analysis of pVHL highlights mutational hot-spots

The tumour-derived mis-sense mutations map evenly to the α - and β -domains, each of the domains containing three of the six most frequently mutated residues [2]. In the α -domain, the H1 helix (fig.24, chapter 2) is the primary target of tumourigenic mutations. It contains the most frequently mutated residue, Arg¹⁶⁷, which has a structural role stabilising the H1 helix and the α - β domain interface, and an additional mutational hotspot, Cys¹⁶², which contacts Elongin C (Fig.25). The third hotspot in the α -domain is Leu¹⁷⁸, and it has dual roles interacting with Elongin C and also stabilising the H2-H3 packing of the α -domain. The remaining α -domain mutations map to residues involved in the packing of the helices (such as Val¹⁷⁰, Ile¹⁸⁰, Leu¹⁸⁴, and Leu¹⁸⁸), or in stabilising the α - β inter-domain interface (Arg¹⁶¹ and Gln¹⁶⁴). Several of these residues also make important contacts to Elongin C (Arg¹⁶¹, Ile¹⁸⁰, and Leu¹⁸⁴). This pattern of mutations in the α -domain solidifies the role Elongin C binding has in the tumour suppressor activity of VHL.

Box 12. 10 Most frequently mutated residues

Residue	Records	Function
R167	54	Packing of α -helices
R161	33	Elongin C binding
V155	24	Elongin C binding
Y98	23	Hyp564 binding
G114	20	HIF binding?
F76	20	HIF binding?
P86	19	HIF binding?
P81	19	HIF binding?
L158	18	Elongin C binding
C162	17	Elongin C binding

As already mentioned in chapter 2, the pVHL residues that interact with Hyp⁵⁶⁴ residue of HIF-1 α are highly conserved in the human, mouse, frog, fly, and worm pVHL orthologues (Fig.28.B, chapter 2) and mutations of Tyr⁹⁸, Ser¹¹¹, and Trp¹¹⁷ of pVHL have been shown to abolish HIF1 α binding [115]. The importance of a pVHL-HIF α interaction is supported by the distribution of VHL tumour-derived missense mutations, which tend to cluster at the Hyp⁵⁶⁴ binding site of pVHL (Fig.35) [2]. All of the five pVHL residues that contact Hyp⁵⁶⁴ are mutated at high frequencies. In fact, Tyr⁹⁸, whose side chain is not important for the structural integrity of the β sandwich but which contacts both the pyrrolidine ring

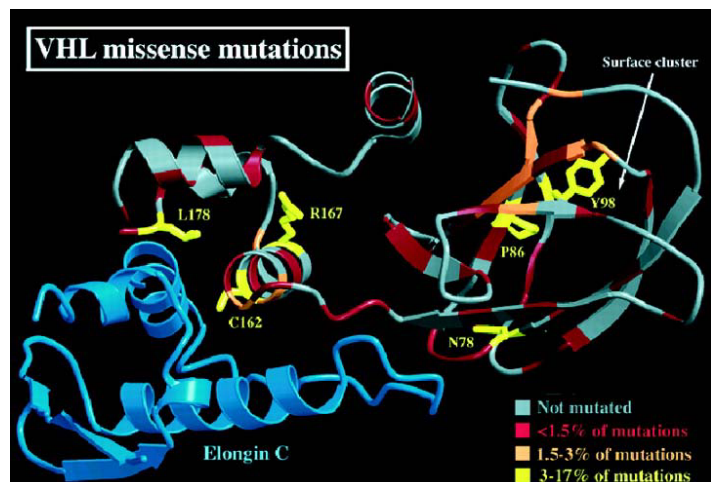


Figure 35. The VHL ribbon diagram is coloured by mutational frequency. Grey indicates an absence of tumour-derived mutations, red less than 1.5% of the total mutations, orange 1.5 to 3% of total mutations, and yellow 3 to 17% [2]. The latter correspond to the six most frequently mutated residues, which are labelled. Elongin C is shown in blue. The mutational cluster of surface residues on the β domain is indicated.
Adapted from Stebbins et al. 1999

for the structural integrity of the β sandwich but which contacts both the pyrrolidine ring

and backbone carbonyl group of Hyp⁵⁶⁴, is the second most frequently mutated amino acid of pVHL (the first one, Arg¹⁶⁷, maps to the α - β inter-domain interface) [111, 128].

Understanding how mutations in pVHL contribute to tumourigenesis is crucial in trying to delineate molecular mechanisms underlying the pathological phenotype. A theory proposed by a renowned cancer researcher has helped our understanding of tumourigenesis, a theory to which *VHL* conforms, and the subject of the next section.

3.3 Knudson's two-hit hypothesis for tumourigenesis

Much of what scientists know about the origins of cancer and the role of tumour suppressors can be traced back 33 years to the elegant theory of cancer researcher Alfred G. Knudson. Widely thought to be one of the most significant theories in modern biology, the "two-hit" theory explains the relationship between the hereditary and nonhereditary, or sporadic, forms of retinoblastoma, a rare cancer affecting one in 20,000 children. Years prior to the age of gene cloning, Knudson's 1971 paper proposed that individuals will develop cancer of the retina if they either inherit one mutated retinoblastoma (*Rb*) gene and incur a second mutation (possibly environmentally induced) after conception, or if they incur two mutations or hits after conception [129]. If only one *Rb* gene functions normally, the cancer is suppressed. Knudson coined these preventive genes anti-oncogenes; other scientists renamed them tumour suppressors.

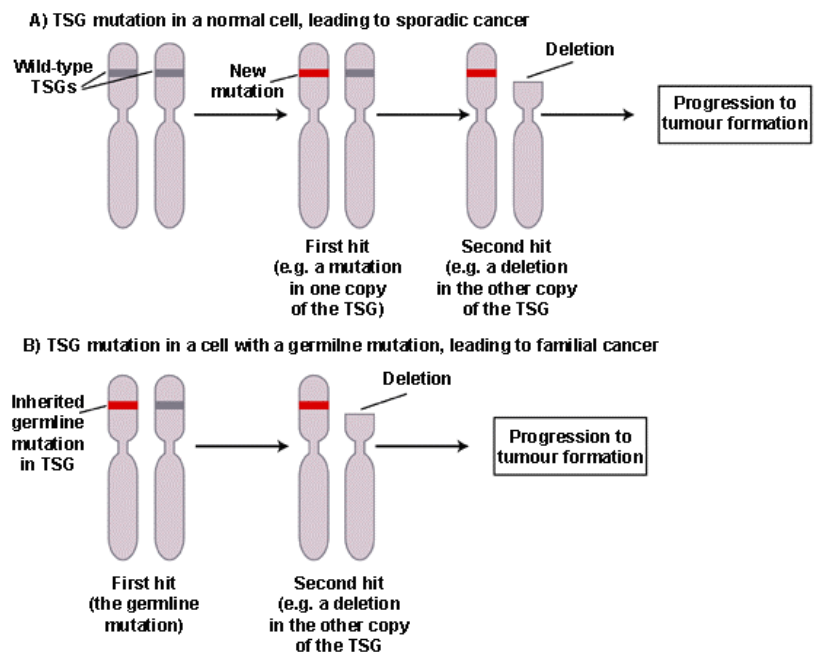


Figure 36. Knudson's two-hit hypothesis for tumourigenesis. (A) Somatic inactivation of both alleles of a tumour suppressor gene (TSG) is necessary for tumour formation. (B) As one inactivated allele has already been inherited, only inactivation of the corresponding TSG allele is necessary for tumour progression.

Adapted from Richards et al. 2002

Knudson's two-hit theory of tumour development may not apply to all cancers, but the basic concept was validated with the cloning of the *Rb* tumour suppressor gene. It was demonstrated that in retinoblastomas, both copies of *Rb* genes are inactivated, thus the 'hits' necessary to transform a cell toward malignancy can be both inherited and acquired. In agreement with this hypothesis, previous analyses of VHL disease-

associated neoplasms have consistently demonstrated both *VHL* gene mutations and deletions in tumours that are associated with the syndrome [79]. That is, people with the disease are born with one mutated copy of the *VHL* gene. Tumours develop when the other, normal, copy is inactivated (by mutation or hyper-methylation) in a susceptible cell. People with two normal copies of the *VHL* gene may also develop sporadic cancers if both copies are inactivated. In this case, the *VHL* gene is inactivated some time after birth.

3.4 Genotype-Phenotype Correlations in VHL Disease

Complex genotype-phenotype associations are a notable feature of VHL disease. As already mentioned in section 1.1, although retinal angiomas and CNS haemangioblastomas are hallmarks of the disease, some families display a high risk of concurrent pheochromocytoma (type 2 VHL) but others do not (type 1 VHL) [35]. Type 2 VHL families can be further subdivided into type 2A (low risk of renal cell carcinoma), type 2B (high risk of renal cell carcinoma) and type 2C (exclusively pheochromocytoma without other characteristics of VHL disease). This is outlined in table 3 and includes some mutations most commonly associated with the phenotype.

VHL disease type	Tumour types observed in families			Germline VHL mutation types most commonly associated with phenotype
	HB	RCC	Phaeo	
Type 1	+	+	-	Deletions and truncations ¹
Type 2A	+	-	+	Missense Tyr98His ² and Tyr112His
Type 2B	+	+	+	Missense
Type 2C	-	-	+	Missense Leu188Val, Val84Leu, Ser80Leu

¹ Truncations include both frameshift and nonsense mutations.
² The 'Black Forest' founder mutation.

In general, type 2 disease is associated with subtle VHL mutations, such as missense mutations, that would be predicted to give rise to conformationally intact pVHL mutants [35, 127, 130-133]. In contrast, type 1 disease is often associated with mutations that should grossly alter the structure of pVHL or lead to complete absence of pVHL. This latter set of observations has led to speculation that type 2 mutants acquire a 'gain of function' that is linked to the induction of pheochromocytoma [43, 111]. Alternatively, it

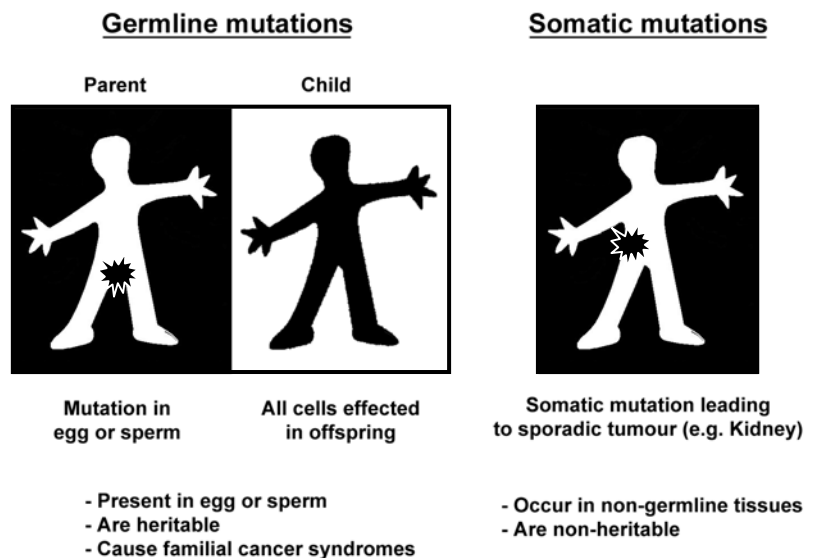
is possible that complete loss of pVHL function is incompatible with pheochromocytoma development.

In addition to regulation of HIF, pVHL has been implicated in the control of extracellular matrix formation and the cell-cycle (functional analysis of pVHL is discussed in more detail in chapter 4) [134-138]. Hoffman *et al.* showed that type 2C pVHL mutants retained the ability to interact with HIF α and to down-regulate HIF α target genes when reintroduced into pVHL-defective tumour cells. This provides a biologically plausible mechanism to account for the low risk of haemangioblastoma associated with these mutants. Furthermore, they demonstrated that pVHL mutant L188V can suppress renal carcinoma growth *in vivo*, suggesting that deregulation of HIF contributes to pVHL-defective renal tumourigenesis. In contrast however, L188V, like classical null pVHL mutants, is defective in promoting extracellular fibronectin matrix assembly. This might suggest that abnormal extracellular matrix formation following pVHL inactivation contributes to the development of pheochromocytoma in the setting of VHL disease, thereby, at least in part, explaining the clinical sub-divisions in VHL disease. These studies strengthen the notion that HIF deregulation plays a causal role in haemangioblastoma and renal carcinoma, and raises the possibility that abnormal fibronectin matrix assembly contributes to pheochromocytoma pathogenesis in the setting of VHL disease.

3.5 Germline Mutations

Germ cells are the reproductive cells of the body, i.e. the sperm and egg cells. Germ-line mutations are those present in a parent that can be passed on to offspring through the egg or sperm cell. Because the mutation is present at conception in the original fertilised egg, when that cell replicates its genetic material and divides, the mutation is

copied in all future cells. Thus, an inherited mutation is present in every cell of the body. A person who inherits a mutation in a specific cancer susceptibility gene, like the VHL gene, can develop cancer more easily, have bilateral or multiple cancers, and at a



younger age than a person born without such a mutation. The reason being that every cell already carries an inherited mutation. Therefore, every cell is already one step closer to malignant transformation.

Germline mutations are found in up to almost 100% of the families fulfilling the clinical VHL criteria [31, 34, 43]. Missense, nonsense, splice site mutations, and micro-deletions and –insertions, are detected in approximately two-thirds of patients [34, 35, 133]. In one-third of the VHL families, large deletions (4-380 kb) are found. Such deletions are demonstrated by southern blot analysis [34], pulsed field gel electrophoresis [139], or fluorescent *in situ* hybridisation (FISH) .

The scope of this thesis does not allow addressing each mutation individually, instead a summary of the more frequent germ-line mutations will be discussed as outlined in table 14. Codon 167 missense mutations are particularly associated with Type 2B VHL disease, with a high incidence of pheochromocytoma within the families. Two specific missense mutations are associated with Type 2A VHL (presenting with pheochromocytoma and haemangioblastoma, but no RCC); these are Tyr98His (the Black Forest mutation) and Tyr112His, otherwise referred to as Y98H and Y112H respectively [35, 140, 141]. Interestingly, a different missense mutation at codon 112 (Tyr112Asn) in one family has given rise to VHL disease that has so far resulted in RCC, retinal and cerebellar haemangioblastoma and one case of pheochromocytoma (Type 2B) [142]. Specific missense mutations have also been observed in families with pheochromocytoma but none of the other features of VHL (Type 2C VHL disease, or familial pheochromocytoma); these are Leu188Val [62, 63], Val84Leu [65] and Ser80Leu [143]. Individuals with these mutations are unlikely to develop haemangioblastomas or RCC. However, some patients with apparently isolated pheochromocytoma have mutations in Type 2B VHL disease (e.g. Arg167Trp); these individuals are at risk of developing the other tumour types [65].

Table 14. Examples of germ-line VHL-mutations and disease class correlations

Mutation	Cases	Class
Y98H	21	Type 2A
Y112H	4	Type 2A
Y112N	1	Type 2B
F119L	5	Type 2B
R167W	21	Type 2B
F119S	1	Type 2C
L188V	5	Type 2C
V84L	1	Type 2C

- Type 1 disease is associated generally with deletions and truncations which include both frameshift and nonsense mutations

The lack of protein-truncating mutations in Type 2 VHL disease suggests a bias against complete loss-of-function mutations for susceptibility to pheochromocytoma; this has been confirmed by mapping of the mutations onto the structure of pVHL [111].

3.6 somatic mutations

In contrast to germline mutations, somatic mutations are confined to somatic cells of an individual (i.e. any cell type except germ cells), and are therefore not heritable. Somatic mutations that occur in tumour suppressor genes in relevant tissues might initiate cancer development. Tumours from VHL patients generally show deletion, mutation or methylation of the wild-type allele such that there is loss of the normal function of *VHL* in tumours. This is characteristic of a tumour suppressor gene. There have been conflicting reports as to whether the spectrum of *VHL* mutations observed in VHL disease differs with respect to the mutations observed in sporadic tumours [121, 122], and as already mentioned, it is possible that some sporadic *VHL* mutations would not be tolerated in the germ line (e.g., if associated with certain "gain-of-function" effects) and that some sporadic *VHL* mutations are non-random because of exposure to specific environmental carcinogens.

In an interesting study by Prowse *et al.*, the mechanism of tumourigenesis in VHL disease tumours was investigated to determine whether there were differences between tumour types or classes of germ-line mutations [144]. Fifty-three tumours (30 RCCs, 15 haemangioblastomas, 5 phaeochromocytomas, and 3 pancreatic tumours) from 33 patients (27 kindreds) with VHL disease were analysed. Overall, 51% of 45 informative tumours showed loss of heterozygosity (LOH) at the VHL locus. In 11 cases it was possible to distinguish between loss of the wild-type and mutant alleles, and in each case the wild-type allele was lost. LOH was detected in all tumour types and occurred in the presence of both germ-line missense mutations and other types of germline mutation associated with a low risk of phaeochromocytoma. Intragenic somatic mutations were detected in three tumours (all haemangioblastomas) and in two of these it was shown to occur in the wild-type allele. This provided the first example of homozygous inactivation of *VHL* by small intragenic mutations in this type of tumour. Hypermethylation of the VHL gene was detected in 33% (6/18) of tumours without LOH, including 2 RCCs and 4 haemangioblastomas. Although hypermethylation of the VHL gene has been reported previously in non-familial RCC and although methylation of tumour-suppressor genes has been implicated in the pathogenesis of other sporadic cancers, this was the first report of somatic methylation in a familial cancer syndrome.

3.6.1 Allelic deletions

In many patients with VHL disease, germ-line mutations of the coding region of the *VHL* gene are absent. Instead, most of these patients exhibit deletion of one entire copy or at least a substantial part of the *VHL* gene [145]. The criteria for establishing VHL disease

are based on clinical diagnosis and identification of *VHL* gene mutations. Although substantial progress has been made in defining the precise mutations causing the disease, approximately 20% of patients with clinically established VHL disease do not show mutations with exhaustive *VHL* gene sequencing analysis [122, 130, 133]. Previous studies have shown that some of these VHL patients carried constitutional deletions of the *VHL* gene [146, 147]. However, there is no simple and reliable technique to detect gene deletions in the germ-line screening of *VHL*.

In the past, pulse field gel electrophoresis has been used to detect VHL germ-line deletions [59, 146, 147]. Presently, quantitative normalised Southern blot analysis is used for deletion screening [34]. However, these techniques are laborious and rely on quantitative comparison of band intensities. Therefore, results can be difficult to interpret and may require confirmation by other methods. In addition, extended deletions can be missed by this technique because of the small size of the genomic probes typically used. In an article published in *Cancer Research* in 1999, Pack *et al.* demonstrated that fluorescent *in situ* hybridization (FISH) can be used to detect deletions in the VHL locus. FISH has already been successfully used in gene mapping studies as well as in the identification of gene alterations, including deletions and translocations, in a variety of human diseases, and was the premise for this study [148]. FISH had until then not been applied to the detection of constitutional *VHL* gene alterations. The advantages of using this technique are manifold, and include: the ability to assess individual cells; detection of variable deletion sizes; technical simplicity; and the ability to identify deletion mosaicism. In the study, Pack *et al.* used FISH and genomic probes that cover the *VHL* locus and its flanking regions to analyse constitutional deletions in patients clinically diagnosed with VHL disease who did not possess *VHL* gene point mutations. They re-examined a group of VHL patients shown previously by single-strand conformation and sequencing analysis not to harbour point mutations in the *VHL* locus. Constitutional deletions were found in 29 of 30 VHL patients in this group using probes that cover the *VHL* locus. Six phenotypically normal offspring from four of these VHL families were then tested: two were found to carry the deletion and the other four were deletion-free. In addition, germ-line mosaicism of the *VHL* gene was identified in one family. In summary, FISH was found to be a simple and reliable method to detect *VHL* germ-line deletions and practically useful in cases where other methods of screening had failed to detect a *VHL* gene abnormality.

3.6.2 Intragenic mutations

Figure 37 below is adapted from Richards *et al.* and develops the distribution of VHL mutations illustrated in Figure 34 by comparing Germline VHL mutations that have been documented in a panel of 120 VHL families from the UK, and Somatic VHL mutations detected in 152 RCCs [35, 132]. Mapping the mutational distributions onto the VHL protein highlights mutational hotspot areas. In both cases, mutations cluster within the α and β domains of VHL disrupting the Elongin C and HIF α interface surfaces. Mutational documentation and generation of data like that illustrated in figure 37 is crucial in trying to identify areas of functional interest within a poly-peptide. In the case of pVHL, it has highlighted the importance of Elongin C and HIF α binding to pVHL.

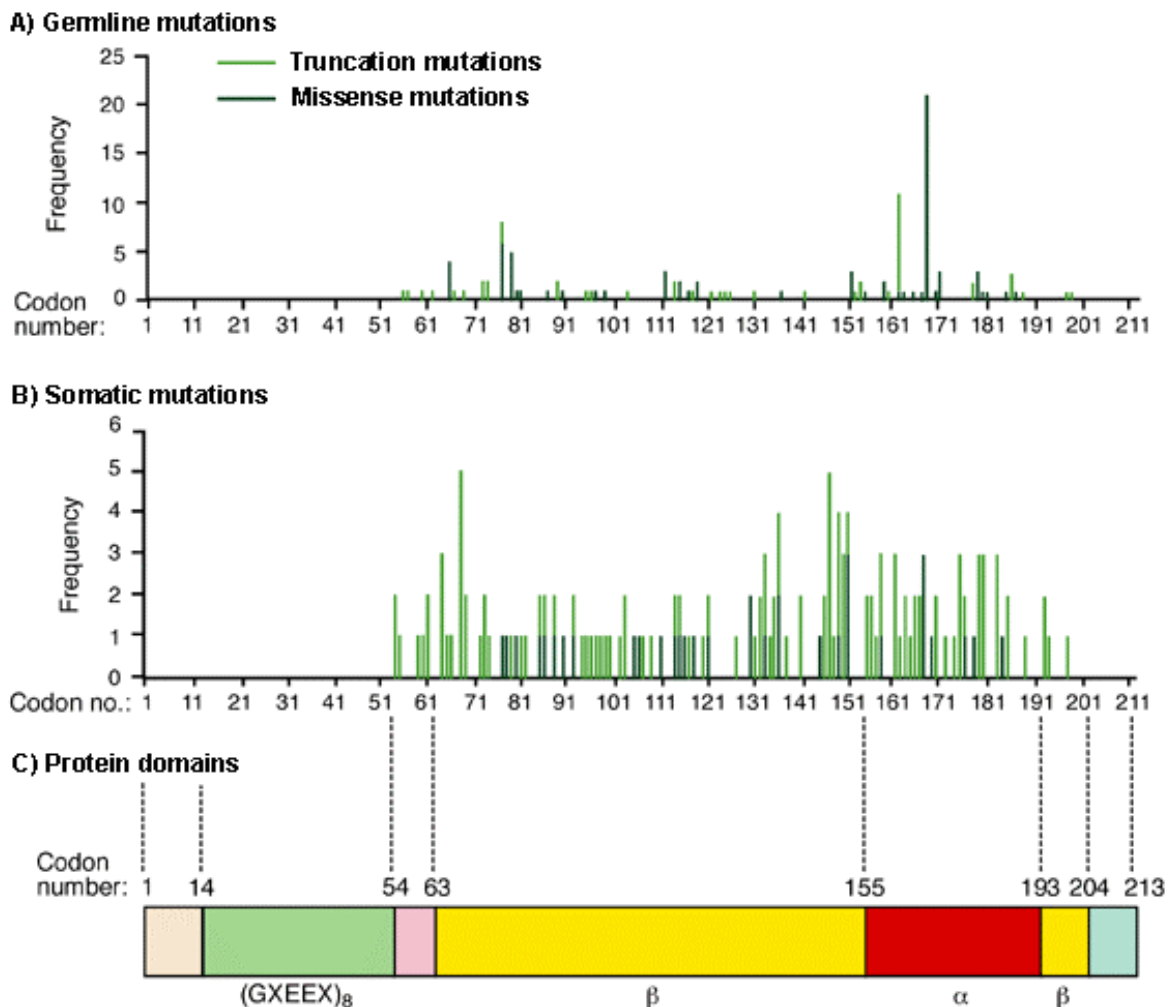


Figure 37. The distribution of intragenic VHL mutations.

Truncating mutations (frameshift and nonsense) are shown with light-green lines; missense mutations are indicated with dark-green lines. (A) Germline VHL mutations in a panel of 120 VHL families from the UK (Crossey *et al.* 1994; Zbar *et al.* 1996). Note that not all of the mutation 'hotspots' were detected in this panel of families. (B) Somatic VHL mutations detected in 152 renal cell carcinomas (RCCs), from the VHL mutation database created by C. Beroud *et al.* 1998. (c) The protein domains encoded by the VHL gene aligned to illustrate that most mutations are in the α - and β -domains.

Adapted from Richards et al. 2002

3.6.3 Methylation

Cancer cells are associated with focal hypermethylation of specific gene promoters. Hypermethylation of gene promoters results in the inactivation of the corresponding genes. This methylation-associated gene silencing has been demonstrated in various genes including tumour suppressor genes – p15, p16, p73 and VHL [149]. Therefore, gene promoter hypermethylation collaborates with other mechanisms of gene inactivation such as deletion and intragenic mutations to fulfil Knudson's hypothesis.

DNA methylation, catalysed by DNA methyltransferase, involves the addition of a methyl group to the carbon 5 position of the cytosine ring in the CpG dinucleotide and results in the generation of methyl-cytosine. Methylation of cytosine to methyl-cytosine in DNA is a heritable genetic alteration which occurs during cell replication in the absence of any change in the genetic sequence. In the normal mammalian genome, the CpG dinucleotides have been progressively depleted from the eukaryotic genome during evolution, and thus are underrepresented in the mammalian genome. However, CpG rich regions, CpG islands, exist and these are often found within the promoter of genes.

The DNA methylation pattern of a cell is accurately reproduced after DNA synthesis and is stably transmitted to the daughter cells. The covalent addition of methyl groups to CpG sites in the newly synthesized DNA strand is mediated by an enzyme known as DNA methyltransferase 1 (DNMT1) (Fig.38). This enzyme is targeted to the replication fork where it efficiently methylates DNA containing hemi-

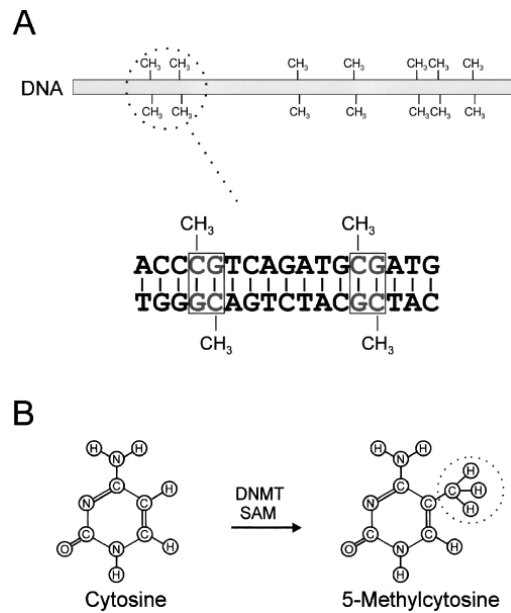


Fig. 38. Schematic overview of DNA Methylation. (A) The human genome is decorated with methyl groups, which occur nearly exclusively at cytosine residues within the symmetric CpG dinucleotide. (B) The postreplicative addition of a methyl group to cytosine is catalyzed by DNA methyltransferase (DNMT), using S-adenosyl-L-methionine (SAM) as a substrate.
Adapted from Worm et al. 2002

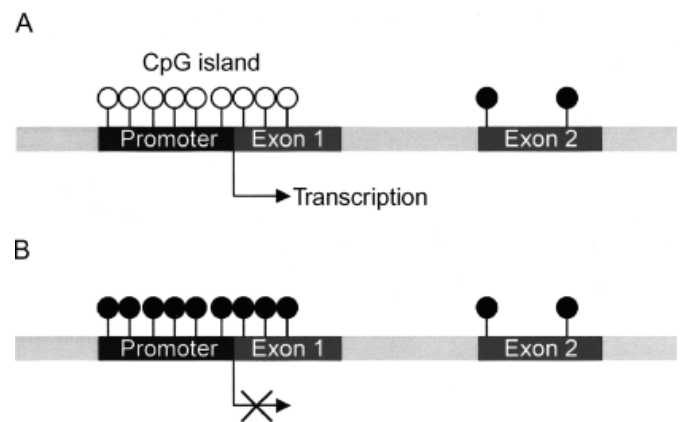


Figure 39. Unmethylated cytosines are found at high densities in CpG islands, which usually map to the promoter and first exon regions of housekeeping genes. (A) The fully unmethylated state of a promoter CpG island (open circles) is associated with transcriptional activity, whereas (B) dense methylation (closed circles) causes transcriptional silencing.
Adapted from Worm et al. 2002

methylated CpGs (postreplicative maintenance methylation). Two additional active DNA methyltransferases have been cloned, DNMT3A and DNMT3B, both of which catalyse the transfer of methyl groups to 'naked' DNA (*de novo* methylation) [150]. The methylation state of promoter CpG islands confers information about the transcriptional activity at these loci. It has been known for many years that, in general terms, there is an inverse relationship between the density of promoter methylation and the transcriptional activity of a gene (Fig.39). However, the actual mechanisms by which DNA methylation modulates gene expression have remained elusive.

Hypermethylation and silencing of tumour suppressor gene expression are emerging as an important mechanism in tumourigenesis. Herman *et al.* reported methylation of a normally unmethylated CpG island in the 5' end of the VHL gene in 19% (5/26) of clear cell renal cell carcinoma cell lines [95]. In these lines, VHL hypermethylation was associated with silencing of the VHL gene transcript, whereas their subsequent chemical demethylation resulted in its re-expression. In addition, Prowse *et al.* demonstrated *de novo* methylation of the wild-type VHL allele in primary tumours from VHL patients concluding that VHL methylation is a specific and important event in the pathogenesis of VHL disease [144]. As already mentioned, they showed hypermethylation detected in 33% of VHL tumours that do not demonstrate LOH, including RCC and haemangioblastoma.

There are now numerous examples of tumour suppressor genes inactivated by aberrant CpG island promoter methylation in human cancers [151, 152]. *De novo* methylation of these genes may occur early in tumour progression and lead to abnormal function of important cellular pathways, including those controlling cell cycle, apoptosis and cell-to-cell growth signalling.

3.7 Somatic mutations in sporadic tumours

Knudson's tumour suppressor gene hypothesis states that familial cancers arise due to the inheritance of a mutated tumour suppressor gene and that a second mutational event involving the wild type allele of that gene leads to malignancy. The model predicts that the more common, sporadic tumours would arise in the same cell-type after somatic inactivation of both copies of the gene responsible for the hereditary cancer [129]. In keeping with its role as a tumour suppressor gene, loss of normal VHL function has been observed in sporadic tumours of the same types as occur in VHL disease. For this reason, identifying and documenting mutations in the VHL gene locus with respect to frequency and consequence is very important. Moreover, by comparing specific VHL inactivating mutations in both germ-line and sporadic tumours, we can define mutational hotspots that help us to functionally investigate VHL function based on structural and

biochemical analysis. This ultimately allows us to propose concepts of VHL involvement in the more common, sporadic tumours that may arise in tissues similar to those that arise in VHL disease. The following sections will detail VHL involvement in sporadic RCC, haemangioblastoma and phaeochromocytoma. Unfortunately, due to data limitation, other sporadic tumours that form in tissue similar to that of tumours in VHL disease could not be discussed. This does not therefore exclude the possibility of VHL involvement in other sporadic tumours of the same type as associated with VHL disease.

3.7.1 Mutations in sporadic renal cell carcinoma

Like cancers of the breast, colon and prostate, kidney cancer occurs in both a hereditary and a sporadic (non-hereditary) form. The year 2003 marked the 10th anniversary of the discovery of the VHL tumour suppressor gene, the first gene identified for hereditary RCC that is now known to be involved in approximately 80% of sporadic RCCs, accounting for some 2% of all adult neoplasma [153]. In many VHL families, the diagnosis of VHL can now be made at birth by detection of VHL gene mutations in blood cells. The finding of frequent VHL gene mutations in tumour tissue from patients with sporadic kidney cancer provides the opportunity for scientists to significantly improve methods for diagnosis of kidney cancer by detecting such mutations, either in tissue removed at surgery or by biopsy or, potentially, by searching for VHL gene mutations in the urine or circulating cells of patients with this disease.

In a study published in 1994, to elucidate the aetiological role of the VHL gene in human kidney tumorigenesis, Gnarr *et al.* analysed localised and advanced tumours from 110 patients with sporadic renal carcinoma for VHL mutations and loss of heterozygosity (LOH) [123]. VHL mutations were identified in 57% of clear cell renal carcinomas analysed and LOH was observed in 98% of those samples. The identification of VHL mutations in a majority of localised and advanced sporadic renal carcinomas indicates that the VHL gene plays a critical part in the origin of this malignancy [123].

In another study carried out by Brauch *et al.* in 2000 to investigate the role of somatic alterations for renal cancer aetiology and prognosis, 227 sporadic renal epithelial tumours were analysed for mutations and hypermethylations in the *VHL* gene. Somatic *VHL* mutations were identified by PCR, single-strand conformation polymorphism analysis, and sequencing, and hypermethylations were identified by restriction enzyme digestion and Southern blotting. Frequencies of *VHL* alterations were established, and an association with tumour type or tumour type and tumour stage was evaluated. *VHL* mutations and hypermethylations were identified in 45% of clear cell renal cell carcinomas (CCRCCs). RCCs carrying *VHL* alterations showed, in nine cases (12%),

mutations at a hot spot involving a thymine repeat (ATT.TTT) in exon 2. Tumour staging was critical to the *VHL* mutation/hypermethylation detection rate in CCRCCs shown by separate evaluation of patients from medical centers in Munich, Heidelberg, and Mainz. The spectrum of pT₁¹⁹, pT₂, and pT₃ CCRCCs and the *VHL* mutation/hypermethylation detection rate varied among these three groups. Altogether, *VHL* alterations were significantly associated with pT₃ CCRCCs. This was the first evidence of frequent somatic *VHL* mutations at a particular site within exon 2 and an association of *VHL* mutations/hypermethylations with a standard prognostic factor.

The spectrum of *VHL* mutations is enormous. As already discussed, almost any nucleotide of the coding sequence may be affected by substitutions, deletions or insertions and other changes may involve methylation. Although most of these alterations seem distributed at random, some occur more frequently. For example, somatic mutations in RCCs cluster within *VHL* exon 2 [123]. Also, RCCs of patients with defined occupational exposure to a human carcinogen, *i.e.*, the organic solvent trichloroethylene, show frequent cytosine to thymine (C→T) transitions and/or a *VHL* hot spot mutation in exon 1 [154]. With the exception of patients with known environmental exposure for which non-random *VHL* mutations may be linked to a specific carcinogen, the origin of frequent mutations at other sites remains elusive. The idea that non-random distribution of somatic *VHL* mutations not only originating endogenously but also from exposure to exogenous carcinogens, is supported by the observation of regional variations in RCC incidence. For example, for yet unknown reasons, the Bas Rhin region of France has one of the highest incidences of RCC in the world [155]. Furthermore, on the molecular level, the findings of a wide spectrum of somatic *VHL* mutation frequencies in patients from Europe, the United States, and Japan are unexplained. Therefore, comprehensive molecular and histo-pathological data analyses of patients from potentially high-risk areas may provide further clues to the aetiology of RCCs and the meaning of somatic *VHL* alterations.

In summary, the contribution of *VHL* mutation to onset of human RCC has been observed in hereditary and is now accepted to be involved in the most cases of sporadic RCCs. Current data shows that *VHL* mutations mainly occurred in clear cell renal cell carcinoma. Tumour-type specificity of *VHL* mutation suggests that different carcinogenic mechanisms underlie different tumour types of RCC, and might determine different biological behaviours of tumours, *e.g.* invasiveness and metastasis. Finally, evidence exists, which suggests that the *VHL* mutation rate might be associated with advanced tumour stage of CCRCC.

¹⁹ "T" describes the primary tumour within the organ. A small "p" (p stands for *pathology*) before the T describes how the cancer cells look under a microscope. **pT1**: The primary tumour is localised to tissue of origin. **pT2**: The tumour is found in tissue of origin, and has begun to invade the blood vessels or lymphatic vessels next to the tumour. **pT3**: The tumour has invaded further blood vessels.

3.7.2 Sporadic mutations in CNS haemangioblastoma

Hemangioblastoma is one of the benign tumours in the central nervous system and is a hallmark of VHL disease. CNS hemangioblastoma is one of the most frequent manifestations of VHL disease, but also may manifest as a sporadic tumour. The molecular basis for the development of sporadic haemangioblastomas is however not known. Previous reports on mutation analysis of the *VHL* gene in VHL disease related and sporadic CNS haemangioblastomas have yielded a wide range of differing results [132, 144, 156-161]. Reported frequencies of loss-of-heterozygosity (LOH) on chromosome 3p in disease related haemangioblastomas are 14% (1/7) [132], 27% (3/11) [144], 66% (2/3) [158], 100% (4/4) [159] and 62% (13/21) [161] with an average of 40%. This indicates that a classic two hit inactivation of the *VHL* gene is a common mechanism in disease-associated haemangioblastomas, i.e germ-line carriers. In a study by Gläsker *et al.*, of the 13 sporadic tumours analysed, 23% showed a single somatic mutation of the *VHL* gene that was not present in the germ-line. 3p LOH was identified in 50% of informative sporadic tumours. No promoter hypermethylation was demonstrated in either disease-related or sporadic tumour investigated in this study, which is in agreement with Tse *et al.* [158] but contradicts investigations by Prowse *et al.* who showed that four out of eight CNS haemangioblastoma analysed, demonstrated hypermethylation, albeit VHL disease-related tumours, not sporadic tumours. Due to the fact that investigations of hypermethylation of the *VHL* gene in CNS haemangioblastomas are based on a small series, it is difficult to draw conclusions, it is nonetheless tempting to suggest that the absence of hypermethylation in sporadic cases of CNS haemangioblastoma reflect an activity associated uniquely with VHL disease-related haemangioblastomas.

Cerebellar haemangioblastoma is a benign central nervous system neoplasm with characteristic proliferation of vascular and stromal cells. There is increasing evidence that the stromal cell population may represent the neoplastic component of haemangioblastoma, whereas the vascular component may be composed of reactive, non-neoplastic cells. Therefore, successful genetic testing for loss of heterozygosity requires selective analysis of target cell populations. In a study by Lee *et al.* [160], tissue micro-dissection was used to selectively analyse the stromal cell component of 20 sporadic cerebellar haemangioblastomas for loss of heterozygosity at the *VHL* gene and somatic *VHL* gene mutations. Allelic deletions at the VHL gene locus were detected in the stromal cell in 10 of 19 (52.6%) informative cases. In all cases, heterozygosity at the VHL gene locus was retained in the vascular component. In two cases, aberrant bands in exon 2 of the VHL gene were demonstrated in the stromal cells by PCR-based single-strand conformation polymorphism analysis, and somatic mis-sense mutations were successfully characterised in two of the sporadic haemangioblastomas by direct

sequencing. The results support the notion that allelic losses and mutations of the VHL tumour suppressor gene play a role in sporadic cerebellar haemangioblastoma tumorigenesis. Furthermore, because the genetic changes were detected in selectively procured stromal cell areas, the data provide strong evidence that the stromal cell represents a neoplastic component of haemangioblastoma. This may explain why VHL-involvement in sporadic cancer may be under-appreciated, as isolation of the target cell population like those studies performed by Lee *et al.*, might be necessary in order to reveal the true implication of VHL in sporadic tumourigenesis.

However, to reiterate Gläscher *et al.*, they found only three (23%) somatic VHL gene mutations in sporadic haemangioblastomas. Only one of these tumours showed biallelic VHL gene inactivation due to an additional LOH of the VHL gene region at 3p. Their findings of relatively low frequencies of somatic VHL gene mutations in sporadic haemangioblastomas and biallelic VHL gene inactivation agree with previous reports, in which somatic mutations have been reported with an average of 18% [156-158, 160]. In previous studies, no sporadic tumour were shown to have biallelic VHL gene inactivation, as these studies did not investigate all inactivating mechanisms, or the tumours retained heterozygosity. By contrast, Gläscher *et al.* investigated all known VHL gene inactivating mechanisms and their results are highly suggestive that biallelic VHL gene inactivation is not a common mechanism in the tumourigenesis of sporadic CNS haemangioblastoma.

In conclusion, it would seem therefore that the data to date, despite the above-mentioned findings by Lee *et al.*, would suggest that the genetic pathways involved in pathogenesis in VHL disease haemangioblastoma versus sporadic haemangioblastoma are distinct. Further investigations on chromosome 3p in CNS haemangioblastomas are warranted to clarify this hypothesis further.

3.7.3 Sporadic mutations in pheochromocytoma

Pheochromocytomas arise sporadically and as an associated tumour of the inherited cancer syndromes VHL, multiple endocrine neoplasia type 2 (MEN 2), and type 1 neurofibromatosis. Germ-line mutations of the VHL tumour suppressor gene are responsible for VHL disease, and germ-line RET proto-oncogene mutations are associated with MEN 2. Bender *et al.* conducted an investigation to examine a large series of 36 VHL-related pheochromocytomas for somatic VHL and RET gene alterations and loss of heterozygosity (LOH) of markers on chromosome arm 3p, hypermethylation of the upstream VHL-CpG island, and LOH of markers at chromosomal arms with putative relevance for MEN 2 and sporadic pheochromocytomas, namely 1p and 22q [162-165]. For comparison, the same analyses were performed in 17 sporadic pheochromocytomas. They found no somatic intragenic mutations within VHL and RET

in any VHL or sporadic pheochromocytoma, and no pheochromocytoma demonstrated upstream *VHL* gene hypermethylation. Interestingly, they found significantly different LOH frequencies between sporadic and VHL tumours; the more than 91% LOH of markers on 3p and the relatively low frequencies of LOH at 1p and 22q (15% and 21%, respectively) in VHL pheochromocytomas argue for the importance of VHL gene deregulation and dysfunction in the pathogenesis of almost all VHL pheochromocytomas. In contrast, the relatively low frequency of 3p LOH (24%) and the lack of intragenic VHL alterations compared with the high frequency of 1p LOH (71%) and the moderate frequency of 22q LOH (53%) in sporadic pheochromocytomas argue for genes other than VHL, especially on 1p, that are significant for sporadic tumourigenesis and suggest that the genetic pathways involved in sporadic versus VHL pheochromocytoma tumourigenesis are distinct.

Originally VHL disease-associated pheochromocytomas were believed to abide by the Knudson two-hit mechanism of tumourigenesis. This was based on 4 studies encompassing a total of only 12 VHL pheochromocytomas and a broad range of 3p LOH frequencies with an average of 50% [144, 162, 166, 167]. The study by Bender *et al.* is based on 36 VHL-associated pheochromocytomas, and demonstrated for the first time that indeed a complete and biallelic 2-hit *VHL* inactivation is a necessary pathogenetic mechanism for these tumours. In more than 91% of such tumours, the second hit is somatic deletion of the 3p region encompassing the remaining wild-type *VHL* allele. In contrast to VHL tumours, sporadic pheochromocytomas have a relatively low frequency of 3p LOH, which supports 4 other reports that demonstrated LOH at 3p in 35% of a total of 52 sporadic tumours [162, 164, 165, 167]. These studies together with the observation of a lack of somatic intragenic *VHL* mutations in sporadic tumours indicate that VHL-related and sporadic pheochromocytomas do not share common pathogenic pathways. Bender *et al.* demonstrate convincingly that although the *VHL* gene plays a principal role in the tumourigenesis of VHL pheochromocytoma, alterations in *VHL* appear in sporadic pheochromocytomas to a significantly lesser extent. Instead, an as yet unidentified factor(s) residing perhaps on 1p plays a major role in sporadic tumourigenesis. Tumour suppressor genes on 22q may also contribute to sporadic pheochromocytoma.

Concluding Remarks

These observations of genetic alterations in VHL-related and sporadic pheochromocytoma (and indeed CNS haemangioblastomas) are in contrast to observations that have been made among inherited cancer syndromes with involvement of tumour suppressor genes to date. Sporadic counterparts of associated tumours in several inherited cancer syndromes share a common genetic aetiology and pathogenic

pathway. The classic example is retinoblastoma, on which the Knudson two-hit hypothesis is based. In heritable retinoblastoma, the first hit is germ-line mutation of the *RB* gene, and the second hit is a somatic mutation or deletion of *RB* [168, 169]. In sporadic retinoblastoma, two somatic mutations affecting *RB* are the genetic basis of tumourigenesis [169]. This is also true of *p53* mutations in Li-Fraumeni syndrome and its sporadic counterpart tumours osteosarcoma, soft tissue sarcomas, and glioblastomas [170, 171], and *APC* mutations in familial adenomatous polyposis and a subset of sporadic colon cancer [172, 173]. With respect to the *VHL* gene, its biallelic inactivation is a well-known feature in VHL-related as well as sporadic renal clear cell carcinomas where inactivation is observed in up to 80% of sporadic cases. However, there are other examples in the literature where the genetic pathway in a hereditary cancer is different from the sporadic counterpart. For example, although germ-line *BRCA1* and *BRCA2* mutations are associated with the hereditary breast-ovarian cancer syndrome, less than 1% of sporadic breast cancers or ovarian cancers harbour somatic *BRCA1* or *BRCA2* mutations [174, 175]. Further, breast carcinomas from *BRCA1* mutation carriers have been described to harbour different genetic alterations compared with their sporadic counterparts [176-178]. Thus, the different frequencies of *VHL* inactivation, and LOH at 1p, 3p, and 22q between VHL disease-associated and sporadic pheochromocytoma suggest that in contrast to renal clear cell carcinoma, different genetic pathways might be involved in hereditary versus sporadic disease, a situation more akin to the *BRCA* loci and breast cancer.

CHAPTER 4

Functional analysis of the VHL tumour suppressor

4.1 Introduction

This chapter outlines the role of pVHL as a substrate recognition component of an E3 ligase complex that specifically targets hypoxia inducible factor α (HIF α) for degradation. It details HIF regulatory mechanisms and hypoxia-induced gene expression and discusses the consequences of this ubiquitin-mediated proteolytic event. Finally, additional substrates, which have been identified for the pVHL E3 ligase complex, and other protein interactions that are either ligase independent or facilitate pVHL's function as an E3 ligase, are discussed.

4.2 pVHL and ubiquitin-mediated proteolysis

The discovery of the complex cascade of the ubiquitin pathway revolutionised the field of protein degradation. It is now clear that degradation of cellular proteins is a highly complex, temporally controlled, and tightly regulated process that plays major roles in a variety of basic pathways during cell life and death, and in health and disease. With the multitude of substrates targeted, and the myriad of processes involved, it is not surprising that aberrations in the pathway are implicated in the pathogenesis of many diseases, as is the case in VHL disease. The discovery of the ubiquitin/proteasome pathway emerged from efforts to understand why intracellular proteolysis, measured as the release of amino acids from intact cells, requires metabolic energy [179]. Key elements of the answer became clear in the early 1980's as a result of the pioneering biochemical studies of Hershko and coworkers. These investigators found that energy, in the form of ATP, is needed to modify proteolytic substrates with ubiquitin, a highly conserved 76 amino acid polypeptide that is joined to a substrate lysine side chain through an isopeptide bond to ubiquitin's C terminus [180, 181]. Ubiquitination occurs through sequential steps catalysed by activating (E1), conjugating (E2), and ligase (E3) enzymes (Fig.40) [182]. The presence of multiple substrate-linked ubiquitins recruits the 26S proteasome, a 2.5 MDa complex that uses energy derived from ATP hydrolysis to unfold the substrate polypeptide chain and translocate it into an interior chamber [183]. Having arrived at this site, the substrate is hydrolysed by a nucleophilic mechanism to

produce small peptides. Ubiquitin is spared from degradation through its release from the substrate (or a substrate fragment) by deubiquitinating enzymes [181]. Thus, there are two independent reasons why ATP is required for intracellular proteolysis: to activate ubiquitin's C-terminus in preparation for conjugation, and to support the proteasome's substrate unfolding and translocation activities.

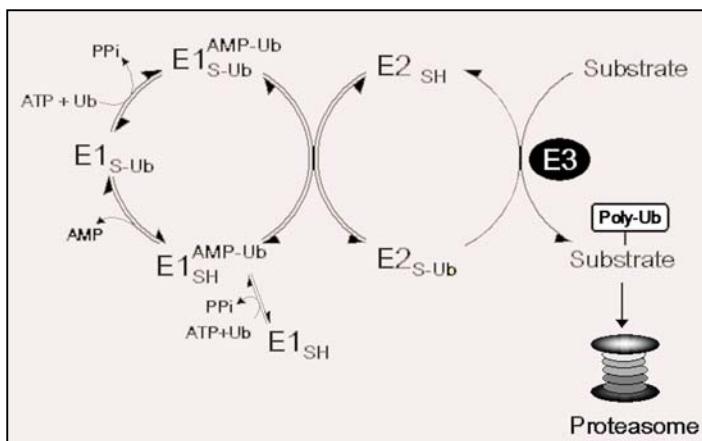


Figure 40. Components and Mechanisms in the Ubiquitin-Proteasome Pathway. Overview of ubiquitin-mediated proteolysis showing how ATP is used in its conjugative and degradative phases. *E1*, *E2*, and *E3* are ubiquitin activating, conjugating, and ligase enzymes, respectively.

As figure 40 illustrates, ubiquitin (Ub) is conjugated to other proteins through an amide bond, called the isopeptide bond, between the C-terminal (glycine 76) residue of Ub and the ϵ -amino group of a lysine residue in an acceptor protein. Ub is activated for conjugation to other proteins by a Ub-activating enzyme (*E1*), which couples ATP hydrolysis to the formation of a high-energy thioester bond between Gly76 of Ub and a specific cysteine residue

of *E1*. The *E1*-linked Ub moiety is moved, in a trans-esterification reaction, from *E1* to a Cys residue of a Ub-conjugating enzyme (*E2*), and from there to a lysine residue of an ultimate acceptor protein, yielding a Ub-protein conjugate. This last step requires the participation of another component, called the *E3*, which acts as the substrate recognition complex recruiting specifically substrates to be ubiquitinated and subsequently degraded. It has been shown by our laboratory and others that pVHL constitutes an *E3* ligase complex, and acts as the substrate recognition component of this complex [184, 185].

4.3 pVHL is a component of an *E3* ubiquitin ligase complex

Because protein degradation must be highly selective in order for the cell not to destroy itself, the substrate recognition step mediated by enzymes called *E3* ubiquitin ligases is crucial. Not surprisingly, given the multitude of substrates, *E3* ligases are a highly diverse group. One way in which the cell achieves such diversity is by engaging numerous substrate-specific adapter proteins that recruit protein substrates to core ubiquitin complexes. A superfamily of *E3* ubiquitin ligase complexes have emerged – the SCF (Skp1-Cdc53/Cul1-F-box protein) family, the APC (Anaphase Promoting Complex) family, and the more recently discovered VCB-Cul2 (VHL-Elongin C/Elongin B-cullin 2)

complex (Fig.41). The SCF family is the exemplar for combinatorial control of E3 ligase specificity. SCF complexes contain adapter subunits called F-box proteins that recognise different substrates through specific protein-protein interaction domains [186]. F-box proteins link up to a core catalytic complex – composed of Skp1, Cdc53 (cullin 1 in metazoans), and the E2 ubiquitin-conjugating enzyme, Cdc34 – through the F-box motif, which is a binding site for Skp1. There are hundreds of F-box proteins, and known targets of SCF complexes range from cell cycle regulatory proteins such as cyclins and CDK inhibitors and transcriptional regulators such as I κ B and β -catenin, among many others [187, 188]. For example, our laboratory demonstrated that the F-box protein SKP2 promotes p27^{Kip1} degradation and induces S phase in quiescent cells [189].

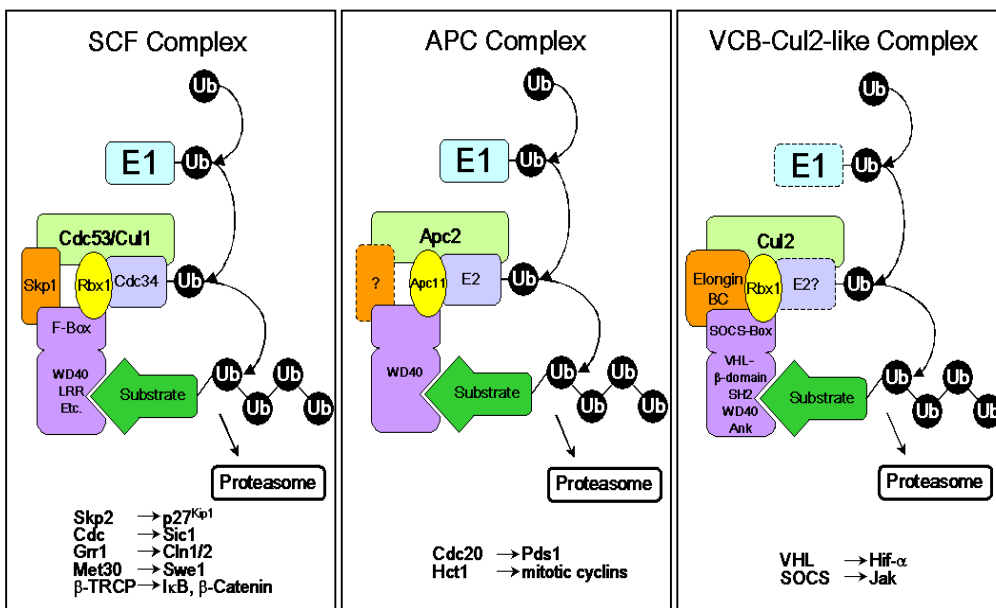


Figure 41. Comparison of the structural homology between SCF, APC and VCB-Cul2 ubiquitin ligase complexes. Each complex interacts with a set of adapter molecules that recruit different binding partners through specific protein-protein interaction domains such as WD40 repeats and leucine-rich repeats (LRR). Representative examples are shown below each complex. Rbx1 and its homologue Apc11 may play a role in tethering components to each other and in activating the E2 enzyme. Question marks indicate speculative components of interactions.

The APC is a second E3 ligase that uses different adapters to target different substrates, which include mitotic cyclins and other proteins that regulate mitosis [190]. Interestingly, the APC2 subunit of the APC complex turned out to be a homologue of Cdc53, fuelling the idea that the SCF and APC complexes had a possible distant relationship. The third complex, composed of pVHL and its associated subunits Elongin B, Elongin C, and cullin 2 was presumed to comprise an E3 ligase complex based on sequence and structural similarity between complex components.

It had been well established that pVHL stably associates with the two regulatory subunits B and C of the trimeric transcription elongation factor, elongin [191-193]. Initial investigation demonstrated that pVHL bound tightly and specifically to elongin B and C subunits and it was proposed that, by virtue of its ability to compete for elongin A, this binding inhibited the activity of the transcriptional elongation complex, SIII, which is a complex consisting of Elongin A, B and C [191]. However this evidence was only shown *in vitro*, and has since never been confirmed. Furthermore the authors acknowledge in a

follow up paper in 1997 that they were unable to prove this *in vivo* and that since pVHL is found in a stable complex with elongin B and C, it is unlikely that pVHL actively competes with elongin A thereby affecting transcriptional elongation. This finding led them to rethink their model and propose an alternative cellular function for the VCB complex. In addition the pVHL-elongin C binding interface represents a 12 amino acid stretch shown to be a mutational hotspot region which further underlines the functional significance of this complex [192]. This region is referred to as the BC-box motif and is contained within the SOCS box domain as explained in chapter 2 [111].

Pause *et al.* further demonstrated that the VCB complex bound a member of the cullin family of proteins, cullin 2, which had been previously shown to be involved in cell-cycle control in yeast, and in cell growth in *C.Elegans*. Cullin 2 interaction was shown to be dependent on the integrity of trimeric VCB complex, and that naturally occurring mutations that interfere with binding of elongin's also eliminate binding to cullin 2.

The emergence of Rbx1 (Ring-box) proved equally important in helping to define the first known function of pVHL. Kamura *et al.* defined Rbx1 as a stoichiometric component of the mammalian VCB-Cul2 complex and, prompted by the finding that Rbx1 interacts directly with the Cdc53 homologue cullin 2, determined that Rbx1 was also an integral component of the human and yeast SCF complexes [194]. Rbx1 is a close homologue of the APC subunit Apc11, which together with Rbx1 defines a distinct subclass of RING finger proteins. The RING finger is a small, metal-binding domain often found in sub-units of multi-protein complexes [111]. In the SCF complex, Rbx1 interacts with Cdc53/Cul1, Cdc34 (E2 enzyme), and with several different F-box proteins, but does not interact with Skp1 [194]. Kamura *et al.* also demonstrated that Rbx1 co-precipitates independently with pVHL and elongin B/C complexes. One pivotal role of Rbx1 is to recruit Cdc34 into the SCF complex by bridging or stabilising the Cdc34-Cdc53 interaction. Furthermore, it has been shown that Rbx1-SCF complexes greatly stimulate the catalytic activity of Cdc34. In addition, Rbx1 has been shown to be required for catalysing Skp2 auto-ubiquitination in the presence of E1, E2 and ubiquitin during the G₀/G₁ phases of the cell cycle [195]. Similarly, the role of Rbx1 within the VCB-Cul2 ligase might therefore be in recruiting an as yet unidentified E2(s) to the complex thereby facilitating more efficient ligase activity.

The first proof that this newly defined VCB-Cul2 complex possessed ligase activity came in 1999 when two independent studies, one of which coming from our own laboratory, demonstrated biochemical evidence that the complex is involved in the process of ubiquitination [184, 185]. Moreover, selected, naturally occurring mutants of pVHL failed to exhibit this activity in ubiquitination assays further highlighting the functional importance of this complex. With the VCB-Cul2 complex established as an E3

ubiquitin ligase with pVHL as the probable substrate recognition component, the search had begun for a substrate(s) for this ligase.

4.4 pVHL targets HIF- α for degradation

By studying the involvement of pVHL in oxygen-regulated gene expression of two VHL-deficient renal carcinoma lines, RCC4 and 786-O, Maxwell *et al.* could demonstrate that the up-regulation of hypoxia-inducible mRNAs in VHL-defective cells extended to a broad range of oxygen-regulated genes and involved a constitutive 'hypoxia pattern' for both positively and negatively regulated genes [114]. VHL disease predisposes sufferers to highly angiogenic tumours [10]. Enhanced glucose metabolism and angiogenesis are classical features of cancer, involving up-regulation of genes that are normally induced by hypoxia [196]. In addition to stimulation by the hypoxic microenvironment, genetic alterations contribute to these effects [196, 197]. Constitutive up-regulation of hypoxically inducible messenger RNAs encoding vascular endothelial growth factor (VEGF) and glucose transporter 1 (GLUT-1) in these tumour cells is correctable by re-expression of pVHL. Furthermore, Maxwell *et al.* investigated the role of pVHL in HIF-1 regulation and tested for interactions between HIF α -subunits and pVHL using a combination of hypoxia and/or proteasomal blockade to induce HIF- α subunits. Anti-pVHL immunoprecipitates of extracts from proteasomally blocked RCC4/VHL²⁰ cells, but not RCC4 cells, contained both HIF-1 α and HIF-2 α . Similar results were obtained with hypoxia in the absence of proteasomal blockade. As HIF-1 activation by hypoxia is mimicked by cobaltous ions and iron chelation, Maxwell *et al.* could also show that the pVHL/HIF-1 α complex could not form in cells exposed to these stimuli, and proposed an iron-dependent model of interaction [198, 199].

While direct evidence of a VCB-Cul2 ligase dependent Hif- α ubiquitination event was at this time not shown, it was presumed, based on the given data, that this was indeed the case. These experiments defined a function for pVHL in the regulation of HIF α . Given the importance of HIF in tumour angiogenesis [200] [201], constitutive HIF α activation is clearly consistent with the angiogenic phenotype of VHL disease. Whether it is a sufficient explanation for oncogenesis is less clear. HIF mediates gene activation not only by hypoxia, but also by growth factors such as insulin and insulin-like growth factor-1 [202]. HIF targets such as molecules involved in enhanced glucose metabolism and angiogenesis [196] [203] are classically up-regulated (by different mechanisms) in many forms of cancer, supporting an important role in tumour progression, although their role in the initiation of oncogenesis is less clear. It is now firmly established that pVHL plays a

²⁰ RCC4/VHL refer to renal cell carcinoma cell where VHL has been reintroduced

central role in regulating this key transcription factor. Figure 42. illustrates a simplified diagrammatic representation of HIF- α control by pVHL.

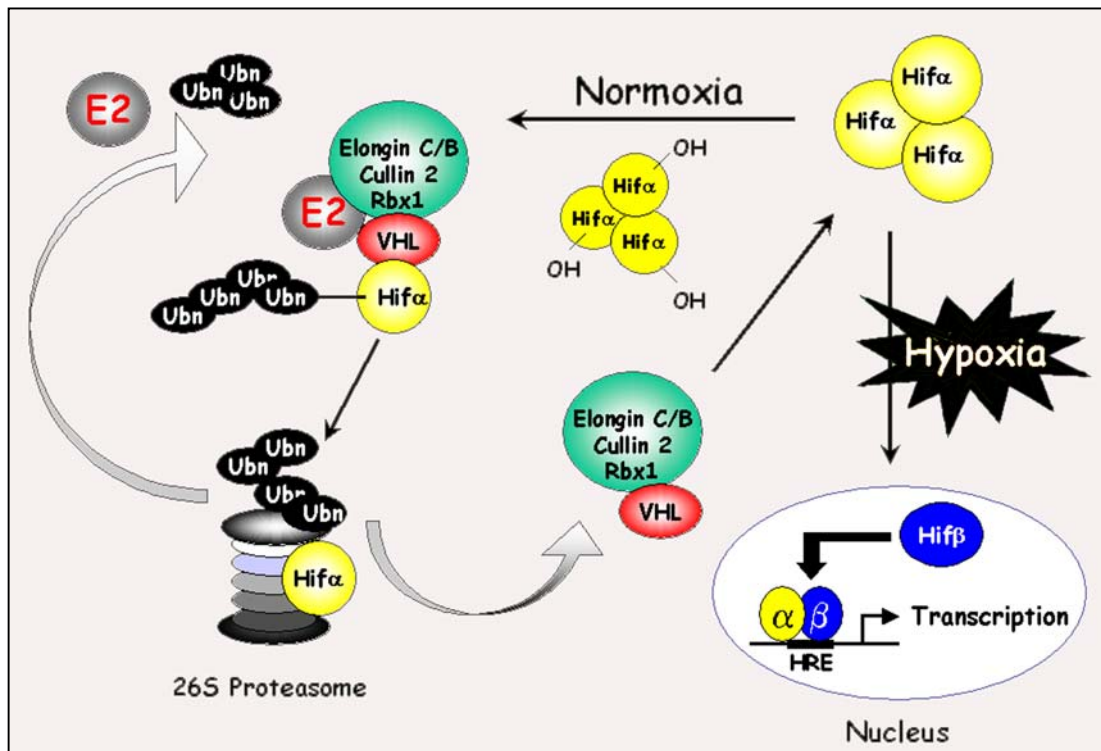


Figure 42. Diagrammatic representation of HIF- α control by the VCB-Cul2 ubiquitin-ligase complex. Under normoxia, HIF α undergoes an hydroxylation event facilitating interaction with pVHL which recruits components of the VCB-Cul2 E3 ubiquitin ligase complex. This complex targets HIF α to the 26S proteasome for degradation. Under hypoxia, HIF α is stabilised, translocates to the nucleus where it dimerises with HIF β , and binds to promoter regions containing a Hypoxia-Responsive-Element (HRE) and thereby initiates transcription of these genes.

4.5 The HIF system

The two subunits, HIF α and HIF β , aryl hydrocarbon receptor nuclear translocator (ARNT), belong to the basic helix-loop-helix (bHLH)-PAS (Per/Amt/Sim) family (Figure 43). HIF α dimerises with HIF β and functions as a transcription factor. The constitutively expressed HIF β resides in the nucleus and acts as a common subunit of multiple bHLH-PAS transcription factors. HIF α constantly varies in its protein level, according to changes in the microenvironmental oxygen concentration. Therefore, the HIF α transcriptional activity is determined by the hypoxic induction and modifications of the HIF α protein level [204]; [205].

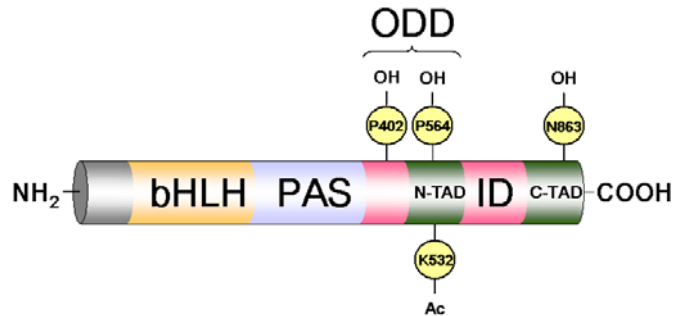


Figure 43. Structural domains and key regulatory residues of HIF-1 α . Domains, residues and abbreviations are explained in the text. OH and Ac represent hydroxylation and acetylation modifications respectively.

Beginning at the N-terminus, HIF-1 α contains the bHLH domain, PAS domain, ID (inhibitory) domain containing the ODD (oxygen-dependent domain), and finally the N- and C-TAD (transactivational domains). These domains are involved in the regulatory machinery of HIF-1 biological activation. The bHLH and PAS domains are required for dimerisation with HIF-1 β and DNA binding [114, 206-208]. The transcriptional activity of HIF-1 is regulated through N-TAD, C-TAD and ID [209]. Under normoxia, the hydroxylation of Pro-402 and Pro-564 in ID or N-TAD of HIF-1 α , respectively, by specific proline hydroxylases is required for the binding of pVHL, which recruits the VCB-Cul2 E3 ubiquitin-protein ligase that targets HIF-1 α for degradation. In the absence of oxygen, the prolyl hydroxylases are not active, consequently the unhydroxylated prolyl-HIF-1 α cannot interact with pVHL [7, 13, 210]. For this reason, these domains are also called oxygen-dependent degradation (ODD) domains. VHL also recruits histone deacetylases (HDAC) that interfere with the transactivation domain function. An asparaginyl hydroxylase, FIH-1 (factor inhibiting HIF-1), which binds to both pVHL and HIF-1 α , also inhibits the transcriptional activity of HIF-1 [19, 211].

The protein level of HIF-1 α is regulated at the level of synthesis and stability. Activation of tyrosine kinases, such as SRC, HER^{neu}, and the IGF and EGF receptors, stimulate the PI3 kinase–PKB–FRAP and ERK/MAPK signal transduction pathways, which lead to the increased translation of HIF-1 α mRNA into protein [212, 213].

Both the HIF- α and HIF- β subunits exist as a series of isoforms encoded by distinct genetic loci. HIF- β subunits are constitutive nuclear proteins, whereas HIF- α subunits are inducible by hypoxia. Among three HIF- α isoforms, HIF-1 α and HIF-2 α appear closely related and are each able to interact with hypoxia response elements (HREs) to induce transcriptional activity [214]. In contrast, HIF-3 α appears to be involved in negative regulation of the response through an alternately spliced transcript termed inhibitory PAS domain protein [215]. Table 15. gives an overview of some HIF-regulated genes (adapted from Semenza et al. [216]).

Aside from pVHL-mediated degradation, reports have shown that p53 can promote Mdm-2 mediated ubiquitination and proteasomal degradation of HIF-1 α through direct interaction with HIF-1 α in hypoxia [217]. The inhibitory PAS domain (IPAS) protein is also reported to target HIF-1 and plays a role as a negative regulator of the hypoxia induced gene expression. The expression of IPAS in hepatoma cells impairs the induction of genes under hypoxic conditions, notably the VEGF gene, and results in retarded tumour growth and tumour

vascular density *in vivo* [215]. Under hypoxic conditions, HIF- α is stabilised and exerts its transcriptional activity by binding to the p300/CBP, SRC-1 (steroid receptor co-activator-1) family co-activators, nuclear redox regulator Ref-1, and molecular chaperone heat shock protein 90 (HSP90) [218-220]. The HIF-1 α -mediated transcriptional regulation is synergistically enhanced by p300/CBP, SRC-1 and Ref-1. The control of HIF-1 α stability by post-translational modification or protein-protein interaction appears to be essential for the transcriptional activity of HIF- α (Fig.45).

Table 15. Examples of Genes regulated by HIF-1
Genes
Growth factor related Endocrine gland-derived VEGF Erythropoietin IGF-II IGF-binding protein I/II/III TGF β 1 VEGF
Receptors FLT-1 α 1B-adrenergic receptor CxCR4
Glucose metabolism Aldolase A (ALDA) Aldolase C (ALDC) Enolase I Glucose transporter 1 Glucose transporter 3 Glyceraldehyde-3-P-dehydrogenase Hexokinase 1 Hexokinase 2 Phosphoglycerate kinase 1 Lactate dehydrogenase A (LDHA) Pyruvate kinase M (PKM)
Others related in vascular growth and metabolism Adenylate kinase 3 Adrenomedulin Ceruloplasmin Collagen type V, α 1 Endothelin-1 ETS-1 Haeme oxygenase-1 LDL receptor-related protein 1 Nitric oxide synthase 2 p21 p35srj plasminogen activator inhibitor 1 (PAI-1) Prolyl-4-hydroxylase α 1 Transferrin Transglutaminase II

In addition to the abovementioned interactions, HIF α has also been shown to bind Jab-1, a protein originally described as a transcriptional co-activator of c-Jun and Jun D [28]. Jab-1 plays a role in a variety of signalling pathways. These include integrin signalling, cell cycle control, and steroid hormone signalling [221-223]. This protein is also known as a subunit, CSN5, of the mammalian COP9 signalosome (CSN) complex, a highly conserved protein complex implicated in diverse biological functions that involve ubiquitin-mediated proteolysis. This subunit has been shown to phosphorylate transcriptional regulators such as c-Jun, I κ B, p105 and p53 [224-226]. Bae *et al.* demonstrated that Jab-1 interacts with the ODD domain of HIF-1 α and in this way may control HIF-1 α stability and activity by competition with p53. The interaction of Jab-1 with HIF-1 α contributes to the up-regulation of the HIF-1 α protein level under hypoxic conditions. However, under normoxia, Jab-1 has no effect on the up-regulation of the HIF-1 α protein level. This is due to the strong affinity of pVHL for HIF-1 α , which leads to the rapid degradation of HIF-1 α . p53 directly interacts with the ODD domain of HIF-1 α and down-regulates the hypoxia-induced expression of HIF-1 α by promoting the ubiquitination of HIF-1 α under hypoxic conditions but not under normal oxygen conditions [114, 217]. The Jab-1 mediated stabilisation of HIF-1 α might therefore, by directly interfering with the HIF1 α -p53 interaction, play a central role in HIF regulation under hypoxic conditions.

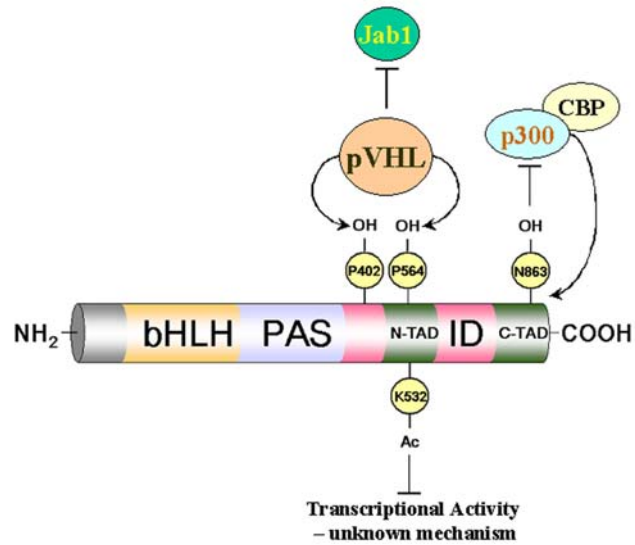


Figure 45. Post-translational control of HIF1 α . Modifications and protein interactions are explained in the text.

Another protein that has been shown to interact with HIF-1 α is ARD1, an acetyltransferase [23]. While there is only one report regarding ARD1 regulation of Hif α , the evidence reported by Jeong *et al.* in *Cell* convincingly describes acetylation of HIF-1 α by ARD1, and that this modification is important in HIF α regulation. Acetylation is found in various proteins, including histones, ERF1, MyoD, GATA-1 and p53 [227-230]. The authors showed that ARD1 binds HIF-1 α more strongly under normoxic conditions than under hypoxic conditions. The over-expression of ARD1 significantly decreases HIF-1 α protein stability, whereas the down-regulation of the ARD1 level with anti-sense ARD1 transfection increases the stability of HIF-1 α . This suggests that ARD1 functions as a negative regulator of HIF-1 α . ARD1 acetylates lysine 532 in the ODD domain of HIF-1 α .

Interestingly, it has been previously reported that lysine 532 is critical for the degradation of HIF-1 α under normoxia [27]. Although it is unclear how the ARD1-mediated acetylation of HIF-1 α leads to its decreased stability, it is proposed that a conformational change of HIF-1 α by the acetylation may effectively facilitate its interaction with pVHL and enhance the subsequent proteosomal ubiquitination of HIF-1 α .

4.5.1 HIF and regulation by protein hydroxylation

As already mentioned, recent analysis of post-translational modifications that mediate processes involving HIF stability has revealed a direct interface with the availability of oxygen through a series of non-haeme, iron-dependent oxygenases that hydroxylate specific HIF- α residues in an oxygen-dependent manner [11-13, 17, 210, 211, 231]. Hydroxylation at two proline residues (Pro402 and Pro564 in human HIF-1 α) mediates interactions with pVHL and the subsequent E3 ubiquitin ligase complex that targets HIF- α for proteasomal destruction (Fig.46). Each site can interact independently with pVHL, potentially contributing to the extremely rapid proteolysis of HIF- α that is observed in oxygenated cells [7]. These sites contain a conserved LxxLAP motif and are targeted by a newly defined prolyl hydroxylase activity that in mammalian cells is provided by three isoforms termed PHD (prolyl hydroxylase domain) 1–3. Determining the relative importance of different PHD isoforms in the regulation of HIF- α and other potential hydroxylation targets is the subject of active research. In a second hydroxylation-dependent control, β -hydroxylation of an asparaginyl residue in the C-terminal activation domain of HIF- α (Asn803 in human HIF-1 α) is regulated by a HIF asparaginyl hydroxylase termed FIH (factor inhibiting HIF) [17, 19]. Hydroxylation at this site blocks interaction of the HIF- α C-terminal activation domain with the transcriptional co-activator p300.

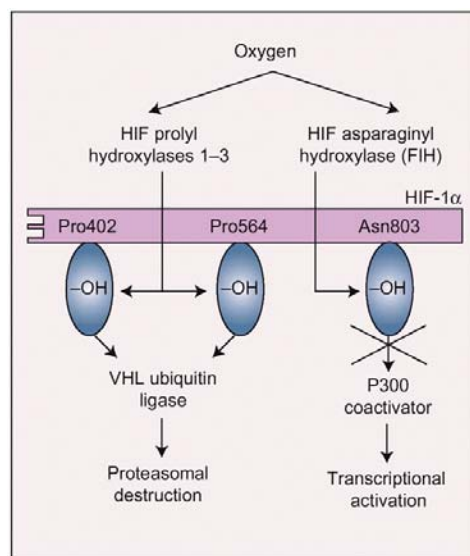


Figure 46. Dual regulation of HIF- α subunits by prolyl and asparaginyl hydroxylation.

Hydroxylation sites are indicated for the human HIF1 α polypeptide.

Adapted from Pugh et al. 2003

In oxygenated cells, these hydroxylation reactions provide a dual mechanism of HIF inactivation that involves proteolytic destruction and inhibition of transcriptional activity. The HIF hydroxylases are all Fe(II)- and 2-oxoglutarate-dependent dioxygenases that have an absolute requirement for molecular oxygen, allowing HIF to escape inactivation in hypoxia. The enzymatic process splits di-oxygen, with one oxygen

atom creating the hydroxylated amino acid, and the other oxidising 2-oxoglutarate to succinate with the release of CO₂ [232]. Fe(II) at the catalytic centre is loosely bound by a 2-histidine-1-carboxylate coordination motif, and may be displaced or substituted by other metals, such as cobaltous ions, with loss of catalytic activity. Given the role of HIF in the regulation of genes involved in the process of angiogenesis, these findings therefore couple angiogenic regulation to metabolic demand through minimal pathways linking molecular oxygen availability, HIF hydroxylase activity, HIF-dependent transcription and angiogenic growth factor expression. They also account for the up-regulation of angiogenic growth factors by cobaltous ions and iron chelators and indicate a route to therapeutic manipulation of angiogenesis.

Characterisation of the HIF pathway has therefore provided a clear focus for the investigation of the role of hypoxia in angiogenesis associated with development, ischemic and hypoxic disease, and neoplasia. Nevertheless, hypoxia influences many other transcriptional pathways, such as those mediated by fos and jun, NF-κB and p53. How these pathways interface with HIF, and whether they involve different targets for currently defined and other predicted protein hydroxylases, is the subject of active investigation. Recent data implicating prolyl hydroxylation in the VHL-dependent ubiquitylation of subunit 1 of RNA polymerase II indicates that regulatory prolyl hydroxylation extends beyond the HIF system and is discussed in the following section.

4.6 Additional ubiquitination targets of pVHL

Reports are available which demonstrate evidence that, in addition to HIF α , pVHL targets other proteins for ubiquitin-mediated proteolysis. While strong genetic evidence is required to establish these substrates as physiologically relevant, they may represent novel aspects of VHL functioning. To date these targets include RNA polymerase II subunits, a subfamily of deubiquitinating enzymes, and activated atypical protein kinase C (table 16).

Table.16 Ubiquitination targets of the VCB-Cul2 E3 ligase

Function	Target	References
Transcription factor	Hypoxia inducible factor α	>100
RNA polymerase II subunit	Hyperphosphorylated RPB1	1
RNA polymerase II subunit	RPB7	1
Deubiquitinating enzymes	VDU-1 and -2	3
Kinase	Atypical protein Kinase C	2

* VDU – VHL-interacting deubiquitinating enzyme

4.6.1 Hyperphosphorylated-RNA polymerase II large subunit, hsRPB1

The finding originates from one group that had previously published work relating to the regulation of tyrosine hydroxylase (TH) by pVHL in rat pheochromocytoma (PC12) cells [233] [234]. Pheochromocytomas express high levels of tyrosine hydroxylase (TH), the rate-limiting enzyme in catecholamine²¹ biosynthesis. The initial observations involved stably transfecting PC12 cells with either wild type or mutated pVHL. It was shown that while wild type pVHL represses levels of TH mRNA and protein, a truncated pVHL mutant, pVHL(1-115), induces accumulation of TH mRNA and protein. The author's present evidence, which suggests that repression results from inhibition of RNA elongation at a downstream region of the TH gene. Hypoxia, a physiological stimulus for TH gene expression, alleviates the elongation block. A truncated pVHL mutant, pVHL(1-115), stimulates TH gene expression by increasing the efficiency of TH transcript elongation. This was the first report showing pVHL-dependent regulation of specific transcript elongation *in vivo*, as well as dominant negative activity of pVHL mutants in pheochromocytoma cells. Furthermore, in a separate report, the group published data demonstrating the first evidence that endogenous pVHL is a physiological regulator of

²¹ Catecholamines include adrenaline, noradrenaline and dopamine. Levels can be measured in blood and urine and elevations may be seen in pheochromocytoma

the catecholaminergic phenotype, thereby suggesting that loss of pVHL function may be causative in pheochromocytoma-associated hyper-catecholaminemia and arterial hypertension [234, 235].

The transition from transcription initiation to elongation involves phosphorylation of the large subunit (Rpb1) of RNA polymerase II on the repetitive carboxyl-terminal domain. The elongating hyper-phosphorylated Rpb1 is subject to ubiquitination, particularly in response to UV radiation and DNA-damaging agents. Regions of Rpb1 and the adjacent subunit 6 of RNA polymerase II (Rpb6) that share sequence and structural similarity with the domain of HIF-1 α that binds pVHL were identified. In agreement with the computational model, Kuznetsova *et al.* showed biochemical evidence that pVHL specifically binds the hyper-phosphorylated Rpb1 in a proline-hydroxylation-dependent manner, thereby targeting it for ubiquitination. The exact role that ubiquitination of hyperphosphorylated Rpb1 by pVHL plays in the function of the RNA polymerase complex remains to be determined. Because ubiquitination of Rpb1 occurs in a transcription-dependent manner, and because the abovementioned observations indicate that pVHL levels effect *in vivo* elongation of TH transcripts, the authors anticipate that ubiquitination of Rpb1 by pVHL complex is likely to regulate efficient transcript elongation through elongation-pause and –arrest sites of specific genes. In particular, given the above, it may be involved in the regulation of TH transcript elongation. This finding is interesting in light of already mentioned data regarding *in vitro* inhibition of the SIII transcriptional elongation complex, where it was suggested that pVHL actively competes for Elongin's B and C from this complex composed of Elongin's A, B and C.

Finally, the authors speculate as to a more universal role of the pVHL-Rpb1 interaction, and that gene regulation may not be limited to the TH gene alone. The authors present data that exhibit regulation of this interaction by UV-stress. Thus pVHL could play a role in the regulation of transcription complexes under conditions of DNA-damage, such as UV irradiation. Reports already exist regarding increased apoptotic susceptibility in pVHL-negative cells following UV treatment when compared to their pVHL wild-type expressing counterparts [236].

4.6.2 RNA polymerase II subunit hsRPB7

Using yeast two-hybrid technology, Na *et al.* showed that pVHL can directly bind to another RNA polymerase II subunit, human Rpb7, through its β -domain [237]. Furthermore, they demonstrated that naturally occurring mutations in this domain could decrease binding. Introducing wild-type pVHL into human kidney tumour cell lines

carrying endogenous mutant non-functional pVHL facilitates ubiquitination and proteasomal degradation of Rpb7, and decreases its nuclear accumulation. pVHL can also suppress Rpb7-induced VEGF promoter transactivation, mRNA expression and VEGF protein secretion.

Three dimensional structural studies of yeast Pol II have revealed that the Rpb4-Rpb7 sub-complex is located between the two major domains that form the DNA-binding cleft of the Pol II complex and suggested that Rpb7 might be involved in inducing tighter closure of the DNA-binding cleft and thus stabilising the Pol II complex [238]. This may help explain why Rpb7 is important in the initiating transcription for a subset of genes during the stress response. How Rpb7 is regulated during the stress response could be crucial for understanding how Pol II functions in the regulation of gene expression.

Together with the finding that pVHL can target another RNA pol II subunit, Rpb1, for proteasomal degradation, indicates that pVHL could regulate gene expression through RNA Pol II subunits [239]. It would be important to identify other genes that could be specifically regulated by Rpb7 other than VEGF, as well as determining their roles in tumourigenesis.

4.6.3 VHL-interacting deubiquitinating enzymes

Following a yeast two-hybrid aimed at identifying pVHL interacting proteins, a novel protein named VHL-interacting deubiquitinating enzyme 1 (VDU1) was identified as being able to directly interact with pVHL *in vitro* and *in vivo* [240]. In a follow-up report, the same group showed that another uncharacterised deubiquitinating enzyme, VDU2, is also bound to pVHL [241]. Based on human and mouse cDNA sequences, VDU1 and VDU2 are identical in approximately 59% of the amino acids with strong homology in the N-terminus and C-terminus and a weaker similarity in the middle region. Both deubiquitinating enzymes contain the signature motifs of the ubiquitin-specific processing protease family and possess deubiquitinating activity. They interact with pVHL β -domain and naturally occurring mutations in this region effect binding. It was also demonstrated that these two proteins can compete with each other to bind to pVHL. Finally, they showed that VDU1 and VDU2 can both be ubiquitinated and degraded in a pVHL-dependent manner. Based on their amino acid sequence homology and functional interaction with pVHL, VDU1 and VDU2 define a subfamily of ubiquitin specific processing proteases. Since deubiquitination, by reversing ubiquitination, has been recognised as an important regulatory step in ubiquitination-related processes, VDU1 and VDU2 could be important substrates of pVHL E3 ligase complex.

Furthermore, Curcio-Morelli *et al.* demonstrated deubiquitination of type 2 iodothyronine deiodinase by enzymes VDU1 and VDU2, and they provide evidence to show that this interaction could help regulate thyroid hormone activation [242]. The type 2 iodothyronine deiodinase (D2) is an integral membrane ER-resident selenoenzyme that activates the pro-hormone thyroxine (T4) and supplies most of the 3,5,3'-triiodothyronine (T3) that is essential for brain development. D2 is inactivated by selective conjugation to ubiquitin, a process accelerated by T4 catalysis and essential for the maintenance of T3 homeostasis. D2 interaction with VDU1 and VDU2 was confirmed in mammalian cells. Both VDU proteins co-localise with D2 in the ER, and their co-expression prolongs D2 half-life and activity by D2 deubiquitination. VDU1, but not VDU2, is markedly increased in brown adipocytes by noradrenaline or cold exposure, further amplifying the increase in D2 activity that results from catecholamine-stimulated *de novo* synthesis. Thus, deubiquitination regulates the supply of active thyroid hormone to brown adipocytes and other D2-expressing cells. The present studies identify D2 as the only known specific substrate of VDU1 and VDU2, which in turn are the first ubiquitin-specific processing proteases known to specifically deubiquitinate an ER-Associated Degradation (ERAD) substrate. Although no functional significance is implied with respect to presence or absence of pVHL, it is interesting to note that pVHL has been shown to partially localise to the ER which might suggest a functional relevance. It is tempting to speculate that pVHL could be involved in down-regulating the deubiquitinating pathways controlled by VDU1 and VDU2. The authors also raise the interesting possibility of these deubiquitinating enzymes being able to deubiquitinate already ubiquitinated substrates of the VCB-Cul2 E3 ligase, i.e. Hif- α , thereby modifying the ubiquitinating capacity of the ligase depending on certain stimuli. While no evidence exists, it has been suggested that pVHL itself undergoes ubiquitin-mediated proteasomal degradation. An interesting question to address is whether regulation of VDU's can facilitate re-employment of ubiquitinated pVHL in cases where it is necessary, and what, if any, would be the pathological outcomes of aberrations in this system.

4.6.4 Atypical protein kinase C

Pal *et al.* were the first group to propose a model of pVHL and PKC functional interaction [243]. They suggested that the well-vascularised tumours associated with VHL disease could, in part, be explained by the fact that under normal conditions, pVHL inhibited protein kinase C (PKC) activity. They demonstrated that when over-expressed, PKC isoforms ζ and δ formed cytoplasmic complexes with pVHL preventing recruitment of these isoforms to the cell membrane where they would otherwise engage in a signal transduction mechanism leading to VEGF up-regulation. Aberrations in this regulatory pathway could therefore result in up-regulation of VEGF, as seen in VHL-associated tumours [243]. In a follow up paper the same group described experiments

demonstrating that the transcription factor Sp1, when bound to a PKC ζ , promotes the transcription of VEGF through phosphorylation of the zinc finger of Sp1 [244]. Interestingly, in the presence of wild-type pVHL, this interaction was shown to be inhibited, and VEGF transcription subsequently repressed. However, these experiments all entailed over-expression studies, and no endogenous interaction of PKC isoforms and pVHL had been shown.

An independent study has confirmed a pVHL-PKC interaction [245]. In their study, Okuda *et al.* demonstrated that pVHL could directly interact with atypical PKC isoforms (aPKC) ζ and λ . They demonstrated that interaction with these two isoforms was mediated through the β -domain of pVHL. It wasn't until a follow up paper from the same group emerged however, that evidence was reported demonstrating that these aPKC isoforms could represent ubiquitination targets of pVHL. They showed that PKC λ is ubiquitinated by the VCB-Cul2 E3 ligase complex, demonstrating ubiquitination of PKC λ *in vivo* and *in vitro*, and that pVHL mediates the ubiquitination of the recombinant activated form of PKC λ through an interaction with the regulatory domain of PKC λ . These results strengthen their previous finding. Together, these results strongly suggest that the VCB-Cul2 complex is responsible for the down-regulation of activated aPKC via the ubiquitin-proteolytic pathway, which terminates aPKC-mediated cellular signalling.

Ubiquitination and degradation of proteins often depend on post-translational modifications. Target proteins for the SCF complex-type ubiquitin ligases, such as β -catenin, p27^{kip}, and I κ B, are recognised by F-box proteins only when phosphorylated at defined amino acid residues [188]; [246]. This molecular mechanism allows quick, phosphorylation-dependent degradation of proteins, which plays crucial roles in the regulation of the cell cycle, growth, and differentiation. As already mentioned, degradation of HIF- α , a target of VCB-Cul2 ubiquitin ligase, is dependent upon a molecular oxygen-mediated hydroxylation event at specific HIF- α residues, which is prevented under hypoxic conditions. Based on this, we are forced to ask how then does pVHL recognise active aPKC? To date, this question remains unanswered.

Contribution of aPKC in the formation of tight junction and actin filament organisation has been reported [247]; [248]. It is interesting to note that pVHL has also been shown to be involved in such cellular events. Ectopic expression of pVHL in VHL-deficient renal cell carcinoma cells induces the formation of focal adhesions and stress fibers, as well as β 1-fibrillar adhesions [249]; [250]. pVHL is also involved in the establishment and maintenance of contact inhibition of cell growth [251]. Taken together, these observations support the idea that some of pVHL's functions as a tumour suppressor are attained at least in part by the control of aPKC activity. Given the

preferential pVHL interaction and ubiquitination/degradation of the active form aPKC, one might predict that the loss of pVHL function leads to the endurance of activated aPKC, which may cause disorders in cytoskeletal organisation and cell-substrate and cell-cell interaction as are commonly observed in tumorigenic cells. This topic is further discussed in the following chapter.

4.7 Alternative pVHL interactions

4.7.1 pVHL interacts and stabilises microtubules

A novel function of pVHL emerged from our laboratory, and as a co-author of this paper published in *Nature Cell Biology* in 2003, contributory results pertaining to this study are outlined in the results section of this thesis. pVHL was shown to specifically bind microtubules through a region in pVHL defined as residues 95-123. This region constitutes part of the α -domain through which Elongin C binds to pVHL. Interestingly a microtubule-pelleting assay in which both endogenous pVHL₃₀ and pVHL₁₉ co-sedimented with polymerised microtubules, showed no other E3 ligase complex components. This suggests that this function of pVHL is independent from its ligase activity. Endogenous immunoprecipitation of pVHL₃₀ showed co-precipitation of α -tubulin in HCT116 cells. Furthermore, integrity of the microtubule network proved to be important with respect to pVHL localisation. Microtubule stabilising and destabilising drugs were used to show that when microtubules are stabilised, pVHL remains cytoplasmic and microtubule-bound. However using vincristine or some other microtubule destabilising drug renders a strong pVHL signal in the nucleus, with concomitant reduction in cytoplasmic signal. It is still not clear whether these differences in localisation patterns reflect an active migration of pVHL into the nucleus upon microtubule destabilising conditions, or whether an active degradation of cytoplasmic pVHL under destabilising conditions occurs. Given the evidence available regarding the ability of pVHL to shuttle in and out of the nucleus in a ran-mediated, exon 2-dependent fashion, it would not be surprising if pVHL could actively move to the nucleus upon microtubule destabilising conditions. This idea will be further explored in chapter 7, part II.

To address the functional significance of pVHL binding to microtubules, and given the fact that stability of the microtubule network is important for pVHL localisation, an assay was established which investigated the potential of ectopically expressed GFPVHL₃₀ to protect microtubules under what would normally be destabilising conditions. The results showed that GFPVHL₃₀ does indeed protect microtubules, but that binding alone was not sufficient to induce this effect as certain VHL point mutants bound, but did not stabilise. Importantly, upon analysis, the point mutants which did not stabilise, could be all classed clinically as those mutants related to type 2A VHL disease, i.e. Y98H and Y112H (with the exception of one type 2C; F119S). A single, but specific amino acid mutation is sufficient. Even Y98N and Y112N retained their stabilising capabilities. Type 2A patients exhibit predisposition to pheochromocytoma and haemangioblastoma but a reduced risk to renal cell carcinoma. The correspondence between type 2A mutants and microtubule stabilisation might suggest a contributory

causal role on behalf of the microtubule network regarding development of malignancies associated with this sub-class of VHL disease, or that the mutational effect somehow mitigates against the RCC predisposition? Trying to explain how this can correlate with the high risk of RCC associated with completely inactivating VHL mutations is difficult. It has been however suggested that as type 2A mutants bind microtubules, perhaps they act as dominant-negative versions of their normally tumour suppressing wild-type counterparts. In this regard, and as postulated in the paper, they could be viewed as oncoproteins.

Due to the difference in localisation of pVHL₃₀ and pVHL₁₉, it might also be suggested that the different translation products, while both capable of binding microtubules and in recruiting HIF α to the VCB-Cul2 complex, differ in their functions due to their sub-cellular locations. As pVHL₁₉ predominantly localises to the nucleus, perhaps it represents the main HIF targeting pVHL species while pVHL₃₀, which demonstrates predominant cytoplasmic localisation, may represent the microtubule binding species. Evidence for pVHL₁₉ acting as a nuclear E3 ligase has already been confirmed [208]. If this is indeed the case, then a functional difference between pVHL₁₉ and pVHL₃₀ has for the first time been described.

4.7.2 TAT-binding protein-1 (TBP1); An ATPase involved in HIF- α degradation

Recently a study emerged by Corn *et al.* demonstrating a novel interaction between the β -domain of pVHL and TAT-binding protein-1 [252]. TBP-1 is a core component of the 19S regulatory particle of the 26S proteasome. The 19S particle contains six ATPases, including TBP-1, that belong to the ATPases-associated-with-different-cellular-activities (AAA) family [252]. The precise role of these ATPases in proteasome function is unknown, but they are thought to mediate the hydrolysis of ATP that is required for proteasome-mediated degradation of intracellular proteins [253]; [254]. In addition, the 19S regulatory particle seems to recognise poly-ubiquitinated substrates and is involved in both the unfolding of target proteins and their subsequent translocation into the 20S proteolytic core [253]; [254]. Three principal observations from their data help to characterise the functional consequences of the pVHL-TBP-1 interaction. First, the ability of TBP-1 to promote Hif-1 α degradation requires an intact ATPase domain, suggesting that this is an energy-dependent process. Second, TBP-1 enhancement of Hif-1 α degradation depends on wild-type pVHL function. Third, TBP-1 does not seem to affect the regulation of ubiquitinated proteins generally, but rather regulates the pVHL E3 ubiquitin ligase pathway in a relatively specific manner. These data support a model in which the 19S regulatory particle acts as a chaperone that promotes substrate unfolding and translocation of target proteins into the 20S proteolytic core [253]; [255]. In

summary, these data suggest a model for the role of TBP-1 in the pVHL-mediated degradation of Hif-1 α . After hypoxic stress in normoxia, wild-type pVHL exists in a complex with Hif-1 α , TBP-1, elongin C and Cul-2 that ubiquitinates Hif-1 α and targets it to the proteasome for degradation. In contrast, complexes containing a pVHL mutant that does not bind TBP-1 (for example, pVHL-P154L) no longer effectively chaperone Hif-1 α to the proteasome, resulting in impaired degradation of Hif-1 α . These results thus provide a novel mechanism for Hif-1 α stabilisation in some pVHL-deficient tumours. Interestingly, a proteomics approach has identified another member of the AAA-family of ATPases which interacts with pVHL, namely p97. This will be discussed in detail in chapter 7.

4.7.3 Tric/CCT; a protein chaperonin involved in VCB assembly

Feldmann *et al.* demonstrated in 1999 that the folding and assembly of VHL into a complex with its partner proteins, elongin B and elongin C, is directly mediated by the chaperonin TRiC, also called CCT [256]. The authors provide evidence which shows that the association of pVHL with TRiC is required for formation of the VHL-elongin B-elongin C complex. They demonstrate that a 55-amino acid domain of pVHL (amino acids 100 to 155) is both necessary and sufficient for binding to TRiC. Hansen *et al.* investigated this interaction further and demonstrated that blocking the interaction of pVHL with elongin B/C resulted in accumulation of pVHL within the TriC complex [257]. pVHL present in purified VHL-TRiC complexes, when added to rabbit reticulocyte lysate, proceeded to form VCB and VCB-Cul2. The authors conclude that, TRiC thus likely functions, at least in part, by retaining VHL chains pending the availability of elongin B/C for final folding and/or assembly.

In 2003, Melville *et al.* used the yeast *Saccharomyces cerevisiae* as a model system to examine *in vivo* the chaperone requirements for assembly of the VBC complex. Human pVHL and elongin B/C expressed in yeast assembled into a correctly folded VBC complex that resembles the complex from mammalian cells. Unassembled VHL did not fold and remained associated with the cytosolic chaperones Hsp70 and TRiC/CCT, in agreement with results from mammalian cells [258]. Analysis of the folding reaction in yeast strains carrying conditional chaperone mutants indicates that incorporation of VHL into VBC requires both functional TRiC and Hsp70. VBC assembly was defective in cells carrying either a temperature-sensitive *ssa1* gene as their sole source of cytosolic Hsp70/SSA function or a temperature-sensitive mutation in CCT4, a subunit of the TRiC/CCT complex. Finally, Friedman *et al.* followed up their initial finding by showing that TRiC is specified by two short hydrophobic beta strands in VHL that, upon folding, become buried within the native structure [259]. These TRiC binding

determinants are disrupted by tumour-causing point mutations that interfere with chaperonin association and lead to mis-folding. The results reveal a class of disease-causing mutations that owing to their ability to disrupt chaperone-mediated folding *in vivo*, ultimately inactivate the protein function of pVHL.

4.7.4 von Hippel-Lindau binding protein – VBP1

Following a yeast 2-hybrid, Tsuchiya *et al.* found four clones; elongin C, the HIV tat-binding protein, the actin-binding protein Filamin (ABP280), and the HIBBJ46 protein they named VBP-1 [260]. They demonstrated that VBP-1 required the C-terminal end of pVHL for binding. It was also established that epitope-tagged pVHL strongly forms complexes with VBP-1 *in vivo*. VBP-1 was widely expressed in various cell lines tested, in which VHL mRNA can also be detected. When the VBP-1 protein was solely expressed, it located to the cytoplasm and did not localise to the nucleus. However, when co-expressed with pVHL, it could translocate to the nucleus. These results indicated that VBP-1 can form a complex with VHL protein *in vivo* and hence pVHL might affect the intracellular localisation of VBP-1 protein.

A recent study demonstrated functional analysis of VBP-1 in the nematode, *C. elegans* [119]. The *C. elegans* VBP-1 gene was expressed in adults only in the gonads and was also expressed in early stage embryos. Double-stranded RNA interference against VBP-1 resulted in an arrest of embryogenesis at morula stages. The authors suggest that the VBP-1 protein product is necessary for morphogenesis. However, since its identification, the significance of a pVHL-VBP1 interaction, if any, remains elusive.

Concluding Remarks

The identification of pVHL as a constituent of an E3 ubiquitin ligase represents a hallmark in VHL biology and served to pave the way for the identification of what is to date the most important aspect of pVHL functioning, proteolytic regulation of hypoxia inducible factor α . The implication of this interaction in the context of tumour growth and progression is the topic of discussion in the final chapter of this introduction. While other potential substrates outlined in this chapter may represent interesting novel aspects to the function of pVHL, the lack of physiological investigation renders these observations momentarily undeveloped. Finally, protein interactions, notably with microtubules, TBP-1 and PKC isoforms are beginning to highlight functions of pVHL separate from its role as a substrate recognition component of an E3 ligase, and may represent novel aspects of pVHL function.

CHAPTER 5

VHL and Tumourigenesis

5.1 Introduction

This chapter summarises current data regarding the role of VHL in tumourigenesis. By analysing animal models where VHL has been specifically targeted, it questions the concept of mutations in pVHL as a causal event in tumour formation and analyses the role of VHL in tumour progression. While HIF-dependency represents the principal mechanism of action underlying known VHL-mediated cellular events to date, efforts are made to highlight HIF-independent functions of *VHL*. The VHL tumour suppressor is emerging as an integral protein in key cellular events leading to cell proliferation, survival, angiogenesis, polarity, invasion and metastasis. This chapter aims at trying to summarise information available regarding these cellular phenomena.

5.2 VHL knockout and functional inactivation studies

To analyse the role of VHL in normal cell growth and differentiation, knockout studies aimed at specific inactivation of the VHL gene have been undertaken. The following section will focus on the complete knockout of the VHL locus and four subsequent studies that have emerged as a result of the need to develop an *in vivo* system for studying the functional requirement of the *VHL* gene.

5.2.1 Complete Knockout: VHL^{-/-}

Gnarra *et al.* developed a mouse line lacking *VHL* [261]. While heterozygous VHL^{+/-} mice appeared phenotypically normal and surviving 15 months without evidence of spontaneous disease, VHL^{-/-} mice died *in utero* at 10.5 to 12.5 days of gestation (E10.5 to E12.5). Homozygous VHL^{-/-} embryos appeared to develop normally until E9.5 to E10.5, when placental dysgenesis developed. Embryonic vasculogenesis of the placenta failed to occur in VHL^{-/-} mice, and haemorrhagic lesions developed in the placenta. Subsequent haemorrhage in VHL^{-/-} embryos caused necrosis and death (Fig.47). These results indicate that VHL expression is critical for normal extra-embryonic vascular development.

Among the earliest differentiation events in the mammalian embryo are those that direct cells to develop into the extra-embryonic tissues, the placenta, the yolk sac, and the amnion (Fig.48). The placenta is derived from trophoblast cells and mesodermal cells from the inner cell mass, and these cell types appear histologically normal in *VHL*-deficient mice. However, loss of normal VHL expression in the trophoblasts and mesodermal cells appears to account for the lack of vasculogenesis in the placenta, leading to placental failure, the major cause of embryonic lethality in *VHL*-deficient mice.

Negative regulation of VEGF expression by VHL is well established and has been demonstrated with respect to pVHL's ability to target HIF for ubiquitin-mediated degradation [114, 200]. HIF is a transcription factor capable of transcribing the VEGF gene. However, in this study, Gnarra *et al.* found VEGF expression to be decreased in *VHL*-deficient placental trophoblasts. This contradicts our understanding of HIF regulation by VHL and subsequent VEGF suppression. Consistent with constitutively active HIF, depletion of VHL should result in an up-regulation of VEGF as seen in *VHL* null tumours [262-264]. In the lethal phenotype observed upon *VHL* depletion in mice, this is however not the case. VEGF is down-regulated in *VHL*^{-/-} placental derived trophoblast cells, and embryos die due to a lack of vascularisation of the placenta. However, it has yet to be fully determined whether this decrease is directly related to VHL inactivation which would indicate an alternative form of regulation in placental trophoblasts than seen in vascular tumours related to VHL disease, or a secondary effect and an early indicator of placental failure.

It is interesting to note that mice deficient for VEGF or its receptors, VEGF-R1 and VEGF-R2, have been developed and show embryonic lethality by E9.5 to E11.5,

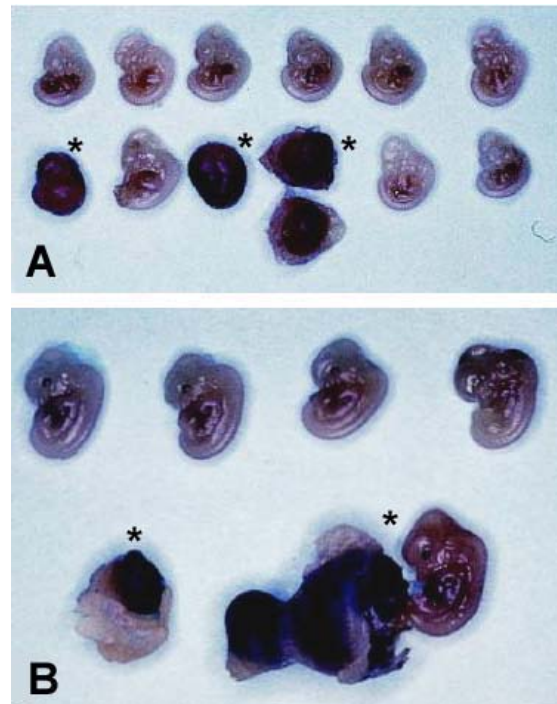


Figure 47. E12.5 embryos from an inter-cross of *VHL* +/- mice. (A) Three abnormal embryos of 12-litter (marked with asterisks). *VHL*^{-/-} embryos are necrotic, and one is shown with haemorrhagic placenta. (B) Another E12.5 litter demonstrating one abnormal embryo and another where the embryo appears normal but is attached to a haemorrhaging placenta.

Adapted from Gnarra et al 1997

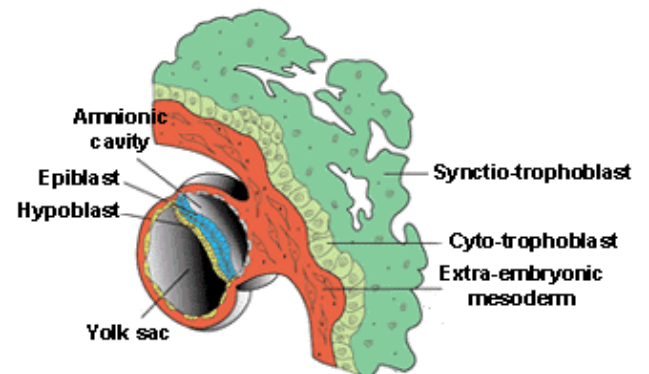


Figure 48. Early mammalian embryonic development. The trophoblast and mesoderm cells are important because they will connect the uterine wall to the embryo, develop into the chorion, and enable the mother to nourish the embryo by forming the placenta.

Adapted from: www.med.unc.edu/embryo

similar to the VHL-deficient embryos described above [265-268]. Lethality in VEGF and VEGF receptor mice appears to involve defects in vasculogenesis as well as haematopoiesis. Interestingly, VEGF heterozygous mice also show embryonic lethality by E10.5 to E11.5, indicating that gene dosage is important for VEGF [265, 268]. These results imply that the decreased VEGF levels seen in *VHL* homozygous embryos may play a contributory role in embryonic lethality, but mechanistically, how this is linked to loss of *VHL* remains unclear.

5.2.2 Heterozygotic predisposition to tumourigenesis: VHL+/-

Chapter 3 explains that genotyping has shown that most, if not all, VHL tumours tested show inactivation of the inherited wild-type VHL allele and retention of the inherited inactivated allele, as predicted by Knudson. In trying to develop a model that would mimic the germ-line situation, Gnarra *et al.* in the aforementioned study observed that heterozygous *VHL* null mice in a C57BL/6 background lived beyond 15 months without evidence of significant disease. Further analysis of VHL mice beyond 15 months was necessary to provide a better understanding of the role of VHL in development and tumourigenesis, and has since emerged. The first evidence provided by Haase *et al.* who contradicted the previous findings, demonstrated that clinical features of VHL disease can indeed be reproduced by targeted mutagenesis of *VHL* in mice [269]. They generated a conditional VHL null allele (2-lox allele) and null allele (1-lox allele) by Cre-mediated recombination in embryonic stem cells. They demonstrated that heterozygote mice for the 1-lox allele develop cavernous haemangiomas of the liver.

Their findings demonstrated that mice heterozygous for a *VHL* null mutation are susceptible to the development of spontaneous vascular tumours, reminiscent of those found in VHL patients. However, the authors are keen to admit that the discrepancy between their observation and the previously reported findings in heterozygous *VHL* knockout mice may result from differences in genetic background. It is well established that differences in genetic background can account for variable phenotypic penetrance of targeted null mutations [270]. The conditional inactivation of the *VHL* gene was carried out in the livers of BALB/c mice. Nonetheless, in contrast to the variety of tumours that arise in the human disease, the tumour spectrum and location in mice were restricted to cavernous haemangiomas of the liver. The authors speculate that in VHL+/- mice, hepatocytes are particularly susceptible to loss or inactivation of their wild-type *VHL* allele. The nature of this inactivation was not ascertained. Furthermore, it remains unclear why vascular tumours in mice occurred in the liver only and why, in contrast to humans, other VHL-associated tumours such as RCC could not be found. It is possible that the development of RCCs in VHL+/- heterozygotes may require additional mutations in other tumour suppressor or modifier genes [271]. Nonetheless, the study shows that inactivation of *VHL* leads to the up-regulation of VEGF, Glut-1, and Epo mRNAs, as well as stabilisation of HIF-2 α in hepatocytes. This finding suggests that pVHL acts as a

global regulator of HIF- α stability, and not only a regulator in VHL disease effected tissues. This points to a more general role of pVHL in the regulation of HIF- α .

Interestingly, two recent reports supporting the above study have been published. Ma *et al.* have undertaken attempts to generate a mouse model that closely mimics the human VHL disease and avoids embryonic lethality by using similar Cre/lox site-specific recombination technology. Under the control of the β -actin promoter, which drives expression in many organs, mice have been shown to develop multiple, hepatic haemangiomas that lead to premature death, as well as angiectasis²² and angiogenesis in multiple organs, including pancreas, kidney, spleen and heart. Furthermore, testes were shown to be unusually small and very low in sperm count resulting in infertility, which represents a potentially novel function of VHL in the process of spermatogenesis. Importantly the authors note that the differences in phenotypic consequence of the heterozygous VHL deleted allele, which were observed among three different mouse strains, suggest that strain-specific modifier genes may provide protection against the formation of hepatic haemangiomas as observed in C57BL/6 mice, or may enhance the development of the vascular phenotype as seen in BALB/c or A/J mice.

The most recent study involving the investigation of whether *VHL* heterozygote mice (*VHL*+/-) exhibit increased susceptibility to tumourigenesis, was published by *Kleyменова et al* [272]. They tested whether *VHL*+/- mice would demonstrate increased susceptibility to renal carcinogenesis when treated with the well-characterised renal carcinogen, streptozotocin. Neither Wild-type nor *VHL*+/- mice exhibited an increase in renal lesions in response to 50-200 mg/kg streptozotocin, however *VHL*+/- mice did develop vascular proliferative lesions of the liver, uterus, ovary, spleen, and heart. Lesions included angiectasis and haemangiosarcoma²³, and were most prominent in the liver. These data along with the previous two studies indicate that heterozygosity at the *VHL* locus predisposes mice to a vascular phenotype, which is consistent with the ability of *VHL* to control key proteins that participate in angiogenesis.

The absence of a kidney phenotype in *VHL* heterozygotes contrasts sharply with mice heterozygous for the *TSC-2*²⁴ tumour suppressor gene. *TSC-2*+/- mice develop spontaneous renal cell tumours with an incidence of 100% by 10 months of age [273, 274]. It is not clear why mice are refractory to *VHL*-related kidney tumours and susceptible to *TSC-2*-related renal cell tumours. This predisposition to renal tumours in *TSC-2* heterozygous mice is especially interesting in light of recent data showing that similar to loss of *VHL* function, loss of *TSC-2* gene function also results in stabilisation of HIF α and increased expression of VEGF [275, 276]. Consistent with stabilisation of HIF-2 α in *TSC-2*-null tumours, *TSC-2* knockout mice also develop hepatic haemangiomas

²² Angiectasis – dilation of lymphatic or blood vessel

²³ haemangiosarcoma - rare malignant neoplasm characterised by rapidly proliferating, extensively infiltrating, anaplastic cells derived from blood vessels and lining irregular blood-filled spaces

²⁴ Tuberous sclerosis complex (TSC) is a human syndrome characterised by a widespread development of benign tumours. This disease is caused by mutations in the *TSC1* or *TSC2* tumour suppressor genes (reviewed in [18])

similar to those that occur in VHL heterozygotes [273]. Interestingly, rats carrying the Eker²⁵ mutation in the TSC-2 gene (TSC-2^{EK/+}) that develop renal cell tumours also develop vascular lesions. Haemangiomas occur in a variety of organs, although these tumours arise predominately in the spleen [277], but unlike the situation in TSC-2 knockout mice, vascular proliferative lesions have not been noted in the hepatic parenchyma of TSC-2^{EK/+} rats.

In conclusion, due to the high degree of cellular heterogeneity in these tumours, neither Kleymenova, Kobayashi nor Haase were able to determine if loss of the wild-type VHL allele occurred in the vascular lesions that develop in VHL (or TSC-2) knockout mice. Although these efforts are continuing, the question of whether the vascular lesions that develop in VHL knockout mice are themselves clonal in origin and follow Knudson's 'two-hit' hypothesis remains an open question. Nonetheless, VHL^{+/-} mice should prove to be a useful model for increasing our understanding of the factors that contribute to vascular tumorigenesis as they provide an *in vivo* system with which to dissect and study the sequence of events leading from pre-neoplastic changes to tumour initiation and progression.

While biochemical and genetic evidence clearly demonstrate that pVHL regulates HIF α degradation to mediate normal cellular responses to changing oxygen concentration, it remains unclear whether deregulation of HIF α has a causal role for tumour formation when *VHL* is mutated. Studies investigating the tumour growth of RCC cell lines in nude mouse models support the idea of HIF-dependent tumour suppressor activities of pVHL. Inhibition of HIF-2 α expression by siRNA inhibits growth of VHL negative tumours [278], while re-introduction of a degradation-resistant mutant of HIF-2 α abolishes the ability of VHL to suppress growth of these cell lines [279]. While these studies display the importance of HIF-2 α in the growth of established tumour cell lines *in vivo*, they do not demonstrate that deregulation of HIF degradation is sufficient to induce *de novo* tumour formation. Importantly, VHL ablation in mouse embryonic stem cells results in smaller tumour formation than controls, in spite of displaying maximal HIF activity [280]. This observation suggests that loss of VHL may actually cause a growth disadvantage in an otherwise normal genetic background and implies that malignancies associated with inactivation of the VHL tumour suppressor may manifest only in the background of other genetic alterations, and are perhaps not solely attributable to loss of VHL. Therefore, in this setting, HIF activity alone is not capable of driving tumour progression. Furthermore, as already mentioned, while re-introduction of VHL into RCC cells eliminated tumour growth, these cells are known to harbour alternative genetic abnormalities [121, 263, 281]. Defining molecular mechanisms with respect to VHL

²⁵ Hereditary RCC occurs in Eker rats that are heterozygous for an insertion mutation in the TSC2 tumour suppressor gene, the Eker mutation. The germ-line mutation renders heterozygous mutants highly susceptible to renal carcinogens. The utility of this model in studying potential renal carcinogens is due to an ordered progression of proliferative renal lesions that can be identified and counted microscopically. The quantitative nature of the model allows for the production of statistically powerful data to understand the relative degree and potency of chemical effects and allow analysis of genetic alterations that may be chemical specific (reviewed in [22]).

alone in an already effected background is therefore difficult and requires caution. Moreover, several lines of evidence suggest that VHL has HIF-independent tumour suppressor functions, namely, a subclass of *VHL* mutations that retain the ability to induce HIF α degradation still predispose to pheochromocytoma-only (type 2C) VHL disease. These findings raise interesting questions as to whether VHL-related tumours are a consequence of aberrant VHL control of HIF α or rather a means of promoting growth advantage within a given genetic background.

5.3 VHL involvement in tumour growth

Development of malignancy requires that tumour cells undergo biological changes allowing them to proliferate, escape apoptosis, form new blood supplies, invade surrounding tissue and metastasise to distant sites. Recent evidence now suggest that VHL loss-of-function results in the deregulation of a number of signalling pathways that play key roles in one or more of these biological processes. The following sections outline VHL involvement in these events and the pathological consequence of its functional inactivation.

5.3.1 Angiogenesis

Figure 49 demonstrates how an angiogenic stimulus ‘activates’ endothelial cells lining an existing micro-vessel to dissolve their underlying basement membrane (BM), forming capillary sprouts in the perivascular connective tissue [282-284]. Key molecules in the angiogenic process are integrins, which might contribute to endothelial cell migration and survival, and proteases such as matrix metalloproteinases (MMPs), which degrade the BM and components of the perivascular

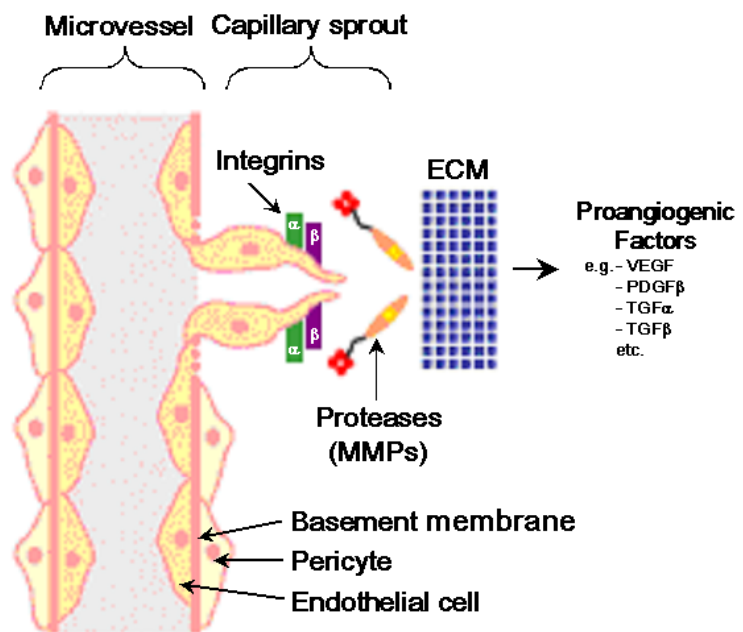


Figure 49. Initial stages of angiogenesis. See text for explanation. Adapted from Lafleur et al.2003

extracellular matrix (ECM) which facilitate liberation of angiogenic factors such as VEGF. VEGF increases vascular permeability, resulting in spillage of plasma proteins such as fibrinogen into the perivascular environment, which contributes to a provisional matrix for further vascular remodelling. Vascular sprouts elongate in the direction of the angiogenic stimulus as a result of the migration and proliferation of the endothelial cells proximal to the migrating front, and gradually form a lumen. Eventually they anastomose²⁶ with each other, forming capillary loops, thus allowing blood flow to begin. Angiogenesis is considered a key step in tumour progression implying a fundamental role for HIF in the later stages of tumour progression. However, the link between VHL loss, HIF activation, and how this relates to loss of growth control remains a key unanswered question.

²⁶ Anastomose - cause to join or open into each other by anastomosis, as of blood vessels

Targeted inactivation of either HIF-1 α or HIF-1 β in the mouse results in abnormal vascular development and embryonic lethality [285-288]. Despite marked reduction in VEGF expression by *HIF-1 α* ^{-/-} embryonic stem cells in hypoxic tissue culture, analysis of the developing *HIF-1 α* ^{-/-} embryos detected a surprising increase in VEGF mRNA expression. This suggests that compensatory stimuli may operate to induce VEGF, and that reduced vascular development may be mediated by other pathways.

Targeted inactivation of *HIF-2 α* results in quite different and variable phenotypes. Though one study showed a defect in vascular remodelling, differing phenotypes have been observed in three other studies [289-292]. The reason for variability is unclear, although it appears more likely to reflect differences in genetic background rather than incompletely inactivated *Hif-2 α* alleles. Overall, reports to date suggest that despite similar activity on HRE-linked reporter genes, HIF-1 α and HIF-2 α have important non-overlapping, non-redundant functions in the regulation of endogenous gene expression in development. The unexpected and variable phenotypes presumably reflect the complexity of these responses.

Experiments on cells bearing inactivating mutations in the HIF pathway have emphasised the importance of HIF (particularly HIF-1 α) on the regulation of genes involved in angiogenesis [200, 285, 286, 293, 294]. For a substantial number of these genes, promoter analysis has also clearly identified HREs that interact directly with HIF. The expression of other genes may be affected indirectly by secondary cascades of gene regulation. Even with respect to a single molecule, there may be many interfaces with hypoxia and hypoxia pathways. This is well-illustrated for VEGF (Fig.50). In hypoxia, VEGF transcription is up-regulated by HIF, mRNA stability is increased by binding of proteins to specific sequences in the 3' UTR, and an internal ribosomal entry site allows preserved translation in the face of normal cellular hypoxic shutdown [294-297]. The biological activity of secreted VEGF is further influenced by hypoxia-inducible expression of the VEGF-R1 receptor, post-transcriptional regulation of the VEGF-R2 receptor and VEGF-induced effects on soluble VEGF-R1, which inhibits VEGF action [298-300].

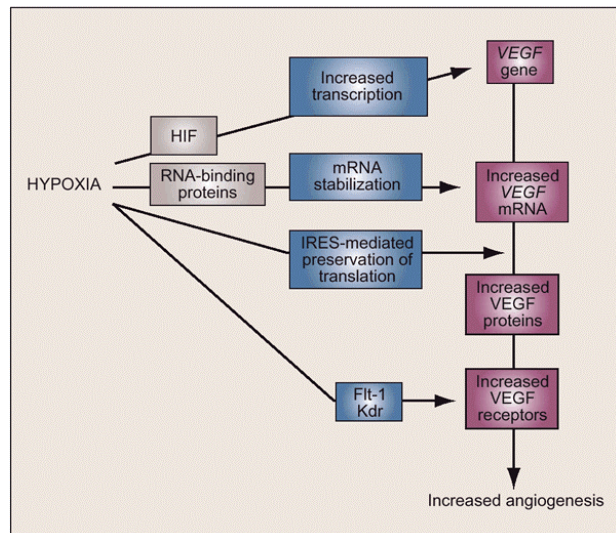


Figure 50. Multiple interfaces of hypoxia pathways with the angiogenic growth factor VEGF. IRES, internal ribosomal entry site. Flt-1 and Kdr are VEGF-R1 and -R2 respectively.

Adapted from Pugh et al. 2003

Microenvironmental activation of HIF in cancer occurs at the simplest level by physiological activation of the oxygen-sensitive pathways by hypoxia within the growing

mass of cells. Findings suggest that reduction of cellular iron availability, as well as hypoxia, may limit proline hydroxylase activity in cancer cells and contribute to the general activation of HIF in tumours.

5.3.2 Growth factors and enhanced cell proliferation

It has been shown that pVHL can suppress certain genes that are over-expressed in renal carcinomas. Some of these genes are proangiogenic genes, and help in our understanding of why VHL derived tumours are highly vascular, and also help us to understand mechanisms of VHL tumour invasion and metastasis. Overproduction of angiogenic factors, like VEGF, might explain why VHL negative tumours are so highly vascularised, but whether this overproduction is sufficient for oncogenesis still remains unknown. Some of these factors that have been implicated in VHL disease are described below.

A number of polypeptide growth factors that stimulate proliferation of normal cells have pathological consequences in tumourigenesis when deregulated. RCC cells lacking functional pVHL over-express various growth factors including PDGF β , VEGF and transforming growth factor (TGF)- α . The latter is a bona fide renal cell mitogen that activates the Ras-Raf-MAP kinase signalling cascade through its cognate EGF cell-surface receptor [301]. Overproduction of TGF- α in RCC cells, at least in part, is HIF-dependent and a major contributory event that confers growth advantage to these cells [302, 303]. Indeed, transgenic expression of TGF- α in mice leads to the formation of multiple renal cysts reminiscent of pre-neoplastic lesions of the human kidney [33, 304, 305]. These findings highlight a direct link between pVHL loss-of-function, activation of HIF and the ensuing deregulated production of a potent growth factor of renal epithelial cells.

5.3.3 Cell survival and apoptotic evasion

Several studies have associated loss of VHL function to decreased susceptibility of cells to undergo apoptosis and promote cell survival [200, 236, 306, 307]. Interestingly, while the molecular pathway(s) is unclear, tumour necrosis factor (TNF)- α , a 17 kDa pro-inflammatory cytokine, has been shown to promote HIF-1 α accumulation and this may involve a VHL-dependent step [308-311]. TNF- α is an endogenous mediator of inflammation and apoptotic cell death [312]. Jung *et al.* recently investigated TNF- α -induced HIF-1 α accumulation and demonstrated that an NF κ B-mediated event normally associated with inflammation and cell survival, caused protein accumulation in normoxic cells [313]. While the report fails to identify the mechanism of HIF-1 α accumulation, it is suggested that this might interfere with the pVHL-mediated HIF-1 α degradation process.

Further studies support the concept of a pVHL-dependent cytotoxicity in RCC cells to TNF- α [314, 315]. In particular it has been reported that RCC cells can be sensitised to TNF- α induced cytotoxicity by re-introducing wild-type VHL [315]. Interestingly, the authors highlight the fact that TNF-receptor engagement by TNF- α triggers the activation of atypical PKC (aPKC), which, through phosphorylation of IKK β , liberates NF κ B thereby initiating transcription of genes involved in apoptosis. pVHL has been shown to directly bind various aPKC isoforms and to target aPKC λ for ubiquitin-mediated degradation [245, 316]. Deregulation of this process may therefore have significant impact on NF κ B transcriptional activity, and ultimately represents a means of promoting a selective pressure for populations of cells lacking functional pVHL to survive under adverse environmental conditions.

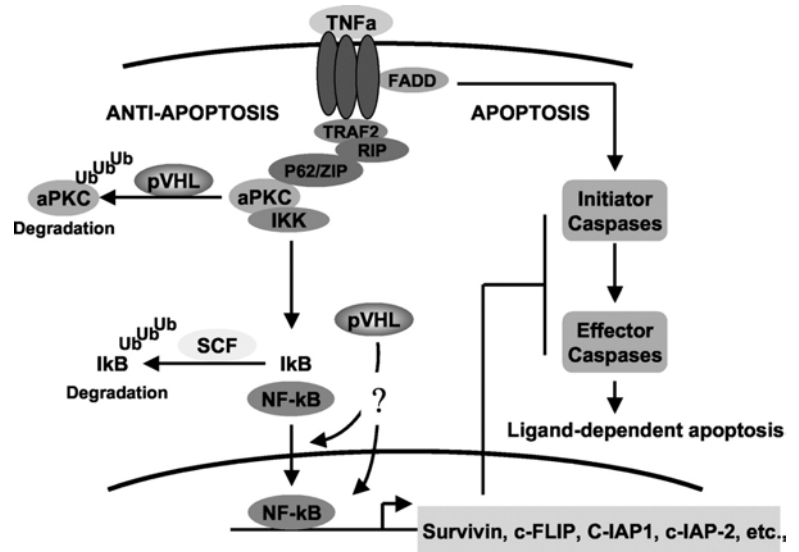


Fig. 51. Model of pVHL involvement in TNF- α -mediated signaling. TNF- α elicits apoptotic and antiapoptotic signals. In the apoptotic pathway, TNFR engagement of TNF- α triggers the activation of caspase-protease cascade leading to programmed cell death. In the anti-apoptotic pathway, TNFR engagement of TNF- α triggers the activation of aPKC, which is in a complex with TRAF2, RIP, and P62/ZIP. Activated aPKC phosphorylates IKK β , which phosphorylates I κ B, triggering its ubiquitination and subsequent degradation. This releases NF κ B from its inhibitor I κ B, allowing the translocation of NF κ B to the nucleus where it activates the transcription of numerous anti-apoptotic genes, including *c-FLIP*, *Survivin*, *c-IAP-1*, and *c-IAP-2*, which are inhibitors of caspases 8 and 3. Thus, completing the anti-apoptotic pathway. One possibility is that pVHL directly targets aPKC for ubiquitin-mediated destruction or pVHL affects the nuclear localisation and activation of NF κ B independent of pVHL-mediated degradation of aPKC.

Adapted from Jung et al. 2003

5.3.4 VHL and the extracellular matrix

Fibronectin is a multifunctional component of the extra-cellular matrix (ECM) that elicits intracellular signals that regulates cell adhesion, proliferation, differentiation, and tumourigenesis [317]. It is an extracellular glycoprotein that binds and signals through heterodimeric cell surface receptors known as integrins²⁷ [318]. Loss of fibronectin matrix organisation has been recognised for many years as a very important event in cellular transformation and is a common feature in most cancer cells. Fibronectin has the ability to decrease the metastatic behaviour of malignant cells by increasing the interaction

²⁷ Integrins are receptor proteins. They are the main way that cells both bind to and respond to the extracellular matrix. They are part of a large family of cell adhesion receptors that are involved in cell-extracellular matrix and cell-cell interactions. Functional integrins consist of two transmembrane glycoprotein subunits, called α and β , that are non-covalently bound. The α subunits all share some homology to each other, as do the β subunits. The receptors always contain one α chain and one β chain and are thus called heterodimeric. Until now 16 α and 8 β subunits have been identified. From these subunits some 22 integrins are formed in nature, which implies that not all possible combinations exist.

between tumour cells and their micro-environment via the integrin receptor family [319]. Several lines of evidence have demonstrated that pVHL interacts with fibronectin and is also responsible for the lack of extra-cellular fibronectin arrays in RCC cells lacking functional pVHL and in *VHL* negative mouse fibroblasts [134, 250, 320]. Although most disease-causing pVHL mutations hinder the regulation of the HIF pathway, every disease-causing pVHL mutant tested to date has failed to promote the assembly of the fibronectin matrix, underscoring its potential importance in VHL disease. Nevertheless, the exact nature of such an association and the mechanism by which *VHL* regulates the assembly of this ECM are poorly understood. It had been postulated that abnormally processed or misfolded fibronectin might accumulate inside cells in the absence of correctly functioning VHL, and that these aberrant fibronectin species, if secreted, could at least potentially interfere with the assembly of normal fibronectin. However, in a study by Esteban-Barragán *et al.*, failure to detect any accumulation of endogenous fibronectin in *VHL* negative cells, as assessed by Western blot of total and intracellular fibronectin, cast doubt on this hypothesis [250]. In addition, neither the use of exogenous normal fibronectin nor culture on fibronectin-coated coverslips improved the ability of VHL negative cells to organise extra-cellular fibronectin. From these findings, they suggest that the abnormal ECM organisation in VHL null RCC cells might require a different explanation. Moreover, they showed that $\alpha 3$, $\beta 1$, αv , and to a lesser extent, $\alpha 2$ and $\alpha 5$ integrins are up-regulated in VHL negative cells demonstrating that the altered assembly of the fibronectin matrix is not attributable to decreased integrin expression. These results are also consistent with the highly migratory phenotype that has been reported previously in VHL null RCC cells [136, 321].

Esteban-Barragán *et al.* demonstrated that the restored ability of VHL positive transfectants to assemble extracellular fibronectin is mediated by $\beta 1$ integrins because it is completely abrogated by $\beta 1$ -blocking antibodies. They propose that an abnormal organisation of $\beta 1$ -fibrillar adhesions²⁸ could help to explain the deficient fibronectin assembly of VHL negative cells. Nevertheless, they cannot formally rule out the possibility that an undetectable amount of abnormal fibronectin is accumulated and secreted in VHL negative cells, interfering with normal fibronectin assembly. Furthermore, the question still remains how VHL regulates the formation of $\beta 1$ -fibrillar adhesions and subsequent fibronectin organisation? VHL could regulate the expression or function of any of the intracellular constituents of the fibrillar adhesion. Given VHL's current role in cytoskeleton stabilisation, it could be modulating proteins, such as the small GTP-binding proteins Rho, Rac, and cdc42, which play an important role in the control of cytoskeleton and regulate the formation of cell-matrix adhesions?

²⁸ There are two major cell-matrix adhesions; focal and fibrillar adhesions. They not only differ in their morphology but also in their constituents. Classic focal adhesions are arrowhead shaped, contain αv or $\beta 1$ integrins, and are rich in talin and vinculin proteins. Conversely, fibrillar adhesions are elongated, contain exclusively $\beta 1$ -integrins, and possess low levels of vinculin and talin.

An interesting twist to this story has recently emerged in a report that a ubiquitin-like molecule called NEDD8 covalently modifies pVHL, and that a non-neddylatable pVHL mutant, while retaining its ability to ubiquitinate HIF, cannot bind to and promote the assembly of the fibronectin matrix. Furthermore, expression of the neddylation-defective pVHL in RCC cells, while restoring the regulation of HIF, was insufficient to suppress the formation of tumours in nude mice models. These results suggest that NEDD8 modification of pVHL plays an important role in fibronectin matrix assembly and that in the absence of such regulation, an intact HIF pathway is insufficient to prevent VHL-associated tumourigenesis.

5.3.5 VHL and cell polarity

Emerging evidence indicates an inhibitory role for pVHL in the regulation of components that have been implicated in establishing/maintaining cell polarity and directed cell migration, in particular protein kinase C (PKC) isoforms. Regulation of insulin growth factor (IGF)-I-mediated cell invasion of RCC cells appears to

be dependent upon PKC δ inhibition by pVHL. This inhibition is mediated through protein-protein interaction involving a domain of pVHL which shows similarity to protein kinase inhibitor (PKI), a natural inhibitor of cAMP-dependent protein kinase (PKA) (table 17) [322]. In contrast to protein-binding inhibition, evidence has shown that pVHL binds both atypical PKC isoforms λ and ζ through its β -domain, and in the case of activated aPKC λ , mediates its turnover as part of pVHL's function as an E3 ligase [245, 316]. While the functional significance of this inhibition remains elusive, given the central role for atypical PKC's, namely aPKC ζ , in establishing cell polarity in conjunction with PAR6 and the GTPase CDC42 [323], one could envisage a scenario whereby loss of pVHL leads to altered cell polarity, and by extension, aberrant cell migration.

Consistent with this above-noted view, pVHL₃₀ has been shown to co-localise with the microtubule network *in vivo* and to promote microtubule stabilisation [107]. Since microtubule dynamics have been intimately linked to the process of directed cell migration [323], this functional association may be an additional element of pVHL's tumour suppressing activity. Indeed, the microtubule stabilising function of pVHL is specifically disrupted by type 2A disease mutants that predispose to a defined tumour spectrum of haemangioblastoma and pheochromocytoma with a low predisposition to develop RCC. It is certainly tempting to draw parallels between the tumour suppressor

Table 17. Comparison of VHL with protein kinase inhibitor regions

Inhibitors	Amino Acid Sequence
PHK substrate	RQM-SFRL
VHL	⁹⁷ PYPTLP--PGTGRRIHSYRGH ¹¹⁵
PKI	TYADFIASGRITGRRNAI--HD
PKC δ	MNRRGAI-KQ

PHK substrate means substrate recognition sequence for phosphorylase kinase. PKI is the inhibitor sequence for cAMP-dependent protein kinase. Adapted from Datta et al. 2000

pathways regulated by pVHL and that by the adenomatosis polyposis tumour suppressor (APC) gene product, whose inactivation is the most frequently observed in hereditary and sporadic colon cancers [324]. Analogous to VHL, APC also binds to microtubules [323], and it has been shown that for APC this association culminates in cytoskeletal rearrangements and changes in cell polarity upon activation of the CDC42-PAR6-aPKC ζ

pathway (summarised in figure 52). Studies aimed at pVHL's role with respect to cell polarity and directed cell migration are therefore clearly warranted.

5.3.6 Branching morphogenesis and vasculogenesis

VHL has been implicated in the process of branching morphogenesis in the fly, *Drosophila Melanogaster*. Here Adryan *et al.* addressed the discrepancy between the fact that mutations in VHL predispose individuals to highly vascularised tumours, while VHL-deficient mice die *in utero* due to a lack of placental vascularisation. To help resolve the contradiction, Adryan *et al.* cloned the *Drosophila VHL* homologue (*d-VHL*) and studied its function [117]. The *Drosophila VHL* homologue has since been shown to bind complex components Cul2, Elongin's B and C, and Rbx1, and that this complex exhibits ligase activity towards the HIF-1 α homologue in flies [118]. Adryan *et al.* showed that during embryogenesis, *d-VHL* is expressed in the developing tracheal regions where tube outgrowth no longer occurs. Reduced *d-VHL* activity caused breakage of the main vasculature accompanied by excessive looping of smaller branches, whereas over-expression caused a general lack of vasculature. Importantly, human VHL can induce the same gain-of-function phenotypes. The authors suggest that VHL could be involved in halting cell migration at the end of vascular tube outgrowth. Loss of VHL activity could therefore lead to disruption of major vasculature, which requires precise cell movement and tube fusion, thus helping to explain the lack of placental vascularisation in VHL-deficient mice. Once the primary vascular structure is laid out, a lack of VHL activity, and hence excessive cell migration and branching, could possibly lead to over-

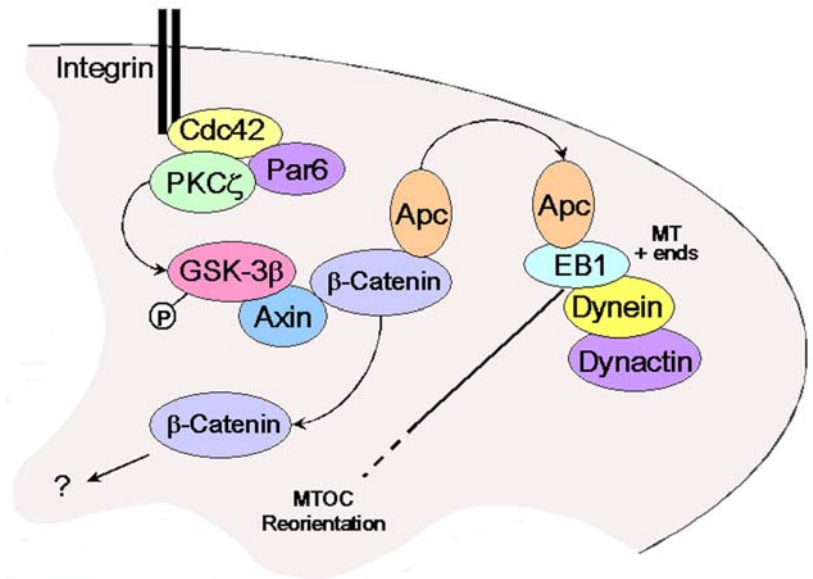


Figure 20. Downstream activating pathways of the Rho-GTPase family of proteins, which include Rho, Rac, and Cdc42, and their participation in cell polarity. Atypical PKC ζ forms a complex including Par6 and Cdc42. Etienne-Manneville *et al.* demonstrated, through the use of primary rat astrocytes in a cell migration assay, that Par6-PKC ζ interacts directly with and regulates glycogen synthase kinase-3 β (GSK-3 β) to promote polarisation of the centrosome and to control the direction of cell protrusion. Cdc42-dependent phosphorylation of GSK-3 β occurs specifically at the leading edge of migrating cells, and induces the interaction of the APC tumour suppressor protein with the plus ends of microtubules.

vascularisation, as observed in the secondary branches of drosophila and in human tumours.

Nonetheless, the question remains what is the true *in vivo* action of VHL in the vasculogenesis pathway? While *in vitro* its contributory role seems apparent, no evidence to date indicates a possible mechanism. Further analysis is necessary to explain these observations.

5.3.7 VHL and tumour cell invasion

Recently, important mediators of cell invasion were shown to be regulated by the pVHL tumour suppressor and these include hepatocyte growth factor (HGF) acting through the Met tyrosine kinase receptor [136, 321, 325-329]. Koochekpour *et al.* examined the HGF responsiveness of VHL-negative RCC cells and found that certain VHL-negative RCC cells were highly invasive and exhibited an extensive branching morphogenesis phenotype in response to HGF when compared to their wt-VHL expressing isogenic counterparts [136]. This same study demonstrated that VHL loss-of-function negatively regulates tissue inhibitor of metalloproteinase 2 (TIMP-2), resulting in the up-regulation of matrix metalloproteinases 2 and 9 (MMP2/9), thereby implicating pVHL in the control of these molecules. Matrix metalloproteinases (MMPs) are responsible for the degradation of ECM and have been associated with cellular invasiveness [330]. Importantly, it has been recently shown that hypoxia promotes tumour cell invasion by inducing the expression of the Met receptor [331]. This establishes a mechanism whereby transformed cells can be spurred to exit a hypoxic microenvironment and invade surrounding tissues, which provide more favourable growth conditions. Given the fact that HIF-1 α has been shown to be involved in Met gene expression, constitutive HIF-1 α activation as a consequence of pVHL deregulation provides a mechanism explaining the observation that expression of HGF and Met receptor is associated with genetic alterations of VHL in primary RCC. Hypoxic cell-sensitisation to HGF has therefore been proposed as an 'invasive switch' which facilitates cell movement away from an area of low oxygen availability, and is dependent on pVHL's ability to degrade HIF α .

5.3.8 VHL and tumour metastasis

Tumour cell migration and metastasis share many similarities with leukocyte trafficking, which is critically regulated by chemokines and their receptors. In a report by Müller *et al.*, the chemokine receptors CXCR4 and CXCR7 were shown to be highly expressed in human breast cancer cells, malignant breast tumours and metastases (Fig.51) [6] [332]. Breast cancer is characterised by a distinct metastatic pattern involving the regional lymph nodes, bone marrow, lung and liver. CXCR4 and CXCR7 respective ligands CXCL12/SDF-1 α and CCL21/6CKine exhibited peak levels of expression in organs

representing the first destinations of breast cancer metastasis. In breast cancer cells, signalling through CXCR4 or CXCR7 has been shown to mediate actin polymerisation and pseudopodia formation, and subsequently induces chemotactic and invasive responses. *In vivo*, neutralising the interactions of SDF-1 α /CXCR4 significantly impairs metastasis of breast cancer cells to regional lymph nodes and lung. Malignant melanoma, which has a similar metastatic pattern as breast cancer but also a high incidence of skin metastases, shows high expression levels of CXCR10 in addition to CXCR4 and CXCR7. Their findings indicated that chemokines and their receptors have a critical role in determining the metastatic destination of tumour cells, thereby fulfilling the chemoattraction theory of tumour metastasis. Interestingly, mice knockout studies of the CXCR4 gene exhibit defects in branching and/or remodelling of certain blood vessels [333]. Furthermore, VEGF has been shown to induce expression of CXCR4 supporting the notion that this chemokine receptor is important in remodelling the vasculature under hypoxia [334].

The gene encoding the chemokine receptor CXCR4 has been discovered as a novel HIF target based on microarray comparison of genetic profiles derived from VHL null RCC cells and their isogenic wild type VHL-expressing counterparts [321]. The fact that *CXCR4* is a hypoxia-inducible gene provided a potential mechanistic explanation for CXCR4 up-regulation during tumour cell evolution. CXCR4-induced surface expression due to VHL loss-of-function confers enhanced migratory potential to RCC cells in response to its cognate ligand stromal-derived factor 1 (SDF1). In addition, CXCR4 might be needed to promote the survival of tumour cells in a hypoxic environment. Thus, the ability of a cell to generate genetic programmes capable of evading unfavourable growth conditions is reflected at least in part by the up-regulation of CXCR4 in response to a hypoxic microenvironment. However, unlike the Met receptor, and perhaps other hypoxic responsive factors that promote cell motility and invasion, CXCR4, due to its chemotactic responsiveness to SDF1, might confer not only a migratory potential but also the

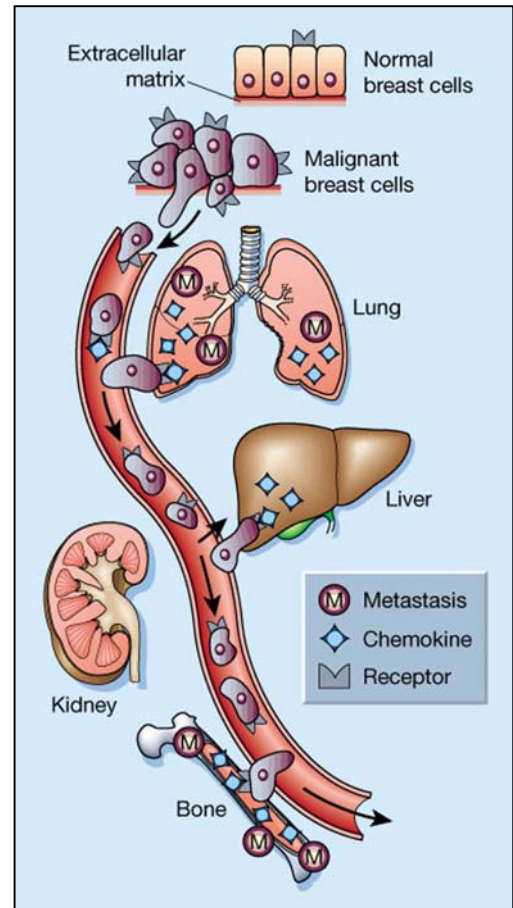


Figure 53. Targeted metastasis of primary breast cancer cells, according to the results of Müller *et al.* Compared with normal breast epithelial cells (top), their malignant counterparts are enriched for the surface expression of the chemokine receptor CXCR4. The chemokines (such as SDF-1 α) that recognise these receptors are released in high quantities only by certain organs, such as bone marrow, liver, and lung. Other organs, such as kidney, skin and brain, contain low amounts of these chemokines. Malignant primary breast cancer cells invade their underlying extracellular matrix and circulate in the blood and lymphatic systems. Breast cancer cells passing through those organs with large amounts of the chemokines will be attracted to leave the circulation and enter the organs. So the final distribution of metastases reflects the relative abundance of chemokines in the different organs, and represents the chemoattractive theory of metastasis. Adapted from Liotta *et al.* 2001

possibility of targeting migrating cells to specific secondary sites. Interestingly, strong CXCR4 expression can be correlated to poor tumour-specific survival in clear cell RCC, reflecting the metastatic potential of these tumours. This further implies that CXCR4 expression levels may influence the metastatic behaviour of these cells. The question remains however, whether CXCR4 up-regulation is a result of a cell's ability to metastasise, or whether this up-regulation itself primes the cell to metastasise. What ever this may represent, a cell's ability to migrate to specific target sites may therefore be determined, in part, by loss of VHL, suggesting that these cells may be primed from an early stage to spread to other sites in the body. CXCR4 could represent a novel target site for therapeutic intervention in the prevention of cancer metastasis, the major cause of death in RCC patients and of many other solid tumours.

Concluding Remarks

Research to date shows that pVHL functions in the correct orchestration of cell proliferation, survival and angiogenesis through the control of the HIF pathway. However, VHL has also been linked to the regulation of cell polarity and directed cell migration in part through its association with aPKC and the microtubule network. Finally, intimate mechanistic linkages have been established between loss-of-function of pVHL and the processes of invasion and metastasis. Thus, a deeper appreciation of the many aspects of VHL biology and their deregulation within a pathological setting will help us to understand the molecular details pertaining to these pathways and key processes of the cancer phenotype.

CHAPTER 6

Materials and Methods

6.1 Materials

6.1.1 General Chemicals

Reagent	Supplier
Acetic acid	BDH
Activated CH sepharose 4B	Pharmacia
Acrylamide	Bio-Rad
Agar	Gibco BRL
Agarose	Progen
Ammonium acetate	BDH
Aprotinin	Boehringer
Bovine serum albumin (BSA)	Sigma
Bio-Rad Protein Assay	Bio-Rad
Bromophenol blue	Ajax
Caesium chloride	BDH
Centricon	Millipore
Chloroform	BDH
Creatine phosphate	Calbiochem
Deoxynucleotide mix	Stratagene
Dextran sulphate	Sigma
D-(-)-Luciferin	Boehringer
DAPI (4'6'-Diamidine-2'-Phenylindole Dihydrochloride)	Boehringer
Diethyl pyrocarbonate (DEPC)	Sigma
Dimethylsulfoxide (DMSO)	Sigma
Sodium hydrogen phosphate (Na ₂ HPO ₄)	BDH
Dithiothreitol (DTT)	Promega
Distilled water	GibcoBRL
DNA Ladder:	
1kb	Promega
- Marker II – (0,12-23.1)	Roche
- Marker III – (0.12-21.2kbp)	Roche
- Marker V – (26-501bp)	Roche
- Marker VI – (Roche
DNA polymerase:	
- cloned <i>Pfu</i>	Stratagene
- Pwo	Roche
- Taq	Stratagene
EN ³ HANCE	NEN TM

Reagent	Supplier
Enhanced chemi-luminescence	Amersham
Ethanol	BDH
Ethidium bromide	Sigma
Ethylenediamine tetra-acetic acid (EDTA)	Boehringer
Ethyleneglycol-bis-(aminoethyl ether)-N,N,N',N'-tetraacetic acid (EGTA)	Sigma
Ficoll	Pharmacia
Formaldehyde	BDH
Glutathione sepharose 4B	Pharmacia
Glycerol	BDH
Hemocyanin, keyhole limpet (KLH), Megathura Crenulata	Calbiochem
Hydrochloric acid	BDH
Hydrogen peroxide	BDH
Isopropanol	BDH
Isopropylthio- β -D-galactoside (IPTG)	BRL
Klenow enzyme	Boehringer
Lambda protein phosphatase	New Eng Bio.
Leupeptin	Auspep
Magnesium chloride	BDH
Magnesium sulfate	BDH
Methanol	BDH
3-(N-Morpholino)propane-sulfonic acid (MOPS)	Sigma
N,N,N',N'-Tetramethylethylenediamine (TEMED)	Bio-Rad
N,N'-methylene bisacrylamide	ICN
Mowiol	Calbiochem
N-2-Hydroxyethylpiperazine-N'-2-ethanesulfonic acid (HEPES)	Boehringer
Nickel chloride	BDH
Nitrocellulose membrane	Schlei. & Schuell
NP-40	Sigma
Oligo-dT cellulose	Pharmacia
Paraformaldehyde	BDH
PCR nucleotide mix	Boehringer
Pepstatin A	Boehringer
Phenol	GibcoBRL
Phenyl-methyl-sulphonyl-fluoride (PMSF)	Boehringer
Polydeoxyinosinic-deoxycytidylic acid (poly [dl:dC])	Sigma
Polyvinyl pyrrolidone	Sigma
Potassium acetate	Amresco
Potassium chloride	Amresco
Potassium ferricyanide	BDH
Potassium ferrocyanide	BDH
Protein A / G sepharose	Pharmacia
Proteinkinase K	GibcoBRL
Propidium iodide (PI)	Sigma
RNase H reverse transcriptase	GibcoBRL
RNase inhibitor	Boehringer
Protease Inhibitor cocktail tablets (competo)	Boehringer
Sodium acetate	BDH
Sodium chloride	BDH

Reagent	Supplier
Sodium dihydrogen orthophosphate (NaH ₂ PO ₄)	BDH
Sodium Dodecyl Sulfate (SDS)	ICN
Sodium Hydroxide	BDH
Spermidine	New Eng bio.
T4 DNA ligase	Sigma
Thrombin (bovine)	Calbiochem
TNT-Coupled reticulocyte lysate system	Promega
Tris(hydroxymethyl)aminomethane (Tris base)	BDH
Tri-Sodium citrate	BDH
Triton X-100	BDH
Tween-20	BDH
Ubiquitin aldehyde	Affiniti
Ubiquitin	Calbiochem
Ubiquitin (K84R)	Bio-Rad
Wheat germ extract	Promega
5-bromo-4-chloro-3-indolyl-B-D-galactopyranoside (X-Gal)	Promega
Xylene cyanol	Ajax
Zeocin	Invitrogen

6.1.2 Drugs and tissue culture reagents

Reagent	Supplier
Actinomycin D	Sigma
Ampicillin	Fisons
β-mercaptoethanol	Sigma
5-Bromo-2'-deoxyuridine (BrdU)	Sigma
Chloramphenicol	Sigma
Cell proliferation kit I (MTT)	Roche
Concanavalin A	Sigma
CSF-1 (recombinant human)	Chiron Corp
Colcemid	Sigma
Cycloheximide	Sigma
Doxorubicin	DBL
Dulbecco's Modified Eagle Medium (DMEM)	GibcoBRL
Etoposide	Sigma
Foetal Bovine calf Serum (FCS)	HycClone
Folic acid	Sigma
G418 (geneticin)	GibcoBRL
Grace's insect medium	Sigma
Hygromycin B	Boehringer
Ionomycin	Sigma
Kanamycin	Sigma
L-asparagine	Sigma
Leptomycin B	Sigma
Lipofectamine	GibcoBRL
Lipofectamin 2000	GibcoBRL
L-Glutamine	Trace
LPS (<i>E.coli</i> 0111:B4)	Sigma
MEK inhibitor	Promega
MEM non-essential amino acids	GibcoBRL

Reagent	Supplier
Methyl α -D-mannopyranoside	Sigma
Nocodazole	Sigma
Oligofectamine	Invitrogen
Optimem	GibcoBRL
Penicillin	Trace
Phorbol 12-myristate 13-acetate (PMA)	Sigma
Phosphate Buffered Saline (PBS)	Trace
Poly-L-Lysine solution	Sigma
Puromycin	GibcoBRL
Renal proximal tubular epithelial cells (RPTEC)	BioWhittake Inc.
RPMI	GibcoBRL
Staurosporine	Dr.B.Hemmings
Streptomycin	Trace
Taxol (Paclitaxel)	Sigma
Trichostatin A	BIOMOL
Trypsin EDTA	GibcoBRL
Trypsin versene	CSL
Vincristine	Sigma

6.1.3 Antibodies

Antigen	Conjugation	Clone / Cat#	Supplier
Acetylated-tubulin		6-11B-1	Sigma
Akt		9272	Cell signaling
ARNT 1 (C-19)		Sc-8076	Santa Cruz
BrdU	FITC	347583	Becton Dickinson
Caesin kinase I α		Sc-6478	Santa Cruz
Caesin kinase I ϵ		610446	BD Pharmingen
β -catenin		14 / C19220	BD Trans. labs
Cyclin A		C-22 / sc-160	Santa Cruz
cyclin B1		H-433 / sc-752	Santa Cruz
Cyclin B1		GNS1 / sc-245	Santa Cruz
Cyclin D1		72-13G / sc-450	Santa Cruz
Cyclin E		HE12 / sc-247	Santa Cruz
Cyclin F		C-20 / sc-952	Santa Cruz
Cyclin G		FL-249 / sc-851	Santa Cruz
Cyclin H		FL-323 / sc-855	Santa Cruz
CDK2		Sc-163-G	Santa Cruz
CDK3		Sc-826	Santa Cruz
CDK4		Sc-260	Santa Cruz
CDK7		Sc-856	Santa Cruz
CXCR4		12G5 / MAB170	R&D Systems Inc.
Drebrin		M2F6 / D029-3	LabForce
Dynein (intermed. chain)		70.1 / D5167	Sigma
E2F-1		05-379	Upstate biotech.
EB1		5 / e46420	BD Trans. labs
Elongation factor 1a		05-235	Upstate Biotech.
EPAS-1 (C-16)		Sc-8712	Santa Cruz
Fibronectin		P1H11/MAB1926	Chemicon Int.
FLAG		M5 or M2	Kodak

Antigen	Conjugation	Clone / Cat#	Supplier
GAL4		5398-1	Clontech
GAL4 (DBD)		RK5C1 / sc-510	Santa Cruz
GFP		7.1 and 13.1	Boehringer
Glut1		GT12-S	JURO
α -Goat IgG	HRP		Amersham
GSK-3		7 / 610202	BD Trans. labs
GST		GST-2 / G1160	Sigma
HA.11		MMS-101R	BAbCO
HDAC6		Sc-5255	Santa Cruz
HDAC6		184	Gift: Tso-Pang Yao
HDAC6		2162	Cell signalling
HIF-1alpha		54 / H72320	BD Trans. labs
HIF-1alpha		NB 100-123	Novus-Biologicals
HIF-2alpha		NB 100-122	Novus-Biologicals
HSP60		MA3-012	Affinity Bioreagents
Lamin A/C (346)		Sc-7293	Santa Cruz
NF κ B p50		Sc-7178	Santa Cruz
NF κ B p65		Sc-109	Santa Cruz
α -Mouse IgG	Cy5	715-175-150	Dianova
α -Mouse IgG	FITC	715-095-150	Dianova
α -Mouse IgG	Texas Red	715-075-150	Dianova
α -Mouse IgG	HRP	NA 931	Amersham
α -Mouse IgG	Alexa 488	A-11029	Molecular Probes
α -Mouse IgG	Texas red 595	T-862	Molecular Probes
Mouse IgG1 κ		M7894	Sigma
Myc (supernatant)		9E10	Cell culture
Myc (c-Myc)		sc-789	Santa Cruz
Myosin II (nonmuscle)		PRB-440P	BabCO
Myosin II (nonmuscle)		CMII23	Dev.Stud.Hyb.Bank
P-Akt (Thr308)		9275	Cell signaling
P-Akt (ser473)		9271	Cell signaling
P-histone		06-570	Upstate
P-I κ B- α (ser32)		9241	Cell signaling
p-cofilin			Cell signaling
P-p44/42 MAP kinase		9101	Cell signalling
P-p70 S6 kinase(Thr 389)		9205	Cell signaling
Prolyl hydroxylase 2		100-137	Novus Biologicals
p21		Sc-397	Santa Cruz
p27		57 / K25020	BD Trans. labs
p27		sc-527	Santa Cruz
p53		Ab-7	Oncogene
p53		Sc-100	Santa Cruz
p53		G59-12 / 14211A	BD Pharmingen
PARP		C2-10 / 556362	BD Pharmingen
PKC- ζ		sc-7262	Santa Cruz
PKC- μ		sc-936	Santa Cruz
PTEN		sc-6818	Santa Cruz
Rabbit IgG (purified)		02-6102	Zymed
α -Rabbit IgG	Cy5	711-175-152	Dianova
α -Rabbit	Texas Red	711-075-152	Dianova

Antigen	Conjugation	Clone / Cat#	Supplier
Rabbit IgG (purified)		02-6102	Zymed
α -Rabbit IgG	Cy5	711-175-152	Dianova
α -Rabbit	Texas Red	711-075-152	Dianova
α -Rabbit IgG	Nanogold		Nanoprobes
α -Rabbit IgG	HRP	NA 934	Amersham
α -Rabbit IgG	Alexa 488	A-11008	Molecular Probes
α -Rabbit IgG	Texas Red 595	T-2767	Molecular Probes
α -Rat IgG	HRP	-	Dako
RNA pol II		MMS-134R	BAbCO
Skp2		monoclonal	Krek Lab
Skp2		Sc-1566	Santa Cruz
T7		69522-3	Novagen
β -TRCP		Sc-8863	Santa Cruz
α -Tubulin		MAS 077 / YL1/2	Harlan Sera-lab
β -Tubulin		Tub 2.1 / T4026	Sigma
γ -Tubulin		GTU-88 / T6557	Sigma
Ubiquitin		MMS-258R	BAbCO
Ufd1		611643	BD Trans. Labs
VCP		612183	BD Trans. Labs
VCP (G-20)		sc-9783	Santa Cruz
VEGF (147)		sc-507	Santa Cruz
VHL-mouse		Ig32 / 65031A	BD Pharmingen
VHL (M-20)		Sc-1534	Santa Cruz
VHL (R-20)		Sc-1535	Santa Cruz
Vimentin		V2258	Sigma
Vimentin		64-740-1	ICN Biochemicals

6.1.4 Radiochemicals

PRO-MIX L- ^{35}S] in vitro cell labelling mix (Amersham) with a specific activity of $>37\text{TBq/mM}$ ($>1000\text{Ci/mM}$) and radioactive concentration of 530 MBq/ml (14.3mCi/ml) was used for metabolic labelling. $[\gamma\text{-}^{32}\text{P}]\text{dATP}$ ($\sim 3000\text{ Ci/mmol}$) were obtained from Amersham as 10mCi/mL solutions.

6.1.5 Restriction Enzymes

Restriction enzymes were purchased from Boehringer, New England Biolaboratories or Promega and used with supplied buffers according to recommended protocols.

6.1.6 Bacterial strains and media

Plasmid DNA was grown in the bacterial strain DH5 α (Life Technologies). Luria modified medium, Luria broth and Terrific broth for growth of bacteria were generated by FMI Media Kitchen staff.

6.1.7 Oligonucleotides

Sequencing oligonucleotides

T7	TAATACGACTCACTATAGGG
T3	ATTAACCCTCACTAAAG
SP6	GATTTAGGTGACACTATAG
M13-5'	GTAAAACGACGGCCAGT
M13-3'	AGCGGATAACAATTTTCACACAGGA
pBabe-P-5'	CCCTAAGCCTCCGCCTCCTCTTCC
pBabe-P-3'	CATGCTTTGCATACTTCTGCCTGC
p97-int-5'	GCCAATGAGACTCATGGTCAT
p97-int-3'	TGAACATAGGGCTGCCAAATC
hHDAC6 ¹¹⁴⁴ -5'	CTGGAGGGTGGCTACAACCTCCGCGCC
hHDAC6 ¹²²⁷ -3'	CATGGGGCAAGGGTCTCCCAGAAGGGT
hHDAC6 ²⁴⁰¹ -5'	GACCCACCACCCTGCTGACCCTGCCA
hHDAC6 ²⁴⁹³ -3'	CCAGTATCTGCGATGGACTTGGATGGT

Oligonucleotides for protein tags

HA	TACCCATACGACGTGCCAGACTACGCT
FLAG	GATTATAAAGATGATGATGATAAA
T7	<u>AGCTT</u> CTCCCTCCTGCTGAAAGAGCTACTCTTG
Myc	CTACAGGTCCTCCTCGGAGATCAGCTTCTGCTCC
NLS	CCAAAGAAGAAGCGCAAGGTC
NES	CTCCCTCCTGCTGAAAGAGCTACTCTT

Oligonucleotides for generation of pcDNA3 / pBABE(puro) -HA/GST/GFP/untagged -VHL constructs

GST-5'	CTCCACGGC <u>AAGCTT</u> ACCATGTCCCCTATACTAGGTTATTGG
GST-3'	CTCCACGGC <u>TCTAGA</u> TCAGTCACGATGAATTCCCGGGGA
GFP-5'	CGC <u>TACGTA</u> ACCATGGTGAGCAAGGGCGAG
GFP-5'	CTCCACGGC <u>GAATTC</u> ACCATGGTGAGCAAGGGCGAGGAG
GFP-3'	CTCCACGGC <u>CTCGAG</u> TTACTTGTACAGCTCCTCGTCCAAATGAAC
VHL ₃₀ -5'	CTCCACGGC <u>GAATTC</u> ACCATGCCCCGGAGGGCGGAGAACTGG
VHL-3'	G <u>CGAATCT</u> CAATCTCCCATCCGTTGATGTGCAAT
VHL ₁₉ -5'	CTCCACGGC <u>GAATTC</u> ACCATGGAGGCCGGGCGGGCCGCGGCC
VHL ₁₋₁₅₇ -3'	CTCCACGGC <u>GGATCC</u> AGTATACACTGGCAG
VHL-STOP	CTCCACGGC <u>GAATTC</u> CAATCTCCCATCCGTTGATGTGCAATGCG
VHL ₁₋₅₃ -3'	CTCCACGGCGGATCCCTCCTCCTCGGCGCCCAGTTCCTC
^{HA} VHL ₃₀ -5'	GCGGATCCACCTACCCATACGACGTGCCAGACTACGCTATGCCCC
^{HA} VHL ₁₉ -5'	GCGGATCCACCTACCCATACGACGTGCCAGACTACGCTATGGAGG
^{NLS} VHL ₃₀ -5'	GCGAATTCCCAAAGAAGAAGCGCAAGGTCATGCCCCGGAGGGCG
^{NLS} VHL ₁₉ -3'	GCGAATTCCCAAAGAAGAAGCGCAAGGTCATGGAGGCCGGGCGG

Oligonucleotides for PROTEOMICS

15301015-5' CTCCACGGCGGATCCACCATGAGCTTCGTGGCATAACGAGGAGCTG
 MYC¹⁵³..-5' GCGAATTCCTACAGGTCCTCCTCGGAGATCAGCTTCTGCTCCATGC
 p97^{MM}-5' GCGGATCCACCATGGCCTCTGGAGCCGAT
 p97^{MM}-3' GCGATTATCTTAGCCATAGAGGTCATCGTC
 MYC^{p97}-5' GCGGATCCACCATGGAGCAGAAGCTTGATCTCCGAGGAGGACCTG
 15301015-3' CTCCACGGCGAATTCTAGCCTGGGGTCTTGGTGGCGAAGGTCAGG
 HA¹⁵³..-5' GCGGATCCACCTACCCATACGACGTGCCAGACTACGCTATGAGCT
 153^{STOP}-3' GCGAATTCCTAGCCTGGGGTCTTGGTGGCGAAGGT
 Dj967n21-5' CGTAAGCAGCGGGAAATCCCCCCCCCTCCC
 Dj967n21-3' CTCCACGGCTCTAGATCAAAGCAGACAAGGAGAAAGAGAATGCCA
 HA^{XP_04}-5' GCGGATCCACCTACCCATACGACGTGCCAGACTACGCTATGGAGG
 XP_04-3' CTCCACGGCGAATTCTTAAGAGTCAGACTCTGGGCATTTTTCG

Oligonucleotides for construct clonings or sequencing

HA^{ODD_{Hif1α}}5' GCGGATCCACCTACCCATACGACGTGCCAGACTACGCTAGCCGAGGAAGA
 ODD^{Hif1α}-3' GCGAATTCTCAGGTCATAGGTGGTTTCTTATACCCACA
 NHE-1-5' CTCCACGGCAAGCTTACCATGGTTCTGCGGTCTGGCATCTGTGGC
 NHE-1-3' CTCCACGGCGGATCCCTGCCCTTGGGGAAGAACGGTTCTCCCTC
 NHE-1-5' CTCCACGGCGGTACCCTGCCCTTGGGGAAGAACGGTTCTCCCTC
 HA^{Npl4}-5' GCAAGCTTACCTACCCATACGACGTGCCAGACTACGCTATGGCCGAGAGC
 Npl4-3' GCGAATTCCTAGGTCCTGGGGAGGCTGCA
 Npl4^{rat}-5' GCAAGCTTACCATGGCCGAGAGCATCATAATCCGT
 HA^{Npl4^{rat}}-5' GCAAGCTTACCTACCCATACGACGTGCCAGACTACGCTATGGCCGAGAGC
 HA^{ufd1}-5' GCAAGCTTACCTACCCATACGACGTGCCAGACTACGCTATGTTCTCTTTCA
 Ufd1-3' GCGGATCCTTAGGGCTTTCTTCCCTTTTT
 Ufd1^{mm}-5' GCGGATCCACCATGTTTTCTTTCAACATGTTTGACCACCCG
 HA^{ufd1^{mm}}-3' GCGGATCCACCTACCCATACGACGTGCCAGACTACGCTATGTTTTCTTTCA
 Ufd1^{MM}-3' GCTTCTAGATTAGGGCTTTCTTCCCTTCTTACG
 HDAC6^{HS}-5' GCAAGCTTACCATGACCTCAACCGGCCAGGAT
 HDAC6^{HS}-5' GCGAGCTCACCATGACCTCAACCGGCCAGGAT
 HDAC6^{HS}-3' GCTTCTAGATTAGTGTGGGTGGGGCATATCCTC
 HDAC6^{HS}-3' GCAGATCTTTAGTGTGGGTGGGGCATATCCTC
 HD6^{FLAG}-3' GCTTCTAGATTATTTATCATCATCATCTTTATAATCGTGTGGGTGGGGCATAT
 CCTCCCCAAA
 HDAC6^{MM}-5' GCGAATTCACCATGACCTCCACCGGCCAAGATTCT
 HDAC6^{MM}-3' GCCTCGAGTTAGTGTGAGTGGGGCATGTCCTC

PHD2-5' GC**GGATCC**ACCATGGCCAATGACAGCGGCGGG
 PHD2-3' GC**GAATTC**CTAGAAGACGTCTTTACCGACCGA

Oligonucleotides to be annealed and inserted into vectors for general usage

NES-5' **AGCTTC**TCCCTCCTCTCGAAAGACTTACTCTTG
 NES-3' **GATCCA**AAGAGTAAGTCTTTCGAGAGGAGGGAGA
 NESM-5' **AGCTT**CTCCCTCCTGCTGAAAGAGCTACTCTTG
 NESM-3' **GATCCA**AAGAGTAGCTCTTTCAGCAGGAGGGAGA
 FLAG-5' **AGCTT**TCTAGAGATTATAAAGATGATGATGATAAAA
 FLAG-3' **AAGAT**CTCTAATATTTCTACTACTACTATTTTTTCGA

Oligonucleotides for antisense VHL approach (pSuper)

VHL^{21mer}-5' GATCCCCGTCATCTTCTGCAATCGCAGTTTCAAGAGAACTGCGATTGCAGA
 AGATGACTTTTTGGAAA
 VHL^{21mer}-3' AGCTTTTCCAAAAAGTCATCTTCTGCAATCGCAGTTCTCTTGAAACTGCGAT
 TGCAGAAGATGACGGG
 VHL^{19mer}-5' GATCCCCGTCATCTTCTGCAATCGCATTCAAGAGATGCGATTGCAGAAGAT
 GACTTTTTGGAAA
 VHL^{19mer}-3' AGCTTTTCCAAAAAGTCATCTTCTGCAATCGCATCTCTTGAATGCGATTGCA
 GAAGATGACGGG

Oligonucleotides for siRNA – target sequences

VHL #1 AAGAGTACGGCCCTGAAGAAGAC
 VHL #2 GTCATCTTCTGCAATCGCAGT
 VHL #3 CTCAATGTTGACGGACAGCCT
 VHL #4 ACACAGGAGCGCATTGCACAT
 p97 AACAGGTAGCCAATGAGACTC
 PHD2 CTTCAGATTCCGGTCGGTAAAG
 MDM2 AACAAAGAGACCCUGGUUAGAC
 CKI- α GGCCAGGCATCCCCAGTTGT
 Cullin 2 AAGAAGTCAGCGAAAGGGATG

6.2 DNA and RNA manipulation

6.2.1 Isolation of plasmid DNA

Nucleobond from Machery-Nagel was used to isolate plasmid DNA. Cultures were inoculated by mini-culture or directly from glycerol stock and left incubate over-night (10-12 hrs) in 100-500ml LB media supplemented with appropriate antibiotic if necessary. The following day, bacteria were pelleted by centrifuging at 5000g for 5mins and the pellet was re-suspended in appropriate volume of S1 buffer supplemented with RNase A (50mM Tris/HCl, 10mM EDTA, 100µg RNase A/ml, pH8.0, stored at 4°C). Samples were lysed in S2 buffer for 5mins at room temperature (200mM NaOH, 1% SDS), followed by addition of S3 buffer (2.80M KAc, pH5.1) and left incubate for a further 5mins on ice. Filter paper was prepared in glass funnels by dampening them with ddH₂O prior to filtration of the lysate. The filtrate was collected and added to DNA binding columns that had already been calibrated with buffer N2 (100mM Tris, 15% ethanol, 900mM KCl adjusted with H₃PO₄ to pH6.3, 0.15% Triton X-100). The filtrate was passed through the column (for low copy plasmids, this was repeated) to allow the plasmid DNA to bind to the column. Contaminants were washed from column using buffer N3 (100mM Tris, 15% ethanol, 1150mM KCl adjusted H₃PO₄ with to pH6.3). Buffer N5 was used to elute the plasmid DNA (warmed to 50°C for low copy plasmids) and DNA was precipitated by addition of approximately 0.8 volumes of isopropanol. Samples were centrifuged at >15,000g for 30mins at 4°C, and the pellets were washed with 70% ethanol and further centrifuged at 15,000g for 10mins at 4°C. Pellet was dried and re-suspended in appropriate amount of ddH₂O or TE buffer. Concentration was calculated by measuring OD₂₆₀.

(NB: Plasmid isolation kits were also used from Qiagen, and followed manufacturer's instructions. Miniprep plasmid isolation was performed using Wizard Plus SV Miniprep kit).

Alternatively – Cesium Chloride preparation

200-400ml culture was grown up over-night, pelleted at 5000rpm for 5mins and re-suspended in 20ml of Solution 1 (50mM Glucose, 25mM Tris/HCl pH8.0, 10mM EDTA pH8.0) containing 3mg/ml lysozyme. After incubation on ice for 10mins, 40ml of solution 2 (0.2M NaOH, 1% SDS – mix fresh) was added, and left incubate for a further 30mins. Samples were centrifuged at 8000rpm for 10mins, and the supernatant collected and passed through gauze into new tubes. 0.6 volumes isopropanol was added, and samples centrifuged at 12000rpm for 10mins. The supernatant discarded and the pellet re-suspended in 8.5ml ddH₂O. 8g of CsCl₂ was prepared in a 15ml polypropylene falcon and 8ml of DNA solution was added. CsCl₂ had to entirely dissolved before continuing. Carefully 640µl of a 10mg/ml stock of ethidium bromide was added and mixed gently. Samples were centrifuged at 3000rpm for 5mins, supernatant removed and centrifuged further at 45,000rpm for 22 hours at 15°C. Following the ultra-centrifugation, there should be a band corresponding to the plasmid DNA. This band was collected and extracted

with the same volume of isobutanol (3-4 times). ddH₂O was added to the extraction solution to make up a final volume of 6ml supplemented with 0.6ml of 3M NaOAc (pH5.2). A further 12ml of 100% ethanol was added and DNA precipitated at -20°C for 60mins. Samples were centrifuged at 13000rpm for 15mins, supernatant discarded and pellet re-suspended in 2-4ml of ddH₂O. Phenol/chloroform extracted and ethanol precipitated as usual. Pellets were re-suspended in an appropriate volume of ddH₂O or TE buffer.

6.2.2 Isolation of DNA from agarose gels

DNA fragments were excised from agarose gels in a minimum volume using a scalpel, and purified using QIAquick Gel Extraction kit from Qiagen.

6.2.3 Isolation of total RNA

Snap-frozen tissue samples were homogenised in F15 Falcon tubes in TRIzol reagent (GibcoBRL). Tissue culture cells were lysed directly in TRIzol reagent. Samples were incubated for 15 minutes at room temperature, 0.2 volumes of chloroform was added, and shaken vigorously for 15 seconds, followed by a further incubation for 5 minutes at room temperature. The mix was then spun at 12000g and 4°C for 15 minutes, separating it into three phases. The upper, clear aqueous phase, containing the RNA, was removed into a fresh eppendorf tube and 0.5 volumes (calculated from the initial volume of TRIzol used) isopropanol added. Following 10 minutes at room temperature, the sample was centrifuged at 12000g and 4°C for 10 minutes to pellet the RNA. The supernatant was discarded, and the pellet washed with 1mL 70% ethanol. After air-drying, the RNA pellet was re-suspended in TE and incubated for 15 minutes at 55°C. Concentration was determined at OD₂₈₀.

6.2.4 Northern Blot Analysis

Gel apparatus was soaked in 0.2M NaOH (20mins) to inactivate any RNase activity and rinsed thoroughly with ddH₂O. Appropriate agarose gel and running buffer (MOPS/EDTA:0.2M MOPS, 50mM Na-acetate, 10mM EDTA, pH7.0, supplemented with 2.2M formaldehyde) was prepared. Samples were equalised with loading buffer and left at 65°C for 10 minutes. 1µl of ethidium bromide was added to each sample before loading onto gel. Following migration, the gel was incubated in 10x SSC for 30 minutes, as was the nylon membrane for 10 minutes. Capillary transfer of RNA from the agarose gel onto membrane was employed. Following transfer, the membrane was washed in 5x SSC for 15 minutes and subjected to UV-cross-linking using a Stratlink.

-Probe preparation as per MEGA-prime DNA Labelling Systems: 25ng/µl of template was used to yield a 50µl reaction volume, which included template, primers and ddH₂O. DNA was denatured at 95°C for 5 minutes, and the following was added - 4µl unlabelled dNTP, 5µl 10x reaction buffer, 5µl radio-labelled dNTP, 2µl enzyme. Reaction mixture was incubated for 10 minutes at 37°C, and stopped upon the addition of 0.2M EDTA. The

mixture was heated for a further 5 minutes at 95°C. Specific activity was calculated for probe, which was then subject to a Nick-spin sepharose G-50 column (Pharmacia-Biotech) to eliminate unincorporated nucleotides and further measured for specific activity which should not drop below 10⁶cpm. Probe was stored at –20°C until ready for use.

- *Pre-hybridisation*: Membrane was incubated for 15 minutes in 65°C pre-warmed Church & Gilbert Hybridisation buffer (0.25M Na₂HPO₄ pH7.3, 1% BSA, 1mM EDTA pH8.0, 7% SDS – all sterile filtered).

- *Hybridisation*: 100µl of salmon sperm DNA (10mg/ml) and probe were denatured by heating to 95°C for 5 minutes, and then added to each other. This DNA mixture was then added to 10ml of C&G buffer and incubated with the membrane at 65°C overnight. The membrane was washed 4x30 minutes with washing buffer (20mM Na₂HPO₄ pH7.3, 1mM EDTA pH8.0, 1% SDS). Following the final wash, the membrane was dried between whatmann paper, and exposed to film.

6.2.5 Construction of plasmids

VHL sub-cloning was derived from pcDNA3-VHL₃₀ following BamHI/EcoRI digestion, unless otherwise stated. pcDNA3-HA-VHL₃₀ (R82P), (P86H), (N90I), (Q96P), (Y112H) were a gift from P. Ratcliffe. All other point mutants of pVHL were generated by a two-step PCR-based mutagenesis procedure using pcDNA3-HA-VHL₃₀ as template. Individual PCR products were subsequently digested with *Bam*HI and *Eco*RI and cloned into pcDNA3-derivative containing an HA epitope. pcDNA3-GST was generated by a one step PCR reaction involving pGEX-2TK and insertion of GST into pcDNA3 HindIII/xbaI. To generate pcDNA3-GST-VHL₃₀/VHL₁₉/VHL₁₋₁₁₅, pcDNA3-GST was cut BamHI/EcoRI. PcDNA3-GST-VHL₁₋₁₅₇ was sub-cloned from pCMV-HAVHL₁₋₁₅₇ BamHI/XbaI.

Retroviral expression of GFP-fusion VHL constructs was obtained by sub-cloning VHL into pBABE(puro). Oligonucleotides were designed to remove the stop codon from VHL by PCR, and the product was sub-cloned BamHI/EcoRI. The GFP sequence was amplified following a one step PCR reaction from the commercially available vector pEGFP-N1 (Clontech) and sub-cloned 3' to the respective VHL construct BamHI/XhoI. To obtain pGST-VHL₃₀ mutants, the corresponding fragments were sub-cloned into pGEX-4T-1 (bacterial expression) or pAc-GST (for expression in Sf9 cells) using *Bam*HI and *Eco*RI. To obtain pcDNA3-HIF1 α and pcDNA3-HIF2 α , both cDNAs were amplified by PCR, subsequently digested with *Bam*HI and *Xba*I, before ligating into pcDNA3. Baculoviral constructs included pvL1393-VHL₃₀ was cloned BamHI/EcoRI from pAC-GST-VHL₃₀; pAC-GST-Elongin C from pvL1393-GST-Elongin C by BamHI/EcoRI; PAC-GHLT(B)-VHL₃₀ from pvL1393-VHL₃₀ by pstI/NcoI. PAC-GHLT(B)-Elongin C was cloned from pvL1393-Elongin C by pstI/NotI. cDNA clones of HNMHC IIA and IIB were gifts from R.Aldestein. pCS2-HDAC6-flag and pCS2-MT-HDAC6-flag were gifts from Dr.S.Hook. p97, pET26-Ufd1 and pET30-Npl4 were gifts from Dr.H.Meyer. p97 was sub-cloned BamHI/EcoRV following PCR amplification of cDNA. Subsequent tags (HA/Myc) were

included within oligonucleotides. pVL1393-p97 was cloned BamHI/NotI. Clones 15301015, dj967n21.3 and XP_045589 were obtained from the IMAGE consortium and amplified via one-step PCR reactions and sub-cloned into appropriate vectors. pcDNA3-15301015 sub-cloning involved a BamHI/EcoRI digestion. For HA or Myc tagged constructs, the tag was included in the oligonucleotide, generating for example pcDNA3-HA-15301015.

All PCR-derived constructs were confirmed by sequence analysis. The primers used for constructing and sequencing the above-described plasmids have been listed within the materials section of this chapter.

6.2.6 Standard recombinant DNA reactions

Standard DNA manipulation techniques such as restriction enzyme digestion, blunting of 3' and 5' overhangs, λ -phosphatase treatment, oligonucleotide annealing/sub-cloning and ligation of DNA fragments were performed by standard methods using enzymes in buffers supplied by the manufacturers.

6.2.7 Polymerase chain reaction

PCR was carried out according to the manufacturers protocol regarding the polymerase employed. Standard usage involved Pfu polymerase. However, the Expand Long Template proofreading PCR system (Boehringer Mannheim) was used for generation of larger DNA fragments used to construct. Taq polymerase was also used.

6.2.8 Reverse transcriptase-PCR

RT-PCR was performed as per manufacturers instructions - GibcoBRL Superscript first-strand synthesis system (cat.#11904-018).

6.2.9 DNA sequencing

Samples were dried down in a speed-vac at approximately 1 μ g per sample, and processed by the automated DNA sequencing facility at the FMI which employs the use of an ABI PRISM 377 DNA sequencer. This sequencer performs slab gel electrophoresis with fluorescence detection of individual nucleotides. Alternatively, samples were sent externally to Microsynth, a commercially available source for sequencing.

6.3 Cell culture

6.3.1 Culture of immortalised cell lines

All cells, unless otherwise stated, were maintained in Dulbecco's Modification of Eagles Medium (DMEM) supplemented with 10% foetal calf serum. NIH-3T3 cells were cultured in DMEM containing 5% bovine calf serum. Renal proximal tubule epithelial cells (RPTECs) were cultured as described by the manufacturer. Stable cell lines expressing

construct of interest routinely involved transfection of construct within a mammalian expression vector, namely pcDNA3. Following transfection, cells were subjected to selective media containing 0.5mg/ml G418 (for neomycin resistance). Cultures were sub-cloned and/or stable pools established under selective media. Cells were counted using a haemocytometer.

6.3.2 Transfection of cells

Transfection of cells was performed using various transfection protocols. For 293 and Hela cells, a calcium phosphate protocol was employed. For more difficult transfections, or for those that required a higher transfection efficiency, lipid-based transfection media were employed, e.g. fugene and lipofectamine 2000.

6.3.3 siRNA transfection of cells

Unless otherwise stated, logarithmically growing cells were transfected to yield a final concentration of 130nM siRNA oligonucleotide mixture (Qiagen). For a 6 well plate, 10 μ l of the oligonucleotide mixture was added to 175 μ l Opimem. In a separate eppendorf, 3 μ l of oligofectamine was added to 15 μ l of Optimem and left to stand for 5 minutes before being added to the oligonucleotide mixture, which was then incubated for a further 20 minutes. Target cells were washed once with medium lacking serum, and 800 μ l of serum free medium was added to the cells. The transfection complex was overlaid and cells were incubated at 37°C for 4 hours. The medium was then supplemented with 500 μ l of medium containing 30% serum and left incubate for appropriate time, normally 24-48 hours. (NB. While most cell lines tested showed significant knockdown of target protein, all attempted experiments demonstrated Hela cells as being the cell line in which most efficient knockdown could be achieved).

6.3.4 Retroviral transduction of cells

In order to generate retroviral pools, the packaging cell line PT-67 (Clontech) was fugene-transfected with pCMV(neo-retro) or with pBABE(puro) constructs. Tissue culture supernatant was harvested 24 hours later, passed through a 0.45 μ m filter and added to target cells in the presence of 0.8 μ g/ml polybrene (detergent). Infected cells were selected by growth in the presence of 1 mg/ml G418 or puromycin. Clones were sub-cultured and/or stable pools (uncloned mass culture) cells were maintained in DMEM supplemented with 10% FCS and 0.5 mg/ml G418 or puromycin.

6.4 Cell cycle analysis

6.4.1 Fluorescent activated cell sorting (FACS)

Cells were trypsinised, washed, pelleted and re-suspended in 300 μ l cold PBS. While vortexing, 1ml of cold (-20°C) 100% ethanol was added drop-wise. Samples were incubated at -20°C overnight (up to one month), pelleted, washed once in PBS, and re-

suspended in 500 μ l of FACS solution (38mM sodium citrate pH7.5; 69 μ M propidium iodide) supplemented freshly with 10 μ g RNase. Cells were left at 37°C for 30mins and read at 488nm using a Becton Dickinson FACS Calibur flow cytometer incorporating a class 3B laser. Cellquest, version 3.13 from Immunocytometry, was used to analyse data.

6.4.2 Arresting cells

Cells were arrested in late G₁/S-phase by a double thymidine (2mM) block or thymidine/aphidicolin block (14hrs thymidine - 14hrs DMEM - 14hrs thymidine or aphidicolin - release). Alternatively, hydroxyurea and mimosine were employed, albeit to a lesser extent. Nocodazole (500ng/ml) was used to block cells at G₂/M. Serum starvation (overnight) and contact inhibition (6 days post confluency with daily medium changes) arrested cells in G₀.

6.5 Protein manipulation

6.5.1 Immunoprecipitation and Western blotting

Immunoprecipitations were performed from cells lysed at 4°C in either TNN buffer (50mM Tris-HCl pH7.5; 120mM NaCl; 5mM EDTA; 0.5% NP-40; 50mM NaF; 0.2mM Na₃VO₄; 1 μ M DTT, 1 μ M PMSF, 1mg/ml aprotinin) or alternatively from whole cell extract, WCE, buffer (20mM Hepes pH7.6; 0.4M NaCl; 25% glycerol, 1mM EDTA; 5mM NaF; 0.1% NP-40; 0.5mM Na₃VO₄; 1mM DTT; 1 μ M PMSF; 1mg/ml aprotinin). Proteins were equalised using Bradford method (Biorad). Lysates were cleared using centrifugation, and pre-cleared using protein A sepharose beads. The immunoprecipitating antibody was added for a period of one hour to overnight. Concentrations varied among antibody, but generally, an average concentration of 2 μ g per 1-2ml of lysate was used. Following IP, protein A sepharose was added for one hour (NB. Protein G sepharose was used in the case of monoclonal antibodies). Beads were washed at least three times in lysis buffer, boiled in laemmli buffer and loaded on an SDS-PAGE gel (NB: where necessary, gradient gels were used as per *Hoefler*).

Immunoblotting was performed onto Nitrocellulose membrane (Schleicher & Schuell) at 400mA for 1-2 hours for min-gels (10x6cm approx.), and 450-500 mA overnight for large gels (13x15cm approx). Membranes were blocked in 5% milk (unless otherwise stated) and incubated with primary antibody in 5% milk from one hour to overnight. Membranes were washed 3x10mins TBST, and further incubated with a relevant HRP-conjugated secondary antibody in 5% milk for one hour. Western blots were processed using enhanced chemi-luminescence according to the manufacturer's instructions.

6.5.2 Cell fractionation

Basic cytoplasmic/nuclear fraction preparation

Cells were harvested from a 10cm plate by scraping in 1ml of ice cold PBS. Cells were pelleted at 5000rpm for 5mins at 4°C. Supernatant was discarded, and the cells resuspended in 400µl of hypotonic buffer (10mM MOPS pH7.5, 10mM KCl, 2mM MgCl₂, 0.1mM EDTA and 5mM DTT). The resuspension was transferred to a chilled dounce homogeniser and lysed with approximately 10 strokes on ice. Lysate was pelleted at 5000rpm for 2-3mins. The supernatant corresponded to the cytosolic extract. Pellet was washed four times in hypotonic buffer containing 0.1% NP40 and spun down again at 5000rpm at 4°C. Pellet was then lysed in extraction buffer (S6K extraction buffer containing 1% NP40) and centrifuged at 14,000rpm for 10mins at 4°C. Supernatant corresponds to nuclear extract.

Optimised for preparation of nuclei

Medium was aspirated from cells from a 10cm well plate and washed twice in PBS. 5ml of DMEM containing cytochalasin B was added and the cells were let incubate for 40mins at 37°C. Cells were washed again twice in PBS, and scraped into a 15ml falcon. Cells were collected by centrifuging at 800g for 5mins. Cells were washed in 2ml of solution 1 (10mM KCl, 1.5mM MgCl₂, 1mM DTT, 0.1mM PMSF, 1µg/ml pepstatin, 1µg/ml leupeptin, and 1µg/ml trypsin inhibitor). Cell pellet was placed on ice and re-suspended in 1ml of solution 1 supplemented with 10µM cytochalasin B. Cells were incubated on ice for 20mins and then transferred to a chilled Weaton glass homogeniser. The plasma membranes were disrupted by approximately 20 gentle strokes (the efficiency of cell breakage could be monitored by phase-contrast microscopy). The homogenate was transferred to a 1ml eppendorf tube. The homogenate was under-layered with 200µl of solution 1 supplemented with 40% sucrose and centrifuged at 800g for 15mins. Aspirate of the supernatant (membrane and cytoplasmic fraction) and the sucrose cushion and re-suspend the pellet accordingly in PBS.

Isolation of mitochondria from tissue culture cells

For a cell pellet of 1-2ml - the cell pellet was re-suspended in 11ml of ice-cold RSB (hypotonic buffer: 10mM NaCl, 1.5mM MgCl₂, 10mM Tris-HCl pH7.5) and transferred to a dounce homogeniser. Cells were allowed to swell for 5-10mins. Add 8ml of 2.5x MS buffer (525mM mannitol, 175mM sucrose, 12.5mM Tris-HCl pH7.5, 2.5mM EDTA pH7.5) to give a final concentration of 1x MS (210mM mannitol, 7.mM sucrose, 5mM Tris-HCl pH7.5, 1mM EDTA pH7.5 – an iso-osmotic buffer to maintain the tonicity of the organelles and prevent agglutination). The homogeniser was covered with parafilm and the homogenate mixed by careful inversion. Homogenate was transferred to a tube for differential centrifugation (total volume 30ml) and centrifuged at 1300g for 5mins to remove nuclei, unbroken cells and large membrane fragments. The supernatant was removed to a new tube and the nuclear spin-step repeated twice. Supernatant was again transferred to a new tube and the mitochondria pelleted at 17000g for 15mins. The

supernatant was discarded and the pellet washed by re-suspending it 1x MS and repeating the 17000g sedimentation. Again the supernatant is discarded and the pellet re-suspended in a suitable volume in appropriate buffer for subsequent work.

6.5.3 Glycerol gradient

A 10-40% glycerol gradient was used in 20mM Hepes pH7.5, 50mM NaCl, 0.1% NP-40 and 0.5mM DTT. A Standard two chamber pump was used to pour gradients into 12.5ml ultra-centrifuge tubes on which was over-layered the protein preparation of interest and a control (catalase 232kDa, aldolase 158 kDa, BSA 67 kDa, ovalalbumin 43kDa). Tubes were placed inside a SW41 rotor and centrifuged at 40,000rpm for 24hrs. Fractions were carefully collected using an automatic collection carousel. From a total of 12.5ml, approximately 60 fractions were collected, from which every 5th sample of the control was ran on a gel and stained with coomassie in order to estimate the size distribution across the various fractions.

6.5.4 Far Western

Protein transfer was performed in methanol-free transfer buffer (192mM Glycine; 25mM Tris; 0.01% SDS). Proteins were de-natured and re-natured on the membrane: At 4°C gently agitate membrane in the following decreasing concentrations of Guanine-HCl in Hyb75 (20mM Hepes pH7.7; 75mM KCl; 0.1mM EDTA; 2.5mM MgCl₂; 0.05% NP-40; 1mM DTT) - 2x5mins 6M; 4x10mins 3M; 4x10mins 1.5M; 4x10mins 0.75M; 4x10mins 0.375M. Block membrane – 2x30mins Hyb75; 1x30mins Hyb75 + 5% milk; 1x30mins Hyb75 + 1% milk. Overlay with probe (made up in Hyb75 and supplemented with proteinases and NaN₃) and incubate overnight at 4°C. Wash 3x15mins with Hyb75. Incubate with antibodies of interest against probe components and develop as normal western blot.

- *Probe Preparation*: Complex components Skp1/Skp2 or pVHL30/ElonginC/ElonginB were co-expressed in Sf9 cells and purified via GST-pulldown. Complexes are verified by western blot analysis and eluted from beads using 15mM Glutathione elution buffer and buffered for glycerol gradient conditions and store at -80°C. Load probe onto glycerol gradient of 10-40% (20mM Hepes pH7.5; 50mM NaCl; 0.1% NP-40; 0.5mM DTT). Comparative standards included catalase 232kDa, aldolase 158kDa, BSA 67 kDa, Ovalbumin kDa. Samples were spun at 40,000rpm for 24 hours in an SW41 rotor. Following fractionation, western blot analysis was performed for every fifth fraction from standards to estimate range of interest. Following this, every second fraction was taken from sample corresponding to this range, and prepared for western blot. Fractions containing complex were pooled. Protein concentration was estimated against BSA standards on a coomassie-stained gel, and concentration of probe used per Far western ranged between 2-3µg.

6.5.5 Metabolic labelling of cells

Logarithmically growing cells are washed twice and incubated for 30mins in methionine-free DMEM without serum (or dialysed). Radioisotopic labelling was performed by incubating cells in methionine-free DMEM supplemented with [³⁵S]-methionine (100µCi/ml) (PROMIX) and 10% dialysed FCS for 4 hours at 37°C in a humidified 10% CO₂ incubator. Following SDS-PAGE protein resolution, signals can be enhanced by incubating gel for 1 hour in destain (acetic acid; methanol, water), 1 hour in EN³HANCE solution, and finally 30mins in water.

6.5.6 *In vitro* transcription/translation reactions

In vitro transcription/translation reactions were made using TNT reticulocyte translation system with the addition of [³⁵S]-L-methionine according to the manufacturer's protocol (2x TNT rabbit reticulocyte lysate; 25x TNT reaction buffer; 50x amino acid mix minus methionine; 1 unit Rnase inhibitor; 1.5µg DNA; 50x TNT T7 RNA polymerase; 40µCi [³⁵S]-methionine; ddH₂O to 50µl).

6.5.7 Generation and affinity-purification of antibodies

Generation and purification of anti-pVHL₃₀ antibody has been described previously [184]. Polyclonal rabbit serum to full-length mouse was raised against the corresponding GST-fusion protein purified from bacteria. Anti-pVHL_{CT} peptide antibody was raised against the synthetic peptide LERLTQERIAHQRMGD, corresponding to the carboxy-terminus of human pVHL. Before injection into rabbits, the peptide was coupled to keyhole limpet hemocyanin (Pierce) by glutaraldehyde coupling. Polyclonal rabbit serum to mouse pVHL was affinity purified by incubation with first a GST affinity column, followed by a GST-pVHL₂₅ fusion protein affinity column, previously prepared by covalently cross-linking the respective proteins to glutathione-Sepharose with dimethylpimelimidate. Anti-peptide antibody was affinity purified by coupling 10mg of synthetic peptide to 1g of CH-Sepharose 4B (Pharmacia) according to manufacturer's protocol. To obtain anti-pVHL_{NT} antibody, polyclonal rabbit serum to human pVHL was affinity purified by incubation with first a GST affinity column, followed by a GST-pVHL₁₋₅₃ fusion protein affinity column. Incubation and elution of antibodies was carried out as described [335]. All commercially available antibodies used, or those given as gifts are listed in the Materials section of this chapter.

6.5.8 Bacterial expression and purification of GST-fusion proteins

E. Coli DH5α containing expression plasmids for GST-fusion proteins were inoculated overnight and the next morning diluted 1/10 in LB containing 0.2mM IPTG. After 4.5 hours of incubation at 37°C, bacteria were harvested by centrifugation at 5,000 rpm for 5 minutes. After resuspending cells in TNN buffer (50mM Tris, 250mM sodium chloride, 5mM EDTA, 0.5 % NP-40, 50mM sodium fluoride, 0.2mM ortho-vanadate, 1mM

dithiothreitol, 10mM PMSF and 1µg/ml aprotinin at pH 7.5), bacteria were sonicated. Cell debris was collected by centrifugation at 5,000 rpm for 5 minutes, and the supernatant transferred to a fresh tube. Meanwhile, Glutathione-sepharose 4B beads were pre-incubated in 5 % milk for 10-15 minutes and washed 2-3 times with TNN buffer, before adding the beads to the bacterial lysate. After 1-2 hours of incubation at 4°C, the beads were collected by centrifugation and washed 3-4 times with TNN buffer. Depending on the experimental setting beads were subsequently washed with other buffers (e. g. kinase buffers), incubated with other proteins (e. g. *in vitro* translated molecules) or processed directly for SDS-PAGE.

6.5.9 Covalent coupling of antibody to protein A sepharose

For general purpose procedures, approximately 2mg of antibody per millilitre of wet beads were bound. The antibodies and protein A sepharose were incubated at room temperature for 1hr with gentle rocking. Beads were washed twice with 10 volumes 0.2 sodium borate (pH9.0) by centrifugation for 5mins or 10,000g for 30 seconds. They were then re-suspended in 10 volumes of 0.2M sodium borate (pH9.0) and the equivalent of 10µl of beads was removed (for subsequent testing). Enough dimethylpimelimidate was added to bring the final concentration to 20mM and incubated for 30mins at room temperature on a shaker. Again remove an equivalent of 10µl of beads. Reaction was stopped by washing the beads once in 0.2M ethanolamine (pH8.0) and incubated for 2hrs at room temperature in 0.2M ethanolamine with gentle mixing. The beads were washed again three times in PBS and stored as a 50% slurry in PBS supplemented with 0.05% sodium azide.

6.5.10 Baculoviral expression of proteins

The Baculovirus Expression Vector System (BEVS) from PharMingen was used as a eukaryotic expression system. The baculovirus DNA used is the *Autographa californica* nuclear polyhedrosis virus (AcNPV). Heterologous genes are cloned into transfer vectors and co-transfection of transfer vector and AcNPV infection of *Spodoptera frugiperda* (Sf9) cells allows recombination between homologous sites, transferring the heterologous gene from the vector to the AcNPV DNA. AcNPV infection of *sf* cells results in the shut-off of host gene expression allowing for a high rate of recombinant mRNA and protein production.

- *Transfection of sf9 cells*: 2×10^6 sf9 per 6cm plate are seeded. 0.5µg BaculoGold DNA (modified AcNPV) is added to 4µg of DNA (cloned into appropriate vector) and left stand 5mins before adding 1ml transfection buffer B (25mM Hepes, pH7.1, 125mM CaCl₂, 140mM NaCl). Cells are aspirated and 1ml of transfection buffer A (Grace's medium containing 10% FCS) is gently added. Transfection mixture is then added to cells, which are then incubated at 27°C for 4 hours. Cells are washed once with 3ml medium, and left at 27°C for 5 days in a further 3ml medium. Supernatant containing virus is collected,

passed through a 0.45µm filter, and used to infect sf9 cells for further amplification of virus or for protein expression.

- *Infection of sf9 cells*: 5×10^6 sf9 cells per 10cm plate are seeded. Infect by overlaying 1ml of virus containing supernatant ($>10^8$ virus particles). Harvest cells 48 hours post infection.

- *Amplification of virus*: 5×10^6 sf9 cells per 10cm plate are seeded. Infect by overlaying 400µl of virus containing supernatant ($\sim 0.4 \times 10^8$ virus particles). Collect supernatant 72 hours post infection. Pass supernatant through a 0.45µm filter and store at 4°C in dark.

6.6 Cellular and biochemical assays

6.6.1 Cell Proliferation Assay

For adherent cell lines, cells were seeded down at $0.5 \times 10^4/100\mu\text{l}$ in a 96-well plate and after 24 hours the medium was replaced. Cells were hence manipulated according to application. The cells were then gently washed in 100µl PBS, and 50µl of 0.5mg/ml of the tetrazolium salt solution (MTT) was added to each well and left incubate at 37°C for one hour (NB. reaction is light sensitive). Following incubation, 200µl DMSO was added as a solubilising agent. The absorbance of each sample is measured spectrophotometrically at λ_{570} . The mean absorbance of each quadruplicate was calculated subtracting the ethanol control. Standard statistical analysis was performed to evaluate any significant findings.

6.6.2 Reporter gene assay

1×10^5 cells per 6 well were seeded down in triplicate. 24 hours later cells are transfected using FUGENE or Lipofectamine 2000 with 100ng/well of the β -galactosidase plasmid for normalisation and 100ng/well reporter plasmid. Cells are washed and lysed in 250µl extraction buffer (0.1M KPO_4 pH 7.8, 0.1% Tritonx100, 1mM DTT). Lysates are centrifuged at 14,000rpm, and 100µl transferred to 96-well plate. Lysates were combined with luciferin reagent (0.3mM luciferin, 22mM MgSO_4 , 37mM glycyl-glycine, 5mM ATP) or with galactose reagent (Galacto reaction kit) for normalisation. Plate was read using a Microlumat plus LB 96V plate reader (Berthold Technologies).

6.6.3 *In vitro* ubiquitination assay

Reaction volume is 20-30µl and is performed at 30°C for 30mins. Reaction mixture: 2µl of I.V.T substrate; S100 extract supplemented with 8µg/µl ubiquitin; 100ng/µl ubiquitin aldehyde; energy regenerating system (20mM Tris pH7.4, 2mM ATP, 5mM MgCl_2 , 40mM creatine phosphate, 0.5µg/µl creatine kinase). I.V.T. is subsequently immunoprecipitated and prepared for western blot.

- *S100 extract preparation*: Cells are lysed for 15-30mins in Hypotonic buffer (20mM Tris pH7.4, 5mM MgCl_2 , 8mM KCl, 1mM dithiothreitol, 0.5mM PMSF, 10µg/ml leupeptin,

1µg/ml pepstatin, 0.1mM PABA, 10µg/ml aprotinin). Lysates are centrifuged at 14,000rpm to remove cell debris. Supernatants are transferred and are further ultracentrifuged at 100,000g for 4 hours.

6.6.4 Microtubule co-sedimentation assay

Cells were washed with ice-cold PBS, scraped into 1 ml of PBS and collected by centrifugation. The cells were solubilised in PTN buffer (100 mM PIPES, 30 mM Tris, 50 mM NaCl, 1 mM EGTA, 1.25 mM EDTA, 1 mM DTT, 1% Triton X-100, pH 6.9) containing protease inhibitors. Supernatants were cleared by centrifugation for 30 minutes at 100,000×g at 25°C. Tubulin (Sigma; 5mg/ml in buffer A: 100 mM MES, 1 mM EGTA, 0.1 mM EDTA, 0.5 mM MgCl₂, 100 µg/ml sucrose, 1 mM DTT, 0.1 mM GTP, 1 µg/ml leupeptin, 1 µg/ml aprotinin, pH 6.8) was polymerised with 50 µM taxol in the presence of 2.5 mM GTP for 30 minutes at 37°C. 50µg of re-polymerised microtubules per assay were pelleted by centrifugation for 30 minutes at 100,000×g at 25°C. The microtubules were resuspended in 60 µl of pre-cleared cell supernatant containing 50µM taxol and incubated for 30 minutes at 37°C. Samples were then centrifuged for 30 minutes at 100,000×g at 25°C, and supernatants and pellets were analysed by SDS-PAGE and immunoblotting. Plasmid DNA was *in vitro* translated using the TNT Quick Coupled Transcription/Translation Systems (Promega). 10 µl of cold *in vitro* translated HA-tagged pVHL was incubated with polymerised microtubules in a total volume of 60µl and processed as described above.

6.6.5 Microtubule stability assay

MT stabilisation assays were performed as described previously (Krylova et al., 2000). Briefly, exponentially growing COS-7 were plated on coverslips and transfected the next day with indicated constructs using Fugene as described by the manufacturer. 44-48 hours post-transfection cells were- treated with 10µM nocodazole for the indicated time points before processing cells for immunofluorescence using anti-acetyl-tubulin and anti-HA (Y11) antibodies. Untagged pVHL was detected using anti-pVHL₃₀ antibody. DNA was stained with DAPI. At least 300 cells per experiment were analysed for an intact MT network. Only cells with intact nuclei and a clearly detectable cytoplasmic signal of HA-pVHL (or pVHL-GFP) were included in the evaluation. Experiments were repeated as blind assays.

The following adjustments were made for experiments described in Part B: exponentially growing COS-7 cells were plated on coverslips and transfected the next day with indicated constructs using Fugene as described by the manufacturer. 18-24 hours post-transfection cells were- treated with 10µM nocodazole for 20 minutes before processing cells for immunofluorescence using anti-α-tubulin (YL1/2), anti-HA (Y11), where in this case the HA-tagged protein represents an additional protein of interest, e.g.p97. Untagged pVHL was detected using anti-pVHL₃₀ antibody. At least 300 cells per

experiment were analysed for an intact microtubule network. Only cells with intact nuclei and a clearly detectable cytoplasmic signal of pVHL and HA-tagged protein of interest were included in the evaluation. In this way, effects of other factors that may alter VHL's ability to stabilise microtubules can be investigated.

6.6.6 *In vitro* phosphorylation of pVHL

GST-fusion constructs were expressed in *E. coli* or sf9 cells and purified using glutathione-Sepharose affinity resin. Purified protein was incubated with kinase of interest in appropriate buffer (e.g. 20-50mM Tris, 10mM MgCl₂, 5mM DTT at pH 7.5) supplemented with 10 μ Ci of [γ -P³²]-ATP (2,000 Ci/mmol). Kinase reactions were performed for 30 minutes at 30°C. Phosphorylated proteins were separated by SDS-PAGE, the gels were dried and visualised by auto-radiographic exposure.

6.7 Imaging

6.7.1 Immunofluorescence microscopy

Exponentially growing cells were plated on coverslips and processed for indirect immunofluorescence microscopy. Cells were washed with wash buffer (PBS/0.05% Tween/EGTA), fixed in 3% paraformaldehyde / 2% sucrose in PBS (pH 7.4) for 10-15 minutes at 37°C and permeabilised using 0.2% Triton X-100 in PBS for 2 minutes at room temperature, or in acetone (-20°C) for 30 seconds. Alternatively, cells were fixed for 5 minutes in methanol/acetone (-20°C) or in freshly prepared 4 % formaldehyde in PBS for 10 minutes at room temperature and permeabilised using acetone (-20°C) for 30 seconds. All subsequent steps were carried out at room temperature. Coverslips were rinsed with wash buffer and incubated for one hour with indicated primary antibody diluted in 1% BSA/1% goat serum in PBS. After three washes with wash buffer for 5 min each, coverslips were incubated with the appropriate secondary antibody. Secondary antibodies included donkey anti-rabbit aminomethylcoumarin (AMCA), donkey anti-mouse fluorescein isothiocyanate (FITC), anti-rat Texas-Red, donkey anti-rabbit FITC and anti-mouse Texas-Red. DNA was counterstained with 1 μ g/ml 1,4,6-diamidino-2-phenylindole (DAPI) or 10 μ g/ml propidium iodide. F-actin was stained with Texas Red-conjugated phalloidin. Coverslips were then inverted into 5 μ l Vecta-shield mounting medium. For labelling of mitochondria, cells were incubated with MitoTracker (M-7512) for 30 minutes at a final concentration of 100nM prior to fixation. Images were obtained with an Eclipse E800 microscope using a CoolPix950 digital camera (Nikon) or with a Fluoview FV500 confocal laser-scanning microscope (Olympus). Photographic images were processed using Adobe Photoshop, version 6.0.

6.7.2 Time-lapse video microscopy

For live microscopy, cells were mounted in purpose-built observation chambers (Type 1, Life Imaging Services, Olten, Switzerland) and imaged at 37°C on a Leica DM-IRBE

inverted microscope using high numerical aperture oil-immersion lenses and a GFP-optimised filter set (Chroma Technology, Brattleboro, Vermont). Images were captured using a MicroMax cooled CCD camera (Princeton Instruments, Trenton, NJ) and MetaMorph Imaging Software (Universal Imaging Corporation, West Chester, PA). Images were taken every 15 s with a 2 s exposure using neutral density filters to prevent photo damage.

- *Image Analysis*: Still images from individual frames of original video recordings were prepared using Metamorph 2.75 (Universal Imaging, West Chester, PA), and pictures were assembled with Adobe Photoshop.

6.8 Proteomics

6.8.1 2D-gel electrophoresis

- *Protein precipitation*: 4x volume methanol was added to protein sample and vortexed. 1x volume chloroform is added to the mixture, vortexed and spun. 3x volumes of ddH₂O was added, vortexed and spun again. Aqueous (upper) phase was discarded. A further 3x volume of methanol was added, vortexed and spun. Supernatant was removed, pellet was dried in speed-vac and stored at -80°C.

- *2D-gel electrophoresis*: Protein pellet was re-suspended in re-hydration buffer (7M urea, 2M thiourea, 4% CHAPS, 1% DTT and 2% Pharmalyte 3-10). Samples were loaded onto onto pH3-10 (minigel) or pH4-7 (large gel) linear IPG strip (Pharmacia) by re-swelling the strips in buffer. Iso-electric focusing for approximately 6.5kV (minigel) or 100kV (large gel) at 20°C was followed by equilibration with 2% DTT followed by 5% iodoacetamide. For second dimension migration, IPG strips were applied to SDS-PAGE gels (12.5% acrylamide, unless otherwise stated) and run at 30mA (minigel) or 200mA (large gel).

- *Gel processing*: Gels were subsequently prepared for western blotting or stained with Colloidal Coomassie Blue G-250. Stained gels were digitalised using *Personal Densitometer SI* (Molecular Dynamics) and statistically evaluated for differences in spot intensity. Stained protein spots were isolated, washed twice with 50% acetonitrile in 0.1M ammonium bicarbonate and evaporated. Gel pieces were reduced with DTT and alkylated with iodo acetamide, washed, dried and swollen in digestion buffer (50mM ammonium bicarbonate, 5mM CaCl₂) containing 12.5µg/mg trypsin for 45 minutes on ice. Samples were centrifuge for 5 minutes at 10,000g following incubation in digestion buffer for 16 hours at 37°C without enzyme. Peptides were identified as outlined below.

6.8.2 Peptide Identification

- **MALDI-TOF**: Protein Identification involved protein digestion using trypsin, and the masses of the generated peptides measured by MALDI-TOF (Tofspec 2E, Micromass) peptide mass fingerprinting. The programme, *ProteinLynxGlobalServer* (PLGS), was used for protein identification.

- **LC-MSMS:** Failing protein identification by peptide mass fingerprinting, protein identification using LC-MSMS was employed. Proteins are digested with trypsin and the peptides are separated by capillary LC online connected to an IonTrap MS (Finnigan Deca XP). In the MS, the peptides are fragmented and the masses of the fragments provide sequence information. The programme *TurboSequest* was used to identify the corresponding proteins. Since proteins are identified with sequence information of single peptides this method can also be used to identify proteins in complex mixtures and to search genomic and EST libraries.

CHAPTER 7

RESULTS – PART I:

Identification of novel VHL interacting proteins

7.1 Introduction

As discussed in chapter 3, genotype-phenotype relations in patients with VHL disease suggest that VHL has multiple functions, and that some of these functions may be tissue specific. Indeed, mutations that give rise to type 2C disease, those corresponding to predisposition to pheochromocytoma but to no other VHL-associated tumours, retain their ability to degrade HIF α . This strongly suggests, that in these individuals, lesions of the adrenal glands arise independent of HIF inactivation, supporting the notion that non-HIF related functions of pVHL exist.

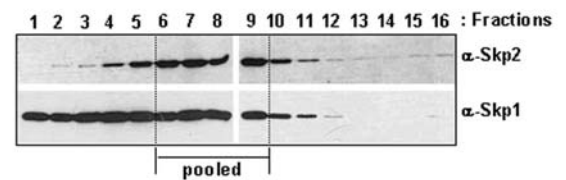
In an attempt to elucidate novel functions of pVHL, or to help further explain already existing knowledge, efforts were made to identify new pVHL-protein interactions. Previous undertakings by various groups had revealed crucial insights into normal VHL functioning within the cell. When beginning this project, VHL-protein interactions were limited to the VCB-Cul2 ligase components [192-194] and the extra-cellular matrix protein fibronectin [134]. Since then many other protein interactions have been identified which have helped our understanding of VHL biology (see chapter 4), and in particular the finding that pVHL interacts with the basic helix-loop-helix transcription factor HIF α and targets it for ubiquitin-mediated proteasomal degradation [114]. This interaction represent a milestone in VHL biology and has helped us to appreciate how VHL is involved in the process of oxygen sensing and the pathological consequences that arise as a result of its deregulation.

Identification and confirmation of pVHL-protein interactions has involved various protein-protein interaction approaches ranging from basic immuno-precipitation reactions to yeast tetra-hybrid systems. It was felt that a new approach of searching for pVHL-protein interactions might facilitate the identification of novel candidates. Some of these methods are outlined below. While initial attempts may not have proved successful, they helped pave the way for a more successful large-scale endogenous proteomics approach and are therefore briefly discussed.

7.2 Towards defining an experimental approach

Initial attempts involved trying to purify the VBC complex (pVHL-Elongin B-Elongin C), which would then be used to screen for novel substrates of the VBC-Cul2 ligase. Far western technology, a method involving the renaturation of proteins on a membrane in the presence of decreasing concentrations of guanidine-HCl, was used to define the specificity of the purified complex. This technique had already been employed by others to show pVHL interactions with fibronectin and HIF2 α [134]. Identification of where the probe binds the membrane would indicate the specificity of the probe and its potential as a tool to screen two λ gt11 expression libraries, human cerebellum and human foetal kidney, in a fashion similar to *Harlow et al.* in the identification of NPAT, a novel substrate for the cyclin E/CDK2 complex shown to promote S-phase entry [336]. In light of the fact that cyclins are involved in substrate specificity of cyclin dependent kinases (CDKs), it seemed important to consider that ligase components could influence the binding of pVHL to other proteins. Therefore it was deemed more suitable to use the ligase complex to probe for new physiological substrates than pVHL alone. Before beginning with purification of the trimeric VBC complex, the experimental parameters were tested using a simpler system – the ability of the dimeric complex, pSkp1-pSkp2, to bind its substrate, the cyclin dependent kinase inhibitor p27. As this was an established interaction, and the complex easier to purify, it was used to define experimental conditions. The approach involved co-expressing GST-Skp1 and untagged pSkp2 in sf9 cells, followed by a GST-pulldown which would co-precipitate pSkp2. After thrombin cleavage from the GSH sepharose, the protein precipitate was separated on a glycerol gradient so as to separate complexed from uncomplexed pSkp1 and pSkp2. Following the glycerol gradient, the fractions were pooled that corresponded to complexed pSkp1-pSkp2 and this was used in far western as a probe to screen constructs previously expressed in bacteria including GST, p21, pVHL, wild-type p27 and a mutated p27 construct (termed p27^{KANA}/_{NADA} which prevents CDK2/Cyclin A binding). Figure 54

A) Purification of pSkp1/pSkp2 complex over a glycerol gradient



B) Far Western demonstrating the specificity of the pSkp1/pSkp2 complex for the CDK inhibitor p27

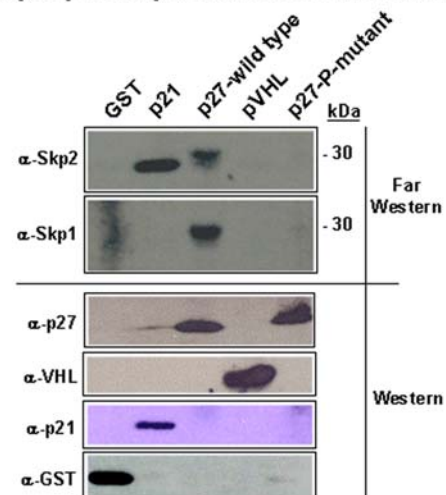


Figure 54. A novel means of mapping the SCF^{Skp2} complex-p27 interaction. A) Following co-expression in sf9 cells, complexed pSkp1 and pSkp2 were isolated over a glycerol gradient. B) The complex pSkp1/pSkp2 was assayed for its binding to renatured GST, p21, pVHL, wild-type and mutant p27. While for pSkp2 a signal is present for both wild-type p27 and p21, the pSkp1 signal which overlays with that of the pSkp2 signal demonstrates that pSkp1 determines specificity of the pSkp1/pSkp2 complex, albeit in this assay. The western blot demonstrates expression of all components.

demonstrates that under these conditions, the pSkp1-pSkp2 complex, and only when complexed, binds wild-type p27 but not mutated p27 thereby representing a novel means of mapping the pSkp2-p27 interaction. Interestingly, a pSkp2 signal was also observed for renatured p21, yet when probed with α -Skp1, the only overlapping signal between pSkp2 and pSkp1 was that of wild-type p27, suggesting that pSkp1 determines, at least in part, substrate specificity of the SCF^{Skp2} complex for p27.

However, while this technique was successful with respect to pSkp1-pSkp2 recognition of wild type p27, trying to purify a VBC trimeric complex of sufficient purity was difficult. All three protein components, pVHL, Elongin B and Elongin C, were co-expressed in sf9 cells and GST-VHL₃₀ successfully precipitated elongins B and C. However problems were encountered when cleaving the protein complex from the glutathione sepharose beads with the ser/thr protease, thrombin. Interestingly, thrombin cleavage resulted not only in cleaving of GST from recombinant pVHL₃₀, but also in specifically cleaving pVHL₃₀ itself. This was completely unexpected. Sequence analysis revealed no particular consensus site, though such sites for thrombin remain poorly defined. Intriguingly, the VHL crystal structure was performed on a VBC complex purified from bacteria, where GST was fused to VHL₁₉ and thrombin-cleaved prior to crystal structure analysis. There is no mention of pVHL cleavage by thrombin. As a result of this cleavage, it was opted to elute the complex using free glutathione, a disadvantage of which was that the complex retained the rather large and bulky GST tag.

Additional challenges arose when purifying the VBC complex over a glycerol gradient. Unlike the gradient shown for pSkp1 and pSkp2, this resulted in smearing of the VBC complex components across many fractions and disruption of the protein complex. Using glycerol gradients to isolate a complex suitably pure to be used as a screening probe was therefore abandoned in favour of large scale sf9 expression using spinner flasks and concentration of the complex using Centricon devices (YM100, 000) of appropriate molecular weight size that retained the complex, but allowed proteins of lower molecular weight to be discarded. Nonetheless, when this complex was used as a probe on far western to probe whole cell extracts derived from 786-0 cells to visualise HIF2 α , the non-specific binding of the probe rendered the approach inappropriate (data not shown). For this reason, the approach was abandoned and an alternative *in vivo* one sought.

The first *in vivo* approach involved establishing stably expressing GST-fusion proteins of pVHL₃₀, pVHL₁₉ and pVHL₁₋₁₅₇, a naturally occurring truncated mutation. Expressing a GST-fused version of pVHL within a mammalian cell line would facilitate large-scale isolation of pVHL and could increase the probability of co-precipitation of protein interactions. Moreover an *in vivo* approach would allow for the identification of physiological substrates, as any binding partners necessary for specific recognition, like elongin C and B, would already be present. Cell lines were established in HEK (293)

cells, a human foetal kidney cell line with high transfection efficiency. Metabolic labelling of these cells using S^{35} -incorporation and subsequent GST-pulldown facilitated an overview of proteins precipitated with the GST fused-proteins of interest, and furthermore allowed comparisons between the selected pVHL forms and GST control. Figure 55 illustrates the results obtained from one such *in vivo* labelling experiment. The conclusion from this experiment was that differences occurred among samples, and that reproducible and specific bands could be seen precipitated with GST-VHL forms that do not precipitate with the GST control. This experiment was the first indication that an *in vivo* approach of this kind could be used to identify pVHL interacting proteins, some of which would hopefully prove to be physiologically relevant.

In order to identify the proteins, GST-pulldown experiments were ran out on large (15cm) SDS-PAGE gels and the bands of interest cut out and processed for peptide mass fingerprinting or LC-MSMS as outlined in material and methods, chapter 6. As the vast majority of bands of interest lay within a 40-200 kDa

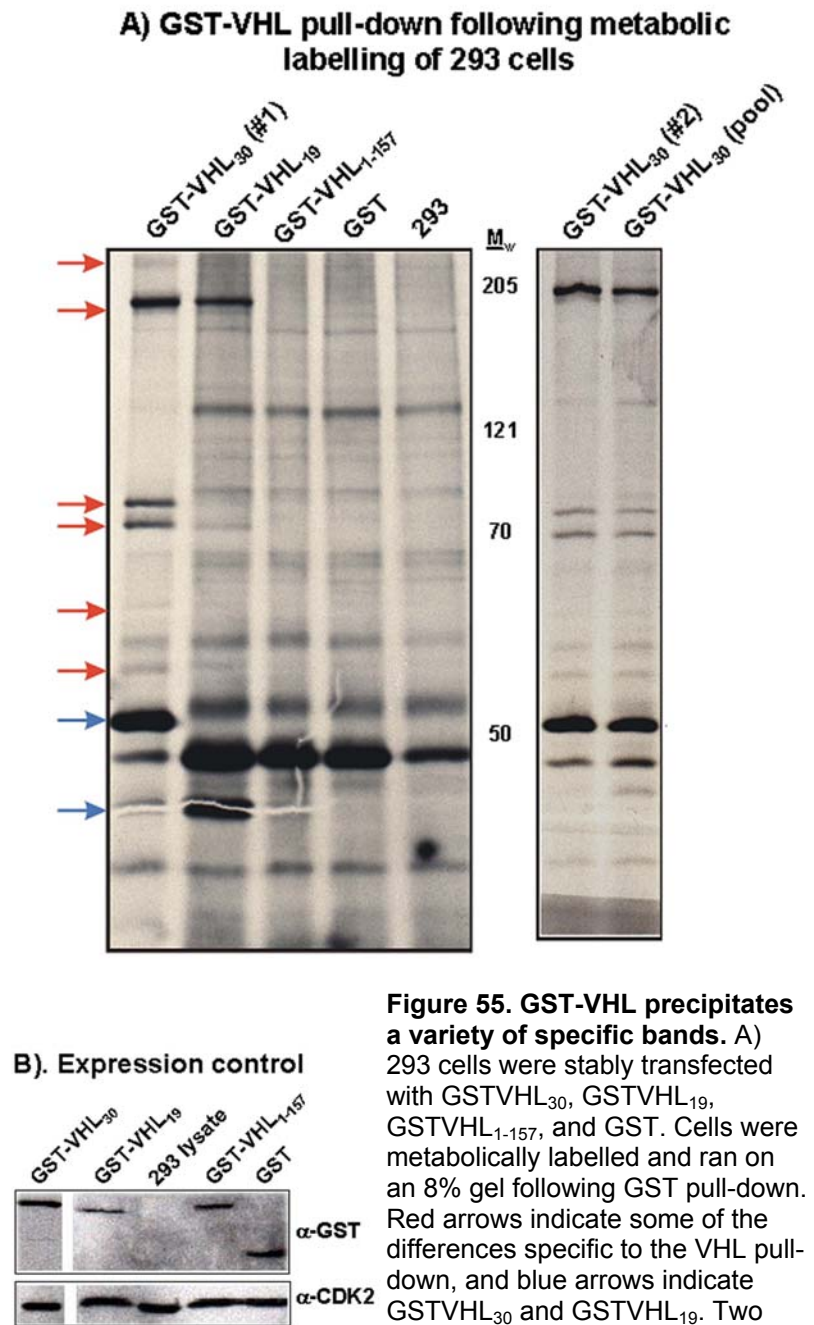


Figure 55. GST-VHL precipitates a variety of specific bands. A) 293 cells were stably transfected with GSTVHL₃₀, GSTVHL₁₉, GSTVHL₁₋₁₅₇, and GST. Cells were metabolically labelled and ran on an 8% gel following GST pull-down. Red arrows indicate some of the differences specific to the VHL pull-down, and blue arrows indicate GSTVHL₃₀ and GSTVHL₁₉. Two independent clones and a mixed pool of GST-VHL₃₀ demonstrate the reproducibility of the results. B) Expression control confirming expression of all cell lines.

Table 18. Results from *in vivo* GST-pulldown

Protein species	kDa	Function
Myosin (MHCIIA)	225	Actin binding motor protein
Cullin 2	80	VBC-Cul2 E3 ligase
Drebrin	70	Actin binding protein
Heat Shock Protein 60	60	Mitochondrial import chaperone
Vimentin	53	A class III intermediate filament

range, 8% gels were ran for greater resolution. The results of the protein identification are summarised in table 18. While other proteins were identified, they mainly represented background, e.g., Keratin, and are not shown. The identification of Cullin 2 demonstrated that the approach not only could identify specific and direct pVHL interactions, but also indirect interactions as cullin 2 does not bind pVHL directly, but rather via elongin C. These proteins were investigated individually, but unfortunately rendered no promising results. No endogenous interaction could be shown for Drebrin, nor HSP60, and in

immunofluorescence, vimentin did not co-localise with pVHL (despite the fact that data exists which has shown that another tumour suppressor, p53, physically associates with vimentin [337]). Initially, the actin motor protein myosin heavy chain nonmuscle type II A (MHCIIA) seemed interesting. Figure 54 outlines an experiment showing that ectopically expressed GST-VHL₃₀ can precipitate endogenous MHCIIA, whereas other GST-fused protein products failed to do so. Given the fact that at this time p53 had been shown to bind the microtubule cytoskeleton, an interaction which facilitated its shuttling in and out of the nucleus, and that evidence supported a similar cellular shuttling for pVHL, it seemed logical to suggest that pVHL may be binding to a component of the cytoskeleton which too may have facilitated its shuttling in and out of the nucleus. For p53, Dynein had been shown as the component capable of bridging p53 to the microtubules. Dynein is a minus-end directed microtubule motor protein. Intriguingly, myosin is also a motor protein, albeit an actin binding motor protein, and at this time it seemed plausible, given the p53 finding, that pVHL could also bind a motor protein that may participate in its intracellular shuttling behaviour. However, despite the result in figure 56, many attempts were made to demonstrate a functional significance for a pVHL-MHCIIA interaction, but to no avail. It has since emerged that MHCIIA frequently occurs in such pull-down experiments, and should be considered with caution. For these reasons, an alternative, more robust assay was developed.

7.3 Endogenous pVHL IP and analysis by mass spectrometry

Previous approaches had failed due to their inability to reproduce an endogenous interaction between pVHL and the identified protein. For this reason, an alternative approach was devised that would circumvent this problem from the outset. A proteomics approach was developed which entailed immuno-precipitating endogenous pVHL and its

Ectopically expressed GST-VHL₃₀ precipitates endogenous MHCIIA

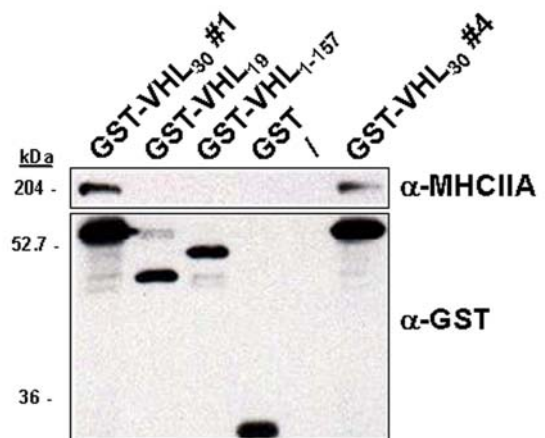
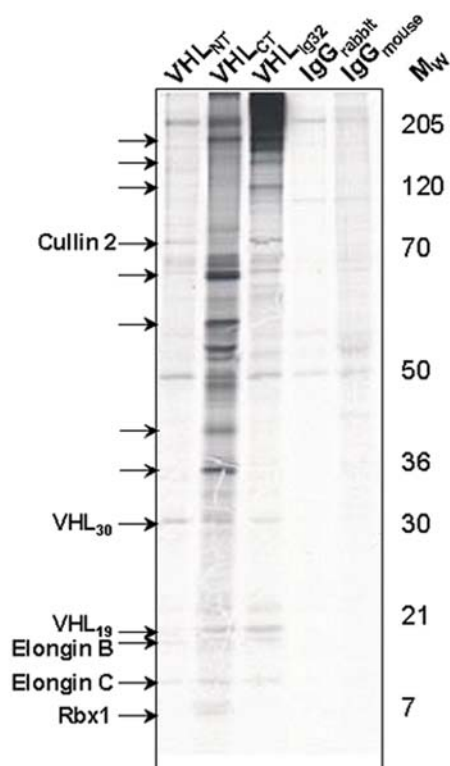


Figure 56. Repetition of GST-pulldown to verify that ectopically expressed GST-VHL₃₀ binds endogenous MHCIIA *in vivo*. Two independent clones of GSTVHL₃₀ demonstrate MHCIIA precipitation, whilst other pVHL constructs do not.

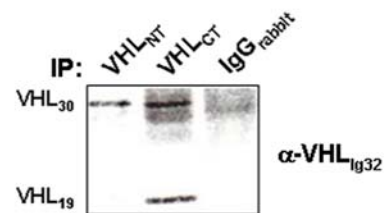
subsequent bound protein partners. In this way, endogenous interactions were established from the beginning, which would facilitate ease of experimental manipulation when confirming the interaction later.

The major obstacle in this approach was in attaining protein amounts sufficient for sequence analysis. Three antibodies capable of immuno-precipitating pVHL were analysed for their efficiency to target pVHL. VHL_{Ig32} is a commercially available monoclonal mouse- α -human antibody recognising both pVHL₃₀ and pVHL₁₉. VHL_{NT} is an antibody raised against full-length pVHL₃₀ but purified to recognise only pVHL₃₀ and not pVHL₁₉. Finally, VHL_{CT} is a polyclonal rabbit- α -human antibody raised against the last 20 amino acids of pVHL and recognises both pVHL₃₀ and pVHL₁₉, thereby reflecting the true abundance of these two proteins with respect to each other. Figure 57 demonstrates an experiment where cells have been metabolically labelled with S³⁵ prior to IP. The result reveals interesting differences between IP reactions, and that the pattern of co-precipitating proteins differs among the different antibodies used. Figure 57(B) further demonstrates recognition of both VHL forms in western blotting following IP with VHL_{CT}

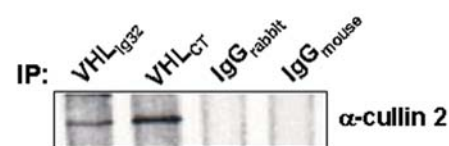
A) Comparison of VHL antibodies in IP following S³⁵-metabolic labelling of HeLa cells



B) VHL_{CT} IP's both VHL₃₀ and VHL₁₉



C) VHL_{CT} IP's cullin 2, an indirect pVHL-protein interacting protein



D) Characterisation of cell line

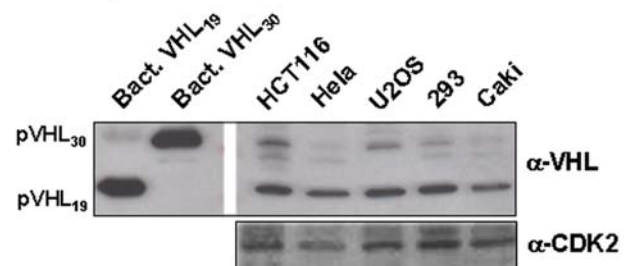


Figure 57. Antibody and cell line characterisation for endogenous proteomics approach. A) 293 cells were metabolically labelled with ³⁵S and prepared for immuno-precipitation by three pVHL specific antibodies, VHL_{Ig32}, VHL_{CT} and VHL_{NT}. B) Comparison of pVHL₃₀ and pVHL₁₉ immuno-precipitation by VHL_{NT} versus VHL_{CT}. C) Cullin 2 precipitation by VHL_{Ig32} and VHL_{CT}. D) Comparison of pVHL levels in five transformed cell lines: HCT116 - human colon carcinoma; HeLa - human cervix carcinoma; U2OS - human osteosarcoma; 293 - human foetal kidney; Caki - human renal cell carcinoma.

compared to VHL_{NT}, and figure 57(C) shows the ability of VHL_{CT} and VHL_{Ig32} to co-precipitate indirect pVHL interacting proteins, namely cullin 2. Due to the efficiency of pVHL recognition in IP reactions, the ability to recognise both pVHL forms, and an unlimited source of antibody, the VHL_{CT} antibody was chosen as the antibody to be employed for the proteomics approach.

The next experimental parameter to be defined was the cell line. Figure 55(D) demonstrates that pVHL levels fluctuate considerably among a panel of different transformed cell lines, especially with respect to their comparative levels of pVHL₃₀. HCT116 cell are immortalised cells derived from a human colon carcinoma. They demonstrated high expression of both pVHL₃₀ and pVHL₁₉, and for this reason were chosen as the cell line to be used.

Initial experiments aimed at attaining enough material for sequencing were hampered by problems of antibody contamination. For this reason, VHL_{CT}, and its corresponding IgG_{rabbit} control, were covalently cross-linked to protein A sepharose beads. This reduced dramatically the extent of antibody contamination and facilitated better visualisation of co-precipitating bands. Furthermore it permitted the use of more antibody, as it was cross-linked to beads at a high concentration, 2mg of antibody per millilitre of beads, thereby facilitating the maximum immuno-precipitation of pVHL. Figure 58 shows the ability of coupled-VHL_{CT} to efficiently immuno-precipitate both pVHL forms, pVHL₃₀ and pVHL₁₉, in HCT116 cells.

For greater resolution of proteins following large-scale immuno-precipitation of pVHL, 2D gel-electrophoresis analysis

Coupled-VHL_{CT} immuno-precipitates pVHL₃₀ and pVHL₁₉ in HCT116

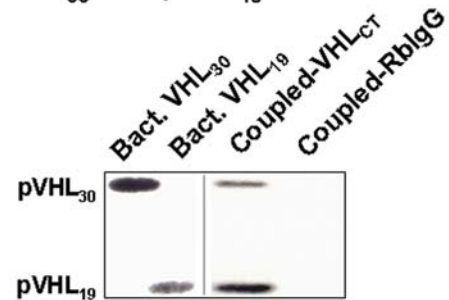


Figure 58. VHL_{CT} coupled to protein A sepharose immuno-precipitates both pVHL₃₀ and pVHL₁₉. Antibody was bound at a concentration of 2mg of antibody per ml of beads.

2D gel overlay of VHL and control IP

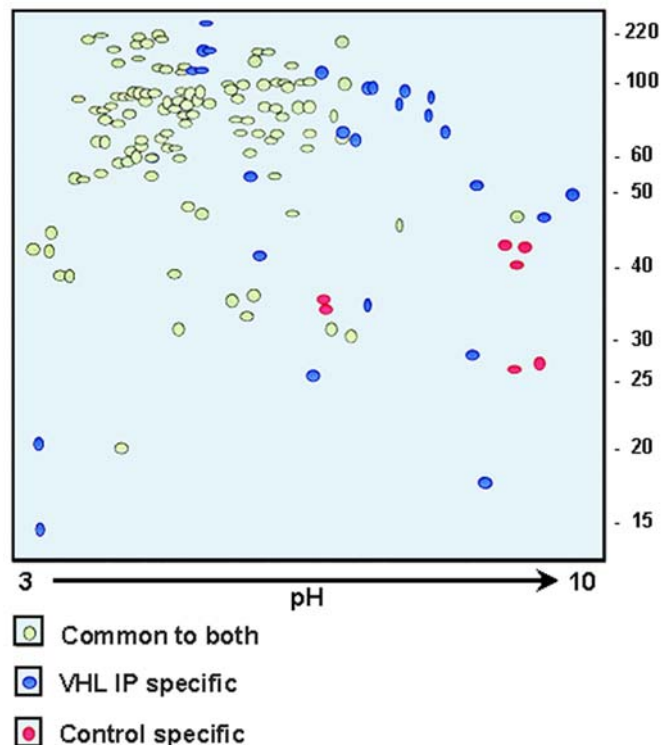


Figure 59. Overlay of trial VHL and control IgG IP to investigate differences specific to pVHL. Samples were separated on 10cm IPTG strips of pH 3 to 10, and ran on 10% SDS-PAGE gels. Gels were stained using colloidal coomassie blue, scanned, and overlaid in Adobe photoshop, version 6.0

was used to separate proteins in two dimensions based on isoelectric focusing and standard SDS-PAGE electrophoresis. While the obvious advantage of enhanced resolution of this approach over its standard one-dimensional counterpart justified its use, one disadvantage was that greater protein amounts were necessary for subsequent protein detection by MALDI-TOF peptide mass fingerprinting or LC-MSMS nano-spray approaches. Figure 59 illustrates a trial experiment to estimate how much material would be required. The gels were stained with colloidal coomassie blue, scanned and overlaid in Adobe photoshop. The aim was to compare protein samples between the pVHL IP reaction and that of its corresponding control in an effort to identify proteins unique to the pVHL IP reaction. Based on this experiment, it was apparent that differences could be seen using this endogenous IP method, but that in order to gain sequence information pertaining to the identity of these candidate pVHL protein partners, the input needed to be further increased.

The final approach involved an experiment consisting of a pVHL IP from approximately 2.25×10^9 HCT116 cells using 1.25ml of coupled VHL_{CT} beads, corresponding to a concentration of 2.5mg of antibody (see material and methods for sample preparation). Cells were grown, lysed and pVHL immuno-precipitated in separate batches so as not to compromise the quality of sample preparation. Following protein precipitation after each IP reaction, the precipitated protein pellet was stored at -80°C until all samples were ready for loading onto the 2D gel. The pellets were pooled together and re-solubilised in the appropriate amount of rehydration buffer overnight. Figure 60 illustrates the results from one such experiment.

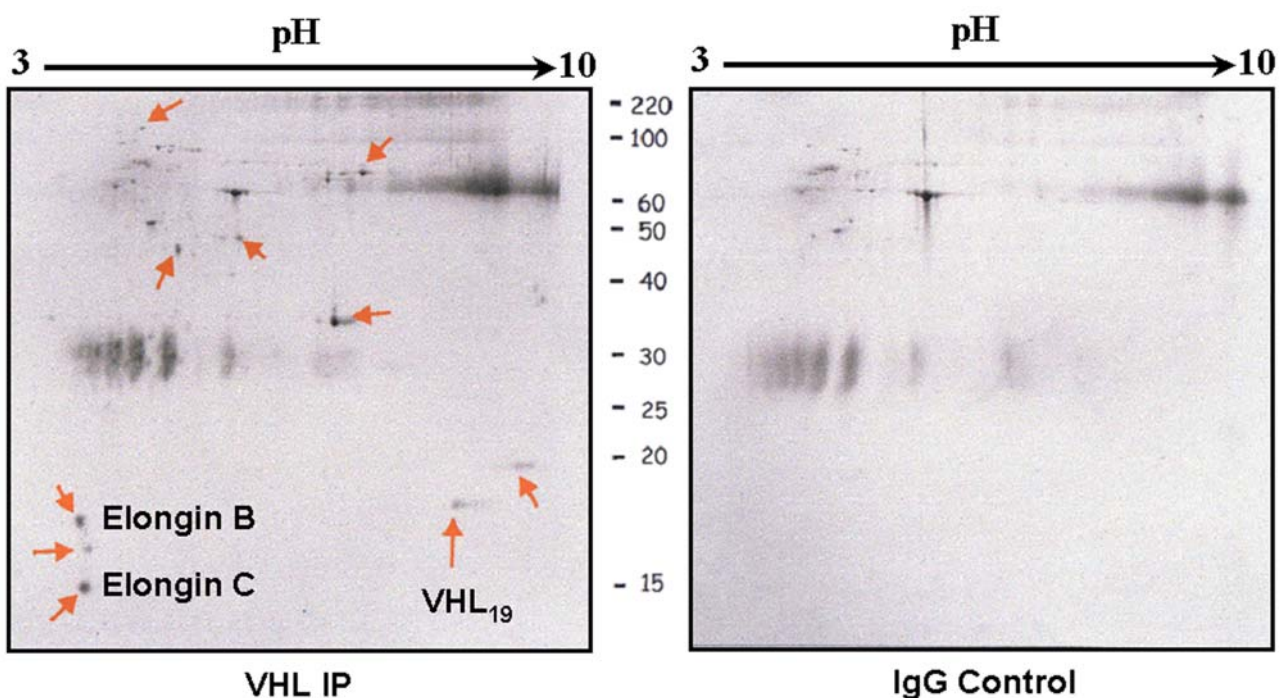


Figure 60. 2D-gel analysis of VHL and control IP from HCT116 cells. Samples were loaded onto a 10cm IPTG strip of pH range 3-10, and further migrated on a 10% SDS-PAGE. Gels were stained using colloidal coomassie to detect proteins. The red arrows indicate some of the differences specific to the VHL IP.

Protein spots that were found in both gels were considered as background, and only those spots unique to the pVHL IP reaction were excised and prepared for analysis. Proteins were first prepared for analysis by MALDI-TOF peptide mass fingerprinting. If detection was unsuccessful, the protein sample was further analysed by LC-MSMS, which employs technology capable of protein identification in a much lower range. Following the attainment of sequence information pertaining to the peptides isolated, protein identification was achieved using two databases; swpnr39.2 and Prowl in NCBI nr 060901. Table 19 outlines the results from this experiment. While 27 spots were excised, many of these spots represent different fragmented versions of the same protein species and therefore appear more than once.

Table 19. Results of protein identification following large-scale pVHL IP.

Sample	MALDI	LC-MSMS	Comments
01E102	Q15369	-	RNA pol
02E102	peptides no hit	Q15370	Elongin B
03E102	Q15370	-	Elongin B
04E102	peptides no hit	P55072, tera_hum	p97; VCP
05E102	peptides no hit	peptides no hit	-
06E102	peptides no hit	-	-
07E102	Keratin I & II	Keratin I, II & IX	-
08E102	weak spectra	-	-
09E102	weak spectra	-	-
10E102	Q9ULR7, dj967n21.3	-	Homologue to
11E102	peptides no hit	Q9ULR7, dj967n21.3	yeast-trans. in.
12E102	dj967n21.3	-	factor 3-gamma
13E102	dj967n21.3	-	
14E102	Q9ULR7, dj967n21.3	-	
15E102	peptides no hit	peptides no hit	
16E102	gi/15301015	-	R-RNA-A
17E102	gi/15301015	-	dimethylases
18E102	gi/15301015/AAH10167	-	
19E102	gi/15301015	-	
20E102	VHL	VHL_human	VHL
21E102	peptides no hit	Q9UJA5, dj967n21.3	-
22E102	Q9UJA5, dj967n21.3	-	-
23E102	peptides no hit	-	-
24E102	peptides no hit	peptides no hit	-
25E102	peptides no hit	peptides no hit	-
26E102	peptides no hit	peptides no hit	-
27E102	peptides no hit	peptides no hit	-

NB: Colours denote proteins of the same species

7.4 pVHL interacts with the AAA-ATPase family member, p97

7.4.1 Introduction

The proteomics approach of section 7.3 revealed that p97, a member of the family of AAA-ATPase's, co-precipitated with pVHL following immuno-precipitation of pVHL by VHL_{CT}. The protein was identified by LC-MSMS identifying 10 peptides all directly corresponding to p97.

The ubiquitous ATPase p97 (also called vasolin-containing protein (VCP) in animals; Cdc48 in yeast; VAT in archaebacteria; AtCDC48 in *Arabidopsis*; TER94 in *Drosophila* and p97 in *Xenopus*) is abundant in all cells, comprising ~1% of all the cell cytosol [338], and participates in several cellular functions. p97 has been shown to be essential for viability in yeast [339] and flies [340]. It has been implicated in post-mitotic homotypic membrane fusion of the endoplasmic reticulum and the golgi apparatus [341, 342], assembly and growth of the nucleus [343], apoptosis [343, 344] and DNA replication [345, 346]. In addition, it has been shown to play a role in the extraction of misfolded luminal and membrane proteins from the endoplasmic reticulum for cytosolic degradation [347-350]. Most interestingly with respect to pVHL biology however, is the fact that p97 has been shown to be involved in the ubiquitin-proteasome-dependent degradation pathway [351-355].

Box 1. The AAA family of proteins

The AAA proteins, members of the larger AAA+ superfamily, are a family of enzymatic machines involved in diverse cellular functions ranging from DNA repair and replication to organelle biogenesis, membrane trafficking, transcriptional regulation, and protein quality control. The characteristic feature of this family is the presence of one or two conserved ATPase domains, referred to as AAA cassettes, which contain Walker A and Walker B motifs that mediate ATP binding and hydrolysis, respectively. AAA proteins were defined as ATPases associated with various cellular activities, but this definition disguises the breadth and importance of their functions and the common structures and mechanisms of action that underlie their activities.

AAA proteins do a lot of heavy work in the cell: erecting or disassembling complexes, unfolding or unwinding macromolecules, and transporting cellular cargo. This mechanical work requires a chemo-mechanical converter, the AAA module, which derives its energy from ATP hydrolysis. AAA modules are composed of 200–250 amino acids (Neuwald *et al.* 1999). The motor module is attached to other domains that act as tool heads, the latter interacting with substrates either directly or through 'adaptor' molecules. The connectors between the motor and the tool heads thus act as coupling devices, converting movements of the motor into the specialized motion required for a particular activity.

AAA proteins have either one (D1) or two non-identical (D1 and D2) AAA modules, each of which consists of a core with an α - β - α nucleotide binding fold and a C-terminal domain with at least three α -helices. AAA modules tend to oligomerise into hexameric rings, with all subunits oriented in the same direction.

Full length p97:

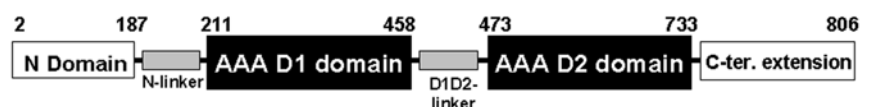
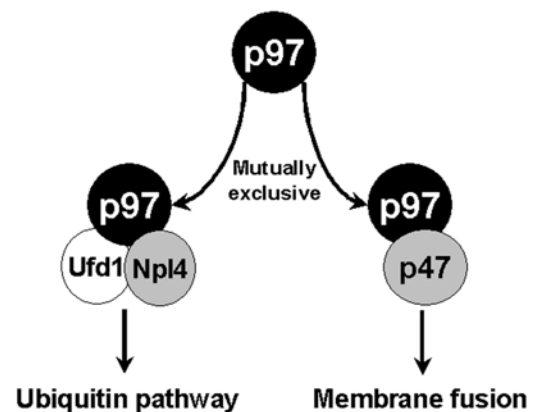


Figure 61. Schematic representation of the different domains of the full-length p97 monomer. p97 contains an N-terminal domain followed by two AAA domains, D1 and D2, which contain the first and second ATPase modules respectively. Gel filtration and light-scattering experiments have shown that p97 forms hexameric complexes.

Interestingly, almost all p97's activities are directly or indirectly related by the ubiquitin-proteasome system. The ubiquitin-proteasome-mediated degradation pathway consists of two sequential steps. The destined substrate is first conjugated with poly-ubiquitin chains, which tag it for proteolysis. The poly-ubiquitinated substrate is then moved, possibly guided by molecular chaperones, to the 26S proteasome for final degradation. The involvement of both p97 and the ubiquitin-proteasome systems in similar cell activities suggests that p97 may act as a chaperone in the ubiquitin-proteasome pathway, thus regulating the various cellular functions through the ubiquitin-proteasome pathway. Both genetic and biochemical studies indicate that this is indeed the case. Mutations in the CDC48 gene result in cell cycle arrest and the accumulation of poly-ubiquitinated proteins in yeast [339, 355]. Depletion of p97 from cell extracts abolishes the ubiquitin-proteasome-mediated degradation of cyclin E, leading to the accumulation of poly-ubiquitinated proteins in mammalian cells [355]. The involvement of p97 in the ubiquitin-proteasome degradation pathway was further supported by the findings that p97 directly binds poly-ubiquitinated proteins, as well as other ubiquitin-proteasome pathway components, such as Ufd1, Ufd2 and Ufd3 (proteins involved in the ubiquitin fusion degradation pathway), and the 26S proteasome [351-353, 356-358].

The ATPase p97 appears to perform different cellular functions depending on its association with cofactors [353]. Mammalian p97 can interact in a mutually exclusive manner with either p47 or a dimer consisting of Ufd1 and Npl4. In mammals, the complex of p97–p47 appears to play a role in the homotypic fusion of ER and Golgi membranes [341, 359, 360]. The p97–p47 complex binds ubiquitinated proteins via a UBA (ubiquitin association) domain in p47, and this domain is essential for its activity in Golgi membrane fusion [361]. In *Saccharomyces cerevisiae*, the complex of Cdc48–Ufd1–Npl4 has been implicated in the release of polypeptides from the ER membrane [362]. This release step is essential for both retrotranslocation of misfolded proteins from the ER into the cytosol, and for the activation of the transcription factor Spt23 from its ER-anchored precursor [363, 364]. SPT23 is a relative of mammalian NF- κ B and controls unsaturated fatty acid levels [348]. It is synthesised as a latent ER/nuclear membrane-localised precursor, and is activated by limited ubiquitin-proteasome degradation, similar to that seen with NF- κ B p105 processing. Mammalian p97 has also been shown to function in retrotranslocation [347], but a requirement for the cofactor Ufd1–Npl4 has not yet been demonstrated.

Mutually exclusive binding of alternative cofactors determines the specific role of p97



Exactly how p97 and its cofactor Ufd1–Npl4 extract polypeptides from the ER membrane during retrotranslocation is unclear. It is not known how the ATPase binds to the ER membrane, nor how the two ATPase domains collaborate to "pull" polypeptides out of the membrane. The mechanism of substrate recognition has been particularly difficult to address because its elucidation requires complex systems in which p97/Cdc48 acts on physiological substrates emerging from the ER membrane. Two possibilities of substrate recognition have been proposed. In one model, p97 would interact directly with an unfolded polypeptide segment as it emerges from the ER membrane. Alternatively, the recognition signal could be a poly-ubiquitin chain attached to a substrate. This model is based on the fact that all polypeptides emerging from the ER undergo poly-ubiquitination, and that this modification is required for the release of substrates from the ER membrane into the cytosol (reviewed in [362]).

The second model is based on the fact that mammalian Ufd1–Npl4 has been shown to bind poly-ubiquitin and has therefore been proposed to mediate substrate binding by p97 [361]. A zinc-binding motif in Npl4, the Npl4 zinc finger (NZF) domain, has been identified as the major binding site for ubiquitin [361, 365]. The relevance of the reported ubiquitin interactions for retrotranslocation is unclear, particularly because the ubiquitin binding to p97 is weak and the yeast homologue of Npl4 lacks an NZF domain. Ye *et al.* have proposed a dual recognition mechanism in which a non-ubiquitinated segment of a substrate is initially recognised by p97 itself, and subsequently, the polyubiquitin chain is bound by both p97 and the cofactor Ufd1–Npl4 [366].

7.4.2 pVHL interacts with p97

Figure 62 is a representation of the proteomics approach undertaken to identify novel pVHL interacting proteins (section 7.3). In the VHL IP a spot corresponding to approximately 100 kDa is present, but absent in the control.

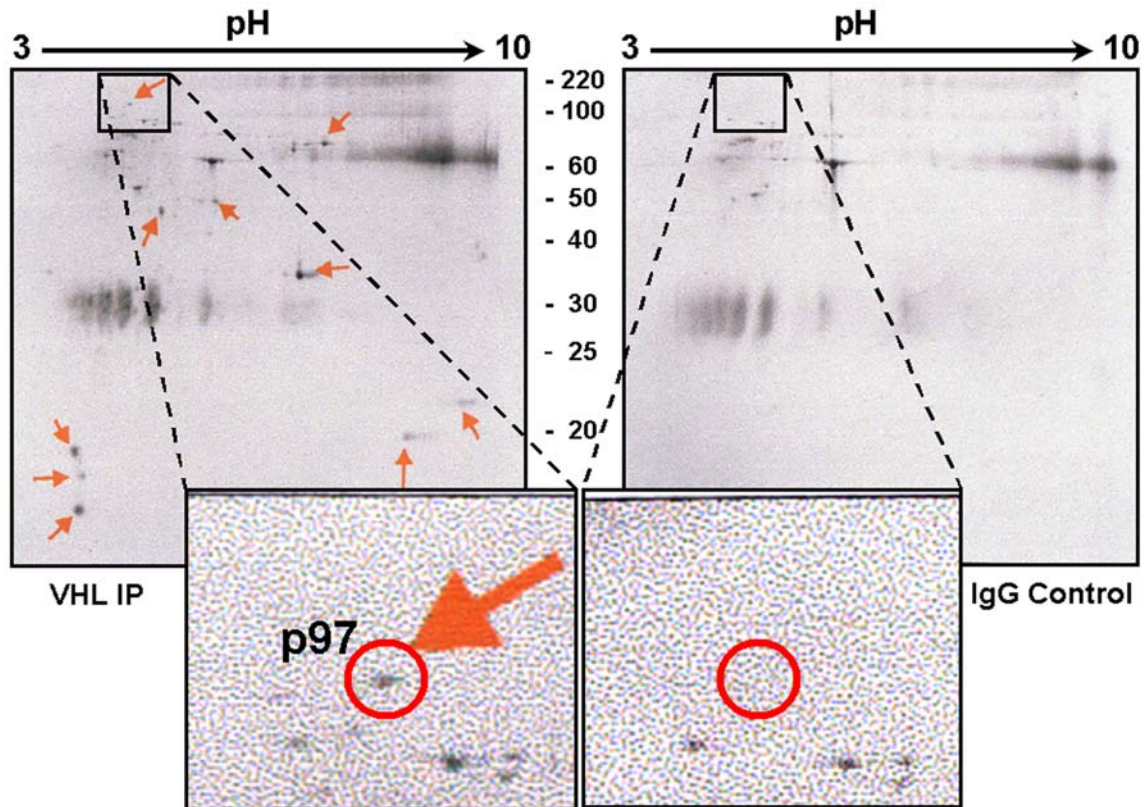


Figure 62. 2D SDS-PAGE of α -VHL IP from HCT116 cells. Isoelectric focusing was performed on 7cm IPTG strips with a pH range of 3-10. Samples were then run on a standard SDS-PAGE gel and stained with colloidal blue as per material and methods. Spots of interest were excised, and prepared for analysis by MALDI-TOF peptide mass fingerprinting, and if necessary LC-MSMS. The sample here illustrates the identification of p97 as a candidate protein specific to the VHL IP.

As outlined below, the identity of p97 was apparent from 10 separate peptides located throughout the p97 open reading frame corresponding to a protein coverage of 15% amino acid count, and 14.5% by mass. The file name *tera_human p55072 homo sapiens* represents the file name as per swpnr39.2, and refers to human p97.

```
>tera_human P55072 homo sapiens (human) – protein coverage: 15% amino acid count; 14.5% by mass
MASGADSKGD DLSTAILKQK NRPNRLIVDE AINEDNSVVS LSQPKMDELQ LFRGDTVLLK GKRRREAVCI VLSDDTCSDE
KIRMNRVVRN NLRVRLGDVI SIQPCPDVKY GKRIHVLPID DTVEGITGNL FEVYLPYFL EAYRPIKGD IFLVRGGMRA
VEFKVVETDP SPYCIVAPDT VIHCEGEPIK REDEEESLNE VGYDDIGGCR KQLAQIKEMV ELPLRHPALF KAIGVKPPRG
ILLYGPPGTG KTLIARAVAN ETGAFFFLIN GPEIMSKLAG ESESNLKAF EEAENAPAI IFIDELDAIA PKREKTHGEV
ERRIVSQLLT LMDGLKQRAH VIVMAATNRP NSIDPALRRF GRFDRFVDIG IPDATGRLEI LQIHTKNMKL ADDVDLEQVA
NETHGHVGAD LAALCSEAAAL QAIRKKMDLI DLEDETIDAE VMNSLAVTMD DFRWALSQSN PSALRETVEE VPQVTWEDIG
GLEDVKRELQ ELVQYPVEHP DKFLKFGMTP SKGVLFGYPP GCGKTLLAKA IANECQANFI SIKGPELLTM WFGESANVR
EIFDKARQAA PCVLFDELD SIAKARGGNI GDGGGAADRV INQILTEMDG MSTKKNVFII GATNRPDIID PAILRPGRLD
QLIYIPLPDE KSRVAILKAN LRKSPVAKDV DLEFLAKMTN GFSGADLTEI CQRACKLAIR ESIESEIRRE RERQTNPSAM
EVEEDDPVPE IRRDHFEAM RFARRSVSDN DIRKYEMFAQ TLQQSRGFGS FRFPSPGNQGA GPSQGSGGGT GGSVYTEDND
DDLGY
```

7.4.3 Verification of a pVHL – p97 interaction

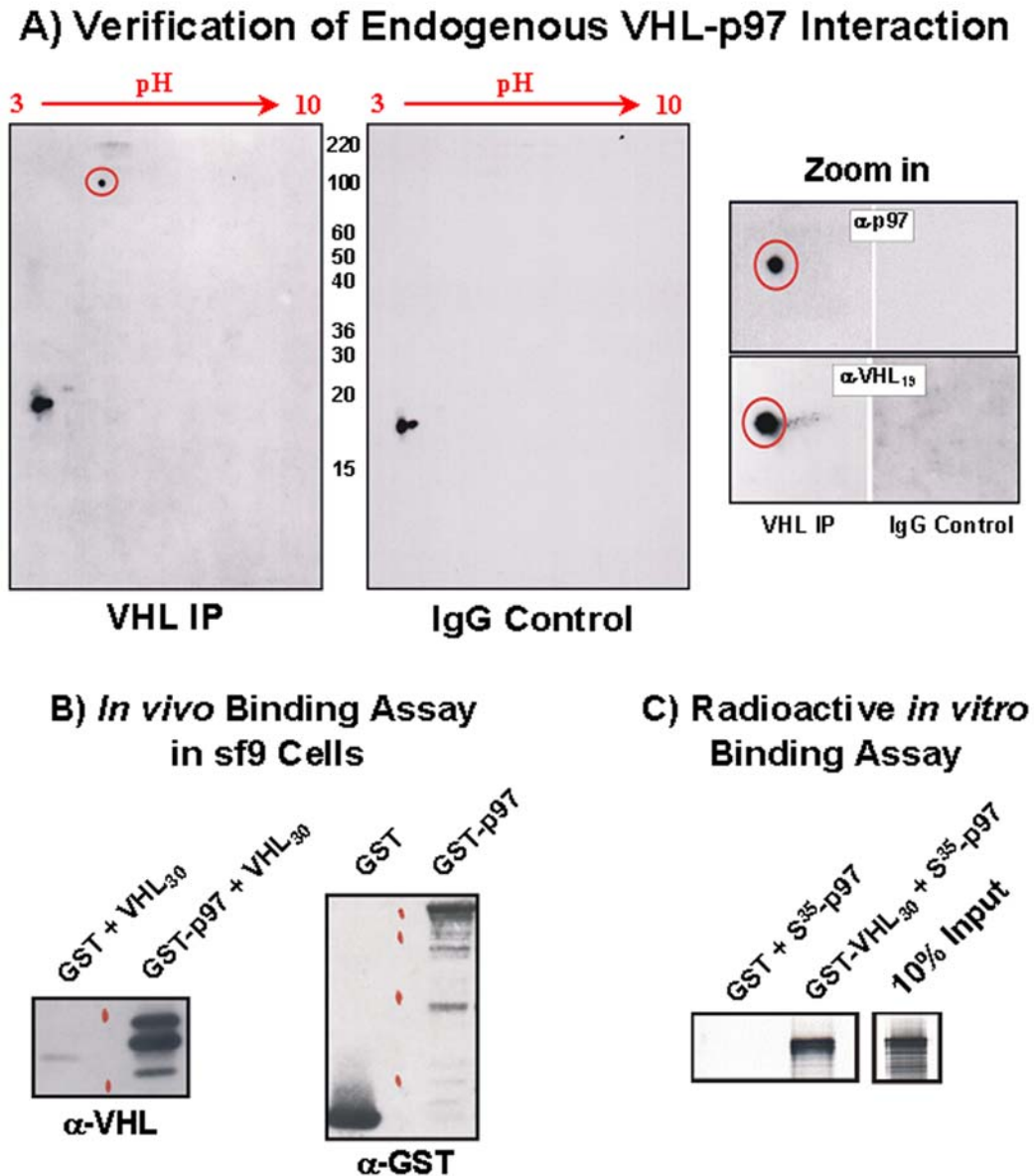


Figure 63. Verification of pVHL-p97 interaction. A) Conformation of an endogenous pVHL-p97 interaction. B) Over-expressed GST fused p97 in sf9 cells specifically precipitates co-expressed untagged VHL₃₀. C) S³⁵-metabolically labelled p97 is specifically precipitated by recombinant GST-VHL₃₀.

Following the identification of p97 by LC-MSMS, it was necessary to investigate the reproducibility of this finding. Figure 63(A) illustrates an identical experiment to that performed for the original LC-MSMS analysis with the exception that the amounts used were far less, and the resultant 2D-gels were processed for western blot analysis instead of being prepared for sequence analysis. A commercially available antibody against p97 was used to probe the membranes. A signal corresponding to p97 is clearly apparent in the VHL IP but completely absent in the IgG_{rabbit} control. The 'zoom in' panel to the right of these blots highlights to a greater magnification the specificity of p97 for the VHL IP, and indeed that the VHL IP itself was successful in immuno-precipitating pVHL. This

experiment was repeated successfully using two independent VHL antibodies, VHL_{CT} as with the original proteomics approach, and VHL_{NT19}, an antibody raised against the N-terminus of pVHL₁₉.

Figure 63(B) shows that when GST-fused p97 is co-expressed with untagged pVHL₃₀ in sf9 cells, then a subsequent GST-pulldown efficiently precipitates pVHL₃₀, whereas GST alone does not. This result further confirms the ability of p97 to interact with pVHL₃₀ *in vivo*. Finally, figure 63(C) demonstrates that *in vitro* translates of p97 when radiolabelled with S³⁵ and then incubated with either recombinant GST-VHL₃₀ or GST, are precipitated uniquely by GST-VHL₃₀ but not GST. This result again strengthens the possibility that p97 and pVHL interact physiologically.

7.4.4 Towards a functional significance for a p97-VHL interaction

7.4.4.1 Sequence analysis

Sequence analysis of p97 has indicated a lack of sequence homology between structural regions in HIF α and also the binding interface region of elongin C known to interact with pVHL. Unlike HIF α , no obvious LxxLAP motif can be observed which might suggest a potential hydroxylation event that could facilitate pVHL binding, and perhaps proteasomal targeting of p97 by pVHL. Nor in the case of Elongin C are residues present in p97 that show significant homology with those residues known to interact with pVHL. The sequences below demonstrate the regions in HIF1 α and Elongin C that were used to search for sequence homology in p97. Sequence analysis could therefore neither identify p97 as a potential substrate nor as a binding partner that may bind in a similar manner to Elongin C.

- **HIF1 α binding interface**

1st Destruction sequence containing Hyp⁵⁶⁴: **DLDLEMLAPYIPMDDDFQLR**

2nd Destruction sequence containing Hyp⁴⁰²: **PDALTLLAPAAGDTIISLDFGSN**

NB. Red indicates conserved residues.

- **Elongin C binding interface**

MDGEEKTYGG CEGPDAMYVK **L**ISSDGHEFI VKREHALTSG **T**IKAMLSGPG Q**F**AENETNEV
 NFREIPSH**V**L SKVCM**Y**FTYK VRY**T**NS**S**TEI **P**EFPIAPEIA **L**ELLMA**N**FL DC

NB. Red indicates residues that bind pVHL. In blue are residues conserved among human, drosophila and yeast elongin C.

7.4.4.2 VHL RNAi does not effect p97 levels

To biochemically consider the possibility that p97 is a target for pVHL-mediated proteasomal degradation, p97 levels were measured in a series of renal cancer cell lines expressing or lacking wild-type pVHL (786-O/A498). By western blot analysis, levels of p97 were comparable between cell lines expressing wild-type pVHL and their non-expressing isogenic counterparts (data not shown). In contrast levels of HIF α , an established pVHL target, were markedly lower in cell lines expressing wild-type pVHL.

Depleting cells of endogenous pVHL does not effect p97 protein levels

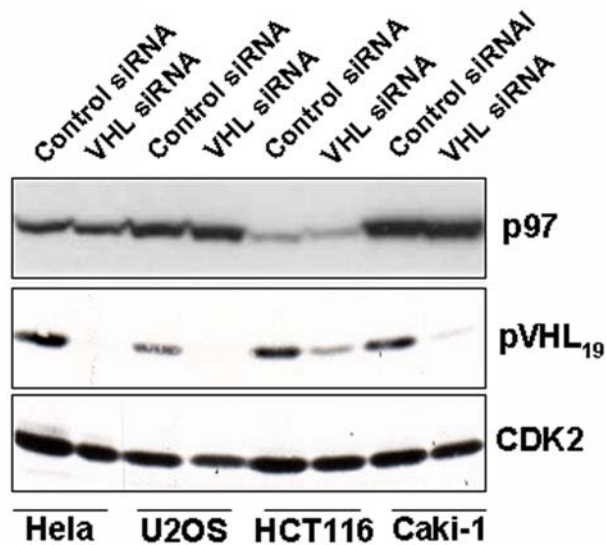


Figure 64. p97 levels in VHL RNAi treated cells. No fluctuations in p97 protein levels are observed when expression of endogenous pVHL is reduced.

An alternative approach to investigate whether p97 is a target of pVHL-mediated proteasomal degradation employed the use of depleting endogenous pVHL by siRNA. Figure 64 demonstrates that when HeLa cells are treated with siRNA oligonucleotides against VHL (see results part III), no fluctuations in p97 protein levels were observed. If p97 were a pVHL-targeted substrate for the VBC-Cul2 E3 ligase, then fluctuations in protein amounts should be observed upon depletion of pVHL. Alternatively the lack of signal change may reflect the fact that p97 is a very abundant protein and that merely down-regulating pVHL, as in the case of siRNA treatment, may not be sufficient to render a response that can be visualised by western blotting. Furthermore, as part III of this results section will outline in more detail, VHL RNAi fails to up-regulate HIF \square in all assays attempted. Perhaps a more radical eradication approach is therefore necessary, for example targeting of VHL via cre-lox recombinase technology, an approach now being established in the laboratory (Frew and Krek). Nonetheless given the previous data that p97 levels do not fluctuate in renal cell carcinoma cells lacking functional pVHL when

compared to their pVHL-expressing isogenic counterparts and that the analysis of the primary sequence has failed to identify any known putative target sequence in p97 by pVHL, it is unlikely that p97 is a target of pVHL-mediated degradation.

7.4.4.3 p97 involvement in proteolytic control of HIF α

As already discussed in the introduction, p97 is involved in a plethora of distinct cellular functions among which includes the process of ubiquitin-mediated proteolytic degradation. p97 forms a homohexamer that binds to several different adapter proteins, and it has been shown that p97 complexes bind poly-ubiquitin chains, exhibiting a chaperone activity that facilitates its 'segregase' function – the ability to separate ubiquitinated proteins from their binding partners. Initial evidence pertaining to this idea was published by Dai *et al* [352]. Here the authors demonstrated that p97 physically and functionally targets the ubiquitinated nuclear factor κ B inhibitor, I κ B α , to the proteasome for degradation. Figure 65 illustrates a model proposed by the authors regarding proteasome presentation of I κ B α by p97 and subsequent liberation of NF- κ B. Since then, p97 has emerged as being an important link in protein degradation and perhaps represents a common mechanism that underlies many of the functions of p97.

Interestingly the notion that pVHL ubiquitin-mediated degradation of HIF α might involve ATPase activity emerged recently. A member of the AAA family, TBP-1 (TAT binding protein 1), was shown to bind to pVHL and was involved in the degradation of HIF1 α . It was shown that this event was energy-dependent, highlighting the requirement for an intact ATPase domain [252]. They demonstrated that pVHL, TBP-1 and HIF1 α subunits form a complex *in vivo* which certain tumour-derived pVHL mutants can disrupt. Interestingly, some pVHL mutations that retain their ability to bind HIF α , did not bind

p97 involvement in I κ B α degradation

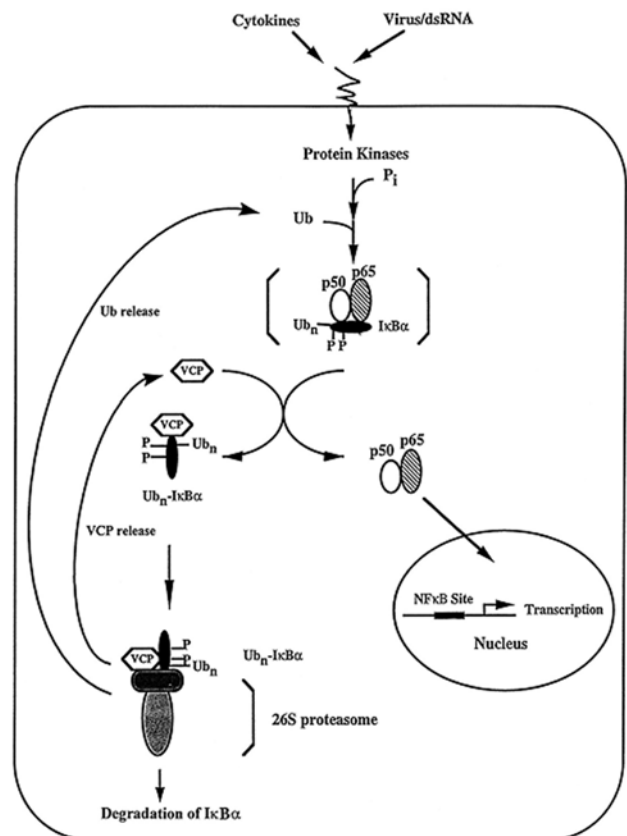


Figure 65. A model proposed by Dai *et al.* regarding the involvement of p97 (VCP) in the proteolytic degradation of I κ B α . In response to stimulation, I κ B α is phosphorylated and poly-ubiquitinated and only then can p97 physically associate with it, thereby liberating NF κ B, which subsequently translocates to the nucleus.

TBP-1, shedding perhaps useful light on a molecular mechanism underlying type 2C disease. These data demonstrate the importance of an ATPase-mediated event in the ubiquitination of HIF α , and therefore support the idea that pVHL may physiologically interact with p97 thereby affecting pVHL-mediated protein degradation of HIF α in a manner similar to TBP-1.

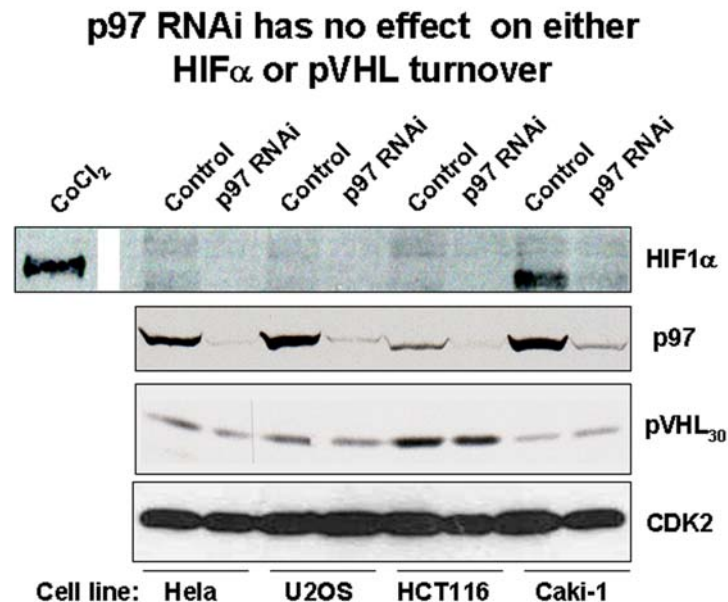


Figure 66. p97 RNAi in different transformed cell lines renders no changes in HIF1 α or pVHL protein levels. Cells were transfected with the siRNA and harvested for western blot after 48 hours.

Given the above, it seems reasonable to suggest that p97 may influence the proteolytic degradation of HIF α via a pVHL dependent interaction. To first test this hypothesis, RNAi against p97 was performed to see if any fluctuations in HIF α levels could be observed when p97 protein levels were reduced. As figure 66 illustrates, no fluctuations in HIF α levels were observed. However, given the fact that HIF α levels are not affected by VHL RNAi (see part III), it seemed unlikely that any fluctuations in HIF α under these experimental conditions would be observed.

A second attempt to investigate the effect of depleting cells of endogenous p97 on HIF α degradation was undertaken. This involved studying the kinetics of HIF α degradation in the presence of p97 RNAi compared to a control RNAi oligonucleotide. No effect on HIF1 α degradation kinetics was observed. However, as figure 87 shows in part III of this chapter, even RNAi against pVHL does not show any changes in the kinetics of HIF degradation. If p97 does affect HIF α degradation, there are two possible explanations why an effect is not observed using siRNA against p97. First, despite the efficacy of the p97 siRNA, only a partial knockdown of p97 expression could be consistently achieved. It is therefore possible that residual p97 is sufficient for HIF α degradation. The presence of even low levels of endogenous wild-type p97 might also

explain why introduction of p97^{QQ}, an ATPase mutant p97, also showed no fluctuation in HIF1 α levels. Therefore, a cell line with a complete knockout of p97 (as with a somatic knockout or embryonic stem cell knockout) might exhibit up-regulated HIF α , which goes unobserved when using siRNA. Secondly, other proteins besides p97 might regulate the pVHL-mediated degradation of HIF α . Based on the above-mentioned regarding TBP-1, we now know this is the case. Clearly, the presence or absence of pVHL is the most important factor in HIF α degradation, as p97 (or TBP-1), does not promote HIF α degradation in pVHL deficient cells. The possibility of alternative proteins that could substitute p97 and promote HIF α degradation suggests that pVHL can still degrade HIF α , albeit less efficiently.

Efforts to identify a p97-HIF α interaction have also been investigated. This approach involved the generation of an ubiquitinated HIF α species, and assaying for the ability of p97 to bind the poly-ubiquitinated protein species. *In vitro* ubiquitination of HIF α had been demonstrated by Ohh *et al* in 2000, where they showed that ubiquitinated Gal4-fused HIF α -ODD was bound by the β -domain of pVHL. Figure 67 shows an ubiquitination assay of HA/Gal4-HIF α -ODD which was incubated in similar reaction conditions as those described by Ohh *et al* and demonstrates a characteristic pattern of bands representing poly-ubiquitinated HIF α -ODD. Preliminary data suggest that GST-p97 bound to beads can precipitate this ubiquitinated HA/Gal4-HIF1 α -ODD, but further confirmation is necessary before any statement is made (data not shown). In light of the developing literature demonstrating increasingly that p97 relies on adapter proteins to execute its functions, it is now apparent that this experiment should be repeated in the presence of an appropriate protein adapter(s) to see if binding can be optimised, i.e. Ufd1 and/or Npl4. These experiments are underway.

In vitro ubiquitination of Hif-1 α ODD

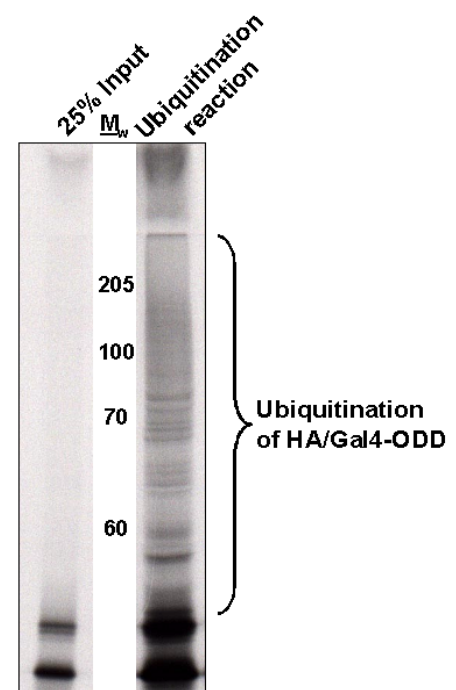
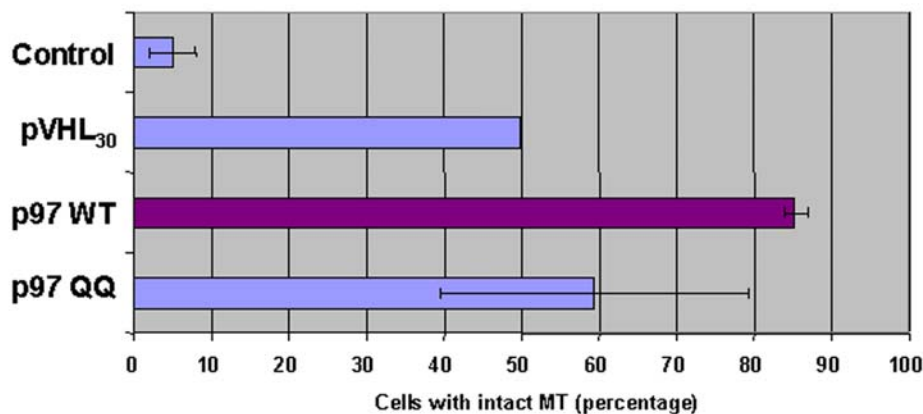


Figure 67. *In vitro* ubiquitination assay using HA/Gal4-HIF α -ODD as substrate. High molecular weight bands represent poly-ubiquitinated substrate.

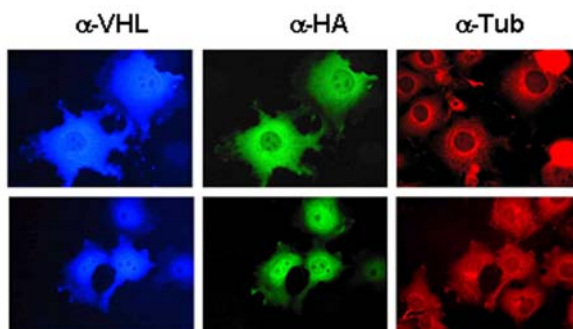
7.4.4.4 Role of p97 in microtubule stability

Other aspects of p97 involvement in pVHL biology have also been investigated, namely the functional significance of a p97-pVHL link in context of pVHL's ability to stabilise microtubules. pVHL has been shown to bind microtubules and to promote their stability in an assay which tested the ability of pVHL to stabilise microtubules under depolymerising conditions (work related to this finding is outlined in part II of this chapter). Interestingly, M. Tagaya and colleagues identified SVIP (small VCP interacting protein) as a novel adaptor protein for p97 [367]. Although SVIP function is as yet unknown, its over-expression in cells caused extensive vacuolation and deformation of ER and also of microtubules.

A) Investigating the role of p97 in microtubule stabilisation



B) Expression of components in microtubule pelleting assay



C) Microtubule pelleting assay: Investigating p97 interaction with MTs

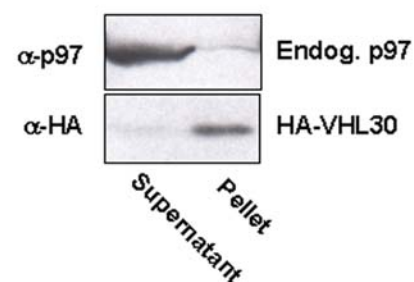


Figure 68. A). Investigating the role of p97 in microtubule (MT) stability. COS-1 cells were transfected with indicated constructs and treated 24 hours later with 5 μ M nocadazole for 4 hours. Cells were prepared for IF, and scored for intact microtubule array. B). Expression control of indicated constructs in pVHL and HA-p97 co-transfections. C). Results from a microtubule-pelleting assay indicating precipitation of over-expressed HA-VHL₃₀ with polymerized microtubules, but not endogenous p97.

An established assay to test the ability of a candidate protein to affect microtubule stability involves treating cells, which have been previously transfected with a protein of interest, with nocadazole, or some other depolymerising agent, and score for intact

microtubule array's after a given period which would normally induce breakdown of the microtubule network in untransfected cells. This assay has shown that for pVHL, microtubule stabilisation is promoted to 50% following transfection of both pVHL₃₀ and pVHL₁₉. Co-transfection of HA-p97 along with pVHL₃₀ in context of this assay was undertaken to investigate whether p97 might affect pVHL's ability to promote microtubule stability. Multiple analyses revealed that in the presence of ectopically expressed p97, microtubule stability was promoted to approximately 85%, thus far exceeding that of pVHL alone. To assess whether the ability of p97 to promote stability was dependent on ectopically expressed pVHL, the effect of transfecting p97 alone was analysed. As figure 68(A) illustrates, the results demonstrated that p97 alone can stabilise microtubules in this assay up to 85%, suggesting that the effect may be independent of over-expressed pVHL. To address the question of whether this stabilisation by p97 relied upon its ATPase activity, p97^{QQ}, a dominant-negative mutant that lacks ATPase activity, was transfected and tested. P97^{QQ} rendered confusing results that fluctuated at times below 20% and reached stability of up to >70%. As results using p97^{QQ} were neither reproducible nor accurate, no conclusion can be made regarding the requirement of an intact ATPase domain in microtubule stability. The ability of p97 to bind microtubules *in vitro* was also investigated. Figure 68(C) shows that, unlike pVHL, p97 does not bind polymerised microtubules *in vitro*. Immuno-fluorescence of p97 supports the pelleting assay in that no co-localisation is observed between p97 and microtubules. Partial localisation is seen associated with the ER, but the predominant signal is a diffuse cytoplasmic signal. Whatever the function of over-expressed p97 is on microtubule stability, it seems that it does not elicit a direct effect through binding, but rather might be involved in functionally regulating other components involved in microtubule stability, like pVHL.

In an effort to investigate cross-talk between pVHL and p97 with respect to microtubule stability, cells were transfected with siRNA oligos against p97, and assayed for the ability of transfected pVHL₃₀ to stabilise microtubules. While a reduction in stability was observed ranging from 35-45% compared to 50%, the reduction is not dramatic. It

would seem that if there is cross-talk between p97 and pVHL regarding microtubule stability, then residual p97 remaining following p97 RNAi is sufficient to maintain microtubule integrity to almost the maximum as seen by transfecting pVHL alone. A complete knockout situation could highlight more significant effects.

Investigation of the effect of p97 downregulation on VHL-stabilisation of microtubules

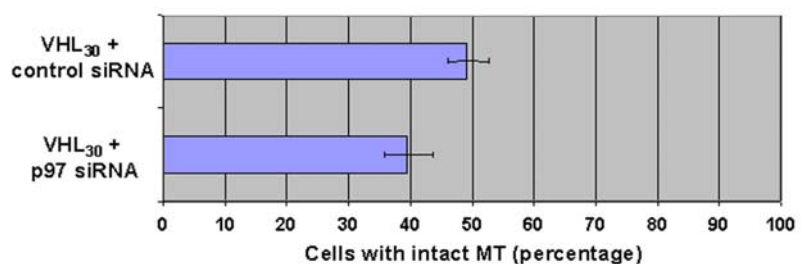


Figure 69. The effect of depleting endogenous p97 by siRNA on pVHL's ability to stabilise microtubules in COS-1 cells. Cells were transfected with siRNA oligos against p97, then transfected with pVHL₃₀ and assayed for microtubule stability.

7.4.4.5 pVHL interacts with HDAC6

Seigneurin-Berny *et al* demonstrated that immuno-purification of endogenous murine histone deacetylase 6 (mHDAC6), a member of the class II HDACs, allowed the identification of two associated proteins [368]. Both were mammalian homologues of yeast proteins known to interact with each other and involved in the ubiquitin signalling pathway: phospholipase A2-activating protein, a homologue of yeast UFD3 (ubiquitin fusion degradation protein 3) and the ATPase p97. Furthermore, using an ubiquitin pull-down approach, several major ubiquitin-binding proteins were identified and mHDAC6 was found to be one of them. All of these findings strongly suggest that mHDAC6 could be involved in the control of protein ubiquitination, thereby establishing a link between protein acetylation and protein ubiquitination and a link that, at least in part, could be mediated by p97.

Histone deacetylases (HDACs) are a family of enzymes whose functions have been overwhelmingly associated with gene expression and chromatin dynamics (reviewed in [369, 370]). However, recent evidence indicates that not all functions of HDACs

are dedicated to regulating gene transcription and chromatin remodelling (reviewed in [371]). The prominent example of such a non-canonical function is illustrated by the cytoplasmic deacetylase HDAC6. Hook *et al.* showed that the C terminus of HDAC6 is both necessary and sufficient for specific association with poly-ubiquitin [372]. In addition, Hubbert *et al.* reported in Nature 2002 that HDAC6 functions as a tubulin deacetylase [373]. They demonstrated that HDAC6 was localised exclusively in the cytoplasm, where it associates with microtubules. Furthermore, they provide evidence that over-expression of HDAC6 promotes chemotactic cell movement, supporting the idea that HDAC6-mediated deacetylation regulates microtubule-dependent cell motility. They thereby suggest that decreasing tubulin acetylation reduces microtubule stability. However, following a brief communication by Gunderson *et al.* in Nature 2003, it is now clear that microtubule stabilisation is in fact not promoted by tubulin acetylation, but rather a modification of already stabilised microtubules. Therefore the cell motility observed by Hubbert *et al.* in cells over-expressing HDAC6 seems to result not from changes in the formation of stable microtubules, but in the degree of tubulin acetylation.

Given the fact that HDAC6 had been shown to bind p97 and other proteins involved in the process of ubiquitination, and that it co-localised with microtubules, it was tested whether HDAC6 could interact with pVHL. Figure 71 demonstrates *in vitro* binding of HDAC6 to pVHL. HDAC6 bound very strongly to pVHL₁₉, but failed to bind the naturally occurring mutant pVHL_{Δexon2}. Fine mapping revealed that the binding interface of HDAC6



Figure 70. In the C-terminal region of HDAC6, a conserved zinc finger-containing domain mediates the specific binding of ubiquitin by HDAC6.

and pVHL lay between residues 93-122 of pVHL. Interestingly, this region corresponds to pVHL's microtubule-binding domain.

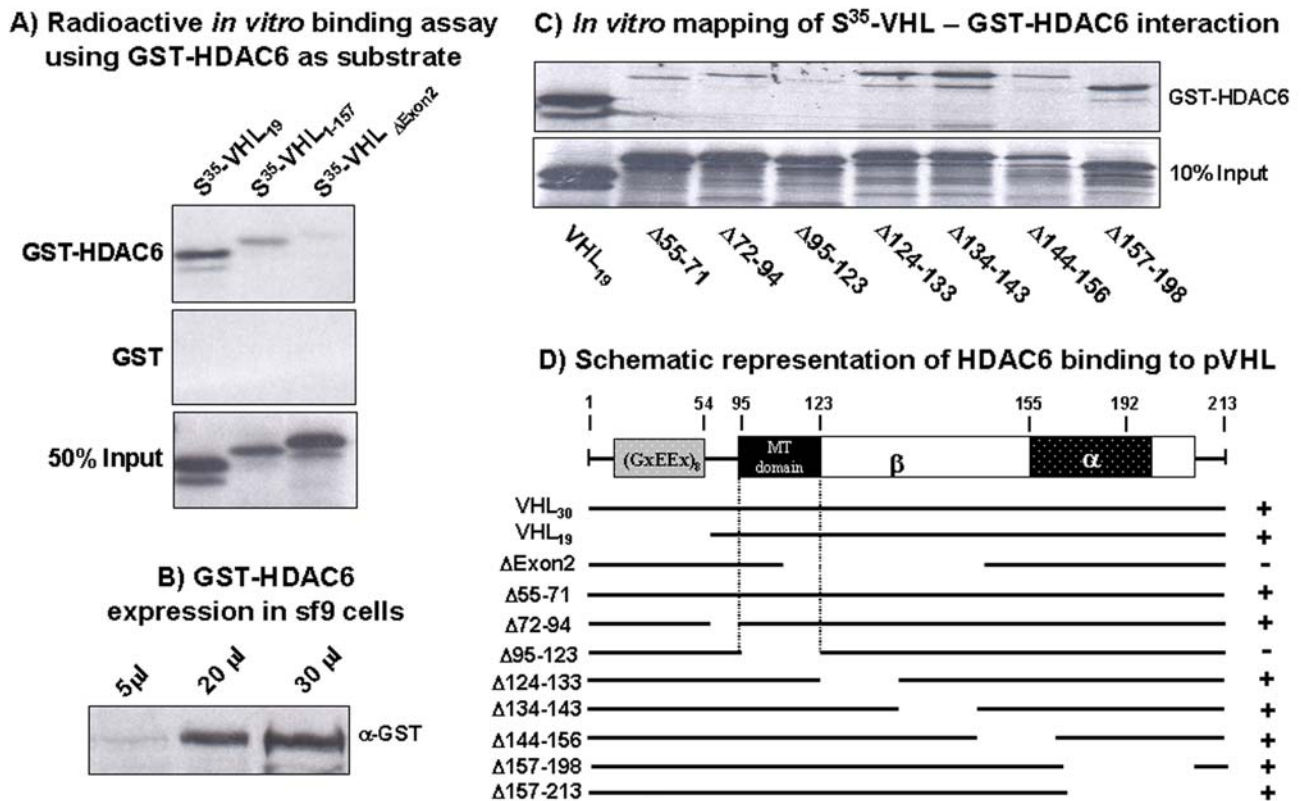
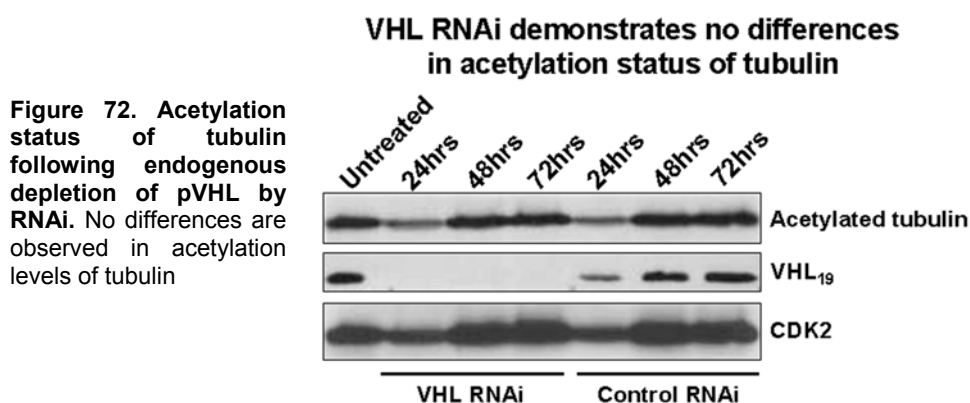


Figure 71. HDAC6 *in vitro* interaction with pVHL. A) Sf9 expressed GST-HDAC6 binds S³⁵-labelled VHL_{19/1-157} but not VHL_{ΔEXON2}. B) Expression of GST-HDAC6 in sf9 cells. C) Mapping of pVHL-HDAC6 identifies residues 95-123 of pVHL as the binding interface.

The significance of this finding remains unclear. Evidence exists that HDAC6 is ubiquitinated *in vitro* and *in vivo* [372], but no evidence has been shown that this is pVHL-dependent. On the contrary, attempts to see whether over-expressing pVHL or depleting cells of endogenous pVHL with siRNA can affect tubulin acetylation, have to date shown no changes in acetylation status. This casts doubt on the idea that pVHL might target HDAC6 for degradation (Fig.72) suggesting that either a pVHL-HDAC6 interaction does not interfere with HDAC6's tubulin deacetylation function, or that under these conditions, depletion of pVHL is not sufficient to effect HDAC6 function.



Further mapping of a HDAC6-pVHL interaction involved investigation of the binding of pVHL mutants within the binding domain $\Delta 95-123$ (Fig.71). Experiments to date suggest that HDAC6 can bind these mutants *in vitro*. If this were indeed the case, then it would seem that mutants that have inactivation of VHL at these sites retain their ability to bind HDAC6. As a functional significance of this interaction has yet to be elucidated it is impossible to draw any conclusions, but it would be tempting to suggest that perhaps mutation at these sites instead of preventing interaction, prevent dissociation, thereby acting to cause pVHL to function inappropriately.

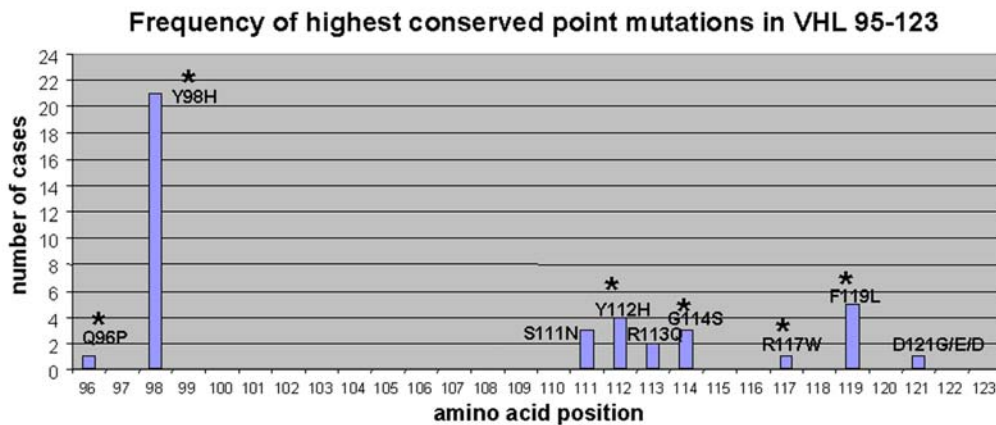


Figure 73. Mutational hotspots within the pVHL microtubule binding domain $\Delta 95-123$. All mutants bind HDAC6 *in vitro* suggesting that mutational inactivation does not hinder an HDAC6-pVHL interaction. Asterixes denote mutants tested.

In the December 12th issue of *Cell*, 2003, a report was published that HDAC6 functions as an adaptor that links cargos of aggregated protein to the minus end-directed motor, cytoplasmic dynein. Molecular motors are the long-haul carriers of eukaryotic cells, moving cargos bi-directionally along microtubule tracks [374]. Misfolded protein aggregates are transported and removed from the cytoplasm by dynein motors via the microtubule network to a novel organelle termed the aggresome where they are processed [375]. The efficient clearance of cytotoxic misfolded protein aggregates is critical for cell survival. However, the means by which dynein motors recognise misfolded protein cargo, and the cellular factors that regulate aggresome formation, remain unknown. Kawaguchi *et al.* discovered that HDAC6, a microtubule-associated deacetylase, is a component of the aggresome. They demonstrated that HDAC6 has the capacity to bind both poly-ubiquitinated misfolded proteins and dynein motors, thereby acting to recruit misfolded protein cargo to dynein motors for transport to aggresomes. Indeed, cells deficient in HDAC6 fail to clear misfolded protein aggregates from the cytoplasm, cannot form aggresomes properly, and are hypersensitive to the accumulation of misfolded proteins. These findings identify HDAC6 as a crucial player in the cellular management of misfolded protein-induced stress. In light of p97's role in retrotranslocation, and the fact that cells lacking functional VHL exhibit deposition of an incorrectly folded fibronectin array might suggest a general role for all three protein components in the malformed protein response, and that this role may, in part, be mediated by direct or indirect interaction with the microtubule network. The potential significance of a p97-pVHL interaction is further discussed in chapter 8.

7.5 pVHL precipitates human homologues of Gcd10p/Gcd14p

7.5.1 Introduction

From the proteomics approach outlined in section 7.3 four additional poly-peptides, of unknown function, were isolated. Figure 74 illustrates their location on a 2D-SDS polyacrylamide gel. Interestingly, poly-peptides C and D, when assembled together, constituted the poly-peptide A. Therefore, it is assumed that C and D correspond to fragmented versions of the same poly-peptide, and from here on reference will only be made to poly-peptides A and B.

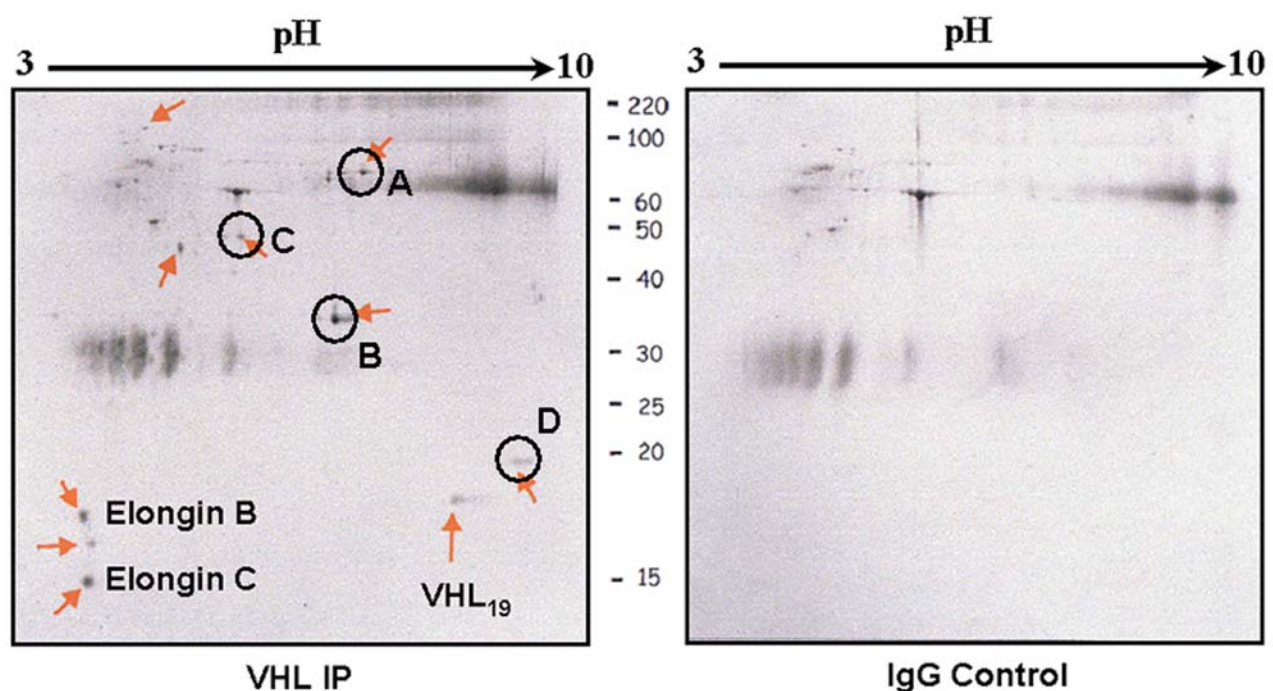


Figure 74. A proteomics approach identified four novel, uncharacterised poly-peptides. The assembled open reading frame of polypeptides C and D were shown to constitute the poly-peptide encoded by A, and therefore represent fragments of the same species.

The sequences overleaf represent the protein coverage of these two novel polypeptides, A and B. Both were identified by peptide mass fingerprinting with peptides totalling to >40% coverage in both cases. Both were uncharacterised protein species. However, NCBI database searches identified homologues for both of these polypeptides in the budding yeast, *Saccharomyces Cerevisiae*.

Protein A: PubMed - XP_045589; 43% Protein coverage

MEGSGEQPGP	QPQHGDHRI	RDGDFVVLKR	EDVFKAVQVQ	RRKKVTFEKQ	WFYLDNVIGH	SYGTAFEVTS
GGSLQPKKKR	EEPTAETKEA	GTDNRNI VDD	GKSQKLTQDD	IKALKDKGIK	GEEIVQQLIE	NSTTFRDKTE
FAQDKYIKKK	KKKYEAITV	VKPSTRILSI	MYAREPGKI	NHMYDTLAIQ	MLTLGNIRAG	NKMI VMETCA
GLVLGAMMER	MGGFGSIIQL	YPGGGPVRAA	TACFGFPKSF	LSGLYEFPLN	KVDSLLHGTF	SAKMLSSEPK
DSALVEESNG	TLEEKQASEQ	ENEDSMAEAP	ESNHPEDQET	METISQDPEH	KGPKERGSKK	DYIQEKQRRQ
EEQRKRHLEA	AALLSERPAD	GLIVASRFHP	TPLLLSLDF	VAPSRPFVVY	CQYKEP LLEC	YTKLRERGGV
INLRLSETWL	RNYQVLPDRS	HPKLLMSGGG	GYLLSGFTVA	MDNLKADTSL	KSNASTLESH	ETEEPAKKR
KCPESDS						

Protein B: PubMed - gi:15301015; 45% Protein coverage

MSFVAYEELI	KEGDTAILSL	GHGAMAVRV	QRGAQTQTRH	GVLRHSDVLI	GRPFSGKVTCT	GRGGWVYVLH
PTPELWTLNL	PHRTQILYST	DIALITMMLL	LRPGSVVCE	GTGSGSVSHA	IIRTIAPTGH	LHTVEFHQQR
AEKAREFQE	HRVGRWTVR	TQDVCRSFG	VSHVADAVFL	DIPSPWEAVG	HAWDALKVEG	GRFCSFSPCI
EQVQRTQAL	AARGFSELST	LEVLPQVYV	RTVSLPPPDL	GTGTDGPAGS	DTSFPRSGTP	MKEAVG
HTGYLTFATK	TPG					

Protein A was identified as having strong sequence homology with a protein found in *Saccharomyces Cerevisiae*, termed Gcd10p. Protein B was also found to have a yeast homologue termed Gcd14p. Gcd10p is found in a nuclear complex with Gcd14p, which contains conserved motifs for binding S-adenosylmethionine (AdoMet) [376, 377]. Evidence exists which suggests that this complex is involved in a crucial methylation event at position 58 on the T-arm (TΨC loop) of initiator methionine transfer RNA ($tRNA_i^{Met}$). The modified nucleoside 1-methyladenosine (m^1A) is found at position 58 in the TΨC loop of many eukaryotic tRNAs. The absence of m^1A from all tRNAs in *Saccharomyces Cerevisiae* mutants lacking Gcd10p elicits severe defects in processing and stability of $tRNA_i^{Met}$. These facts, plus the demonstration that $gcd14\Delta$ cells lacked m^1A , strongly suggested that Gcd10p/Gcd14p complex is the yeast $tRNA(m^1A)$ methyltransferase [(m^1A)MTase].

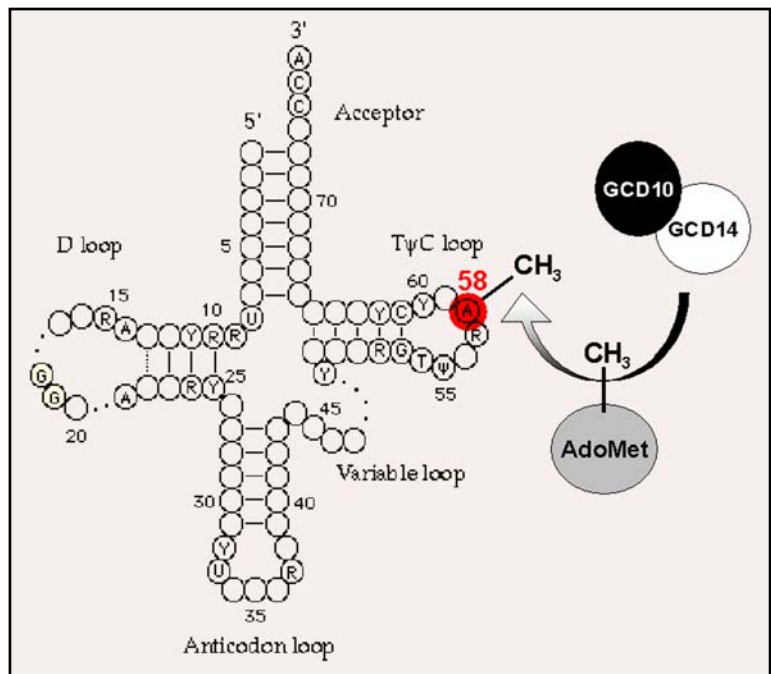


Figure 75. In *S.Cerevisiae*, the Gcd10p/Gcd14p complex functions as a methyltransferase transferring a methyl group from the methyl-donor S-adenosylmethionine onto adenine 58 positioned on the T-arm (TΨC loop) of $tRNA_i^{Met}$. Sequence homology would suggest that Proteins A and B found in a pVHL pulldown are the mammalian counterparts of this complex.

The maturation of tRNA occurs through a series of posttranscriptional processing steps, including splicing, end-trimming, and base or ribose modifications. Modified nucleosides have been identified in all cellular RNAs, but the tRNAs by far contain the greatest number and variety of modifications. Of these, the most widely distributed and

prevalent tRNA modification is base or ribose methylation. Several tRNA modification enzymes have been cloned and characterised from eubacteria and eukaryotes. Remarkably, only one tRNA modification, the subject of this report, has been found to be essential for cell growth under normal conditions. In other instances, the modifications are required for efficient decoding during protein synthesis [378]. A 2'-O-phosphoribosyl modification of A64 in tRNA_i^{Met} prevents inappropriate interaction of the initiator with translation elongation factor 1 α [379].

The occurrence of 1-methyladenosine (m¹A) at position 58 of the T Ψ C loop has been reported in tRNAs from all three kingdoms [378], suggesting an evolutionarily conserved role in tRNA structure or function. In the yeast *Saccharomyces Cerevisiae*, m¹A58 is widespread but not universal, occurring in 21 of 32 sequenced tRNAs [380]. This modification seems to be crucial only for tRNA_i^{Met} because a null mutation in *GCD10* that eliminates m¹A in all yeast tRNAs leads specifically to reduced processing and stability of the initiator. This defect is lethal unless tRNA_i^{Met} is overproduced in the *gcd10* Δ mutant to compensate for reduced accumulation of mature initiator [376]. It was proposed that m¹A58 is singularly required for tRNA_i^{Met} production because it contributes to a unique substructure involving tertiary interactions between the T Ψ C and D loops [381].

Temperature-sensitive *gcd14* mutations lead to accumulation of precursors and reductions in mature tRNA_i^{Met}, and exacerbate the effects of a temperature-sensitive *gcd10* mutation on cell growth and tRNA_i^{Met} production. Furthermore, the lethal phenotype of a *gcd14* Δ allele has been shown to be suppressed by over-expressing tRNA_i^{Met} [377]. It was predicted that the defect in tRNA_i^{Met} processing observed in *gcd14* mutants also derives from the absence of m¹A in tRNA.

Most of the known tRNA methyltransferases (MTases) use S-adenosylmethionine (AdoMet) as the methyl donor, and most contain a domain comprised of four conserved motifs (I, post-I, II, and III) [382]. The three-dimensional structures of several MTases reveal that motifs I and post-I directly contact AdoMet, and mutation of motif I impairs AdoMet binding. The presence of motifs I, post-I, and II in Gcd14p suggested that it can bind AdoMet and function directly as the yeast tRNA(m¹A)MTase [376]. Because all well-characterised tRNA MTases are single-subunit enzymes, the role of Gcd10p was more difficult to predict. The Gcd10p/Gcd14p complex could be a two-subunit tRNA(m¹A)MTase, requiring Gcd10p for intrinsic enzymatic activity. Alternatively, Gcd10p might function in nuclear localisation of the complex, or as a tRNA chaperone, and be required for m¹A formation only *in vivo*.

In a report by Anderson *et al*, they report that the purified Gcd10p/Gcd14p complex demonstrated tRNA(m¹A)MTase activity and that a mutation in motif I of the

putative AdoMet binding domain in Gcd14p eliminated this (m¹A)MTase activity *in vitro* thereby abolishing m¹A formation *in vivo*. These results prove that Gcd10p and Gcd14p function directly in m¹A formation in yeast tRNAs. Purified Gcd14p alone was shown to have no enzymatic activity and was defective for tRNA binding compared with the Gcd14p/Gcd10p complex. These findings, combined with the previous demonstration that Gcd10p alone has RNA binding activity [383], leads to the supposition that Gcd10p is required for tight binding of the tRNA substrate. Thus, the AdoMet and tRNA binding functions required for m¹A formation seem to depend on distinct subunits of a two-component tRNA methyltransferase as depicted in figure 73.

7.5.2 Towards defining a function for a pVHL-protein A/B interaction

Protein B (Gcd14p homologue) was cloned from the image consortium (see chapter 6, materials and methods). Protein A (Gcd10p homologue) posed problems when cloning due to a lack of construct availability. Nonetheless, it has since been cloned in collaboration with another doctoral student, P.Ballschmieter. *In vitro* binding assays involving radio-labelling of protein B with S³⁵ and incubation with pVHL expressed as GST-fused poly-peptides in sf9 cells, demonstrated that protein B can bind GST-VHL₃₀ and GST-VHL₁₉ *in vitro* (figure 76). Antibodies have since been raised against Protein B, and preliminary evidence exists showing that ectopically expressed protein B can precipitate endogenous pVHL thereby confirming the *in vitro* result in figure 76 (Ballschmieter, Barry and Krek, data not shown). Furthermore, ectopically and endogenously expressed protein A has recently been shown to co-precipitate over-expressed and endogenous pVHL, and importantly that ectopically expressed protein A and protein B co-precipitate (Ballschmieter, Barry and Krek, data not shown). These results confirm that complex formation occurs *in vivo*, and that this complex is capable of interacting with pVHL.

Nonetheless, despite the fact that these proteins complex *in vivo*, and that this complex precipitates endogenous pVHL, no physiological relevance is available to assign any potential significance to this interaction. Firstly, evidence that this complex is the mammalian orthologue is necessary, that is, that complexed proteins A and B can demonstrate methylation activity. Secondly the role, if any, pVHL plays in context of protein methylation must be investigated. These studies are underway.

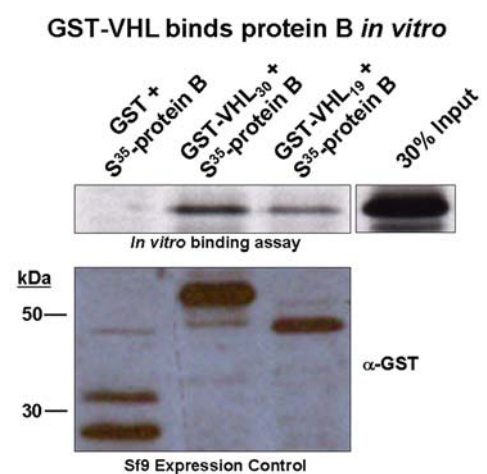


Figure 76. GST-VHL₃₀ and GST-VHL₁₉ bind radiolabelled protein B, the assumed Gcd14p mammalian homologue based on sequence similarity.

Concluding remarks

This section has outlined the development of a novel experimental approach for identifying new pVHL protein interactions. In a field that has been exhaustively examined for novel pVHL partners, this approach was successful in isolating two candidates that may help to shed light on the role of pVHL in tumourigenesis. The first, p97, represents an ATPase, and binding assays have confirmed this interaction both *in vivo* and *in vitro*. Current literature would support a model where p97 may facilitate pVHL-mediated Hif α degradation, a hypothesis under investigation. Preliminary data would also support a role of p97 in the stabilisation of microtubules, thereby linking its function to that of pVHL's in microtubule regulation. Finally, pVHL has been shown to bind the microtubule binding histone deacetylase HDAC6 *in vitro*, and that this binding is mediated through its microtubule binding domain. Given the fact that p97 also binds HDAC6 and that all three proteins are involved in the malformed protein response, suggests a putative functional interaction of all three in this process that may, at least in part, be mediated by the microtubule cytoskeleton.

In addition, pVHL has been shown to interact with two uncharacterised proteins, which show homology to a conserved complex in yeast, namely the tRNA(m1A) methyltransferase. Preliminary data have confirmed the interaction, but further experimentation is needed to confirm whether this complex is the true mammalian orthologue of its yeast counterparts, and what the effect *VHL* may have in the process of methylation. The significance and potential impact these interactions might have on VHL biology is further discussed in chapter 8.

RESULTS – PART II:

Investigating pVHL intracellular dynamics

7.6 Introduction

This section outlines the contribution made to an article published in *Nature Cell Biology* in December 2002 regarding the association of pVHL with microtubules and the effect that disruption of the microtubule cytoskeleton has on pVHL intracellular localisation [107].

Tumour suppressor proteins control the proliferation and survival of normal cells; consequently, their inactivation by gene mutations can initiate or drive cancer progression. Most tumour suppressors have been identified by genetic screening, and in many cases their function and regulation are poorly understood. Many such proteins have recently been shown to contain nuclear transport signals that facilitate their "shuttling" between the nucleus and cytoplasm [384]. This type of dynamic intracellular movement not only regulates protein localisation, but also often impacts on function. Tumour suppressors including APC [385], p53 [386], BRCA1 [387], and also VHL [99] cross the nuclear envelope and the impact of regulated nuclear import/export on protein function is only beginning to be appreciated.

When beginning this project, work, pioneered in particular by Stephen Lee, had shown that nuclear/cytoplasmic localisation of over-expressed pVHL was a cell density dictated event, and that in densely grown cells, pVHL was predominantly cytoplasmic, whereas in sparse cultures, most of the protein was detected in the nucleus [99]. Lee *et al.* also identified a putative nuclear localisation signal (table 20). They developed their findings further, and provided evidence suggesting that VHL-GFP shuttles between the nucleus and cytoplasm in a transcription-dependent, Ran-mediated manner and that deletion mutants of pVHL lacking exon 2 failed to do so [388],[389]. The fact that exon 2 mutants over-expressed in 786-0 cells failed to suppress HIF2 α as demonstrated by up-regulation of the HIF regulated gene GLUT1 (glucose transporter) suggested that shuttling may be important for pVHL tumour suppressor activity.

Table 20. Putative VHL nuclear import/export signals

VHL Nuclear localisation sequence and import pathway:			
Import Elements	Sequence	Receptor/pathway	References
Bipartite NLS	¹ PRR(X) ₅₃ RPRPV ⁶⁰	Importin- α/β	Lee <i>et al</i> 1996
VHL nuclear export sequence and export pathway:			
Export Elements	Sequence	Receptor/pathway	References
Exon 2	a.a. 114-154	CRM1-independent	Lee <i>et al</i> 1999

A) Retroviral expression of GFP in NIH3T3 cells

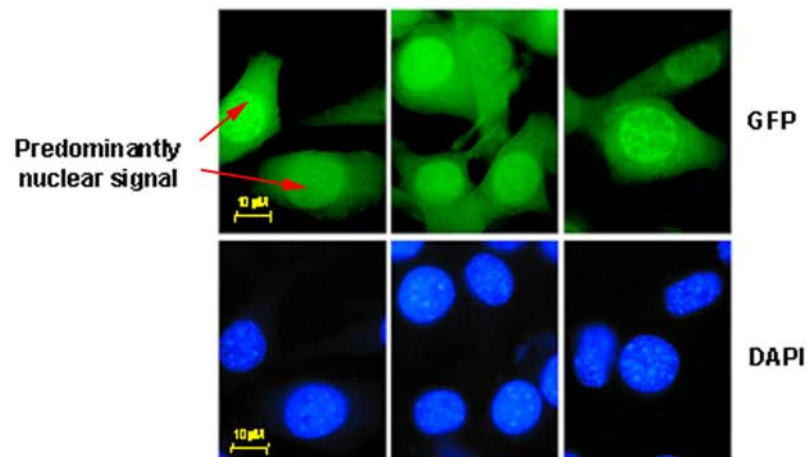
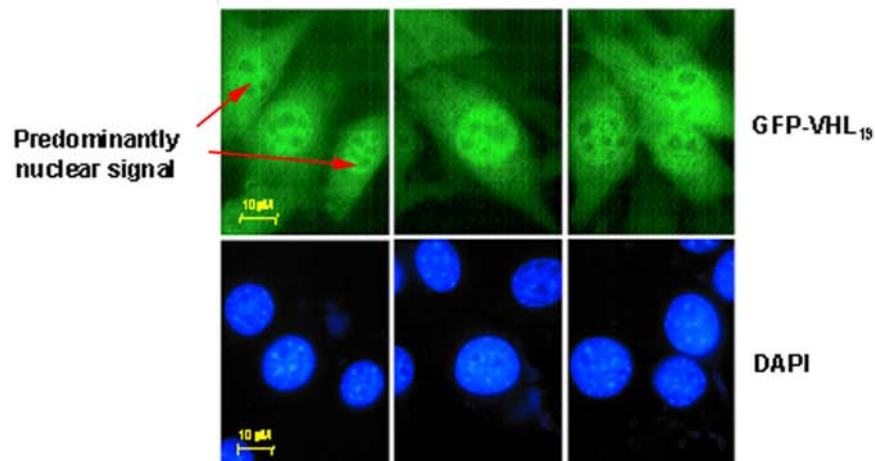
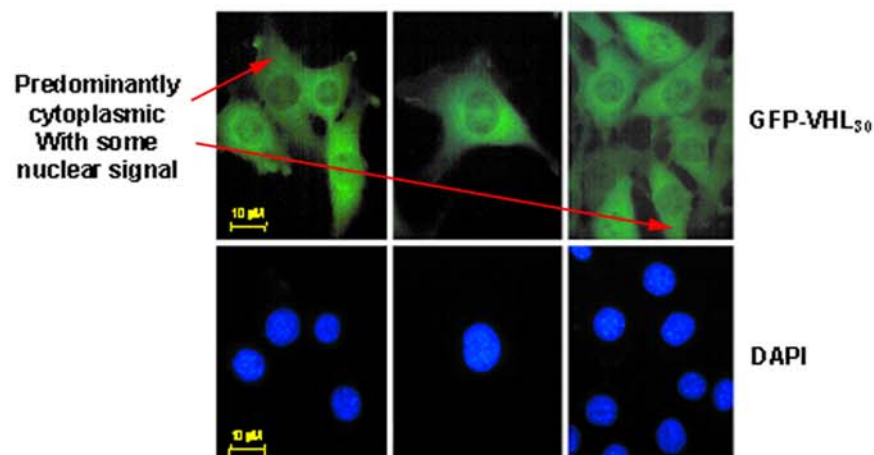
B) Retroviral expression of GFP-VHL₁₉ in NIH3T3 cellsC) Retroviral expression of GFP-VHL₃₀ in NIH3T3 cells

Figure 77. Localisation of GFP-VHL₃₀ and GFP-VHL₁₉ following retroviral transduction in NIH3T3 mouse fibroblasts. A) GFP expression following retroviral transduction. B) GFP-VHL₁₉ expression demonstrates that GFP-VHL₁₉ localises predominantly to the nucleus. C) GFP-VHL₃₀ localises predominantly to the cytoplasm.

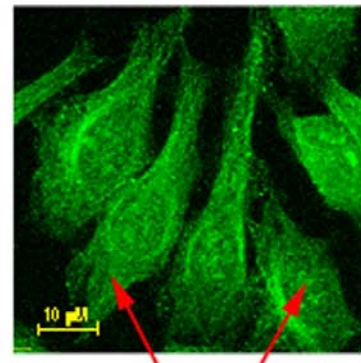
7.6.1 Intracellular localisation of ectopically expressed pVHL₁₉ and pVHL₃₀

While it was clear that pVHL, at least when over-expressed, could localise in both the nucleus and cytoplasm, and that an active transport between both cellular compartments was likely, no understanding of why this might be the case was available, and no consideration to different pVHL forms, namely pVHL₃₀ and pVHL₁₉, had been given. For this reason, it was interesting to investigate participation of both protein species in this cellular event. Figure 77 demonstrates that GFP-VHL₃₀ and GFP-VHL₁₉ localise differently. Like GFP alone, GFP-VHL₁₉ localises predominantly to the nucleus showing some cytoplasmic signal. In contrast, GFP-VHL₃₀ localises predominantly to the cytoplasm, showing some nuclear localisation. The findings were in accordance with previous reports.

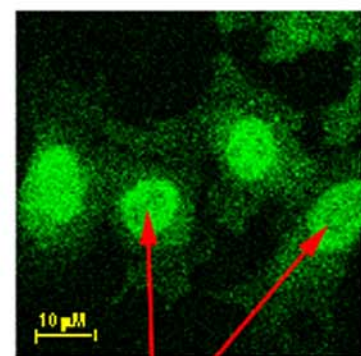
7.6.2 Intracellular localisation of endogenous pVHL₃₀

Endogenous visualisation of pVHL₃₀ by indirect immuno-fluorescence confirmed the previous exogenous approaches in that pVHL₃₀ was predominantly cytoplasmic, but could also localise to the nucleus. The results showed however much clearer than before, that pVHL₃₀ could at times be localised uniquely to the nucleus, uniquely to the cytoplasm, or present in both simultaneously (Fig.78). In light of an article that emerged at the time regarding p53's ability to associate with cellular microtubules [390], which facilitated its transport to the nucleus in a dynein-dependent fashion, it seemed reasonable to suggest that pVHL may, like some other tumour suppressor proteins (p53 and APC), be capable of participating in nuclear/cytoplasmic trafficking in a cytoskeletal-dependent manner. As the first part of this chapter outlines, initial attempts were aimed at defining an interaction between pVHL and the actin

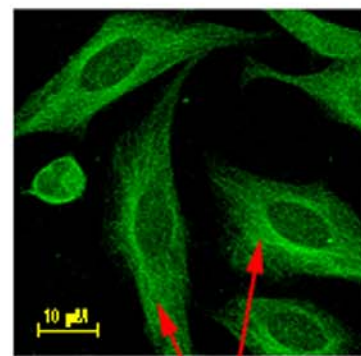
A) pVHL₃₀ IF demonstrates Distinct nuclear and cytoplasmic signals



Cytoplasmic Nuclear



Nuclear



Cytoplasmic

B) VHL_{NT} only recognises pVHL₃₀



Figure 78. Endogenous pVHL₃₀ patterns stained with VHL_{NT} in HeLa cells. A) pVHL₃₀ localises uniquely in the nucleus, uniquely in the cytoplasm, or a mixture of the two. B) IP demonstrating the specificity of VHL_{NT} for pVHL₃₀.

cytoskeleton based on the observation that GST-VHL₃₀ co-precipitated the actin-binding motor protein myosin heavy chain type IIA (MHCIIA). However, when experiments cast doubt on a true *in vivo* interaction between pVHL and MHCIIA, attention was again reverted towards the microtubule cytoskeleton. Subsequent immuno-fluorescence demonstrated that endogenous pVHL₃₀ did indeed co-localise with assembled microtubules (Fig.77). While *in vitro* assays have demonstrated that pVHL₁₉ can also bind assembled microtubules [107], the endogenous distribution of both pVHL forms suggests that only pVHL₃₀ participates in an *in vivo* microtubule association.

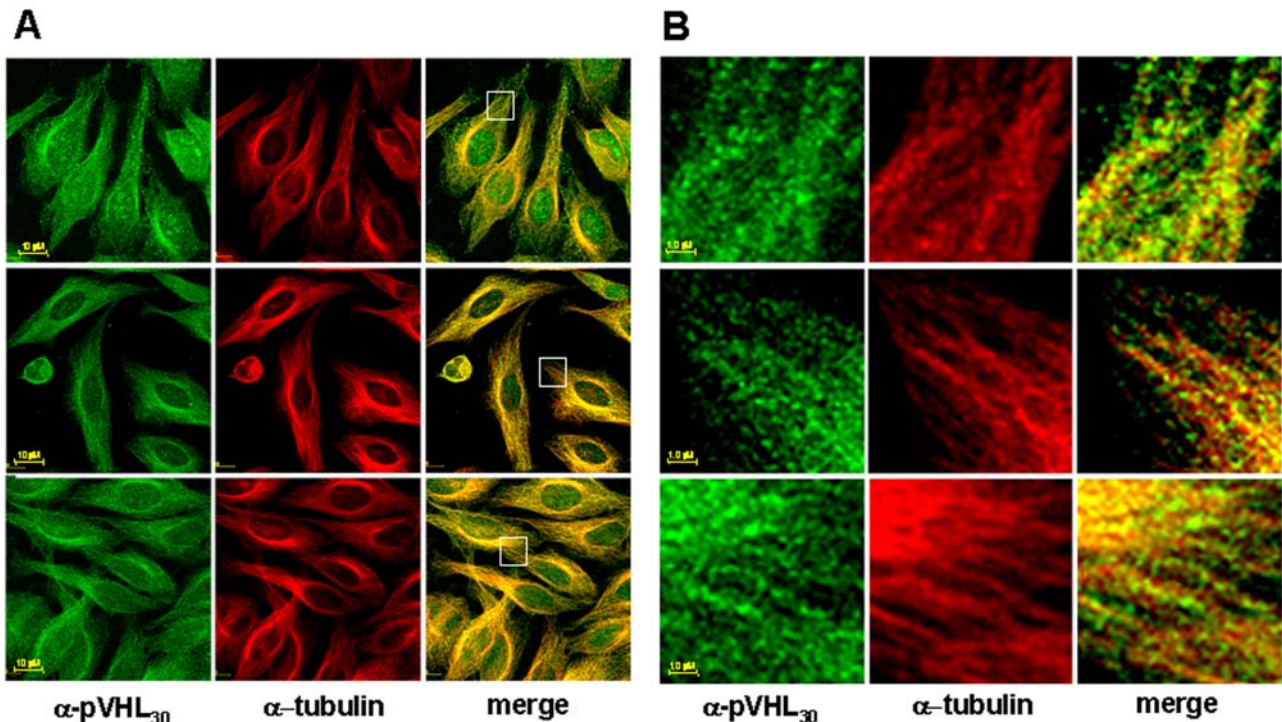


Figure 79. Endogenous pVHL₃₀ co-localises with microtubules. A) HeLa cells were double-labelled with VHL_{NT} and anti-tubulin (Tub27b) and slides processed by confocal microscopy. B) An enlargement of the highlighted area in (A) demonstrating the association of pVHL₃₀ with microtubules at a higher magnification.

7.6.3 The importance of microtubule stability in pVHL₃₀ intracellular localisation

While cytoplasmic pVHL₃₀ had been shown to associate with microtubules, endogenous pVHL₃₀ could nonetheless at times still be observed either partially or totally in the nucleus. Approaches were undertaken to examine the endogenous dynamics of pVHL₃₀ and involved reinvestigating already documented observations – cell density and transcriptional-dependent shuttling - as well as observing pVHL₃₀ localisation throughout the cell cycle. While differences in localisation patterns were observed, conclusions were difficult to make based on the inconsistent observations. Contact inhibition did indeed seem to affect pVHL₃₀ localisation, but in contrast to Lee *et al*, confluent cultures showed a predominantly nuclear signal, whereas sparse cultures showed a predominantly cytoplasmic localisation. No obvious changes in localisation or expression were observed throughout the cell cycle, with the exception that during mitosis, pVHL₃₀ can bind the spindle apparatus (Hergovich and Krek, unpublished). However, when investigating

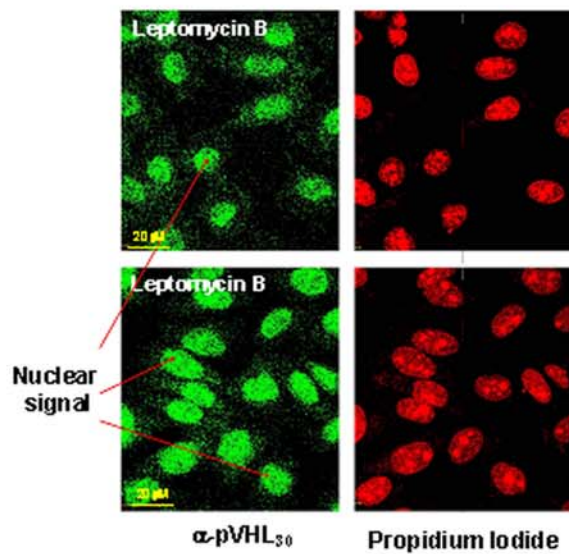
transcription-dependent trafficking of pVHL₃₀, the results were striking. In cells treated with Actinomycin D, an RNA polymerase II inhibitor, or leptomycin B, an inhibitor of CRM-1 dependent protein nuclear export, pVHL₃₀ was observed to be uniquely nuclear (Fig.80.A). This was unexpected, given the fact that Lee *et al.* had recently published that while VHL-GFP is sensitive to ongoing RNA polymerase II activity, it is not affected by treatment with leptomycin B [389].

Interestingly, co-staining for microtubules highlighted an important observation, namely that in cells that exhibited a nuclear pVHL₃₀ signal, no intact microtubules were observed. This does not mean that the drug treatment by leptomycin B or Actinomycin D directly depolymerises microtubules, nor that pVHL₃₀ shuttles in a CRM1-dependent fashion, but rather that this treatment might mimic a stress response resulting in the breakdown of the microtubule network and subsequent re-localisation of pVHL₃₀.

7.6.4 The effect of microtubule stabilising/destabilising drugs on pVHL₃₀ intracellular localisation

To further analyse this observation, cells were treated with drugs that were known to destabilise microtubules. Treatment with vincristine, nocodazole or colcemide all disrupted microtubules, and all resulted in a uniquely nuclear signal of pVHL₃₀, whereas untreated cells

A) Leptomycin B treatment of Hela cells



B) pVHL₃₀ sub-cellular localisation is affected by MT stability

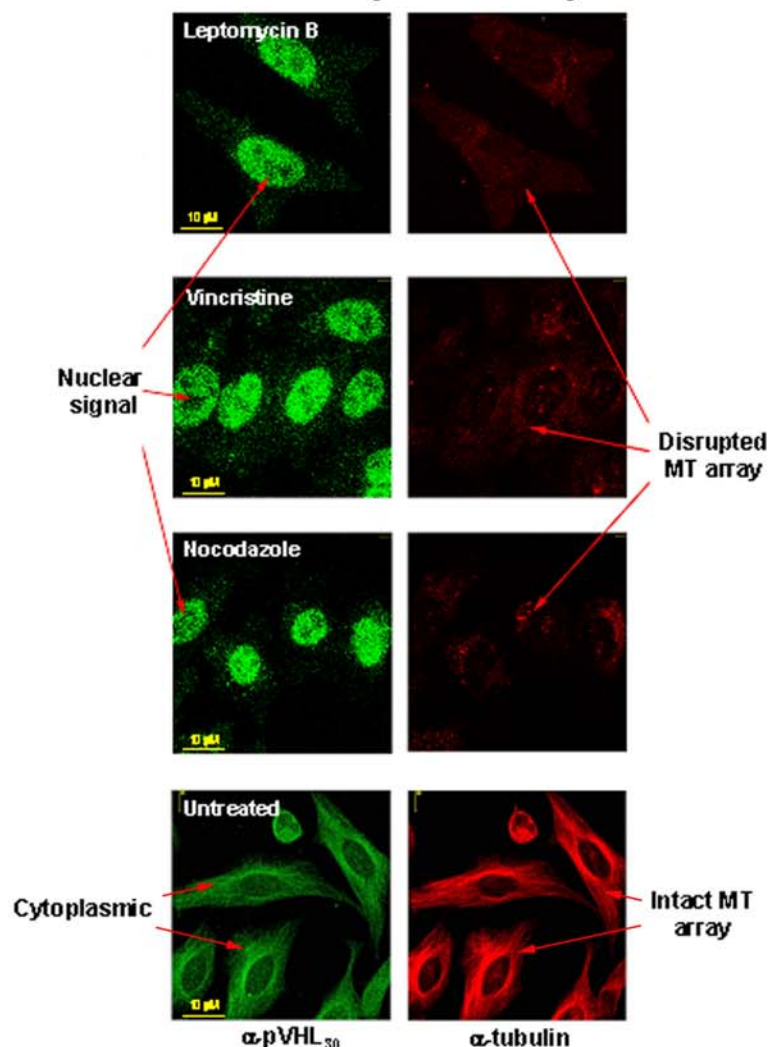
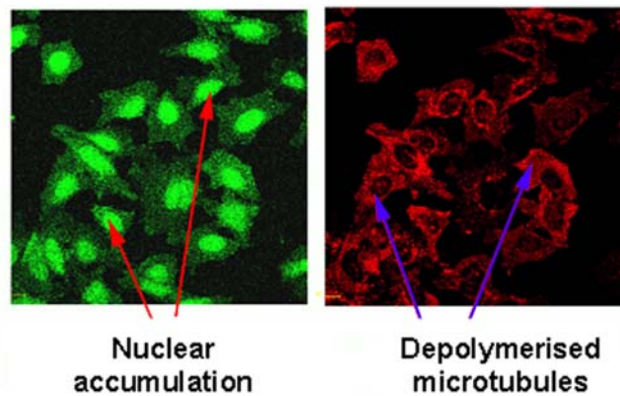


Figure 80. pVHL₃₀ nuclear accumulation corresponds to a disruption of the microtubule network. A) Leptomycin B treatment resulted in a nuclear accumulation of pVHL₃₀, but also a breakdown in microtubule array. B) HeLa cells treated with known depolymerising agents render the same pVHL₃₀ nuclear accumulation as with leptomycin B, whereas untreated cells that maintain an intact microtubule array show a cytoplasmic pVHL₃₀ signal.

retained a cytoplasmic, microtubule-associated pVHL₃₀ localisation pattern (Figs 78(B), 79(A)). Furthermore, when cells were treated with a microtubule stabilising drug like Taxol, a strong pVHL₃₀ signal was retained in the cytoplasm (Fig.81.B). Nonetheless, taxol treated cells also exhibited some nuclear staining. While Taxol stabilises microtubules, it renders them inactive, and thereby creates a non-physiological environment for the cell, which may in part be interpreted as stress. Perhaps for this reason, despite the stabilised microtubule network, more nuclear staining is observed than would be expected for untreated. Regardless, maintaining microtubule

A) Microtubule destabilising drug-treated Hela cells



B) Microtubule stabilising drug-treated Hela cells

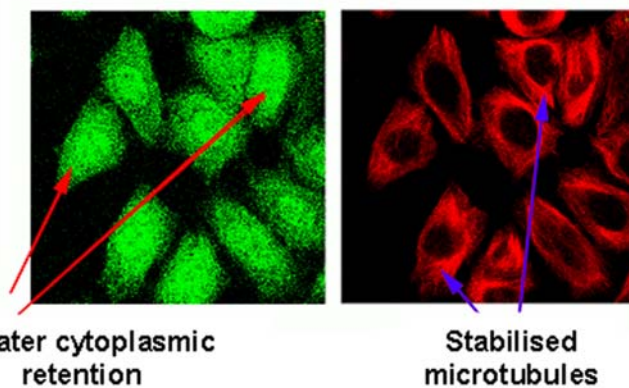


Figure 81. Microtubule stability affects pVHL₃₀ nuclear/cytoplasmic localisation. A) Treatment of Hela cells with vincristine, a microtubule depolymerising agent, caused pVHL₃₀ to localise predominantly in the nucleus. B) Treatment of Hela cells with Taxol, a microtubule stabilising agent gives rise to a greater pVHL₃₀ cytoplasmic retention.

integrity resulted in pVHL cytoplasm retention. At this point it became apparent that the microtubule architecture was implicated in pVHL₃₀ intracellular localisation and that disrupting microtubules resulted in pVHL₃₀ re-localising to the nucleus. Disruption could be induced by drug induced depolymerisation, or seemingly by other treatments that are registered as stress by the cell, like global inhibition of transcription by Actinomycin D, or drug treatment by leptomycin B. Unfortunately, various attempts to visualise pVHL₃₀ migration to the nucleus by time-lapse video microscopy following treatment of cells with a microtubule depolymerising agent were unsuccessful in demonstrating this live. Moreover, while immuno-fluorescence data is convincing, biochemical data is missing to show that cellular fractionation in the presence or absence of a microtubule destabilising drug can show fluctuations in nuclear and cytoplasmic pools of pVHL₃₀. This has been attempted, but for technical reasons has been unsuccessful. It is thought that due to its small size, pVHL₃₀ simply diffuses through the nuclear pores upon mechanical disruption of the cells. Perhaps cross-linking cells with glyceraldehyde prior to lysing may prevent passive diffusion of proteins which are below the nuclear pore exclusion size and could represent a solution to this problem.

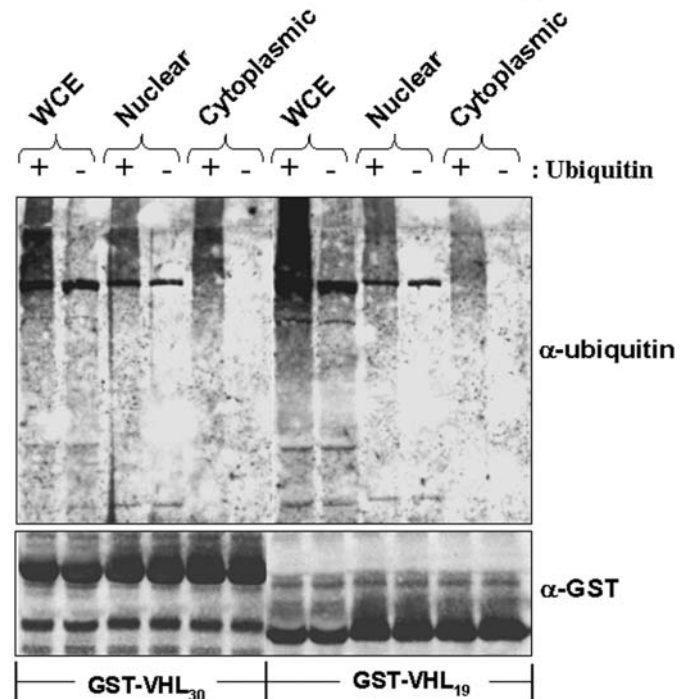
7.6.5 Recombinant VHL₃₀ and VHL₁₉ can exhibit both nuclear and cytoplasmic ubiquitination activity

Given the fact that pVHL₁₉ predominantly localises to the nucleus and pVHL₃₀ to the cytoplasm, it was interesting to investigate their respective ubiquitination activity with respect to nuclear and cytoplasmic intracellular compartments.

More specifically, the question asked was whether pVHL₁₉ could exhibit ubiquitination activity in the cytoplasm, and whether pVHL₃₀ could exhibit ubiquitination activity in the nucleus. If this were not the case, then their intracellular separation might be based on their ubiquitination activity capacity. A crude assay was used to test this which involved reconstituting an *in vitro* ubiquitination assay with either GST-VHL₃₀ or GST-VHL₁₉ as the source of ligase. The reaction mixture involved the addition of an E1 enzyme, cdc34 - as E2, ATP as a source of energy, ubiquitin aldehyde and finally a concentrated lysate input which would provide additional components

necessary for pVHL activity. This lysate input was divided into whole cell extracts, nuclear lysate preparations, and cytoplasmic preparations with the intention of investigating whether specific components were located in either compartment that might be necessary for the ubiquitination activity of either pVHL₃₀ or pVHL₁₉. Finally these reactions were performed in the presence or absence of ubiquitin. As figure 82 illustrates, both GST-VHL₁₉ and GST-VHL₃₀ were capable of generating ubiquitination activity in both cytoplasmic and nuclear fractions, albeit to a lesser extent than the whole cell extract. This activity is reflected by a black smear in the high molecular weight range.

A) Investigation of pVHL₃₀ and pVHL₁₉ cytoplasmic and nuclear ubiquitination activity



B) Nuclear/cytoplasmic fractionation of lysate input for ubiquitination assay

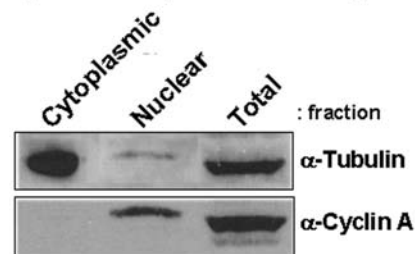


Figure 82. Comparison of the ubiquitination activity of pVHL₃₀ and pVHL₁₉ with respect to sub-cellular localisation. A) GST-VHL forms were purified from sf9 cells and incubated with appropriate ubiquitination assay components (see text) supplemented with lysate derived from WCE (whole cell extract), nuclear extract, or cytoplasmic extract in the presence or absence of ubiquitin. Activity is reflected by high molecular weight black smear. B) The fractionation of HeLa cells prior to ubiquitination assay. Tubulin is used as a cytoplasmic marker, and cyclin A for the nuclear fraction.

While it was shown that pVHL₃₀ did not bind other VBC-Cul2 E3 ligase components when microtubule-bound, its nuclear localisation would be devoid of any microtubule association. It was therefore presumed that, when in the nucleus, pVHL₃₀ could reconstitute an E3 ligase complex. If this was indeed the case, then a scenario was beginning to emerge that VBC-Cul2 activity could also be a nuclear event, and not merely a cytoplasmic event as previously thought. Evidence supporting this idea was published by Berra *et al* in 2001, which showed that HIF1 α could indeed be degraded in both cellular compartments and with the same kinetics [208]. This is in contrast to the mechanism that controls p53 degradation by MDM2 which requires ubiquitinated p53 expulsion from the nucleus before being degraded [386]. Experiments at the time were thus aimed at trying to show that pVHL₃₀ might be entering the nucleus following hypoxic insult in order to degrade HIF α in the nucleus following re-oxygenation, thereby mounting an efficient response that would rapidly down-regulate HIF α (NB. HIF α half-life is 5-8 minutes). Such studies were published during the course of this work by Groulx *et al.* who showed that ubiquitinated forms of HIF α , as well as VHL-ubiquitinated-HIF α complexes, are found solely in the nuclear compartment of normoxic or re-oxygenated VHL-competent cells [391]. However, in contrast to Berra *et al.* who suggested that HIF α could be degraded within the nucleus by nuclear proteasomes, Groulx *et al.* demonstrate that HIF α localises exclusively in the nucleus of hypoxic cells but is exported to the cytoplasm upon re-oxygenation following nuclear ubiquitination. Nonetheless, regardless of where HIF α is degraded, both groups demonstrated that HIF α could be ubiquitinated in the nucleus, thus highlighting the need for a pVHL presence in this compartment capable of mounting an efficient response following hypoxia. While pVHL₁₉ presumably operates to prevent any unwarranted HIF activity in normoxic cells, one could envisage a scenario whereby cells, following hypoxia, accumulate pVHL₃₀ in the nucleus in order to assist the already present pVHL₁₉ to ubiquitinate HIF α as quickly and efficiently as possible. It is tempting to suggest that this transport to the nucleus, analogous to p53, may be along microtubules, whose subsequent disruption upon stress signalling, as with hypoxia, facilitates pVHL₃₀'s nuclear accumulation.

Interestingly a paper emerged last year in Cancer Cell, which described a novel anti-tumour and anti-angiogenic agent currently in clinical trials, 2-methoxyestradiol (2ME2). Administration of 2ME2 resulted in a down-regulation of HIF α , and that this down-regulation was dependent upon disruption of interphase microtubules [392]. The authors suggest that their data establishes this drug as an inhibitor of HIF α and provides a mechanistic link between the disruption of the microtubule cytoskeleton and inhibition of angiogenesis. By extension, perhaps one aspect of pVHL tumour suppressor activity *in vivo* is to re-locate to the nucleus following a hypoxic cue, which not only facilitates down-regulation of HIF α , but by uncoupling itself from its microtubule-association, pVHL₃₀ re-location also destabilises the microtubule cytoskeleton. The question however remains whether microtubule disruption is the causal event in pVHL₃₀ re-location to the nucleus, or whether pVHL₃₀ re-location is the causal event in microtubule disruption.

Which ever this represents, the findings documented here may represent a possible molecular mechanism that can, in part, explain the down-regulation of Hif α following 2ME2 treatment, and by extension, can therefore be implied in normal physiological cellular control. Interestingly, cytoplasmic retention of 53 has been shown to be dependent on vimentin, an intermediate filament protein scaffold [337]. Disruption of intermediate filaments causes p53 to accumulate in the nucleus. Whether disruption of the cytoskeleton is a general phenomenon of tumour suppressor nuclear re-localisation remains unstudied.

Concluding Remarks

This section has demonstrated the initial findings that pVHL is functionally linked to the cytoskeleton. It demonstrates that in normal logarithmically growing cells, GFPVHL₃₀ and GFPVHL₁₉ exhibit different localisation patterns. Endogenous pVHL₃₀ resides predominantly in the cytoplasm where it co-localises with the microtubule network. Disruption of the microtubule cytoskeleton renders nuclear re-localisation of pVHL₃₀. The reason for this is unclear, but postulated to be involved in mounting an efficient response in conjunction with pVHL₁₉ to target Hif α for proteolytic degradation following its accumulation due to hypoxic stress, or some alternative means of rendering a HIF response. This work contributed to an article in *Nature Cell Biology*, where it was further shown that pVHL can protect microtubules from depolymerisation, and that certain tumour derived mutations in *VHL*, while capable of binding microtubules, could not stabilise them. These mutants could be all classed clinically as those mutants related to type 2A VHL disease where patients exhibit predisposition to pheochromocytoma and haemangioblastoma but a reduced risk to renal cell carcinoma. The correspondence between type 2A mutants and microtubule stabilisation might suggest a contributory causal role on behalf of the microtubule network regarding development of malignancies associated with this sub-class of VHL disease, or that the mutational effect somehow mitigates against the RCC predisposition.

RESULTS – PART III:

Investigating VHL RNA Interference

7.1 Introduction

pVHL functional inactivation studies at the time of commencing this project had relied predominantly on the comparison of tumour derived cell lines lacking functional pVHL and comparing findings to an isogenic counterpart into which pVHL had been reintroduced. These cells, which include 786-0, A498, RCC4, are RCC derived cell lines, whose pVHL status is not entirely clear. It could be argued that, they are non-functional with respect to known pVHL functions, but whether all pVHL functioning is effected is unclear. Furthermore as RCC cells are known to harbour a myriad of genetic alterations aside from those associated with pVHL, drawing conclusions about observations solely attributable to pVHL based on reintroduction of pVHL into these cell lines is difficult.

For this reason, an alternative approach was sought. Attempts at targeting pVHL by anti-sense oligonucleotide approaches had failed. However, at the time, small interfering RNA (siRNA) oligonucleotides were beginning to emerge as a potential tool that could be used to effectively, and specifically knockdown target proteins in mammalian cell culture. The laboratory had not established this technology, and the aim of the project was to establish siRNA as a standard reagent to be used, and in particular to analyse the effect of depleting cells of endogenous pVHL.

Post-transcriptional gene silencing (PTGS), which was originally thought to be a phenomenon limited to petunias and other plant species, represents one of the most highlighted areas of molecular biology [393]. It is now understood that PTGS occurs in both plants and animals and has roles in viral defence and transposon silencing. From an experimental point of view, the most exciting development stemming from PTGS is RNA interference (RNAi) – PTGS initiated by the introduction of double stranded RNA (dsRNA) – as a tool to knock down expression of specific genes [393, 394]. Cells can be transfected with dsRNA oligonucleotides, and within hours of transfection, results can already be observed for many proteins targeted in this way. Compared to the time spent generating knock out models in organism like mice or flies, this approach is fast becoming the molecular biologists prerequisite before attempting any timely knockout strategies. Due to its ability to manipulate gene expression experimentally, RNAi is currently being applied to probe gene function on a whole-genome scale. However, one disadvantage using RNAi is that targeting results in knockdown in protein expression, not

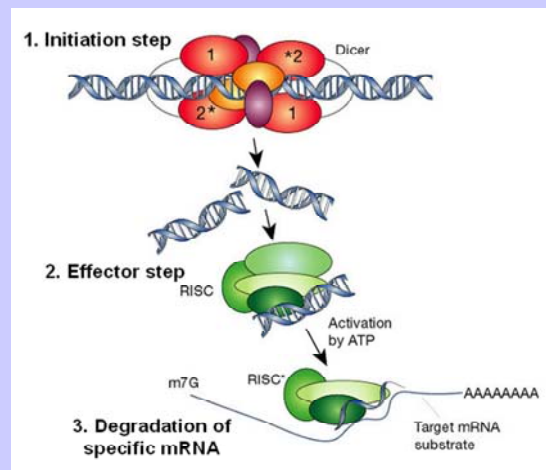
knockout, and if residual amounts of a candidate protein are sufficient to fulfil its function, then unfortunately RNAi is unlikely to render significant results.

Box 2. The Biochemical Mechanism of RNAi

It is generally accepted that RNAi includes both an initiation and effector step. In the initiation step, input dsRNA is digested into 21-23 nucleotide small interfering RNAs (siRNAs). Evidence indicates that siRNAs are produced when the enzyme Dicer, a member of the RNase III family of dsRNA-specific ribonucleases, processively cleaves dsRNA (introduced directly or via a transgene or virus) in an ATP-dependent, processive manner. Successive cleavage events degrade the RNA to 19-21 bp duplexes (siRNAs), each with 2-nucleotide 3' overhangs (Hannon *et al* 2002; Bernstein *et al* 2001).

In the effector step, the siRNA duplexes bind to a nuclease complex to form what is known as the RNA-induced silencing complex, or RISC. An ATP-dependent unwinding of the siRNA duplex is required for activation of the RISC. The active RISC then targets the homologous transcript by base pairing interactions and cleaves the mRNA ~12 nucleotides from the 3' terminus of the siRNA (Hammond *et al* 2001; Sharp *et al* 2001; Hutvagner *et al* 2002). Although the mechanism of cleavage is to date unclear, research indicates that each RISC contains a single siRNA and an RNase that appears to be distinct from Dicer (Hannon *et al* 2002).

Because of the remarkable potency of RNAi in some organisms, an amplification step within the RNAi pathway has also been proposed. Amplification could occur by copying of the input dsRNAs, which would generate more siRNAs, or by replication of the siRNAs themselves. Alternatively or in addition, amplification could be effected by multiple turnover events of the RISC.



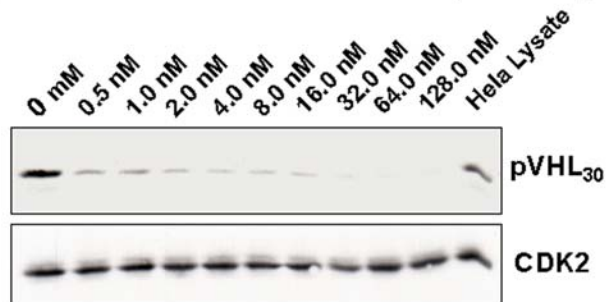
Adapted from Hannon *et al* 2002

7.2 VHL RNA interference

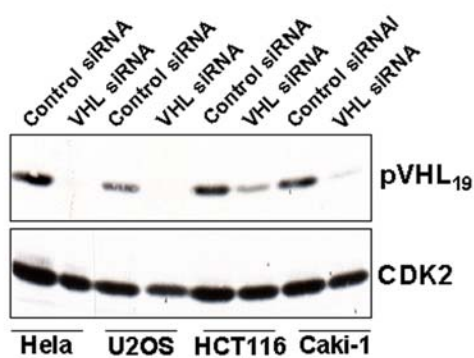
RNA oligonucleotides corresponding to a 19 base pair stretch of the VHL coding region were ordered and prepared as per materials and methods. HeLa cells were chosen as a cell line to define an optimal working concentration. Cells were treated with differing concentrations of oligos for 48 hours and samples prepared for western blotting. Figure 83(A) demonstrates a dose dependent down-regulation of pVHL₃₀. A final concentration of 128nM of dsRNA was used for all future experiments unless otherwise stated. Figure 83(B) illustrates the results obtained from transfecting four different human tumour derived cell lines with siRNA oligos against VHL. The results demonstrate that maximal pVHL₁₉ knockdown is achieved in HeLa cells. All subsequent experiments were hence carried out in HeLa cells unless otherwise stated. Figure 81 demonstrates VHL RNAi time dependency. Samples were first transfected over a 24-96 hour period. Figure 83.C(i) shows that maximal knockdown is reached after only 24 hours, and that this level of

knockdown is maintained up to 96 hours, and presumably beyond. Figure 83.C(ii) highlights more dramatically the efficacy of pVHL knockdown. VHL RNAi can elicit an effect 3-4 hours post-transfection, reaching a near maximum after a mere 5 hours.

A) VHL RNAi - concentration dependency



B) Comparison of VHL RNAi in human tumour cell lines



C) VHL RNAi - Time dependency

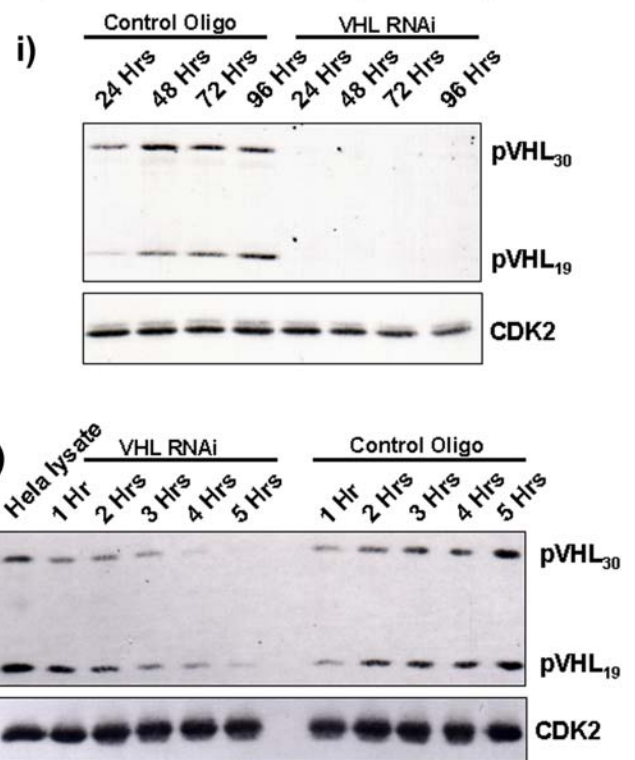


Figure 83. Defining VHL RNAi conditions. A) pVHL depletion by siRNA oligos is concentration dependent. A final concentration of 128nM was defined as an optimal concentration for future experiments. B) Four different tumour derived cell lines were analysed for the efficiency of VHL RNAi. C) Time dependent knockdown of pVHL by RNAi. i) HeLa cells were transfected with oligos and harvested 24-96 hours post-transfection. Maximal knockdown was observed after 24 hours. ii) Cells were transfected with oligos and harvested 0-5 hours post-transfection. Knockdown is observed after 4 hours.

Finally, cells were analysed for adverse affects, which might be either VHL RNAi specific, or technique related. Figure 84 overleaf demonstrates that cells proliferated normally and that cell viability of both VHL and control RNAi was comparable to untreated control. Furthermore, FACs analysis demonstrated that cell growth profiles were unaffected (data not shown). These results indicated that VHL RNAi does not result in a defect in cell proliferation or viability. Furthermore, it demonstrates that the experimental conditions used were not toxic.

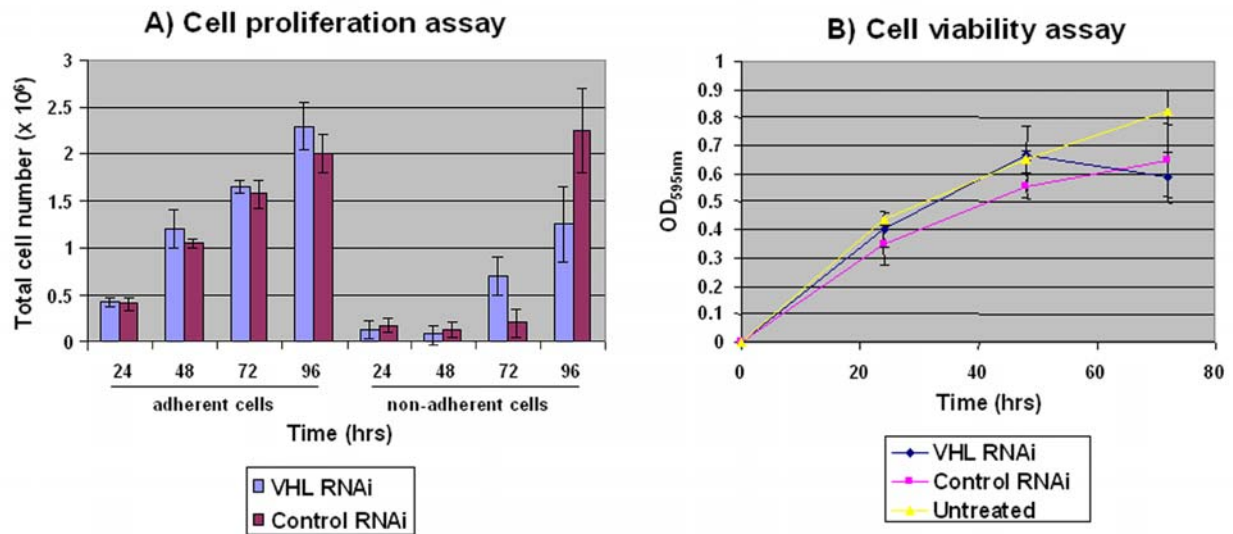


Figure 84. VHL RNAi does not affect cell proliferation. A) Counting adherent and non-adherent, a measure of cell death, show no proliferation defects. B) A cell viability assay using tetrazolium (MTT) salt incorporation. No significant difference in viability is observed with VHL RNAi treated cells.

7.3 VHL RNAi does not up-regulate HIF- α protein levels nor HIF transcriptional activity

As discussed in chapter 5, negative regulation of VEGF expression by VHL is well established and has been demonstrated with respect to pVHL's ability to target HIF for ubiquitin-mediated degradation [114, 200]. However, Gnarra *et al.* found VEGF expression to be decreased in VHL-deficient placental trophoblasts. This contradicts our understanding of HIF regulation by VHL and subsequent VEGF suppression. Consistent with constitutively active HIF, depletion of VHL should result in an up-regulation of VEGF as seen in VHL null tumours [262-264]. In the lethal phenotype observed upon VHL depletion in mice, this is however not the case. VEGF is down-regulated in VHL^{-/-} placental derived trophoblast cells, and embryos die due to a lack of vascularisation of the placenta. However, it has yet to be fully determined whether this decrease is directly related to VHL inactivation which would indicate an alternative form of regulation in placental trophoblasts than seen in vascular tumours related to VHL disease, or a secondary effect and an early indicator of placental failure. Nonetheless, in this scenario, an inability to up-regulate HIF in the absence of pVHL has lethal consequence for the developing embryo.

Haase *et al.* demonstrated that knockout of the *VHL* gene in mice can lead to a stabilisation of HIF [269]. The conditional inactivation of the *VHL* gene in the livers of BALB/c mice shows that inactivation of *VHL* leads to the up-regulation of VEGF, Glut-1, and Epo mRNAs, as well as stabilisation of HIF-2 α in hepatocytes. This finding suggests that pVHL acts as a global regulator of HIF- α stability, and not only a regulator in VHL disease effected tissues, which points to a more general role of pVHL in the regulation of HIF α . Additionally, a very recent report from our laboratory suggests that specific VHL

inactivation in neuronal precursor cells in the brain results in increased vasculogenesis in brain tissue, reflective of up-regulated Hif α in the absence of pVHL (Ballschmieter and Krek). While additional studies are needed, this finding may for the first time demonstrate that inactivating pVHL in the brain is sufficient to cause brain manifestations like those observed in CNS haemangioblastoma, and thereby supporting the idea that inactivating mutations in the VHL gene are a causal role in these tumour formations. These and other studies have clearly demonstrated the role of pVHL in HIF degradation, but given the fact that VHL^{-/-} mice die *in utero* due to lack of placental vasculogenesis owing at least in part to a reduction in Hif α activity, the discrepancy between this and the highly vascularised tumours associated with VHL disease reflecting up-regulated Hif α activity, remains unexplained.

The first question to address therefore was whether endogenous depletion of pVHL in cell culture was sufficient to render a HIF response. Figure 85.A is a representation of multiple attempts to visualise Hif1 α on western blot following VHL RNAi. While the positive control, CoCl₂ treated Hela cells, showed positive for Hif1 α , no signal is seen when depleting cells of endogenous pVHL. To ensure that the result seen by western blot was not simply a reflection of the fact that any fluctuations in Hif-1 α went unobserved due to the lack of detection sensitivity, a reporter assay using the VEGF-reporter gene was analysed to investigate any HIF-induced transactivation that might be increased by depletion of endogenous pVHL by RNAi. Figure 85(B) demonstrates that the positive control, Hif1 α Δ proline, elicits strong transactivation of the VEGF-reporter, whereas VHL and control siRNA oligo-treated samples were indistinguishable. The result therefore demonstrates that VHL RNAi does not cause any detectable up-regulation in HIF activity.

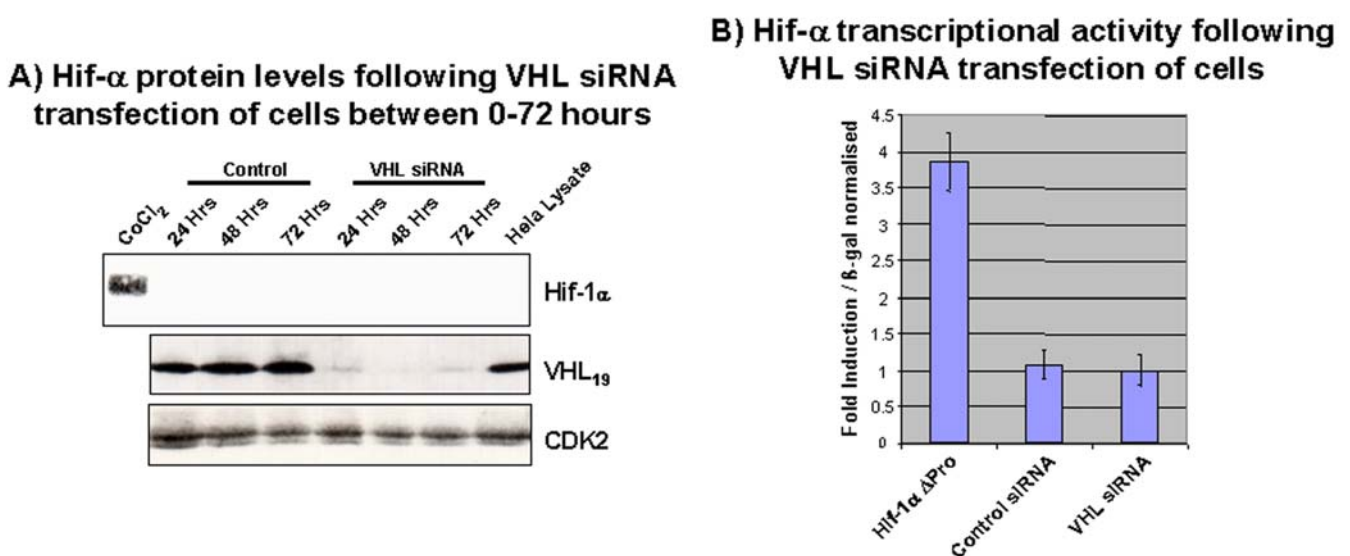


Figure 85. Depleting HeLa cells of endogenous pVHL, does not increase HIF α protein levels, or HIF transcriptional activity. A) HeLa cells were treated with VHL siRNA over a 24-72 hour period and prepared for western blot analysis to see if protein levels of HIF α had changed. B) Cells treated with VHL siRNA and appropriate controls were prepared for VEGF-reporter gene transactivation analysis. HIF-1 α Δ Pro refers to a HIF1 α mutant which has both proline residues, P564 and P402, mutated to facilitate constitutive HIF α activation.

The next parameter to investigate was whether the kinetics of Hif-1 α degradation could be affected in the presence of VHL RNAi. HeLa cells were treated with CoCl₂ for 4 hours to induce a hypoxic response, and re-oxygenation was mimicked by changing the medium to that of medium lacking CoCl₂. The cells were harvested at various time points, and the speed of Hif-1 α degradation examined. Figure 86 demonstrates an example of one such experiment. The result shows no obvious changes in Hif-1 α degradation kinetics in the presence of VHL RNAi. This result is surprising, in light of the fact that pVHL is considered the principle ligase for HIF. Two conclusions can be drawn from this experiment. Either residual amounts of pVHL that remain following down-regulation of pVHL by RNAi are sufficient to suppress HIF, even after a hypoxic insult or that an alternative HIF ligase can replace pVHL under these conditions. Given the fact that HIF continues to be negatively regulated in placental derived trophoblast cells of the VHL^{-/-} mice, it seems plausible that other mechanism of HIF proteolytic control are physiologically more relevant than perhaps thought. Reports already exist demonstrating that p53 promotes Mdm2-mediated ubiquitination and proteasomal degradation of HIF-1 α [217]. Perhaps under these circumstances, Mdm2 compensates for the loss of pVHL in Hif-1 α degradation.

Hif-1 α degradation Kinetics following VHL RNAi

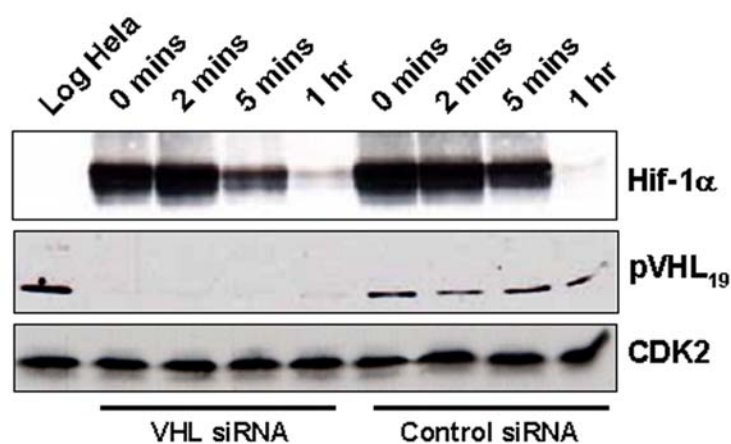


Figure 86. Kinetics of Hif1 α degradation following hypoxia mimetic, CoCl₂, are not affected by VHL RNAi. HeLa cells were transfected with VHL and control siRNA oligos 48hrs prior to CoCl₂ treatment for 4 hrs. They were then released into fresh medium and harvested at the noted time points.

Interestingly, a report emerged from Berra *et al.* demonstrating that specific silencing of proline hydroxylase 2 (PHD2) using siRNA is sufficient to stabilise and activate Hif-1 α in normoxia in all human cells investigated. They demonstrated a dose dependent Hif-1 α response to PHD2 siRNA under normoxia, an increase in Hif-1 α immunofluorescence signal following RNAi, and reporter assays demonstrated Hif-1 α activity under normoxia following PHD2 knockdown. Intriguingly, they state that the same is observed for VHL, but no data is shown. In fact, VHL RNAi has to date never been published, and international correspondence with peers has confirmed the inability to show a consistent and reproducible HIF up-regulation in response to VHL depletion by

RNAi. The question therefore was whether the finding that PHD2 knockdown really was sufficient to mount a HIF response, and if so, why the same could not be observed for VHL RNAi. Figure 87 represents a reporter assay whereby, HeLa cells were investigated for their transactivation capacity of a VEGF-reporter gene following siRNA treatment. RNAi for pVHL, Mdm2, a potential alternative Hif-1 α ligase, and PHD2 were performed. The same oligonucleotides as published by Berra *et al.* were used to target PHD2. As the figure demonstrates, with the exception of the positive

HIF-1 α transcriptional activity following VHL, MDM2 and PHD2 RNAi

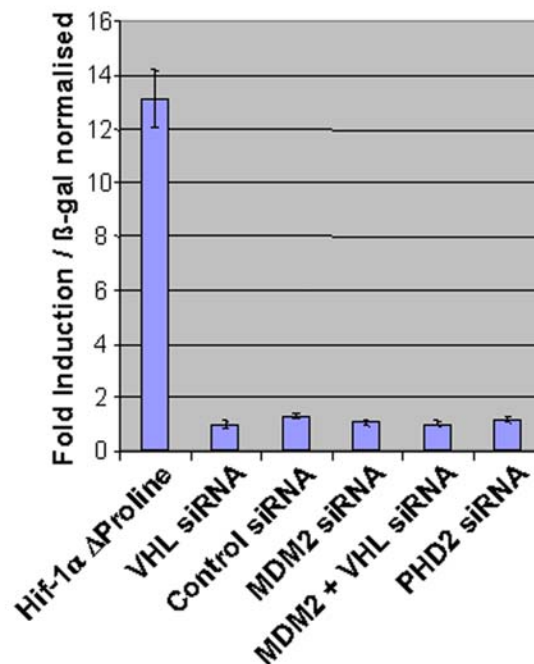


Figure 87. No transactivation activity of a VEGF-reporter gene is observed in HeLa cells treated with siRNA for pVHL, Mdm2 or PHD2. Cells were transfected singularly or in combination 48hrs prior to preparation for reporter assay.

control, a non-degradable Hif-1 α mutant, no significant transactivation activity was observed amongst the various siRNA treated cells. Even when siRNA oligos for VHL and Mdm2 were combined, no fluctuations in activity were observed. These results contradict those published by Berra *et al.*, and cast serious doubt on whether depletion of one proline hydroxylase isoform is sufficient to up-regulate Hif-1 α . Nonetheless, the question remains why no HIF response is seen in the absence of pVHL. Cre-lox specific targeting of *VHL* in mouse embryonic fibroblasts is being established in the laboratory (Frew and Krek). Interestingly, no HIF response has to date been observed in these cells, despite efficient targeting of the *VHL* gene. This observation supports those observed for VHL RNAi. For this reason, it merits further investigation, which ultimately may help explain the phenomenon of down-regulated HIF target genes in the developing placenta of VHL^{-/-} mice.

7.4 VHL RNAi confirms pVHL regulation of phosphorylated cofilin

Collaborative work between Joanna Listzwan, a former doctoral student in the laboratory, and the proteomics centre at Novartis, Basel, had demonstrated that following a proteomics approach aimed at identifying novel proteins differentially expressed in 786-0 VHL^{-/-} cells and their isogenic counterparts stably expressing HA-pVHL₃₀, several candidate proteins shown to be involved in cell shape changes were identified. In particular, levels of phosphorylated cofilin were approximately 2.5 fold higher in 786-0

vector control cell line when compared to their isogenic counterpart expressing re-introduced HA-VHL₃₀. This finding was later confirmed by 2D gel western blotting, comparing phospho-cofilin levels between 786-0 cells expressing or lacking pVHL (Lisztwan and Krek; unpublished). However, evidence lacked regarding whether endogenous depletion of pVHL from cells that normally express wild-type pVHL, would show increases in phospho-cofilin levels, or whether this observation was a phenomenon of 786-0 cells. Collaborative work investigating the affect of VHL RNAi on phospho-cofilin levels demonstrated for the first time that depleting cells of endogenous pVHL increased the level of phospho-cofilin. Figure 88 illustrates these findings, thereby confirming independently the original proteomics result. Up-regulation of phospho-cofilin represents the first consistent and reproducible readout from VHL RNAi treatment.

Cofilin is an actin depolymerising factor, whose phosphorylation is mediated by LIM-kinase (LIMK) [395]. LIMK was initially identified in a screen for a novel member of the c-Met/HGF receptor tyrosine kinase family [396], and to date is known to consist of two members, LIMK1 and LIMK2. Recently, it has been shown that both LIMK1 and LIMK2 regulate actin cytoskeletal reorganisation downstream of the Rho family GTPases, and LIMK-induced actin cytoskeletal rearrangement is mediated by the phosphorylation of cofilin [397, 398]. Therefore, LIMK may be a key component of a fundamental signal transduction system that connects extracellular stimuli to intracellular actin cytoskeletal rearrangements in a distinct biological context.

pVHL was shown not to interact with cofilin, but rather its upstream kinase, LIMK (Lisztwan and Krek, unpublished). This

Depletion of endogenous pVHL confirms pVHL's effect on phosphorylated cofilin

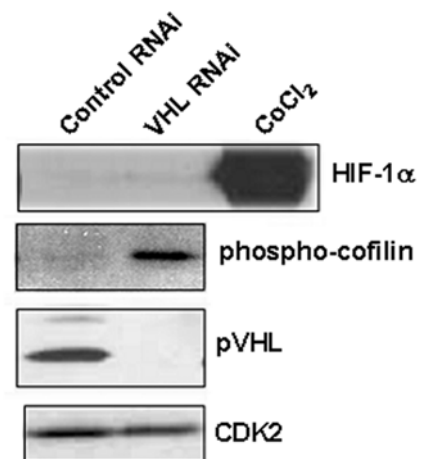


Figure 88. VHL siRNA in HeLa cells results in up-regulation of phospho-cofilin. HeLa cells were transfected 48hrs prior to preparation for western blot analysis. While no fluctuations in HIF α are observed, a known target of the VCB-Cul2 ligase, phospho-cofilin is up-regulated in the absence of pVHL.

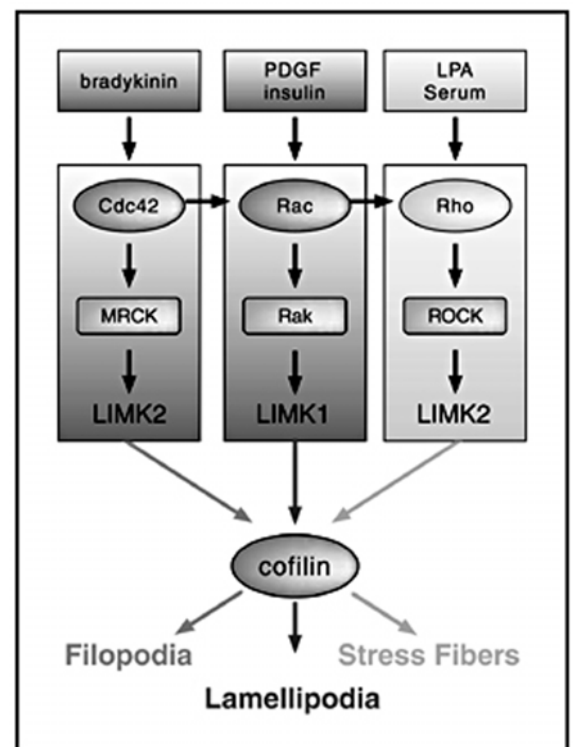


Figure 89. Signal transduction of LIMKs and cofilin mediated by the Rho family GTPases in actin cytoskeletal dynamics. Activated LIMK catalyses phosphorylation of cofilin. Phosphorylated cofilin cannot bind actin and is impaired in its activity to depolymerise actin filaments, thus leading to actin filament stabilisation. Activation of Cdc42, Rac, and Rho specifically induces formation of actin reorganisation-based cellular structures of filopodia, lamellipodia or membrane ruffling, and stress-fibers, respectively. In cellular signalling, LIMK1 is specifically activated by Rac via activation of a well-known Rac effector, Pak. In contrast, LIMK2 activity is enhanced by Rho and Cdc42, which are mediated by their specific effectors, ROCK and MRCK α , respectively.

Adapted from Takahashi et al. 2003

interaction has been shown to inhibit phosphorylation of cofilin by LIMK1, thereby helping to explain the results from the initial proteomics approach and subsequent RNAi data. However the biological significance of this inhibitory interaction remains unclear. Previous work has suggested that reintroduction of pVHL into RCC cells lacking pVHL promotes the assembly of stress fibres, focal adhesion formation and cell spreading - all reflective of changes in the actin cytoskeleton. Whether pVHL's effects on the actin cytoskeleton are direct remains to be determined, but it is interesting to note that although LIMK is activated by all three Rho GTPase family members, each GTPase promotes very different morphological changes (Fig.89) [399]. Rearrangements in the actin cytoskeleton are conducive to cell shape changes and motility, and aberrations in their control may be reflected in the highly invasive or migratory phenotype of certain tumour cells, as seen with cells derived from RCC. Reintroduction of pVHL into RCC cells lacking functional pVHL has been shown to decrease the migratory and invasive behaviour of these cells [136]. Furthermore, contact inhibition, a feature often lost in transformed cells, has been shown to be restored in RCC upon pVHL reintroduction [249, 251]. Interestingly, recent evidence from our laboratory suggests that phospho-cofilin accumulates upon cell contact (Sayi and Krek, unpublished). Given the fact that pVHL has been shown to relocalise upon cell confluency, that depletion of pVHL augments phospho-cofilin levels and that pVHL itself has already been shown to affect the actin cytoskeleton [249], it must be assumed that pVHL is functionally involved in actin cytoskeletal rearrangements. Interestingly, as already mentioned in chapter 5, VHL^{-/-} MEFs are no longer capable of assembling an extracellular fibronectin matrix. Taken together with the fact that pVHL binds microtubules, is involved in integrin receptor expression and that RCC cells lacking pVHL exhibit a highly migratory phenotype, the involvement of pVHL in cell shape changes which culminate in the migratory phenotype observed for VHL^{-/-} RCC cells may in part therefore be explained by pVHL's affect on phospho-cofilin. Further studies are clearly warranted.

Concluding Remarks

The recent studies on RNAi have taken the research world by storm. The ability to quickly and easily create loss-of-function phenotypes has researchers rushing to learn as much as they can about RNAi and the characteristics of effective siRNAs. In the future, RNAi may even hold promise for development of gene-specific therapeutics. This section has outlined the investigation of endogenous depletion of pVHL from cultured tumour cells using RNA interference, and the physiological impact this may have. pVHL was observed to be maximally knocked down after 5 hours, and that this was sustained for up to 96+ hours. HIF activation was not up-regulated following pVHL knockdown. This could represent the inefficiency of pVHL RNAi, or the fact that residual amounts of pVHL are sufficient to target Hif α for degradation. As no VHL RNAi has to date been published, one could speculate however, that this scenario may be more complicated. Perhaps alternative mechanisms are initiated upon pVHL depletion that control HIF and identification of this mechanism(s) could prove important in explaining the discrepancy between the highly vascularised tumours associated with VHL disease, and the lack of placental vasculogenesis that result in embryonic lethality in VHL^{-/-} mice. Finally, as a collaborative undertaking, VHL RNAi confirmed the observation that down-regulation of pVHL results in a concomitant up-regulation in phosphorylated cofilin. Given the role of cofilin in cell shape changes and movement, deciphering the mechanism of this interaction may prove important in understanding the highly invasive and metastatic properties of RCC cells where VHL is found inactivated.

CHAPTER 8

Discussion and Future Perspectives

This chapter is divided into two sections. The first section outlines a peer review currently in press in *Trends in Molecular Medicine*, entitled; The von Hippel Lindau Tumour Suppressor; a multi-faceted inhibitor of tumourigenesis. This review was based on the work detailed in chapters 1-5 and serves as a critical synopsis of these chapters. It attempts to review our current understanding of VHL in tumour growth and progression.

The second part of this chapter aims at briefly summarising the work outlined in chapter 7 submitted as partial fulfilment of this doctoral thesis. Emphasis is given to how this work will be continued and the potential impact it might have on VHL biology.

Discussion – Part I

The von Hippel Lindau tumour suppressor: A multi-faceted inhibitor of tumourigenesis

Robert E. Barry and Wilhelm Krek¹

Institute of Cell Biology

ETH Hönggerberg

CH-8093 Zurich

Switzerland

¹ Corresponding author:

Wilhelm Krek

Tel: + 41 1 633 3447

Fax: + 41 1 633 1357

Email: wilhelm.krek@cell.biol.ethz.ch

Abstract

Proteolytic degradation of hypoxia inducible factor (HIF) α by the von Hippel-Lindau (VHL) tumour suppressor protein, pVHL, has emerged as a key cellular mechanism in the control of adaptive gene expression programmes in response to changes in oxygen levels. Inactivation of this mechanism is phenotypically depicted by the vascular nature of VHL-associated tumours and has also recently been associated with the processes of invasion and metastasis. However, the complex genotype-phenotype correlations, which are a hallmark of VHL disease, demonstrate that the function of pVHL is likely to extend beyond its critical role in oxygen signal transduction and may include roles of pVHL in the regulation of microtubule dynamics, cell polarity and directed cell migration. Studies aimed at defining the normal function of VHL in these processes will help identify molecular mechanisms underlying pVHL-associated tumorigenesis.

VHL disease

The identification of genes that cause rare familial cancer syndromes has yielded fundamental insights into the mechanisms of tumourigenesis that underlie sporadic cancers. This concept applies very well to VHL disease, an autosomal dominantly inherited familial cancer syndrome that affects between 1 in 36,000-45,500 live births [10, 400]. In accordance with Knudson’s two-hit tumour suppressor model, tumours from VHL patients with a germ-line *VHL* mutation display somatic inactivation of the remaining wild-type allele [129]. VHL disease is characterised by a diverse, but defined, array of tumours (summarised in Table 1 and Figure 1). Patients are classed into two general types depending on the risk of developing pheochromocytoma. Type 1 patients do not develop pheochromocytoma whereas type 2 patients do. Type 2 is further sub-divided based on the development or absence of haemangioblastoma and renal cell

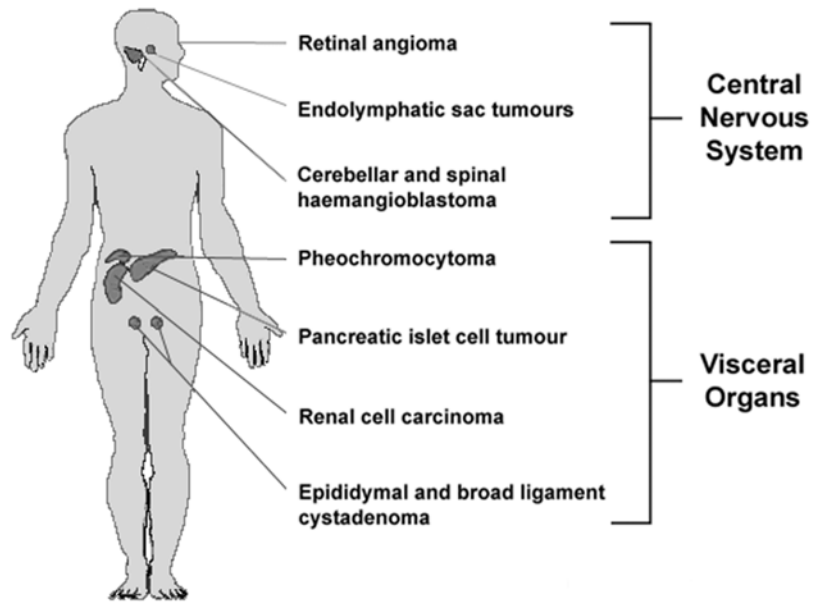


Figure 1. Tumours associated with von Hippel-Lindau disease.

Table 1. Tumour frequency and age of onset

	Frequency (Average)	Age of onset (range)
Central Nervous System		
Craniospinal haemangioblastoma	69%	29 (9-78)
Endolymphatic sac tumours	10%	22 (12-50)
Retinal angioma	47%	25 (1-67)
Visceral organs		
Pheochromocytoma	13%	30 (5-58)
Pancreatic islet cell tumours	42%	36 (5-70)
Renal cell carcinoma	30%	39 (16-67)
Epididymal cystadenoma	42%	Unknown
Broad ligament cystadenoma	Unknown	Unknown

Adapted from references Lonser et al 2003; Maddock et al 1993; Maher et al 1990; Ricjards 1998

Table 2. Clinical sub-divisions in VHL disease

Class	Tumour types observed in families		
	Haem.	RCC	Phaeochr.
Type 1	+	+	–
Type 2A	+	–	+
Type 2B	+	+	+
Type 2C	–	–	+

Haem. – Haemangioblastoma; RCC – Renal cell carcinoma; Phaeochr. - Pheochromocytoma

carcinoma (RCC) (Table 2).

Germ-line mutations are found in up to 100% of families fulfilling the clinical VHL criteria [31, 34, 43].

Mis-sense, non-sense, splice site mutations, and micro-deletions and insertions, are detected in approximately two-thirds of patients

[34, 35, 133] while in the remaining one-third of VHL families, large deletions (4-380 kb) are found. Box

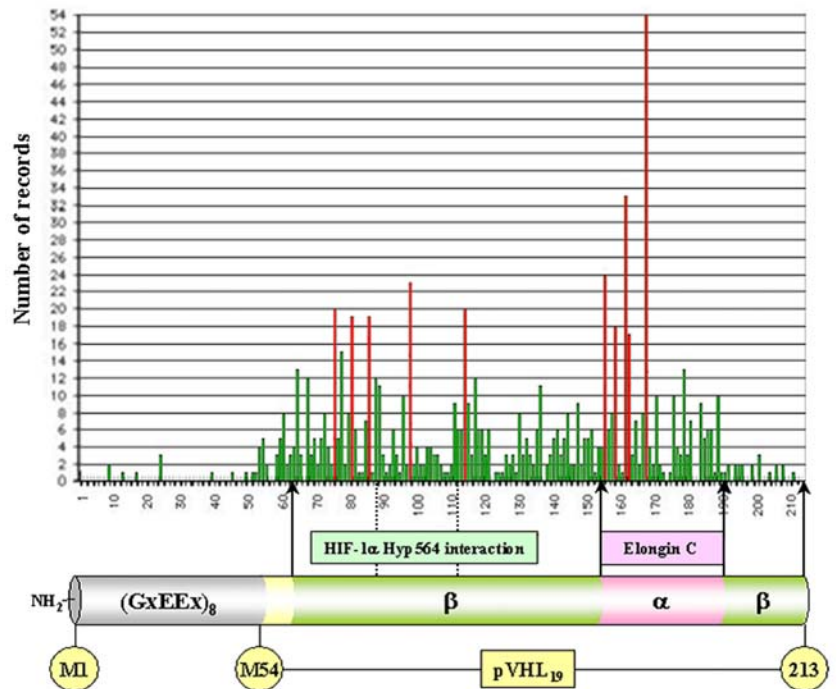
1 outlines the ten most frequently occurring *VHL* mutations and highlights the functional significance

of these residues. Box 1 outlines the ten most frequently occurring *VHL* mutations and highlights the

functional significance of these residues. Interestingly, the pattern of mutations present in familial VHL

disease correlates with clinical sub-classification in terms of predisposition to tumour type. In

general, mis-sense mutations are associated with the development of



Box 1. 10 Most frequently mutated residues

Residue	Records	Function
R167	54	Packing of α -helices
R161	33	Elongin C binding
V155	24	Elongin C binding
Y98	23	Hyp564 binding
G114	20	HIF binding?
F76	20	HIF binding?
P86	19	HIF binding?
P81	19	HIF binding?
L158	18	Elongin C binding
C162	17	Elongin C binding

Figure 2. Distribution of VHL-mutations are concentrated in the HIF α and Elongin C binding domains.

Red bars highlight the ten most frequent mutations as outlined in box 2. Below is the VHL protein structure illustrating the acidic N-terminal region and internal methionine at position 54 which gives rise to the second protein product, pVHL₁₉. pVHL is divided into an α - and β -domain. The α -domain is responsible for binding elongin C, and consists of 3 α -helices. The β -domain is defined as the substrate recognition domain of pVHL and consists of a β -sandwich located between residues 63-154, and an α -helix between residues 193-204. Noteworthy, residues 88-111 constitutes the pVHL- Hyp564 interacting interface which harbours the frequently mutated residue Y98, the ‘black forest’ founder mutation. Some 823 germ-line and somatic mutations have been collected so far (www.umd.be) [2, 8, 9].

Box 2. Examples of germ-line VHL-mutations and disease class correlations

Mutation	Cases	Class
Y98H	21	Type 2A
Y112H	4	Type 2A
Y112N	1	Type 2B
F119L	5	Type 2B
R167W	21	Type 2B
F119S	1	Type 2C
L188V	5	Type 2C
V84L	1	Type 2C

- Type 1 disease is associated generally with deletions and truncations which include both frameshift and nonsense mutations.

type 2 disease, whereas gross deletions or mutations that lead to truncated versions of pVHL are primarily associated with the development of type 1 disease. Moreover, as outlined in box 2, specific point mutations in *VHL* predispose to distinct clinical sub-classifications of disease. For example, Y98H predisposes to type 2A disease while R167W gives rise to type 2B [2]. Thus, the type of germ-line mutation strongly determines the clinical manifestation of VHL disease, suggesting that VHL may have multiple and tissue-specific tumour suppressor functions.

Importantly, sporadic forms of the same tumour types that are common in familial VHL disease display bi-allelic somatic inactivation of the *VHL* gene through a variety of mechanisms including mutation, deletion and hypermethylation [144]; [124]; [123]; [125]; [122]; [126]; [95]. For example, inactivation of *VHL* has been demonstrated in 70-80% of all sporadic clear cell RCC, the major form of RCC, which accounts for approximately 2% of all cancer deaths worldwide [51]. In addition, almost half the number of patients diagnosed with RCC have

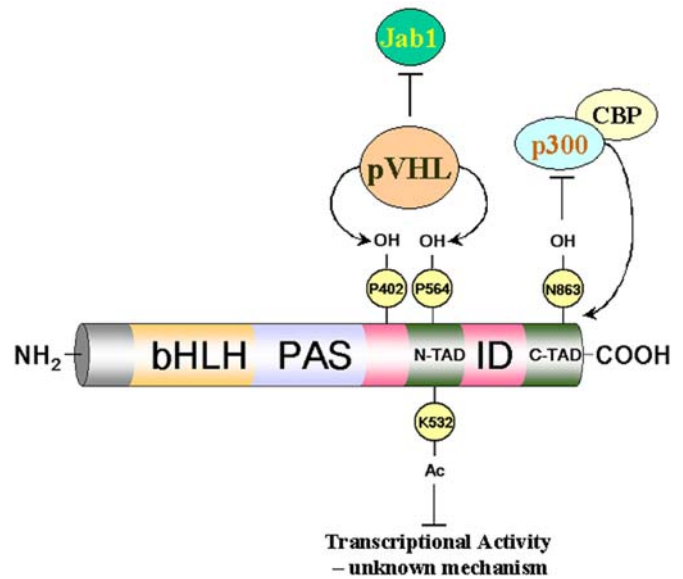


Figure 3. pHIF-1 α domains and regulation through post-translational modification. Ac – acetylation; N/C-TAD – transactivation domains; ID – inhibitory domain containing the oxygen dependent domain (ODD) which harbours both VHL binding prolines; bHLH – basic helix-loop-helix domain; PAS – Per/Amt/sim

Box 3. HIF control by post-translational modification

Hydroxylation at two proline residues mediates interactions with the β -domain of pVHL [7, 8]. Each site can interact independently with pVHL, potentially contributing to the extremely rapid proteolysis of HIF- α that is observed under normoxic conditions. These sites contain a conserved LxxLAP motif and are targeted by proline hydroxylases that in mammalian cells are provided by three isoforms termed PHD 1–3 [11–13]. In a second hydroxylation-dependent control, β -hydroxylation of an asparaginyl residue in the C-terminal activation domain of HIF- α , Asn803 in human HIF-1 α , is regulated by a HIF asparaginyl hydroxylase called FIH (factor inhibiting HIF) [17]; [19]. Hydroxylation at this site prevents binding of the transcriptional co-activators p300/CBP. Under normoxic conditions, these hydroxylation reactions provide a dual mechanism of HIF inactivation that involves proteolytic destruction and inhibition of transcriptional activity [20]. These hydroxylases are all Fe(II)- and 2-oxoglutarate-dependent dioxygenases that require molecular oxygen. HIF α therefore becomes stabilised under hypoxic conditions where oxygen availability is low. Furthermore, an acetyltransferase, ARD1, acetylates Lys532, a residue previously shown to effect HIF α stability, thereby negatively regulating it [23]; [27]. Jab1, a transcriptional co-activator, has been shown to positively regulate HIF α [28].

metastatic disease on presentation. Metastatic RCC has an extremely poor prognosis, with a median survival of less than 1 year. Therefore, the need to understand how pVHL normally effects its tumour suppressor activity is essential if we are to appreciate the pathological consequence of its mutational deregulation and subsequent role in tumourigenesis. This review details the advances that have been made in this regard, and addresses questions that remain to be answered.

Functional analysis of pVHL

The VHL gene located on chromosome 3p25-p26 [80, 147] encodes a single 4.7 kb mRNA which gives rise to two protein products; a polypeptide of 213 amino acids (pVHL₃₀) and, resulting from internal initiation of translation, a second polypeptide of 180 amino acids (pVHL₁₉) [102, 120]. VHL mRNA and protein are ubiquitously expressed [94] [95] [90] [3], implying that tissue-specific expression cannot account for the complex tumour pattern observed in VHL disease. pVHL₃₀ is distinguished from pVHL₁₉ by the presence of eight acidic N-terminal pentameric amino acid repeats. Both protein products are detected *in vivo*. While the functional distinction between pVHL₃₀ and pVHL₁₉ remains elusive to date, they have been shown to exhibit different sub-cellular localisations in that pVHL₁₉ is predominantly nuclear, while pVHL₃₀ localises to both nuclear and cytoplasmic compartments, and when cytoplasmic, can associate with the microtubule network [107]. This implies that functional differences may exist. Noteworthy, all known inactivating mutations reside within a region of the VHL gene common to both protein products, arguing that the development of VHL tumours may require simultaneous inactivation of both pVHL₃₀- and pVHL₁₉-associated functions. *VHL* knockout studies in mice revealed an essential role for pVHL in development [261]. Homozygous *VHL*^{-/-} embryos die between E10.5 to E12.5 due to lack of placental vasculogenesis. Furthermore, efforts to develop *in vivo* models of VHL disease have shown that *VHL*^{+/-} heterozygote mice develop blood vessel tumours of the liver [269] and further studies have also confirmed the finding that *VHL* heterozygosity could predispose mice to a vascular phenotype which appears consistent with the ability of pVHL to control the

expression of genes whose products participate in angiogenesis, a critical stage in tumour progression [5, 272].

The most established function of pVHL to date has been as a substrate recognition component of an E3 ubiquitin protein ligase complex comprising pVHL, Elongin C, Elongin B, Cullin 2 and the RING finger protein, Rbx1, referred to as the VCB-Cul2 complex [184, 185]. In this setting, pVHL targets the α -subunits of HIF for ubiquitin-mediated proteolysis under normal oxygen conditions [114]. This suppresses a transcription programme normally engaged by HIF as part of the cell's adaptive response to low oxygen (hypoxia) such as the activation of vascular endothelial growth factor (VEGF), a potent angiogenic factor [401] [20]. The stabilisation of HIF in response to hypoxia involves the inactivation of prolylhydroxylases that modify HIF at specific proline residues in an oxygen-dependent manner. Proline hydroxylation marks HIF for degradation by the VCB-Cul2 E3 ligase complex (Figure 3; Box 3). Noteworthy, naturally occurring mutations cluster in hotspots and predominantly affect elongin C and HIF- α interface regions of pVHL (see Figure 3) [109]; [2].

While biochemical and genetic evidence clearly demonstrate that pVHL regulates HIF α degradation to mediate normal cellular responses to changing oxygen concentration, it remains unclear whether deregulation of HIF α has a causal role for tumour formation when *VHL* is mutated. Studies investigating the tumour growth of RCC cell lines in nude mouse models support the idea of HIF-dependent tumour suppressor activities of pVHL. Inhibition of HIF-2 α expression by siRNA inhibits growth of VHL negative tumours [278], while re-introduction of a degradation-resistant mutant of HIF-2 α abolishes the ability of VHL to suppress growth of these cell lines [279]. While these studies display the importance of HIF-2 α in the growth of established tumour cell lines *in vivo*, they do not demonstrate that deregulation of HIF degradation is sufficient to induce *de novo* tumour formation. Importantly, VHL ablation in mouse embryonic stem cells

results in smaller tumour formation than controls, in spite of displaying maximal HIF activity [280]. This observation suggests that loss of VHL may actually cause a growth disadvantage in an otherwise normal genetic background and implies that malignancies associated with inactivation of the VHL tumour suppressor may manifest only in the background of other genetic alterations, and are perhaps not solely attributable to loss of VHL. Therefore, in this setting, HIF activity alone is not capable of driving tumour progression. Furthermore, as already mentioned, while re-introduction of VHL into RCC cells eliminated tumour growth, these cells are known to harbour alternative genetic abnormalities [121, 263, 281]. Defining molecular mechanisms with respect to VHL alone in an already effected background is therefore difficult and requires caution.

Moreover, several lines of evidence suggest that VHL has HIF-independent tumour suppressor functions, namely, a subclass of *VHL* mutations that retain the ability to induce HIF α degradation still predispose to pheochromocytoma-only (type 2C) VHL disease. These findings raise interesting questions as to whether VHL-related tumours are a consequence of aberrant VHL control of HIF α or rather a means of promoting growth advantage within a given genetic background.

VHL as a multi-faceted tumour suppressor

Development of malignancy requires that tumour cells undergo biological changes allowing them to proliferate, escape apoptosis, form new blood supplies, invade surrounding tissue and metastasise to distant sites. Recent evidence now suggest that VHL loss-of-function results in the deregulation of a number of signalling pathways that play key roles in one or more of the above-noted biological processes.

A number of polypeptide growth factors that stimulate proliferation of normal cells have pathological consequences in tumourigenesis when deregulated. RCC cells lacking functional

pVHL over-express various growth factors including PDGF β , VEGF and transforming growth factor (TGF)- α . The latter is a bona fide renal cell mitogen that activates the Ras-Raf-MAP kinase signalling cascade through its cognate EGF cell-surface receptor [301]. Overproduction of TGF- α in RCC cells, at least in part, is HIF-dependent and a major contributory event that confers growth advantage to these cells [302, 303]. Indeed, transgenic expression of TGF- α in mice leads to the formation of multiple renal cysts reminiscent of pre-neoplastic lesions of the human kidney [33, 304, 305]. These findings highlight a direct link between pVHL loss-of-function, activation of HIF and the ensuing deregulated production of a potent growth factor of renal epithelial cells.

Several studies have associated loss of VHL function to decreased susceptibility of cells to undergo apoptosis and promote cell survival [200, 236, 306, 307]. Interestingly, while the molecular pathway(s) is unclear, tumour necrosis factor (TNF)- α has been shown to promote HIF-1 α accumulation and this may involve a VHL-dependent step [308-311]. TNF- α , a pro-inflammatory cytokine, is an endogenous mediator of inflammation and apoptotic cell death [312]. Jung et al. recently investigated TNF- α -induced HIF-1 α accumulation and demonstrated that an NF κ B-mediated event normally associated with inflammation and cell survival, caused protein accumulation in normoxic cells [313]. While the report fails to identify the mechanism of HIF-1 α accumulation, it is suggested that this might interfere with the pVHL-mediated HIF-1 α degradation process. Further studies support the concept of a pVHL-dependent cytotoxicity in RCC cells to TNF- α [314, 315]. In particular it has been reported that RCC cells can be sensitised to TNF- α induced cytotoxicity by re-introducing wild-type VHL [315]. Interestingly, the authors highlight the fact that TNF-receptor engagement by TNF- α triggers the activation of atypical PKC (aPKC), which, through phosphorylation of IKK β phosphorylation, liberates NF κ B thereby initiating transcription of genes involved in apoptosis. pVHL has been shown to directly bind various aPKC isoforms and to target aPKC λ for ubiquitin-mediated degradation [245, 316].

Deregulation of this process may therefore have significant impact on NF κ B transcriptional activity, and ultimately represents a means of promoting a selective pressure for populations of cells lacking functional pVHL to survive under adverse environmental conditions.

pVHL has also been implicated in tumour invasion and metastasis, which represent complex multi-step processes requiring the proteolytic degradation of the basement membrane and tissue matrix, changes in cell polarity and motility, and the attachment and detachment of cells to extracellular matrix (ECM) [283]; [284]. pVHL-dependent remodelling of the ECM can be inferred by its link to fibronectin [318]. Fibronectin has the ability to decrease the metastatic behaviour of malignant cells by increasing the interaction between tumour cells and their micro-environment via the integrin receptor family [319]. Several reports have demonstrated that inactivation of pVHL tumour suppressor function is linked to abnormal extra-cellular fibronectin arrays in RCC cells lacking functional pVHL and in *VHL*^{-/-} mouse fibroblasts [134]; [320]; [250]; [402]. However, the exact nature of such an association and the mechanism by which VHL regulates the assembly of this ECM remain poorly understood. Nevertheless, the restored ability of pVHL-positive transfectants to assemble extracellular fibronectin was shown to be mediated by β 1 integrins implying that pVHL controls ECM assembly, at least in part, via integrin signalling [250]. A recent development has demonstrated that an ubiquitin-like molecule, NEDD8, covalently modifies pVHL, and that a non-neddylatable pVHL mutant, while retaining its ability to degrade HIF, fails to promote the assembly of a fibronectin matrix. Furthermore, expression of the neddylation defective pVHL in RCC cells, while restoring the regulation of HIF, was insufficient to suppress the formation of tumours in nude mice models. These results suggest an important role for NEDD8 modification of pVHL in the assembly of a fibronectin matrix, and that in this context HIF control is not sufficient to prevent VHL-associated tumourigenesis.

Emerging evidence indicates an inhibitory role for pVHL in the regulation of components that have been implicated in establishing/maintaining cell polarity and directed cell migration, in

particular protein kinase C (PKC) isoforms. Regulation of insulin growth factor (IGF)-I-mediated cell invasion of RCC cells appears to be dependent upon PKC δ inhibition by pVHL. This inhibition is mediated through protein-protein interaction involving a domain of pVHL which shows similarity to protein kinase inhibitor (PKI), a natural inhibitor of cAMP-dependent protein kinase (PKA) [322]. In contrast to protein-binding inhibition, evidence has shown that pVHL binds both atypical PKC isoforms λ and ζ through its β -domain, and in the case of activated aPKC λ , mediates its turnover as part of pVHL's function as an E3 ligase [245, 316]. While the functional significance of this inhibition remains elusive, given the central role for atypical PKC's, namely aPKC ζ , in establishing cell polarity in conjunction with PAR6 and the GTPase CDC42 [323], one could envisage a scenario whereby loss of pVHL leads to altered cell polarity, and by extension, aberrant cell migration.

Consistent with this above-noted view, pVHL₃₀ has been shown to co-localise with the microtubule network *in vivo* and to promote microtubule stabilisation [107]. Since microtubule dynamics have been intimately linked to the process of directed cell migration [323], this functional association may be an additional element of pVHL's tumour suppressing activity. Indeed, the microtubule stabilising function of pVHL is specifically disrupted by type 2A disease mutants that predispose to a defined tumour spectrum of haemangioblastoma and pheochromocytoma with a low predisposition to develop RCC. It is certainly tempting to draw parallels between the tumour suppressor pathways regulated by pVHL and that by the adenomatous polyposis tumour suppressor (APC) gene product, whose inactivation is the most frequently observed in hereditary and sporadic colon cancers [324]. Analogous to VHL, APC also binds to microtubules [323], and it has been shown that for APC this association culminates in cytoskeletal rearrangements and changes in cell polarity upon activation of the CDC42-PAR6-aPKC ζ pathway. Studies aimed at pVHL's role with respect to cell polarity and directed cell migration are therefore clearly warranted.

Recently, important mediators of cell invasion and metastasis were shown to be regulated by the pVHL tumour suppressor and these include hepatocyte growth factor (HGF) acting through the Met tyrosine kinase receptor and the chemokine receptor CXCR4, implicated in organ-specific metastasis [136, 321]. Koochekpour et al. examined the HGF responsiveness of VHL-negative RCC cells and found that certain VHL-negative RCC cells were highly invasive and exhibited an extensive branching morphogenesis phenotype in response to HGF when compared to their wt-VHL expressing isogenic counterparts [136]. This same study demonstrated that VHL loss-of-function negatively regulates tissue inhibitor of metalloproteinase 2 (TIMP-2), resulting in the up-regulation of matrix metalloproteinases 2 and 9 (MMP2/9), thereby implicating pVHL in the control of these molecules. Matrix metalloproteinases (MMPs) are responsible for the degradation of ECM and have been associated with cellular invasiveness [330]. Importantly, it has been recently shown that hypoxia promotes tumour cell invasion by inducing the expression of the Met receptor [331]. This establishes a mechanism whereby transformed cells can be spurred to exit a hypoxic microenvironment and invade surrounding tissues, which provide more favourable growth conditions. Given the fact that HIF-1 α has been shown to be involved in Met gene expression, constitutive HIF-1 α activation as a consequence of pVHL deregulation provides a mechanism explaining the observation that expression of HGF and Met receptor is associated with genetic alterations of VHL in primary RCC. Hypoxic cell-sensitisation to HGF has therefore been proposed as an ‘invasive switch’ which facilitates cell movement away from an area of low oxygen availability, and is dependent on pVHL’s ability to degrade HIF α .

The gene encoding the chemokine receptor CXCR4 has been discovered as a novel HIF target based on microarray comparison of genetic profiles derived from VHL null RCC cells and their isogenic wild type VHL-expressing counterparts [321]. CXCR4 has been previously implicated in directing malignant breast cancer cells to specific target organs, thereby fulfilling

the chemoattraction theory of tumour metastasis [6] [332]. Interestingly, CXCR4 is highly expressed in malignant breast cancer cells but not in normal breast epithelial cells [6]. The fact that *CXCR4* is a hypoxia-inducible gene provided a potential mechanistic explanation for CXCR4 up-regulation during tumour cell evolution. CXCR4-induced surface expression due to VHL loss-of-function confers enhanced migratory potential to RCC cells in response to its cognate ligand stromal-derived factor 1 (SDF1). In addition, CXCR4 might be needed to promote the survival of tumour cells in a hypoxic environment. Thus, the ability of a cell to generate genetic programmes capable of evading unfavourable growth conditions is reflected at least in part by the up-regulation of CXCR4 in response to a hypoxic microenvironment. However, unlike the Met receptor, and perhaps other hypoxic responsive factors that promote cell motility and invasion, CXCR4, due to its chemotactic responsiveness to SDF1, might confer not only a migratory potential but also the possibility of targeting migrating cells to specific secondary sites. Interestingly, strong CXCR4 expression can be correlated to poor tumour-specific survival in clear cell RCC, reflecting the metastatic potential of these tumours. This further implies that CXCR4 expression levels may influence the metastatic behaviour of these cells. The question remains however, whether CXCR4 up-regulation is a result of a cell's ability to metastasise, or whether this up-regulation itself primes the cell to metastasise. What ever this may represent, a cell's ability to migrate to specific target sites may therefore be determined, in part, by loss of VHL, suggesting that these cells may be primed from an early stage to spread to other sites in the body. CXCR4 could represent a novel target site for therapeutic intervention in the prevention of cancer metastasis, the major cause of death in RCC patients and of many other solid tumours.

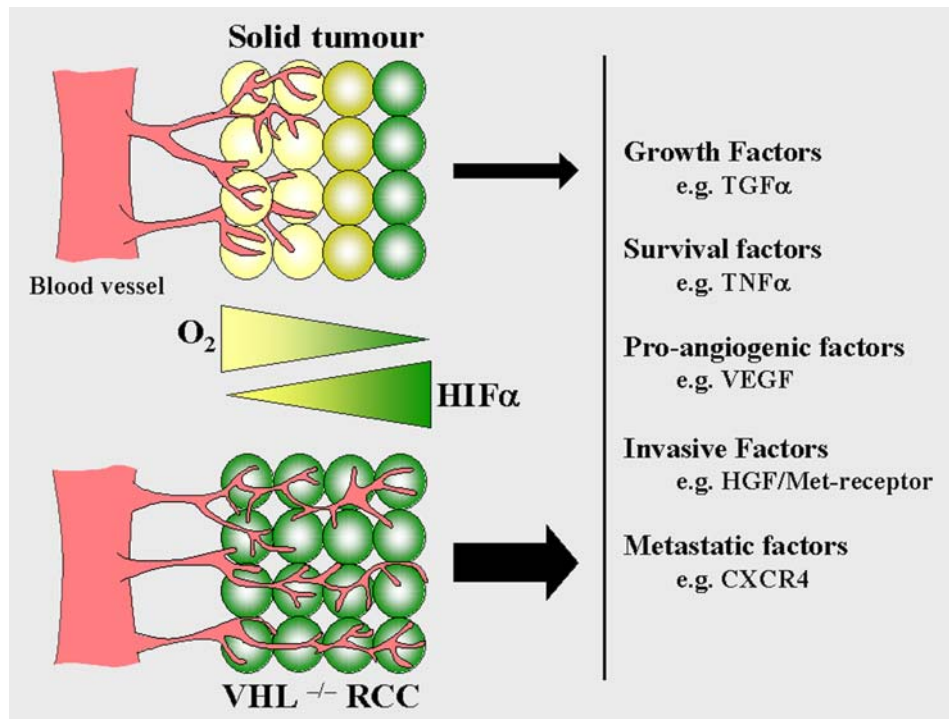


Figure 4. The role of HIF in conferring tumour growth potential. In solid tumours, HIF α is stabilised under conditions of low oxygen due to lack of vascularisation and the subsequent evolution of a hypoxic microenvironment. In a VHL null tumour, HIF α is constitutively active, and can initiate genetic programmes within the entire population of cells that would normally be activated only under hypoxic conditions. Inappropriate up-regulation of genes is, in the case of VHL null tumours, independent of oxygen status. This may help explain, in part, why VHL^{-/-} RCC exhibits an aggressive phenotype.

Concluding Remarks

Research to date shows that pVHL functions in the correct orchestration of cell proliferation, survival and angiogenesis through the control of the HIF pathway. However, VHL has also been linked to the regulation of cell polarity and directed cell migration in part through its association with aPKC and the microtubule network. Finally, intimate mechanistic linkages have been established between loss-of-function of pVHL and the processes of invasion and metastasis. Thus, a deeper appreciation of the many aspects of VHL biology and their deregulation within a pathological setting will help us to understand the molecular details pertaining to these pathways and key processes of the cancer phenotype.

Part II

Discussion and Future Perspectives

The identification of novel pVHL interactions helps us to understand the physiological role of pVHL and allows us to propose models of how inappropriate pVHL function can result in a pathological consequence. Part I of chapter 7 outlined a novel approach for identifying pVHL interactions. By immuno-precipitating endogenous pVHL on a large scale, followed by proteomic identification of co-precipitating proteins, new pVHL interactions have been isolated. This section briefly discusses the proteins found in this proteomics approach, the results obtained to date, and future perspectives concerning these interactions.

8.1 p97 in HIF regulation

The finding that pVHL interacts with a member of the AAA ATPase family, p97, has highlighted the importance of energy dependency in pVHL mediated events. This is not the first evidence that an ATPase can bind an E3 ubiquitin ligase. In yeast, it has recently been shown that UBR1 and UFD4, two E3 ubiquitin ligases of *Saccharomyces Cerevisiae*, interact with RPT4 and RPT6, two ATPases of the 19S proteasome [403]. The data presented in this thesis provide evidence for an endogenous interaction between a component of an E3 ubiquitin ligase, pVHL, and an ATPase, which can associate with the 26S proteasome in mammalian cells *in vivo*, p97. Interestingly, during the course of this work, another already mentioned study emerged demonstrating the interaction of an ATPase with a component of an E3 ubiquitin ligase, namely Tat-binding protein-1 with pVHL. This study has demonstrated the importance of an energy dependent chaperone activity that facilitates Hif-1 α presentation to the proteasome and subsequent proteolytic degradation. This study supports a concept whereby p97, an ATPase of the same family as TBP-1, may participate in a similar process to ensure efficient Hif- α degradation in normoxic cells.

Although reduction in p97 expression using siRNA did not result in detectable levels of Hif-1 α , there are three possible explanations for this. First, despite the efficacy of the p97 siRNA, it was only possible to achieve a partial knockdown of p97 expression. This is probably due to variable transfection efficiencies for the RNAi oligo in different cell lines or the partial efficiency of siRNA to completely inhibit p97 expression. Therefore, in

assays for Hif-1 α degradation in cells treated with p97 siRNA, there was always some residual p97 present in the cell. The presence of even low levels of endogenous wild-type p97 might also explain why over-expression of p97^{QQ}, an ATPase mutant p97, did not result in elevated levels of Hif-1 α in normoxia. Therefore, it is predicted that a cell line with a complete knockout of p97 (as with a somatic knockout or embryonic stem cell knockout) might show higher normoxic levels of Hif-1 α than observed with cells having only a partial knockout of p97 using siRNA. Second, other proteins besides p97 might regulate the pVHL-mediated degradation of Hif-1 α . Certainly the presence or absence of pVHL is the most important factor for clearing Hif-1 α , as p97 does not promote Hif1 α degradation in pVHL-deficient cells. The possibility of additional chaperones implies that even with a complete loss of p97, pVHL might still be able to degrade Hif1 α , albeit less efficiently. Certainly in light of the finding that TBP-1 facilitates Hif-1 α degradation, it seems that there may be various energy-dependent chaperone-like proteins with similar functions. The third reason, and something under active investigation, is that unlike TBP-1, p97 functions seem to be dictated according to the adaptor protein(s) that it complexes with. We have already discussed in chapter 7 that p47 directs p97 to act in the post-mitotic fusion of Golgi membranes. Furthermore other accessory components, namely a complex of Ufd1-Npl4, have been shown to direct p97 to function in the retrotranslocation pathway. In yeast, the Cdc48-Ufd1-Npl4 complex has been shown to move poly-ubiquitinated polypeptides from the ER membrane into the cytosol for their subsequent degradation by the proteasome. Given the fact that adaptor proteins direct p97 function, it seems logical that targeting these proteins by RNAi may render more telling results than p97 itself because p97 is so abundant, representing some 1% of the total cytosol making efficient depletion by RNAi difficult. Further experimentation is required to investigate the role of Ufd1 and Npl4 in the process of Hif- α degradation, and current work involves the targeting of both of these adapter proteins by siRNA in an attempt to up-regulate Hif- α in normoxic cells.

It remains to be seen upon re-oxygenation after hypoxic stress, whether the pVHL-p97 interaction can be enhanced, and also whether other ligase components co-precipitate with p97. This would further support a role for p97 involvement in Hif- α degradation. It would also be very interesting to reinvestigate the kinetics of p97 degradation following endogenous depletion of Ufd1 and/or Npl4. Evidence that these proteins might interfere with Hif- α degradation would further implicate p97 in Hif- α regulation. Taken together, it seems plausible that aberrations in the pVHL-p97 interaction may provide a novel mechanism for Hif-1 α stabilisation in some pVHL-deficient tumours and further define a role for derangements of proteasome function in human cancer. A simplified model of the involvement of p97 in Hif α degradation is schematically depicted in figure 90.

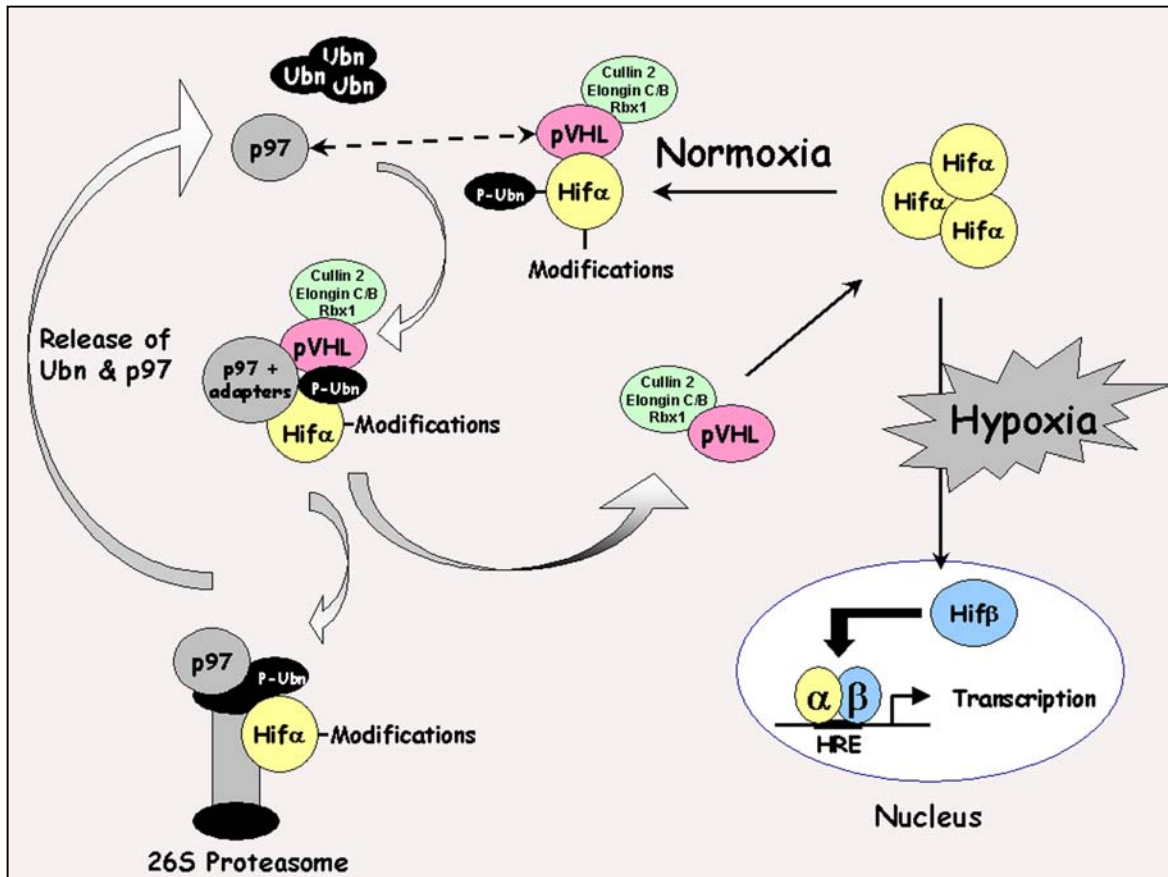


Figure 90. Proposed model for p97 involvement in pVHL-mediated Hif α proteolytic degradation. Endogenous p97 interacts with pVHL and ubiquitin, and this interaction may facilitate a p97 interaction with ubiquitinated and modified Hif α . In a fashion analogous to TBP-1, an energy dependent step might allow p97 to chaperone Hif α to the proteasome where it is subsequently degraded. Unlike TBP-1 however, adapter proteins may facilitate p97 recognition of modified and ubiquitinated Hif α . Identification of these species would prove important.

8.2 p97 and the malformed protein response

p97 has also been shown to be involved in retrotranslocation of proteins from the ER. Newly synthesised proteins in the ER of eukaryotic cells are subject to rigorous quality control, which consists of a sophisticated protein proofreading and elimination mechanism. When misfolded or improperly assembled proteins emerge in the lumen of the ER, they are exported back to the cytosolic side of the ER (an event called retrotranslocation), conjugated with poly-ubiquitin and subsequently degraded by the 26S proteasome (Fig.91). This process, named ERAD (ER-associated degradation), is capable of destroying both

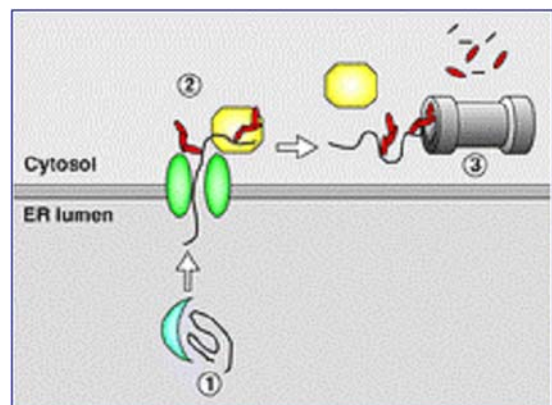


Figure 91. p97 involvement in ER associated degradation (ERAD). A misfolded polypeptide is poly-ubiquitinated and retrotranslocated to the cytosolic side of the ER where it is recognised by p97 (yellow). This interaction then facilitates the poly-ubiquitinated (red) misfolded polypeptide to be presented to the proteasome in an ATP-dependent manner for subsequent degradation.

integral membrane proteins and luminal proteins. In the past, a series of efforts have shown that p97 is required in ERAD and acts as a molecular chaperone that extracts the ubiquitinated proteins from the ER membrane before their final degradation by the proteasome [347, 349, 350, 363, 364, 404]. This may, at least in part, explain the accumulation of ubiquitinated proteins when p97 is inactivated [347]. This is interesting for two reasons. Firstly, RCC cells lacking functional pVHL exhibit deposition of misfolded fibronectin resulting in an aberrant fibronectin matrix assembly. This inappropriate deposition is corrected upon reintroduction of wild-type, but not mutant, pVHL [134]. It would seem therefore, at least in the case of fibronectin, pVHL might also be involved in protein proofreading and the misfolded protein response. Secondly, as already mentioned in section 7.4.4.5, pVHL has been shown to bind HDAC6, albeit *in vitro*. HDAC6 has been shown to be a component of the aggresome and exhibits the capacity to bind both poly-ubiquitinated misfolded proteins and dynein motors, thereby acting to recruit misfolded protein cargo to dynein motors for transport to aggresomes [375]. Indeed, cells deficient in HDAC6 fail to clear misfolded protein aggregates from the cytoplasm, cannot form aggresomes properly, and are hypersensitive to the accumulation of misfolded proteins. These findings identify HDAC6 as a crucial player in the cellular management of misfolded protein-induced stress. For these reasons, a role for pVHL, HDAC6 and p97 in the context of controlling protein folding seems plausible and merits further attention. As no yeast VHL homologue exists, it is difficult to investigate as most studies to date regarding retrotranslocation and ERAD have been performed in yeast. Nonetheless, targeted inactivation of p97 and/or HDAC6 in RCC cells with and without re-introduced wild-type VHL could offer some interesting insights. For example, it would be interesting to see whether the restored extracellular fibronectin matrix assembly observed when wild-type VHL is re-introduced in 786-0 cells can be reversed upon inactivation of p97 and/or HDAC6 in these cells by RNAi or introduction of a dominant-negative version of either protein. This would clearly indicate that they are functioning together in a pathway that facilitates deposition of correctly folded fibronectin, and that aberrations in this interaction may account for the incorrect extracellular matrix assembly, a characteristic of cancer cells, and an event which facilitates tumour invasion and metastasis.

8.3 A potential role for pVHL in the critical methylation of tRNA_i^{met}

In addition to p97, the novel proteomics approach to find new pVHL interactions identified a protein complex which demonstrates structural homology to the yeast tRNA (1-methyladenosine) methyltransferase, Gcd10p/Gcd14p. This finding would be the first evidence linking pVHL to RNA methylation activity. The consequence, if any, of this interaction is unclear, though *in vitro* and *in vivo* evidence demonstrate that the complex forms, and that pVHL binds this complex in mammalian cells. In collaboration with another doctoral student, P.Ballschmieter, efforts are currently being made to investigate whether this homologous human complex is capable of exhibiting methyltransferase

activity as has already been shown for Gcd10p/Gcd14p in the critical methylation event at position 58 in the TΨC loop of yeast initiator methionine tRNA. With both components cloned and antibodies raised against them, it is now possible to address the question of whether this mammalian complex can exhibit methyltransferase activity, and whether it is the true mammalian orthologue of Gcd10p/Gcd14p. If this is the case, it will be interesting to investigate the effect that naturally occurring mutants of pVHL might have on this activity. Such functional studies may expose a sub-class of VHL mutants that could be linked to a particular VHL disease type. Efforts are being made to investigate whether other VCB-Cul2 ligase components co-precipitate with the complex, which might indicate whether this potential methyltransferase is targeted by pVHL for proteolytic degradation. However, sequence analysis has revealed no evidence in either protein that might suggest that either could be bound by pVHL in a manner similar to Hif α .

One problem that remains unclear for the yeast Gcd10p/GCD14p is how this complex exercises substrate specificity. All yeast tRNAs where the sequence has been determined contain adenine at position 58, but only 21 of 32 sequenced tRNAs contain m¹A (methyladenosine) at this position [380]. Thus, it is important to determine how the Gcd10p/Gcd14p complex discriminates against the subset of tRNAs that lack m¹A. One suggestion is that Gcd10p specifically binds only those nascent tRNA transcripts destined for m¹A methylation and presents them to Gcd14p for modification. An alternative possibility is that Gcd10p contributes only non-specific RNA binding affinity to the complex and that Gcd14p imposes tRNA-substrate specificity at the step of methyl group transfer. This would be akin to certain aminoacyl-tRNA synthetases that distinguish cognate from noncognate tRNAs primarily at the catalytic step rather than at the tRNA binding step [405]. In mammalian cells however, it is tempting to suggest that substrate specificity might be conferred by pVHL, which through its interaction with the methyltransferase complex, facilitates specific substrate methylation. This is purely speculative, and no evidence exists which suggests that pVHL can exhibit any RNA binding ability, but a theory certainly interesting to test.

Protein kinases that phosphorylate the alpha subunit of eukaryotic initiation factor 2 (eIF2 α) are activated in stressed cells and negatively regulate protein synthesis. Phenotypic analysis of targeted mutations in murine cells reveals a novel role for eIF2 α kinases in regulating gene expression in the malformed protein response and in amino acid starved cells. When activated by their cognate upstream stress signals, the mammalian eIF2 kinases PERK and GCN2 repress translation of most mRNAs but selectively increase translation of Activating Transcription Factor 4 (ATF4), resulting in the induction of the downstream gene CHOP (GADD153) (Fig.92). This is the first example of a mammalian signalling pathway homologous to the well studied yeast general control response in which eIF2 α phosphorylation activates the transcriptional activator *GCN4* whose translation in yeast has been shown to be increased upon amino

acid starvation resulting in transactivation of many genes involved in amino acid biosynthesis. Mammalian cells thus utilise an ancient pathway to regulate gene expression in response to diverse stress signals [406]. Interestingly, Gcd10p and Gcd14p were first identified genetically as repressors of *GCN4* mRNA translation in *S.Cerevisiae*, linking this complex to a general stress control pathway, which seems to be conserved in mammalian cells. [377].

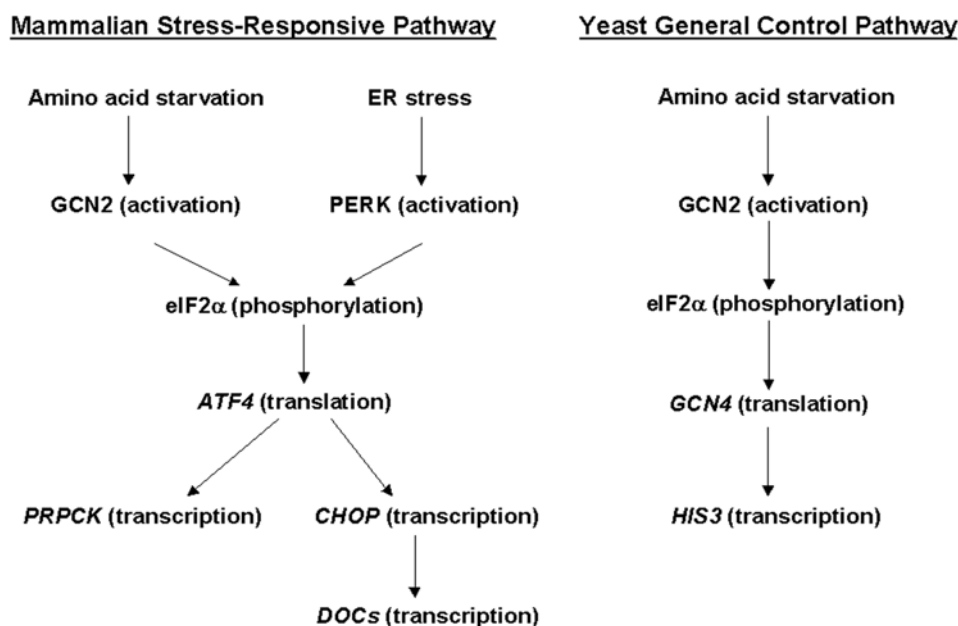


Figure 92. Comparison of genes in the yeast general control response and the homologous mammalian stress response pathway described in the text. The mode by which each gene is regulated is indicated in parenthesis. *PEPCK* refers to gluconeogenic enzyme phosphoenolpyruvate carboxykinase, activated by *ATF4*. *HIS3* is representative of the genes activated by yeast Gcn4p.

Adapted from Harding et al. 2000

Hypoxia profoundly influences tumour development and response to therapy. While progress has been made in identifying individual gene products whose synthesis is altered under hypoxia, little is known about the mechanism by which hypoxia induces a global down-regulation of protein synthesis. A critical step in the regulation of protein synthesis in response to stress is the phosphorylation of translation initiation factor eIF2 α on Ser51, which leads to inhibition of new protein synthesis. Koumenis *et al.* reported that exposure of human diploid fibroblasts and transformed cells to hypoxia led to phosphorylation of eIF2 α , a modification that was readily reversed upon reoxygenation [407]. Expression of a transdominant, nonphosphorylatable mutant allele of eIF2 α attenuated the repression of protein synthesis under hypoxia. The endoplasmic reticulum (ER)-resident eIF2 α kinase PERK was hyperphosphorylated upon hypoxic stress, and overexpression of wild-type PERK increased the levels of hypoxia-induced phosphorylation of eIF2 α . Cells stably expressing a dominant-negative PERK allele and mouse embryonic fibroblasts with a homozygous deletion of PERK exhibited attenuated phosphorylation of eIF2 α and reduced inhibition of protein synthesis in response to

hypoxia. PERK^{-/-} mouse embryo fibroblasts failed to phosphorylate eIF2 α and exhibited lower survival after prolonged exposure to hypoxia than did wild-type fibroblasts. These results indicate that adaptation of cells to hypoxic stress requires activation of PERK and phosphorylation of eIF2 α and suggest that the mechanism of hypoxia-induced translational attenuation may be linked to ER stress and the malformed-protein response.

We have already seen in chapter 7, part II, that stress signals can render pVHL intra-cellular localisation changes. It seems therefore that pVHL sub-cellular localisation can reflect the cellular microenvironment, and that under sub-optimal conditions, or conditions which induce a stress response, pVHL re-localises to the nucleus, an event exemplified by the fact that drug-induced disruption of microtubules causes pVHL₃₀ to accumulate in the nucleus. Interestingly, the Gcd10p/Gcd14p complex has been shown to complex within the nucleus. Also of interest is the fact that the ability of 786-0 cells to exit the cell cycle upon serum deprivation is achieved only when wild type-pVHL is reintroduced into these cells, further supporting a role for pVHL in nutrient signalling [137]. In a manner analogous to Gcd10p/Gcd14p inhibition of *GCN4*, one could envisage a scenario whereby, stress signalling which results in phosphorylation of eIF2 α , could render a nuclear accumulation of pVHL, which in turn would negatively regulate the methyltransferase complex (protein A/B complex) identified by proteomics, thereby relieving the inhibitory effect this complex might have on ATF4, the mammalian *GCN4* counterpart. While the link is of course tenuous, given the fact that pVHL is a central component of oxygen signalling, and that hypoxia results in activation of eIF2 α , it is plausible to suggest a role of pVHL in the context of protein synthesis regulation within the mammalian stress-response pathway, and that this role could be to mediate a critical methyltransferase activity.

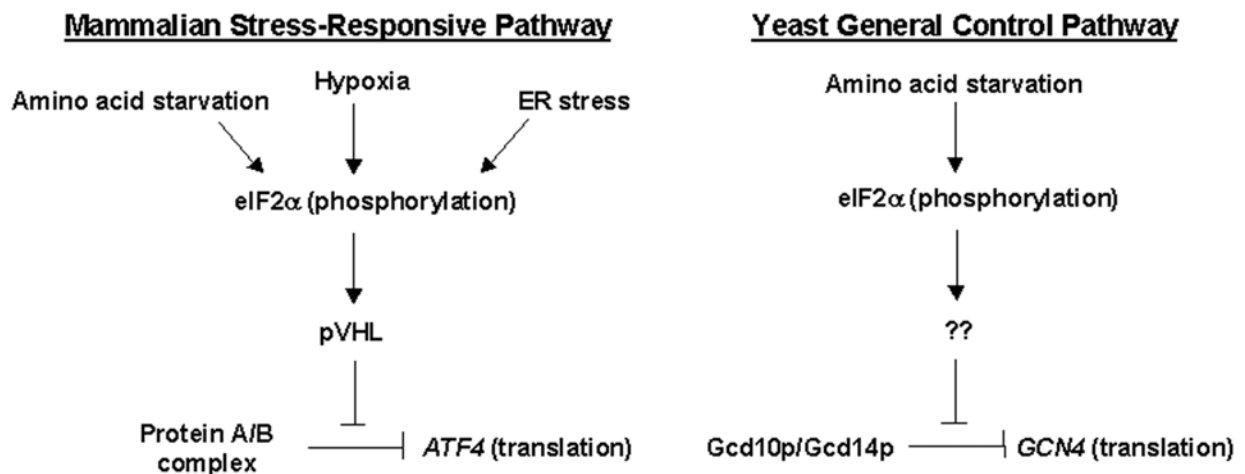


Figure 93. Model proposed regarding the involvement of pVHL and Gcd10p/Gcd14p homologous complex (protein A/B complex) identified in a proteomics approach to identify novel pVHL interacting proteins. As Gcd10p/Gcd14p have been shown to repress *GCN4* in yeast, an analogous situation is proposed for mammalian cells where pVHL functions to positively regulate ATF4 translation by suppressing the protein A/B complex upon appropriate stimuli.

Finally, given the fact that eIF2 has also been implicated in the malformed protein response further implies a functional significance of pVHL involvement in this signalling cascade. Considering the involvement of p97 in retrotranslocation and ERAD, the role of HDAC6 in transport of malformed proteins, and the fact that pVHL is involved in correctly folded fibronectin deposition, one must assume that pVHL's role in the malformed response is somewhat unappreciated. Current research in our laboratory is emerging that might suggest that post-translational modification of pVHL could be involved in regulating fibronectin deposition (Frew and Krek). Given the implications of an aberrant extracellular matrix assembly in tumour growth and progression clearly justifies further studies of pVHL in the malformed protein response, and may be in part be explained by its potential role in the regulation of protein synthesis.

8.4 pVHL intracellular dynamics

Part II of chapter 7 demonstrated work which contributed to published data pertaining to the ability of pVHL₃₀ to protect microtubules from depolymerisation (for further discussion please refer to Hergovich *et al.* 2003 [107]). The experiments demonstrated differential localisation of ectopically expressed GFPVHL₃₀ and GFPVHL₁₉, with GFPVHL₃₀ residing predominantly in the cytoplasm, and GFPVHL₁₉ in the nucleus. This observation was confirmed by endogenous localisation of pVHL₃₀ to the cytoplasm. In addition, it was shown that cytoplasmic pVHL₃₀ can associate with the microtubule network, disruption of which resulted in pVHL₃₀ accumulating in the nucleus. It is believed that this translocation facilitates a more efficient, nuclear targeting of Hif α for proteolytic degradation following an hypoxic insult, or other, alternative signals that induce Hif α accumulation. This hypothesis is supported by literature that emerged during the course of this work [208, 391].

Interestingly, Schraml *et al.* have investigated the relevance of nuclear and cytoplasmic VHL expression in renal carcinoma progression [408]. The authors observed that combined nuclear and cytoplasmic pVHL expression was associated with low histological grade, early tumour stage, and better prognosis, suggesting that the ability of pVHL to localise to both the nucleus and the cytoplasm may have potential relevance for the biological behaviour of clear-cell RCC. This is the first evidence linking VHL shuttling to a pathological consequence if deregulated. Taken together it seems plausible to suggest that pVHL₃₀ localisation reflects its functional activity, and factors affecting the stability of the microtubule cytoskeleton result in intracellular alterations in pVHL₃₀ dynamics which, when deregulated, may result in a pathological phenotype.

8.5 VHL RNA interference

Endogenous depletion of pVHL by RNAi rendered no HIF response, nor were the kinetics of Hif α degradation affected upon VHL siRNA treatment of cells. These results, as discussed in part III of chapter 7, might be explained in two ways. Either residual amounts of pVHL that remain following RNAi treatment are sufficient to regulate Hif α , or that compensatory mechanisms are activated upon pVHL depletion which target Hif α for degradation in the absence of pVHL. Given the importance of HIF control, the latter would not be surprising. Hif α regulation is known to be controlled at many levels (see chapter 4), and while pVHL is considered the principle ligase for Hif α , other means of Hif α regulation may be activated in the absence of pVHL. As mentioned in chapter 7, to date, no VHL RNAi has been published, and peers in the field have communicated similar results regarding Hif α status following VHL RNAi. Furthermore, while published VHL^{-/-} MEFs have been shown to exhibit up-regulated Hif α levels, similar targeting of VHL by CRE-lox recombinase technology in our own laboratory, has not demonstrated any up-regulation in Hif α (Frew and Krek). It would seem therefore that the depletion of pVHL and the consequence this may have on Hif α is more complicated than thought. While VHL^{-/-} tumours are highly vascularised owing, at least in part, to the HIF-induced up-regulation of potent angiogenic factors like VEGF, the discrepancy still remains with the fact that VHL^{-/-} mice die due to a lack of placental vasculogenesis. If VHL RNAi is reflecting a similar situation as that observed for the trophoblast cells in VHL^{-/-} mice, then this may represent a system that could be used to delineate the molecular mechanism underlying this embryonic lethality.

Finally, confirmation of the role of pVHL in the phosphorylation status of cofilin has further implicated pVHL in cofilin-mediated cell shape changes and may help to explain the highly migratory phenotype of VHL^{-/-} RCC cells. Lim kinase-1 (LIMK1) knockout mice have recently been developed in the laboratory (Sayi, Lehembre and Krek). As LIMK is the established kinase demonstrated to phosphorylate cofilin, and also a pVHL binding partner (Lisztwan and Krek, unpublished), these mice will prove important in studying the implication of pVHL in LIMK-cofilin mediated actin cytoskeleton rearrangements.

8.6 Therapeutic intervention in VHL disease

Current surgical techniques aim to reduce morbidity and mortality in VHL patients are limited in their effectiveness, and the generation of specific biological and/or chemical therapies for VHL tumours would be beneficial. This is the reason why understanding the molecular basis of VHL disease is so important. Experimental investigations like those outlined in this thesis, help to identify pathways in which the VHL tumour suppressor is implicated, and ultimately may expose areas of potential therapeutic intervention.

When considering therapeutic intervention in VHL disease, it is important to appreciate that VHL is a multi-functional tumour suppressor, resulting in a vast array of different cellular consequences. Interfering with one aspect of VHL biology, may therefore have more serious repercussions elsewhere. For this reason, it is suggested that therapeutic intervention should be devised to target several aspects involved in VHL disease. Box 20 outlines potential sites of therapeutic intervention, already being targeted in the clinics, or currently under investigation.

Box 21. Sites for therapeutic consideration in VHL disease

Negative regulation by VHL	Examples of Inhibitors	Studies
pHIF α	Histone deacetylase inhibitors Nitric oxide releasing compounds Non-steroidal anti-inflammatory drugs	Kim <i>et al.</i> 2001 Semenza <i>et al.</i> 2001 Jones <i>et al.</i> 2002
Growth factors + Receptors e.g. VEGF	Synthetic antagonists e.g. SU5416	Aiello <i>et al.</i> 2002
Additional receptor molecules - Integrin receptors - Chemokine receptors - Cytokine receptors - IGF1 receptor - aPKC	Receptor signalling blockade e.g. β 1-blocking antibodies e.g. CXCR4-blocking antibodies e.g. EGFR tyrosine kinase inhibitors e.g. antisense IGF-IR oligonucleotides Isoform specific PKC inhibitors e.g. xanthonolignoids	Esteban <i>et al.</i> 2002 Muller <i>et al.</i> 2001[6] Sweeney <i>et al.</i> 2003 Chernicky <i>et al.</i> 2002 Saraiva <i>et al.</i> 2003
Scatter factor signalling	HGF competitor inhibitors	Kuba <i>et al.</i> 2000
Metalloproteinases	IGF-IR kinase inhibitor	Zhang <i>et al.</i> 2003
Positive regulation by VHL	Effector	Studies
Re-introduction of VHL Introduction of VHL peptide	wild-type VHL Residues 104-123	Kamada <i>et al.</i> 2001 Datta <i>et al.</i> 2001

Clinical trials of specific VEGF inhibitors are underway in VHL patients with kidney and CNS tumours, and many other anti-angiogenic drugs are under evaluation in other cancer patients [45, 409, 410]. If effective, these might inhibit the growth of hypervascular VHL tumours. Attempts are also being made to develop gene therapy for treatment of VHL tumours (and sporadic RCC in which pVHL function has been lost), initially using recombinant adenovirus to express the normal VHL gene [411]. Such methods are in their infancy, but there is hope that further advances in understanding the function of the pVHL tumour suppressor will lead ultimately to effective therapies for the prevention or treatment of VHL tumours.

Concluding Remarks

It is clear that inactivation of the *VHL* gene is a key event in the development of tumours in VHL disease and also in the development of a large proportion of sporadic tumours of the same tissue types as those found in this cancer syndrome. Wild-type pVHL has multiple interactions with other cellular proteins and elicits multiple effects on target genes. The major finding to date in VHL biology is the fact that pVHL constitutes an E3 ligase and targets hypoxia inducible factor α for proteolytic degradation. This discovery has led to a molecular mechanism that helps, at least in part, explain the role of pVHL in tumorigenesis. Loss of pVHL leads to increased levels of Hif α under normoxic conditions, resulting in over-expression of hypoxia-inducible genes such as VEGF. This is likely to be one of the key events that results in tumour growth. However, other pVHL functions also are important, most notably the role of pVHL in fibronectin assembly. Therefore, there is still considerable work to do to elucidate clearly the key functions of pVHL that are critical for tumour suppression. For example, little is known about how expression of *VHL* is regulated and experiments are needed to identify the transcription factors that control *VHL* mRNA expression. Similarly, analysis of pVHL is required to determine whether its levels are regulated under different conditions, and whether its function is controlled by post-translational modifications such as phosphorylation. Our laboratory is currently studying the significance of a potential post-translational modification of pVHL that may help explain its interaction with the microtubule network. Similar studies may also help clarify the role of pVHL in fibronectin deposition, a function believed to be independent from its HIF activity.

Analysis of many different *VHL* mutations is under way to determine whether the different VHL phenotypes are related to the ability of the mutant proteins to retain certain protein-binding functions. Much of the research to date has concentrated on RCC (because of the availability of cell lines), but it is likely that there might be tissue-specific functions that relate to pheochromocytoma, haemangioblastoma or other tumours related to VHL disease that have yet to be identified.

Finally, continued efforts in delineating VHL biology and the pathological consequence of its deregulation are crucial if we are to understand the physiological function of the von Hippel-Lindau tumour suppressor, and its role in tumorigenesis. Only by detailing the molecular mechanism of VHL function can we begin to propose effective therapeutic strategies that could combat this life threatening condition and offer hope to those who suffer from VHL disease and VHL disease-related cancer.

References

1. Thoenes, W., S. Storkel, and H.J. Rumpelt, *Histopathology and classification of renal cell tumors (adenomas, oncocytomas and carcinomas). The basic cytological and histopathological elements and their use for diagnostics*. Pathol Res Pract, 1986. 181(2): p. 125-43.
2. Beroud, C., et al., *Software and database for the analysis of mutations in the VHL gene*. Nucleic Acids Res, 1998. 26(1): p. 256-8.
3. Corless, C.L., et al., *Immunostaining of the von Hippel-Lindau gene product in normal and neoplastic human tissues*. Hum Pathol, 1997. 28(4): p. 459-64.
4. Choyke, P.L., et al., *von Hippel-Lindau disease: genetic, clinical, and imaging features*. Radiology, 1995. 194(3): p. 629-42.
5. Ma, X., et al., *VHL gene alterations in renal cell carcinoma patients: novel hotspot or founder mutations and linkage disequilibrium*. Oncogene, 2001. 20(38): p. 5393-400.
6. Muller, A., et al., *Involvement of chemokine receptors in breast cancer metastasis*. Nature, 2001. 410(6824): p. 50-6.
7. Masson, N., et al., *Independent function of two destruction domains in hypoxia-inducible factor-alpha chains activated by prolyl hydroxylation*. Embo J, 2001. 20(18): p. 5197-206.
8. Maddock, I.R., et al., *A genetic register for von Hippel-Lindau disease*. J Med Genet, 1996. 33(2): p. 120-7.
9. Maher, E.R., J.R. Yates, and M.A. Ferguson-Smith, *Statistical analysis of the two stage mutation model in von Hippel-Lindau disease, and in sporadic cerebellar haemangioblastoma and renal cell carcinoma*. J Med Genet, 1990. 27(5): p. 311-4.
10. Kaelin, W.G., Jr., Maher ER, *The VHL tumour suppressor paradigm*. TIG, 1998. 14(10): p. 423-426.
11. Epstein, A.C., et al., *C. elegans EGL-9 and mammalian homologs define a family of dioxygenases that regulate HIF by prolyl hydroxylation*. Cell, 2001. 107(1): p. 43-54.
12. Ivan, M., et al., *HIFalpha targeted for VHL-mediated destruction by proline hydroxylation: implications for O2 sensing*. Science, 2001. 292(5516): p. 464-8.
13. Jaakkola, P., et al., *Targeting of HIF-alpha to the von Hippel-Lindau ubiquitylation complex by O2-regulated prolyl hydroxylation*. Science, 2001. 292(5516): p. 468-72.
14. von Hippel, E., *Über eine sehr seltene Erkrankung der Netzhaut*. von Graefes Arch Ophth, 1904. 59: p. 83-106.
15. Lindau, A., *Studien über kleinhirncysten. Bau, pathogenese und beziehungen zur angiomatosis retinae*. Acta Pathet Microbiol Scandinav, 1926. Suppl.1: p. 1-128.
16. Glushien, A.S., *Pheochromocytoma. It's relationship to the neurocutaneous syndromes*. Am J Med. Vol. 14. 1953. 318-27.
17. Lando, D., et al., *Asparagine hydroxylation of the HIF transactivation domain a hypoxic switch*. Science, 2002. 295(5556): p. 858-61.
18. Manski, T.J., et al., *Endolymphatic sac tumors. A source of morbid hearing loss in von Hippel-Lindau disease*. Jama, 1997. 277(18): p. 1461-6.
19. Mahon, P.C., K. Hirota, and G.L. Semenza, *FIH-1: a novel protein that interacts with HIF-1alpha and VHL to mediate repression of HIF-1 transcriptional activity*. Genes Dev, 2001. 15(20): p. 2675-86.
20. Pugh, C.W. and P.J. Ratcliffe, *Regulation of angiogenesis by hypoxia: role of the HIF system*. Nat Med, 2003. 9(6): p. 677-84.

21. Clifford, S.C. and E.R. Maher, *Von Hippel-Lindau disease: clinical and molecular perspectives*. Adv Cancer Res, 2001. 82: p. 85-105.
22. Maher ER, Y.J., Harries R, Benjamin C, Harris R, Moore AT, Ferguson-Smith MA, *Clinical features and natural history of von Hippel-Lindau disease*. Q J Med, 1990. 77(283): p. 1151-63.
23. Jeong, J.W., et al., *Regulation and destabilization of HIF-1alpha by ARD1-mediated acetylation*. Cell, 2002. 111(5): p. 709-20.
24. Richards, F.M., et al., *Molecular genetic analysis of von Hippel-Lindau disease*. J Intern Med, 1998. 243(6): p. 527-33.
25. Goldfarb, D.A., *Nephron-sparing surgery and renal transplantation in patients with renal cell carcinoma and von Hippel-Lindau disease*. J Intern Med, 1998. 243(6): p. 563-7.
26. Chang, S.D., et al., *Treatment of hemangioblastomas in von Hippel-Lindau disease with linear accelerator-based radiosurgery*. Neurosurgery, 1998. 43(1): p. 28-34; discussion 34-5.
27. Tanimoto, K., et al., *Mechanism of regulation of the hypoxia-inducible factor-1 alpha by the von Hippel-Lindau tumor suppressor protein*. Embo J, 2000. 19(16): p. 4298-309.
28. Bae, M.K., et al., *Jab1 interacts directly with HIF-1alpha and regulates its stability*. J Biol Chem, 2002. 277(1): p. 9-12.
29. Lamiell, J.M., F.G. Salazar, and Y.E. Hsia, *von Hippel-Lindau disease affecting 43 members of a single kindred*. Medicine (Baltimore), 1989. 68(1): p. 1-29.
30. Poirer, R.E.a.J., *In: Manual of Neuropathology*. 2nd ed. 1978, Philadelphia: WB Saunders. 49-51.
31. Melmon, R.S.W., *Lindau's disease: review of the literature and study of a large kindred*. Am J Med, 1964. 36: p. 595-617.
32. Richards, F.M., *Molecular pathology of von Hippel-Lindau disease and the VHL tumour suppressor gene*. Expert reviews in mol med, 2001: p. 1-27.
33. Kaelin, W.G., Jr., *Molecular basis of the VHL hereditary cancer syndrome*. Nat Rev Cancer, 2002. 2(9): p. 673-82.
34. Stolle, C., et al., *Improved detection of germline mutations in the von Hippel-Lindau disease tumor suppressor gene*. Hum Mutat, 1998. 12(6): p. 417-23.
35. Zbar, B., et al., *Germline mutations in the Von Hippel-Lindau disease (VHL) gene in families from North America, Europe, and Japan*. Hum Mutat, 1996. 8(4): p. 348-57.
36. Sgambati, M.T., et al., *Mosaicism in von Hippel-Lindau disease: lessons from kindreds with germline mutations identified in offspring with mosaic parents*. Am J Hum Genet, 2000. 66(1): p. 84-91.
37. Wanebo, J.E., et al., *The natural history of hemangioblastomas of the central nervous system in patients with von Hippel-Lindau disease*. J Neurosurg, 2003. 98(1): p. 82-94.
38. Resche F, M.J., Mantoura J, de Kersaint-Gilly A, Andre MJ, Perrin-Resche I, Menegalli-Boggelli D, Lajat Y, Richard S, *Haemangioblastoma, haemangioblastomatosis, and von Hippel-Lindau disease*. Adv Tech Stand Neurosurg, 1993. 20: p. 197-304.
39. Grossniklaus, H.E., et al., *Retinal hemangioblastoma. A histologic, immunohistochemical, and ultrastructural evaluation*. Ophthalmology, 1992. 99(1): p. 140-5.
40. Alexander, L.J. and K.N. Moates, *Cavernous hemangioma of the retina*. J Am Optom Assoc, 1988. 59(7): p. 539-48.
41. Marks E, A.D., Thomann K., *Primary eyecare in systemic disease*. 1st ed. 1995, Connecticut: Appleton & Lange. 525-534.

42. Annesley, W.H., Jr., et al., *Fifteen year review of treated cases of retinal angiomatosis*. *Trans Am Acad Ophthalmol Otolaryngol*, 1977. 83(3 Pt 1): p. OP446-53.
43. Maher, E.R. and W.G. Kaelin, Jr., *von Hippel-Lindau disease*. *Medicine (Baltimore)*, 1997. 76(6): p. 381-91.
44. Kreusel, K.M., et al., *Ruthenium-106 brachytherapy for peripheral retinal capillary hemangioma*. *Ophthalmology*, 1998. 105(8): p. 1386-92.
45. Aiello, L.P., et al., *Rapid and durable recovery of visual function in a patient with von hippel-lindau syndrome after systemic therapy with vascular endothelial growth factor receptor inhibitor su5416*. *Ophthalmology*, 2002. 109(9): p. 1745-51.
46. Heffner, D.K., *Low-grade adenocarcinoma of probable endolymphatic sac origin A clinicopathologic study of 20 cases*. *Cancer*, 1989. 64(11): p. 2292-302.
47. Wenig BM, H.D., *Endolymphatic sac tumors: fact or fiction?* *Adv Anat Pathol*, 1996. 3.: p. 378-87.
48. Asano, K., et al., *A case of endolymphatic sac tumor with long-term survival*. *Brain Tumor Pathol*, 1999. 16(2): p. 69-76.
49. Benecke, J.E., Jr., et al., *Adenomatous tumors of the middle ear and mastoid*. *Am J Otol*, 1990. 11(1): p. 20-6.
50. Kempermann, G., H.P. Neumann, and B. Volk, *Endolymphatic sac tumours*. *Histopathology*, 1998. 33(1): p. 2-10.
51. McLaughlin, J.K. and L. Lipworth, *Epidemiologic aspects of renal cell cancer*. *Semin Oncol*, 2000. 27(2): p. 115-23.
52. Karumanchi, S.A., J. Merchan, and V.P. Sukhatme, *Renal cancer: molecular mechanisms and newer therapeutic options*. *Curr Opin Nephrol Hypertens*, 2002. 11(1): p. 37-42.
53. Poston, C.D., et al., *Characterization of the renal pathology of a familial form of renal cell carcinoma associated with von Hippel-Lindau disease: clinical and molecular genetic implications*. *J Urol*, 1995. 153(1): p. 22-6.
54. Hes, F.J., et al., *Management of renal cell carcinoma in von Hippel-Lindau disease*. *Eur J Clin Invest*, 1999. 29(1): p. 68-75.
55. Walther, M.M., et al., *Renal cancer in families with hereditary renal cancer: prospective analysis of a tumor size threshold for renal parenchymal sparing surgery*. *J Urol*, 1999. 161(5): p. 1475-9.
56. Zbar B, K.W., Maher E, Richard S, *Third international meeting on von Hippel-Lindau disease*. *Cancer Res*, 1999. 59: p. 2251-3.
57. Pavlovich, C.P., et al., *Percutaneous radio frequency ablation of small renal tumors: initial results*. *J Urol*, 2002. 167(1): p. 10-5.
58. Bender, B.U., et al., *Functioning thoracic paraganglioma: association with Von Hippel-Lindau syndrome*. *J Clin Endocrinol Metab*, 1997. 82(10): p. 3356-60.
59. Richard, S., et al., *Pheochromocytoma as the first manifestation of von Hippel-Lindau disease*. *Surgery*, 1994. 116(6): p. 1076-81.
60. Schimke, R.N., D.L. Collins, and P.G. Rothberg, *Functioning carotid paraganglioma in the von Hippel-Lindau syndrome*. *Am J Med Genet*, 1998. 80(5): p. 533-4.
61. Walther, M.M., et al., *Clinical and genetic characterization of pheochromocytoma in von Hippel-Lindau families: comparison with sporadic pheochromocytoma gives insight into natural history of pheochromocytoma*. *J Urol*, 1999. 162(3 Pt 1): p. 659-64.
62. Neumann, H.P., et al., *Consequences of direct genetic testing for germline mutations in the clinical management of families with multiple endocrine neoplasia, type II*. *Jama*, 1995. 274(14): p. 1149-51.

63. Ritter, M.M., et al., *Isolated familial pheochromocytoma as a variant of von Hippel-Lindau disease*. J Clin Endocrinol Metab, 1996. 81(3): p. 1035-7.
64. van der Harst, E., et al., *Germline mutations in the vhl gene in patients presenting with pheochromocytomas*. Int J Cancer, 1998. 77(3): p. 337-40.
65. Crossey, P.A., et al., *Molecular genetic diagnosis of von Hippel-Lindau disease in familial pheochromocytoma*. J Med Genet, 1995. 32(11): p. 885-6.
66. Eng, C., et al., *Mutations in the RET proto-oncogene and the von Hippel-Lindau disease tumour suppressor gene in sporadic and syndromic pheochromocytomas*. J Med Genet, 1995. 32(12): p. 934-7.
67. Hes, F.J. and M.A. Feldberg, *Von Hippel-Lindau disease: strategies in early detection (renal-, adrenal-, pancreatic masses)*. Eur Radiol, 1999. 9(4): p. 598-610.
68. Kopf, D., et al., *Octreotide scintigraphy and catecholamine response to an octreotide challenge in malignant pheochromocytoma*. Clin Endocrinol (Oxf), 1997. 46(1): p. 39-44.
69. Ilias, I., et al., *Superiority of 6-[18F]-fluorodopamine positron emission tomography versus [131I]-metaiodobenzylguanidine scintigraphy in the localization of metastatic pheochromocytoma*. J Clin Endocrinol Metab, 2003. 88(9): p. 4083-7.
70. Walther, M.M., et al., *Management of hereditary pheochromocytoma in von Hippel-Lindau kindreds with partial adrenalectomy*. J Urol, 1999. 161(2): p. 395-8.
71. Neumann, H.P., et al., *Adrenal-sparing surgery for pheochromocytoma*. Br J Surg, 1999. 86(1): p. 94-7.
72. Hammel, P.R., et al., *Pancreatic involvement in von Hippel-Lindau disease. The Groupe Francophone d'Etude de la Maladie de von Hippel-Lindau*. Gastroenterology, 2000. 119(4): p. 1087-95.
73. Horton, W.A., V. Wong, and R. Eldridge, *Von Hippel-Lindau disease: clinical and pathological manifestations in nine families with 50 affected members*. Arch Intern Med, 1976. 136(7): p. 769-77.
74. Martz, C.H., *von Hippel-Lindau disease: a genetic condition predisposing tumor formation*. Oncol Nurs Forum, 1991. 18(3): p. 545-51.
75. Gruber, M.B., et al., *Papillary cystadenoma of epididymis: component of von Hippel-Lindau syndrome*. Urology, 1980. 16(3): p. 305-6.
76. Meyer, J.S., L.M. Roth, and J.L. Silverman, *Papillary Cystadenomas of the Epididymis and Spermatic Cord*. Cancer, 1964. 17: p. 1241-7.
77. Kragel, P.J., et al., *Papillary cystadenoma of the epididymis. A report of three cases with lectin histochemistry*. Arch Pathol Lab Med, 1990. 114(7): p. 672-5.
78. Glenn GM, C.P., Zbar BH et al., *Problems in Urologic Surgery: Benign and malignant tumors of the kidney*. von Hippel Lindau disease: Clinical aspects and molecular genetics, ed. A. EE. 1990, Philadelphia: JB Lippincott. 312-337.
79. Gaffey, M.J., S.E. Mills, and J.C. Boyd, *Aggressive papillary tumor of middle ear/temporal bone and adnexal papillary cystadenoma. Manifestations of von Hippel-Lindau disease*. Am J Surg Pathol, 1994. 18(12): p. 1254-60.
80. Seizinger, B.R., et al., *Von Hippel-Lindau disease maps to the region of chromosome 3 associated with renal cell carcinoma*. Nature, 1988. 332(6161): p. 268-9.
81. Latif, F., et al., *Identification of the von Hippel-Lindau disease tumor suppressor gene*. Science, 1993. 260(5112): p. 1317-20.
82. Kuzmin, I., et al., *Identification of the promoter of the human von Hippel-Lindau disease tumor suppressor gene*. Oncogene, 1995. 10(11): p. 2185-94.
83. Fujita, N., et al., *Methylation-mediated transcriptional silencing in euchromatin by methyl-CpG binding protein MBD1 isoforms*. Mol Cell Biol, 1999. 19(9): p. 6415-26.

84. Zatyka, M., et al., *Genetic and functional analysis of the von Hippel-Lindau (VHL) tumour suppressor gene promoter*. J Med Genet, 2002. 39(7): p. 463-72.
85. Kadonaga, J.T., et al., *Isolation of cDNA encoding transcription factor Sp1 and functional analysis of the DNA binding domain*. Cell, 1987. 51(6): p. 1079-90.
86. Minie, M.E., T. Kimura, and G. Felsenfeld, *The developmental switch in embryonic rho-globin expression is correlated with erythroid lineage-specific differences in transcription factor levels*. Development, 1992. 115(4): p. 1149-64.
87. Merchant, J.L., et al., *Epidermal growth factor stimulation of the human gastrin promoter requires Sp1*. J Biol Chem, 1995. 270(11): p. 6314-9.
88. Zhang, D.E., et al., *Sp1 is a critical factor for the monocytic specific expression of human CD14*. J Biol Chem, 1994. 269(15): p. 11425-34.
89. Cohen, H.T., et al., *Sp1 is a critical regulator of the Wilms' tumor-1 gene*. J Biol Chem, 1997. 272(5): p. 2901-13.
90. Richards, F.M., et al., *Expression of the von Hippel-Lindau disease tumour suppressor gene during human embryogenesis*. Hum Mol Genet, 1996. 5(5): p. 639-44.
91. Renbaum, P., et al., *Isolation and characterization of the full-length 3' untranslated region of the human von Hippel-Lindau tumor suppressor gene*. Hum Genet, 1996. 98(6): p. 666-71.
92. Kolomietz, E., et al., *The role of Alu repeat clusters as mediators of recurrent chromosomal aberrations in tumors*. Genes Chromosomes Cancer, 2002. 35(2): p. 97-112.
93. Yulug, I.G., A. Yulug, and E.M. Fisher, *The frequency and position of Alu repeats in cDNAs, as determined by database searching*. Genomics, 1995. 27(3): p. 544-8.
94. Kessler, P.M., et al., *Expression of the Von Hippel-Lindau tumor suppressor gene, VHL, in human fetal kidney and during mouse embryogenesis*. Mol Med, 1995. 1(4): p. 457-66.
95. Herman, J.G., et al., *Silencing of the VHL tumor-suppressor gene by DNA methylation in renal carcinoma*. Proc Natl Acad Sci U S A, 1994. 91(21): p. 9700-4.
96. Los, M., et al., *Expression pattern of the von Hippel-Lindau protein in human tissues*. Lab Invest, 1996. 75(2): p. 231-8.
97. Iliopoulos, O., et al., *Tumour suppression by the human von Hippel-Lindau gene product*. Nat Med, 1995. 1(8): p. 822-6.
98. Duan, D.R., et al., *Characterization of the VHL tumor suppressor gene product: localization, complex formation, and the effect of natural inactivating mutations*. Proc Natl Acad Sci U S A, 1995. 92(14): p. 6459-63.
99. Lee, S., et al., *Nuclear/cytoplasmic localization of the von Hippel-Lindau tumor suppressor gene product is determined by cell density*. Proc Natl Acad Sci U S A, 1996. 93(5): p. 1770-5.
100. Hinds, P.W., *The retinoblastoma tumor suppressor protein*. Curr Opin Genet Dev, 1995. 5(1): p. 79-83.
101. Nigro, J.M., et al., *Mutations in the p53 gene occur in diverse human tumour types*. Nature, 1989. 342(6250): p. 705-8.
102. Schoenfeld, A., E.J. Davidowitz, and R.D. Burk, *A second major native von Hippel-Lindau gene product, initiated from an internal translation start site, functions as a tumor suppressor*. Proc Natl Acad Sci U S A, 1998. 95(15): p. 8817-22.
103. Ye, Y., et al., *Subcellular localization of the von Hippel-Lindau disease gene product is cell cycle-dependent*. Int J Cancer, 1998. 78(1): p. 62-9.

104. Shiao, Y.H., et al., *The von Hippel-Lindau tumor suppressor targets to mitochondria*. *Cancer Res*, 2000. 60(11): p. 2816-9.
105. Schoenfeld, A.R., E.J. Davidowitz, and R.D. Burk, *Endoplasmic reticulum/cytosolic localization of von Hippel-Lindau gene products is mediated by a 64-amino acid region*. *Int J Cancer*, 2001. 91(4): p. 457-67.
106. Dingwall, C. and R.A. Laskey, *Nuclear targeting sequences--a consensus?* *Trends Biochem Sci*, 1991. 16(12): p. 478-81.
107. Hergovich, A., et al., *Regulation of microtubule stability by the von Hippel-Lindau tumour suppressor protein pVHL*. *Nat Cell Biol*, 2003. 5(1): p. 64-70.
108. Kishida, T., et al., *Cellular proteins that bind the von Hippel-Lindau disease gene product: mapping of binding domains and the effect of missense mutations*. *Cancer Res*, 1995. 55(20): p. 4544-8.
109. Lonergan, K.M., et al., *Regulation of hypoxia-inducible mRNAs by the von Hippel-Lindau tumor suppressor protein requires binding to complexes containing elongins B/C and Cul2*. *Mol Cell Biol*, 1998. 18(2): p. 732-41.
110. Zhang, J.G., et al., *The conserved SOCS box motif in suppressors of cytokine signaling binds to elongins B and C and may couple bound proteins to proteasomal degradation*. *Proc Natl Acad Sci U S A*, 1999. 96(5): p. 2071-6.
111. Stebbins, C.E., W.G. Kaelin, Jr., and N.P. Pavletich, *Structure of the VHL-ElonginC-ElonginB complex: implications for VHL tumor suppressor function*. *Science*, 1999. 284(5413): p. 455-61.
112. Kile, B.T., et al., *The SOCS box: a tale of destruction and degradation*. *Trends Biochem Sci*, 2002. 27(5): p. 235-41.
113. Min, J.H., et al., *Structure of an HIF-1alpha -pVHL complex: hydroxyproline recognition in signaling*. *Science*, 2002. 296(5574): p. 1886-9.
114. Maxwell, P.H., et al., *The tumour suppressor protein VHL targets hypoxia-inducible factors for oxygen-dependent proteolysis*. *Nature*, 1999. 399(6733): p. 271-5.
115. Ohh, M., et al., *Ubiquitination of hypoxia-inducible factor requires direct binding to the beta-domain of the von Hippel-Lindau protein*. *Nat Cell Biol*, 2000. 2(7): p. 423-7.
116. Gao, J., et al., *Cloning and characterization of a mouse gene with homology to the human von Hippel-Lindau disease tumor suppressor gene: implications for the potential organization of the human von Hippel-Lindau disease gene*. *Cancer Res*, 1995. 55(4): p. 743-7.
117. Adryan, B., et al., *Tracheal development and the von Hippel-Lindau tumor suppressor homolog in Drosophila*. *Oncogene*, 2000. 19(24): p. 2803-11.
118. Aso, T., et al., *Drosophila von Hippel-Lindau tumor suppressor complex possesses E3 ubiquitin ligase activity*. *Biochem Biophys Res Commun*, 2000. 276(1): p. 355-61.
119. Woodward, E.R., et al., *Comparative sequence analysis of the VHL tumor suppressor gene*. *Genomics*, 2000. 65(3): p. 253-65.
120. Iliopoulos, O., M. Ohh, and W.G. Kaelin, Jr., *pVHL19 is a biologically active product of the von Hippel-Lindau gene arising from internal translation initiation*. *Proc Natl Acad Sci U S A*, 1998. 95(20): p. 11661-6.
121. Gnarr, J.R., et al., *Molecular cloning of the von Hippel-Lindau tumor suppressor gene and its role in renal carcinoma*. *Biochim Biophys Acta*, 1996. 1242(3): p. 201-10.
122. Whaley, J.M., et al., *Germ-line mutations in the von Hippel-Lindau tumor-suppressor gene are similar to somatic von Hippel-Lindau aberrations in sporadic renal cell carcinoma*. *Am J Hum Genet*, 1994. 55(6): p. 1092-102.

123. Gnarr, J.R., et al., *Mutations of the VHL tumour suppressor gene in renal carcinoma*. Nat Genet, 1994. 7(1): p. 85-90.
124. Foster, K., et al., *Somatic mutations of the von Hippel-Lindau disease tumour suppressor gene in non-familial clear cell renal carcinoma*. Hum Mol Genet, 1994. 3(12): p. 2169-73.
125. Shuin, T., et al., *Frequent somatic mutations and loss of heterozygosity of the von Hippel-Lindau tumor suppressor gene in primary human renal cell carcinomas*. Cancer Res, 1994. 54(11): p. 2852-5.
126. Kenck, C., et al., *Mutation of the VHL gene is associated exclusively with the development of non-papillary renal cell carcinomas*. J Pathol, 1996. 179(2): p. 157-61.
127. Neumann, H.P. and B.U. Bender, *Genotype-phenotype correlations in von Hippel-Lindau disease*. J Intern Med, 1998. 243(6): p. 541-5.
128. Ohh, M., et al., *Synthetic peptides define critical contacts between elongin C, elongin B, and the von Hippel-Lindau protein*. J Clin Invest, 1999. 104(11): p. 1583-91.
129. Knudson, A.G., Jr., *Mutation and cancer: statistical study of retinoblastoma*. Proc Natl Acad Sci U S A, 1971. 68(4): p. 820-3.
130. Chen, F., et al., *Germline mutations in the von Hippel-Lindau disease tumor suppressor gene: correlations with phenotype*. Hum Mutat, 1995. 5(1): p. 66-75.
131. Glavac, D., et al., *Mutations in the VHL tumor suppressor gene and associated lesions in families with von Hippel-Lindau disease from central Europe*. Hum Genet, 1996. 98(3): p. 271-80.
132. Crossey, P.A., et al., *Identification of intragenic mutations in the von Hippel-Lindau disease tumour suppressor gene and correlation with disease phenotype*. Hum Mol Genet, 1994. 3(8): p. 1303-8.
133. Maher, E.R., et al., *Phenotypic expression in von Hippel-Lindau disease: correlations with germline VHL gene mutations*. J Med Genet, 1996. 33(4): p. 328-32.
134. Ohh, M., et al., *The von Hippel-Lindau tumor suppressor protein is required for proper assembly of an extracellular fibronectin matrix*. Mol Cell, 1998. 1(7): p. 959-68.
135. Los, M., et al., *Regulation of the urokinase-type plasminogen activator system by the von Hippel-Lindau tumor suppressor gene*. Cancer Res, 1999. 59(17): p. 4440-5.
136. Koochekpour, S., et al., *The von Hippel-Lindau tumor suppressor gene inhibits hepatocyte growth factor/scatter factor-induced invasion and branching morphogenesis in renal carcinoma cells*. Mol Cell Biol, 1999. 19(9): p. 5902-12.
137. Pause, A., et al., *The von Hippel-Lindau tumor suppressor gene is required for cell cycle exit upon serum withdrawal*. Proc Natl Acad Sci U S A, 1998. 95(3): p. 993-8.
138. Stickle, N.H., et al., *pVHL modification by NEDD8 is required for fibronectin matrix assembly and suppression of tumor development*. Mol Cell Biol, 2004. 24(8): p. 3251-61.
139. Richards, F.M., et al., *Detailed genetic mapping of the von Hippel-Lindau disease tumour suppressor gene*. J Med Genet, 1993. 30(2): p. 104-7.
140. Brauch, H., et al., *Von Hippel-Lindau (VHL) disease with pheochromocytoma in the Black Forest region of Germany: evidence for a founder effect*. Hum Genet, 1995. 95(5): p. 551-6.
141. Chen, F., et al., *Genotype-phenotype correlation in von Hippel-Lindau disease: identification of a mutation associated with VHL type 2A*. J Med Genet, 1996. 33(8): p. 716-7.

142. Bradley, J.F., et al., *Two distinct phenotypes caused by two different missense mutations in the same codon of the VHL gene*. *Am J Med Genet*, 1999. 87(2): p. 163-7.
143. Woodward, E.R., et al., *Genetic predisposition to pheochromocytoma: analysis of candidate genes GDNF, RET and VHL*. *Hum Mol Genet*, 1997. 6(7): p. 1051-6.
144. Prowse, A.H., et al., *Somatic inactivation of the VHL gene in Von Hippel-Lindau disease tumors*. *Am J Hum Genet*, 1997. 60(4): p. 765-71.
145. Pack, S.D., et al., *Constitutional von Hippel-Lindau (VHL) gene deletions detected in VHL families by fluorescence in situ hybridization*. *Cancer Res*, 1999. 59(21): p. 5560-4.
146. Zbar, B., *Von Hippel-Lindau disease and sporadic renal cell carcinoma*. *Cancer Surv*, 1995. 25: p. 219-32.
147. Richards, F.M., et al., *Mapping the Von Hippel-Lindau disease tumour suppressor gene: identification of germline deletions by pulsed field gel electrophoresis*. *Hum Mol Genet*, 1993. 2(7): p. 879-82.
148. Kuwano, A., et al., *Detection of deletions and cryptic translocations in Miller-Dieker syndrome by in situ hybridization*. *Am J Hum Genet*, 1991. 49(4): p. 707-14.
149. Baylin, S.B., et al., *Alterations in DNA methylation: a fundamental aspect of neoplasia*. *Adv Cancer Res*, 1998. 72: p. 141-96.
150. Bestor, T.H., *The DNA methyltransferases of mammals*. *Hum Mol Genet*, 2000. 9(16): p. 2395-402.
151. Robertson, K.D., *DNA methylation, methyltransferases, and cancer*. *Oncogene*, 2001. 20(24): p. 3139-55.
152. Worm, J. and P. Guldborg, *DNA methylation: an epigenetic pathway to cancer and a promising target for anticancer therapy*. *J Oral Pathol Med*, 2002. 31(8): p. 443-9.
153. Pavlovich, C.P. and L.S. Schmidt, *Searching for the hereditary causes of renal-cell carcinoma*. *Nat Rev Cancer*, 2004. 4(5): p. 381-93.
154. Brauch, H., et al., *Trichloroethylene exposure and specific somatic mutations in patients with renal cell carcinoma*. *J Natl Cancer Inst*, 1999. 91(10): p. 854-61.
155. Parkin, D.M. and C.S. Muir, *Cancer Incidence in Five Continents. Comparability and quality of data*. *IARC Sci Publ*, 1992(120): p. 45-173.
156. Kanno, H., et al., *Somatic mutations of the von Hippel-Lindau tumor suppressor gene in sporadic central nervous system hemangioblastomas*. *Cancer Res*, 1994. 54(18): p. 4845-7.
157. Oberstrass, J., et al., *Mutation of the Von Hippel-Lindau tumour suppressor gene in capillary haemangioblastomas of the central nervous system*. *J Pathol*, 1996. 179(2): p. 151-6.
158. Tse, J.Y., et al., *Molecular genetic analysis of the von Hippel-Lindau disease tumor suppressor gene in familial and sporadic cerebellar hemangioblastomas*. *Am J Clin Pathol*, 1997. 107(4): p. 459-66.
159. Vortmeyer, A.O., et al., *von Hippel-Lindau gene deletion detected in the stromal cell component of a cerebellar hemangioblastoma associated with von Hippel-Lindau disease*. *Hum Pathol*, 1997. 28(5): p. 540-3.
160. Lee, J.Y., et al., *Loss of heterozygosity and somatic mutations of the VHL tumor suppressor gene in sporadic cerebellar hemangioblastomas*. *Cancer Res*, 1998. 58(3): p. 504-8.
161. Glasker, S., et al., *Reconsideration of biallelic inactivation of the VHL tumour suppressor gene in hemangioblastomas of the central nervous system*. *J Neurol Neurosurg Psychiatry*, 2001. 70(5): p. 644-8.

162. Khosla, S., et al., *Loss of heterozygosity suggests multiple genetic alterations in pheochromocytomas and medullary thyroid carcinomas*. J Clin Invest, 1991. 87(5): p. 1691-9.
163. Moley, J.F., et al., *Consistent association of 1p loss of heterozygosity with pheochromocytomas from patients with multiple endocrine neoplasia type 2 syndromes*. Cancer Res, 1992. 52(4): p. 770-4.
164. Mulligan, L.M., et al., *Genetic events in tumour initiation and progression in multiple endocrine neoplasia type 2*. Genes Chromosomes Cancer, 1993. 6(3): p. 166-77.
165. Vargas, M.P., et al., *Loss of heterozygosity on the short arm of chromosomes 1 and 3 in sporadic pheochromocytoma and extra-adrenal paraganglioma*. Hum Pathol, 1997. 28(4): p. 411-5.
166. Crossey, P.A., et al., *Molecular genetic investigations of the mechanism of tumorigenesis in von Hippel-Lindau disease: analysis of allele loss in VHL tumours*. Hum Genet, 1994. 93(1): p. 53-8.
167. Zeiger, M.A., et al., *Loss of heterozygosity on the short arm of chromosome 3 in sporadic, von Hippel-Lindau disease-associated, and familial pheochromocytoma*. Genes Chromosomes Cancer, 1995. 13(3): p. 151-6.
168. Friend, S.H., et al., *A human DNA segment with properties of the gene that predisposes to retinoblastoma and osteosarcoma*. Nature, 1986. 323(6089): p. 643-6.
169. Cavenee, W.K., et al., *Expression of recessive alleles by chromosomal mechanisms in retinoblastoma*. Nature, 1983. 305(5937): p. 779-84.
170. Malkin, D., et al., *Germ line p53 mutations in a familial syndrome of breast cancer, sarcomas, and other neoplasms*. Science, 1990. 250(4985): p. 1233-8.
171. Fults, D., et al., *p53 mutation and loss of heterozygosity on chromosomes 17 and 10 during human astrocytoma progression*. Cancer Res, 1992. 52(3): p. 674-9.
172. Nishisho, I., et al., *Mutations of chromosome 5q21 genes in FAP and colorectal cancer patients*. Science, 1991. 253(5020): p. 665-9.
173. Cottrell, S., et al., *Molecular analysis of APC mutations in familial adenomatous polyposis and sporadic colon carcinomas*. Lancet, 1992. 340(8820): p. 626-30.
174. Futreal, P.A., et al., *BRCA1 mutations in primary breast and ovarian carcinomas*. Science, 1994. 266(5182): p. 120-2.
175. Lancaster, J.M., et al., *BRCA2 mutations in primary breast and ovarian cancers*. Nat Genet, 1996. 13(2): p. 238-40.
176. Bebb, D.G., et al., *Absence of mutations in the ATM gene in forty-seven cases of sporadic breast cancer*. Br J Cancer, 1999. 80(12): p. 1979-81.
177. Armes, J.E., et al., *Distinct molecular pathogeneses of early-onset breast cancers in BRCA1 and BRCA2 mutation carriers: a population-based study*. Cancer Res, 1999. 59(8): p. 2011-7.
178. Sigbjornsdottir, B.I., et al., *Chromosome 8p alterations in sporadic and BRCA2 999del5 linked breast cancer*. J Med Genet, 2000. 37(5): p. 342-7.
179. Simpson, M.V., *The release of labeled amino acids from the proteins of rat liver slices*. J Biol Chem, 1953. 201(1): p. 143-54.
180. Ciechanover, A., et al., *ATP-dependent conjugation of reticulocyte proteins with the polypeptide required for protein degradation*. Proc Natl Acad Sci U S A, 1980. 77(3): p. 1365-8.
181. Hershko, A., et al., *Proposed role of ATP in protein breakdown: conjugation of protein with multiple chains of the polypeptide of ATP-dependent proteolysis*. Proc Natl Acad Sci U S A, 1980. 77(4): p. 1783-6.

182. Hershko, A., et al., *Components of ubiquitin-protein ligase system. Resolution, affinity purification, and role in protein breakdown.* J Biol Chem, 1983. 258(13): p. 8206-14.
183. Baumeister, W., et al., *The proteasome: paradigm of a self-compartmentalizing protease.* Cell, 1998. 92(3): p. 367-80.
184. Lisztwan, J., et al., *The von Hippel-Lindau tumor suppressor protein is a component of an E3 ubiquitin-protein ligase activity.* Genes Dev, 1999. 13(14): p. 1822-33.
185. Iwai, K., et al., *Identification of the von Hippel-lindau tumor-suppressor protein as part of an active E3 ubiquitin ligase complex.* Proc Natl Acad Sci U S A, 1999. 96(22): p. 12436-41.
186. Bai, C., et al., *SKP1 connects cell cycle regulators to the ubiquitin proteolysis machinery through a novel motif, the F-box.* Cell, 1996. 86(2): p. 263-74.
187. Patton, E.E., A.R. Willems, and M. Tyers, *Combinatorial control in ubiquitin-dependent proteolysis: don't Skp the F-box hypothesis.* Trends Genet, 1998. 14(6): p. 236-43.
188. Maniatis, T., *A ubiquitin ligase complex essential for the NF-kappaB, Wnt/Wingless, and Hedgehog signaling pathways.* Genes Dev, 1999. 13(5): p. 505-10.
189. Sutterluty, H., et al., *p45SKP2 promotes p27Kip1 degradation and induces S phase in quiescent cells.* Nat Cell Biol, 1999. 1(4): p. 207-14.
190. Peters, J.M., *SCF and APC: the Yin and Yang of cell cycle regulated proteolysis.* Curr Opin Cell Biol, 1998. 10(6): p. 759-68.
191. Duan, D.R., et al., *Inhibition of transcription elongation by the VHL tumor suppressor protein.* Science, 1995. 269(5229): p. 1402-6.
192. Pause, A., et al., *The von Hippel-Lindau tumor-suppressor gene product forms a stable complex with human CUL-2, a member of the Cdc53 family of proteins.* Proc Natl Acad Sci U S A, 1997. 94(6): p. 2156-61.
193. Kibel, A., et al., *Binding of the von Hippel-Lindau tumor suppressor protein to Elongin B and C.* Science, 1995. 269(5229): p. 1444-6.
194. Kamura, T., et al., *Rbx1, a component of the VHL tumor suppressor complex and SCF ubiquitin ligase.* Science, 1999. 284(5414): p. 657-61.
195. Wirbelauer, C., et al., *The F-box protein Skp2 is a ubiquitylation target of a Cul1-based core ubiquitin ligase complex: evidence for a role of Cul1 in the suppression of Skp2 expression in quiescent fibroblasts.* Embo J, 2000. 19(20): p. 5362-75.
196. Hanahan, D. and J. Folkman, *Patterns and emerging mechanisms of the angiogenic switch during tumorigenesis.* Cell, 1996. 86(3): p. 353-64.
197. Shweiki, D., et al., *Vascular endothelial growth factor induced by hypoxia may mediate hypoxia-initiated angiogenesis.* Nature, 1992. 359(6398): p. 843-5.
198. Goldberg, M.A., S.P. Dunning, and H.F. Bunn, *Regulation of the erythropoietin gene: evidence that the oxygen sensor is a heme protein.* Science, 1988. 242(4884): p. 1412-5.
199. Wang, G.L. and G.L. Semenza, *Desferrioxamine induces erythropoietin gene expression and hypoxia-inducible factor 1 DNA-binding activity: implications for models of hypoxia signal transduction.* Blood, 1993. 82(12): p. 3610-5.
200. Carmeliet, P., et al., *Role of HIF-1alpha in hypoxia-mediated apoptosis, cell proliferation and tumour angiogenesis.* Nature, 1998. 394(6692): p. 485-90.
201. Maxwell, P.H., et al., *Hypoxia-inducible factor-1 modulates gene expression in solid tumors and influences both angiogenesis and tumor growth.* Proc Natl Acad Sci U S A, 1997. 94(15): p. 8104-9.
202. Zelzer, E., et al., *Insulin induces transcription of target genes through the hypoxia-inducible factor HIF-1alpha/ARNT.* Embo J, 1998. 17(17): p. 5085-94.

203. Dang, C.V. and G.L. Semenza, *Oncogenic alterations of metabolism*. Trends Biochem Sci, 1999. 24(2): p. 68-72.
204. Semenza, G.L., *Regulation of mammalian O₂ homeostasis by hypoxia-inducible factor 1*. Annu Rev Cell Dev Biol, 1999. 15: p. 551-78.
205. Minet, E., et al., *Transduction pathways involved in Hypoxia-Inducible Factor-1 phosphorylation and activation*. Free Radic Biol Med, 2001. 31(7): p. 847-55.
206. Salceda, S., et al., *Complex role of protein phosphorylation in gene activation by hypoxia*. Kidney Int, 1997. 51(2): p. 556-9.
207. Huang, L.E., et al., *Regulation of hypoxia-inducible factor 1alpha is mediated by an O₂-dependent degradation domain via the ubiquitin-proteasome pathway*. Proc Natl Acad Sci U S A, 1998. 95(14): p. 7987-92.
208. Berra, E., et al., *Hypoxia-inducible factor-1 alpha (HIF-1 alpha) escapes O₂-driven proteasomal degradation irrespective of its subcellular localization: nucleus or cytoplasm*. EMBO Rep, 2001. 2(7): p. 615-20.
209. Ruas, J.L., L. Poellinger, and T. Pereira, *Functional analysis of hypoxia-inducible factor-1 alpha-mediated transactivation. Identification of amino acid residues critical for transcriptional activation and/or interaction with CREB-binding protein*. J Biol Chem, 2002. 277(41): p. 38723-30.
210. Bruick, R.K. and S.L. McKnight, *A conserved family of prolyl-4-hydroxylases that modify HIF*. Science, 2001. 294(5545): p. 1337-40.
211. Hewitson, K.S., et al., *Hypoxia-inducible factor (HIF) asparagine hydroxylase is identical to factor inhibiting HIF (FIH) and is related to the cupin structural family*. J Biol Chem, 2002. 277(29): p. 26351-5.
212. Zhong, H., et al., *Modulation of hypoxia-inducible factor 1alpha expression by the epidermal growth factor/phosphatidylinositol 3-kinase/PTEN/AKT/FRAP pathway in human prostate cancer cells: implications for tumor angiogenesis and therapeutics*. Cancer Res, 2000. 60(6): p. 1541-5.
213. Laughner, E., et al., *HER2 (neu) signaling increases the rate of hypoxia-inducible factor 1alpha (HIF-1alpha) synthesis: novel mechanism for HIF-1-mediated vascular endothelial growth factor expression*. Mol Cell Biol, 2001. 21(12): p. 3995-4004.
214. Tian, H., S.L. McKnight, and D.W. Russell, *Endothelial PAS domain protein 1 (EPAS1), a transcription factor selectively expressed in endothelial cells*. Genes Dev, 1997. 11(1): p. 72-82.
215. Makino, Y., et al., *Inhibitory PAS domain protein is a negative regulator of hypoxia-inducible gene expression*. Nature, 2001. 414(6863): p. 550-4.
216. Semenza, G.L., *HIF-1 and tumor progression: pathophysiology and therapeutics*. Trends Mol Med, 2002. 8(4 Suppl): p. S62-7.
217. Ravi, R., et al., *Regulation of tumor angiogenesis by p53-induced degradation of hypoxia-inducible factor 1alpha*. Genes Dev, 2000. 14(1): p. 34-44.
218. Arany, Z., et al., *An essential role for p300/CBP in the cellular response to hypoxia*. Proc Natl Acad Sci U S A, 1996. 93(23): p. 12969-73.
219. Carrero, P., et al., *Redox-regulated recruitment of the transcriptional coactivators CREB-binding protein and SRC-1 to hypoxia-inducible factor 1alpha*. Mol Cell Biol, 2000. 20(1): p. 402-15.
220. Minet, E., et al., *Hypoxia-induced activation of HIF-1: role of HIF-1alpha-Hsp90 interaction*. FEBS Lett, 1999. 460(2): p. 251-6.
221. Rossetti, G., et al., *Integrin-dependent regulation of gene expression in leukocytes*. Immunol Rev, 2002. 186: p. 189-207.
222. Tomoda, K., Y. Kubota, and J. Kato, *Degradation of the cyclin-dependent-kinase inhibitor p27Kip1 is instigated by Jab1*. Nature, 1999. 398(6723): p. 160-5.

223. Chauchereau, A., et al., *JAB1 interacts with both the progesterone receptor and SRC-1*. J Biol Chem, 2000. 275(12): p. 8540-8.
224. Wolf, D.A., C. Zhou, and S. Wee, *The COP9 signalosome: an assembly and maintenance platform for cullin ubiquitin ligases?* Nat Cell Biol, 2003. 5(12): p. 1029-33.
225. Seeger, M., et al., *A novel protein complex involved in signal transduction possessing similarities to 26S proteasome subunits*. Faseb J, 1998. 12(6): p. 469-78.
226. Bech-Otschir, D., et al., *COP9 signalosome-specific phosphorylation targets p53 to degradation by the ubiquitin system*. Embo J, 2001. 20(7): p. 1630-9.
227. Ogryzko, V.V., et al., *Histone-like TAFs within the PCAF histone acetylase complex*. Cell, 1998. 94(1): p. 35-44.
228. Boyes, J., et al., *Regulation of activity of the transcription factor GATA-1 by acetylation*. Nature, 1998. 396(6711): p. 594-8.
229. Kouzarides, T., *Histone acetylases and deacetylases in cell proliferation*. Curr Opin Genet Dev, 1999. 9(1): p. 40-8.
230. Kouzarides, T., *Acetylation: a regulatory modification to rival phosphorylation?* Embo J, 2000. 19(6): p. 1176-9.
231. Yu, F., et al., *HIF-1alpha binding to VHL is regulated by stimulus-sensitive proline hydroxylation*. Proc Natl Acad Sci U S A, 2001. 98(17): p. 9630-5.
232. Schofield, C.J. and Z. Zhang, *Structural and mechanistic studies on 2-oxoglutarate-dependent oxygenases and related enzymes*. Curr Opin Struct Biol, 1999. 9(6): p. 722-31.
233. Kroll, S.L., et al., *von Hippel-Lindau protein induces hypoxia-regulated arrest of tyrosine hydroxylase transcript elongation in pheochromocytoma cells*. J Biol Chem, 1999. 274(42): p. 30109-14.
234. Schnell, P.O., et al., *Regulation of tyrosine hydroxylase promoter activity by the von Hippel-Lindau tumor suppressor protein and hypoxia-inducible transcription factors*. J Neurochem, 2003. 85(2): p. 483-91.
235. Bauer, A.L., et al., *Endogenous von Hippel-Lindau tumor suppressor protein regulates catecholaminergic phenotype in PC12 cells*. Cancer Res, 2002. 62(6): p. 1682-7.
236. Schoenfeld, A.R., et al., *The von Hippel-Lindau tumor suppressor gene protects cells from UV-mediated apoptosis*. Oncogene, 2000. 19(51): p. 5851-7.
237. Na, X., et al., *Identification of the RNA polymerase II subunit hsRPB7 as a novel target of the von Hippel-Lindau protein*. Embo J, 2003. 22(16): p. 4249-59.
238. Jensen, G.J., et al., *Structure of wild-type yeast RNA polymerase II and location of Rpb4 and Rpb7*. Embo J, 1998. 17(8): p. 2353-8.
239. Kuznetsova, A.V., et al., *von Hippel-Lindau protein binds hyperphosphorylated large subunit of RNA polymerase II through a proline hydroxylation motif and targets it for ubiquitination*. Proc Natl Acad Sci U S A, 2003. 100(5): p. 2706-11.
240. Li, Z., et al., *Ubiquitination of a novel deubiquitinating enzyme requires direct binding to von Hippel-Lindau tumor suppressor protein*. J Biol Chem, 2002. 277(7): p. 4656-62.
241. Li, Z., et al., *Identification of a deubiquitinating enzyme subfamily as substrates of the von Hippel-Lindau tumor suppressor*. Biochem Biophys Res Commun, 2002. 294(3): p. 700-9.
242. Curcio-Morelli, C., et al., *Deubiquitination of type 2 iodothyronine deiodinase by von Hippel-Lindau protein-interacting deubiquitinating enzymes regulates thyroid hormone activation*. J Clin Invest, 2003. 112(2): p. 189-96.

243. Pal, S., et al., *The von Hippel-Lindau gene product inhibits vascular permeability factor/vascular endothelial growth factor expression in renal cell carcinoma by blocking protein kinase C pathways.* J Biol Chem, 1997. 272(44): p. 27509-12.
244. Pal, S., et al., *Activation of Sp1-mediated vascular permeability factor/vascular endothelial growth factor transcription requires specific interaction with protein kinase C zeta.* J Biol Chem, 1998. 273(41): p. 26277-80.
245. Okuda, H., et al., *Direct interaction of the beta-domain of VHL tumor suppressor protein with the regulatory domain of atypical PKC isoforms.* Biochem Biophys Res Commun, 1999. 263(2): p. 491-7.
246. Carrano, A.C., et al., *SKP2 is required for ubiquitin-mediated degradation of the CDK inhibitor p27.* Nat Cell Biol, 1999. 1(4): p. 193-9.
247. Suzuki, A., et al., *Atypical protein kinase C is involved in the evolutionarily conserved par protein complex and plays a critical role in establishing epithelia-specific junctional structures.* J Cell Biol, 2001. 152(6): p. 1183-96.
248. Coghlan, M.P., M.M. Chou, and C.L. Carpenter, *Atypical protein kinases C lambda and -zeta associate with the GTP-binding protein Cdc42 and mediate stress fiber loss.* Mol Cell Biol, 2000. 20(8): p. 2880-9.
249. Kamada, M., et al., *von Hippel-Lindau protein promotes the assembly of actin and vinculin and inhibits cell motility.* Cancer Res, 2001. 61(10): p. 4184-9.
250. Esteban-Barragan, M.A., et al., *Role of the von Hippel-Lindau tumor suppressor gene in the formation of beta1-integrin fibrillar adhesions.* Cancer Res, 2002. 62(10): p. 2929-36.
251. Baba, M., et al., *Tumor suppressor protein VHL is induced at high cell density and mediates contact inhibition of cell growth.* Oncogene, 2001. 20(22): p. 2727-36.
252. Corn, P.G., et al., *Tat-binding protein-1, a component of the 26S proteasome, contributes to the E3 ubiquitin ligase function of the von Hippel-Lindau protein.* Nat Genet, 2003. 35(3): p. 229-37.
253. Braun, B.C., et al., *The base of the proteasome regulatory particle exhibits chaperone-like activity.* Nat Cell Biol, 1999. 1(4): p. 221-6.
254. Ferrell, K., et al., *Regulatory subunit interactions of the 26S proteasome, a complex problem.* Trends Biochem Sci, 2000. 25(2): p. 83-8.
255. Liu, C.W., et al., *Conformational remodeling of proteasomal substrates by PA700, the 19 S regulatory complex of the 26 S proteasome.* J Biol Chem, 2002. 277(30): p. 26815-20.
256. Feldman, D.E., et al., *Formation of the VHL-elongin BC tumor suppressor complex is mediated by the chaperonin TRiC.* Mol Cell, 1999. 4(6): p. 1051-61.
257. Hansen, W.J., et al., *Diverse effects of mutations in exon II of the von Hippel-Lindau (VHL) tumor suppressor gene on the interaction of pVHL with the cytosolic chaperonin and pVHL-dependent ubiquitin ligase activity.* Mol Cell Biol, 2002. 22(6): p. 1947-60.
258. Melville, M.W., et al., *The Hsp70 and TRiC/CCT chaperone systems cooperate in vivo to assemble the von Hippel-Lindau tumor suppressor complex.* Mol Cell Biol, 2003. 23(9): p. 3141-51.
259. Feldman, D.E., et al., *Tumorigenic mutations in VHL disrupt folding in vivo by interfering with chaperonin binding.* Mol Cell, 2003. 12(5): p. 1213-24.
260. Tsuchiya, H., T. Iseda, and O. Hino, *Identification of a novel protein (VBP-1) binding to the von Hippel-Lindau (VHL) tumor suppressor gene product.* Cancer Res, 1996. 56(13): p. 2881-5.
261. Gnarr, J.R., et al., *Defective placental vasculogenesis causes embryonic lethality in VHL-deficient mice.* Proc Natl Acad Sci U S A, 1997. 94(17): p. 9102-7.

262. Siemeister, G., et al., *Reversion of deregulated expression of vascular endothelial growth factor in human renal carcinoma cells by von Hippel-Lindau tumor suppressor protein*. *Cancer Res*, 1996. 56(10): p. 2299-301.
263. Iliopoulos, O., et al., *Negative regulation of hypoxia-inducible genes by the von Hippel-Lindau protein*. *Proc Natl Acad Sci U S A*, 1996. 93(20): p. 10595-9.
264. Gnarr, J.R., et al., *Post-transcriptional regulation of vascular endothelial growth factor mRNA by the product of the VHL tumor suppressor gene*. *Proc Natl Acad Sci U S A*, 1996. 93(20): p. 10589-94.
265. Ferrara, N., et al., *Heterozygous embryonic lethality induced by targeted inactivation of the VEGF gene*. *Nature*, 1996. 380(6573): p. 439-42.
266. Shalaby, F., et al., *Failure of blood-island formation and vasculogenesis in Flk-1-deficient mice*. *Nature*, 1995. 376(6535): p. 62-6.
267. Fong, G.H., et al., *Role of the Flt-1 receptor tyrosine kinase in regulating the assembly of vascular endothelium*. *Nature*, 1995. 376(6535): p. 66-70.
268. Carmeliet, P., et al., *Abnormal blood vessel development and lethality in embryos lacking a single VEGF allele*. *Nature*, 1996. 380(6573): p. 435-9.
269. Haase, V.H., et al., *Vascular tumors in livers with targeted inactivation of the von Hippel-Lindau tumor suppressor*. *Proc Natl Acad Sci U S A*, 2001. 98(4): p. 1583-8.
270. LeCouter, J.E., et al., *Strain-dependent embryonic lethality in mice lacking the retinoblastoma-related p130 gene*. *Development*, 1998. 125(23): p. 4669-79.
271. Martinez, A., et al., *Role of chromosome 3p12-p21 tumour suppressor genes in clear cell renal cell carcinoma: analysis of VHL dependent and VHL independent pathways of tumorigenesis*. *Mol Pathol*, 2000. 53(3): p. 137-44.
272. Kleymenova, E., et al., *Susceptibility to vascular neoplasms but no increased susceptibility to renal carcinogenesis in Vhl knockout mice*. *Carcinogenesis*, 2004. 25(3): p. 309-315.
273. Kobayashi, T., et al., *A germline insertion in the tuberous sclerosis (Tsc2) gene gives rise to the Eker rat model of dominantly inherited cancer*. *Nat Genet*, 1995. 9(1): p. 70-4.
274. Onda, H., et al., *Tsc2(+/-) mice develop tumors in multiple sites that express gelsolin and are influenced by genetic background*. *J Clin Invest*, 1999. 104(6): p. 687-95.
275. Liu, M.Y., L. Poellinger, and C.L. Walker, *Up-regulation of hypoxia-inducible factor 2alpha in renal cell carcinoma associated with loss of Tsc-2 tumor suppressor gene*. *Cancer Res*, 2003. 63(10): p. 2675-80.
276. Brugarolas, J.B., et al., *TSC2 regulates VEGF through mTOR-dependent and -independent pathways*. *Cancer Cell*, 2003. 4(2): p. 147-58.
277. Everitt, J.I., et al., *Hereditary renal cell carcinoma in the Eker rat: a rodent familial cancer syndrome*. *J Urol*, 1992. 148(6): p. 1932-6.
278. Zimmer, M., et al., *Inhibition of hypoxia-inducible factor is sufficient for growth suppression of VHL-/- tumors*. *Mol Cancer Res*, 2004. 2(2): p. 89-95.
279. Kondo, K., et al., *Inhibition of HIF2alpha Is Sufficient to Suppress pVHL-Defective Tumor Growth*. *PLoS Biol*, 2003. 1(3): p. E83.
280. Mack, F.A., et al., *Loss of pVHL is sufficient to cause HIF dysregulation in primary cells but does not promote tumor growth*. *Cancer Cell*, 2003. 3(1): p. 75-88.
281. Gunawan, B., et al., *Prognostic impacts of cytogenetic findings in clear cell renal cell carcinoma: gain of 5q31-qter predicts a distinct clinical phenotype with favorable prognosis*. *Cancer Res*, 2001. 61(21): p. 7731-8.
282. Norrby, K., *Angiogenesis: new aspects relating to its initiation and control*. *Apmis*, 1997. 105(6): p. 417-37.

283. Aznavoorian, S., et al., *Molecular aspects of tumor cell invasion and metastasis*. Cancer, 1993. 71(4): p. 1368-83.
284. Liotta, L.A., *Tumor invasion and metastases--role of the extracellular matrix: Rhoads Memorial Award lecture*. Cancer Res, 1986. 46(1): p. 1-7.
285. Iyer, N.V., et al., *Cellular and developmental control of O₂ homeostasis by hypoxia-inducible factor 1 alpha*. Genes Dev, 1998. 12(2): p. 149-62.
286. Ryan, H.E., J. Lo, and R.S. Johnson, *HIF-1 alpha is required for solid tumor formation and embryonic vascularization*. Embo J, 1998. 17(11): p. 3005-15.
287. Kotch, L.E., et al., *Defective vascularization of HIF-1alpha-null embryos is not associated with VEGF deficiency but with mesenchymal cell death*. Dev Biol, 1999. 209(2): p. 254-67.
288. Maltepe, E., et al., *Abnormal angiogenesis and responses to glucose and oxygen deprivation in mice lacking the protein ARNT*. Nature, 1997. 386(6623): p. 403-7.
289. Peng, J., et al., *The transcription factor EPAS-1/hypoxia-inducible factor 2alpha plays an important role in vascular remodeling*. Proc Natl Acad Sci U S A, 2000. 97(15): p. 8386-91.
290. Compornolle, V., et al., *Loss of HIF-2alpha and inhibition of VEGF impair fetal lung maturation, whereas treatment with VEGF prevents fatal respiratory distress in premature mice*. Nat Med, 2002. 8(7): p. 702-10.
291. Tian, H., et al., *The hypoxia-responsive transcription factor EPAS1 is essential for catecholamine homeostasis and protection against heart failure during embryonic development*. Genes Dev, 1998. 12(21): p. 3320-4.
292. Scortegagna, M., et al., *Multiple organ pathology, metabolic abnormalities and impaired homeostasis of reactive oxygen species in Epas1-/- mice*. Nat Genet, 2003. 35(4): p. 331-40.
293. Krishnamachary, B., et al., *Regulation of colon carcinoma cell invasion by hypoxia-inducible factor 1*. Cancer Res, 2003. 63(5): p. 1138-43.
294. Levy, N.S., et al., *Hypoxic stabilization of vascular endothelial growth factor mRNA by the RNA-binding protein HuR*. J Biol Chem, 1998. 273(11): p. 6417-23.
295. Liu, Y., et al., *Hypoxia regulates vascular endothelial growth factor gene expression in endothelial cells. Identification of a 5' enhancer*. Circ Res, 1995. 77(3): p. 638-43.
296. Forsythe, J.A., et al., *Activation of vascular endothelial growth factor gene transcription by hypoxia-inducible factor 1*. Mol Cell Biol, 1996. 16(9): p. 4604-13.
297. Stein, I., et al., *Translation of vascular endothelial growth factor mRNA by internal ribosome entry: implications for translation under hypoxia*. Mol Cell Biol, 1998. 18(6): p. 3112-9.
298. Waltenberger, J., et al., *Functional upregulation of the vascular endothelial growth factor receptor KDR by hypoxia*. Circulation, 1996. 94(7): p. 1647-54.
299. Gerber, H.P., et al., *Differential transcriptional regulation of the two vascular endothelial growth factor receptor genes. Flt-1, but not Flk-1/KDR, is up-regulated by hypoxia*. J Biol Chem, 1997. 272(38): p. 23659-67.
300. Barleon, B., et al., *Vascular endothelial growth factor up-regulates its receptor fms-like tyrosine kinase 1 (FLT-1) and a soluble variant of FLT-1 in human vascular endothelial cells*. Cancer Res, 1997. 57(23): p. 5421-5.
301. Knebelmann, B., et al., *Transforming growth factor alpha is a target for the von Hippel-Lindau tumor suppressor*. Cancer Res, 1998. 58(2): p. 226-31.
302. Gunaratnam, L., et al., *Hypoxia inducible factor activates the transforming growth factor-alpha/epidermal growth factor receptor growth stimulatory pathway in VHL(-/-) renal cell carcinoma cells*. J Biol Chem, 2003. 278(45): p. 44966-74.
303. de Paulsen, N., et al., *Role of transforming growth factor-alpha in von Hippel-Lindau (VHL)(-/-) clear cell renal carcinoma cell proliferation: a possible*

- mechanism coupling VHL tumor suppressor inactivation and tumorigenesis. Proc Natl Acad Sci U S A, 2001. 98(4): p. 1387-92.*
304. Lowden, D.A., et al., *Renal cysts in transgenic mice expressing transforming growth factor-alpha. J Lab Clin Med, 1994. 124(3): p. 386-94.*
 305. Everitt, J.I., et al., *Altered expression of transforming growth factor-alpha: an early event in renal cell carcinoma development. Mol Carcinog, 1997. 19(3): p. 213-9.*
 306. Devarajan, P., et al., *The von Hippel-Lindau gene product inhibits renal cell apoptosis via Bcl-2-dependent pathways. J Biol Chem, 2001. 276(44): p. 40599-605.*
 307. Potter, C. and A.L. Harris, *Hypoxia Inducible Carbonic Anhydrase IX, Marker of Tumour Hypoxia, Survival Pathway and Therapy Target. Cell Cycle, 2004. 3(2): p. 164-7.*
 308. Hellwig-Burgel, T., et al., *Interleukin-1beta and tumor necrosis factor-alpha stimulate DNA binding of hypoxia-inducible factor-1. Blood, 1999. 94(5): p. 1561-7.*
 309. Albina, J.E., et al., *HIF-1 expression in healing wounds: HIF-1alpha induction in primary inflammatory cells by TNF-alpha. Am J Physiol Cell Physiol, 2001. 281(6): p. C1971-7.*
 310. Haddad, J.J. and S.C. Land, *A non-hypoxic, ROS-sensitive pathway mediates TNF-alpha-dependent regulation of HIF-1alpha. FEBS Lett, 2001. 505(2): p. 269-74.*
 311. Sandau, K.B., et al., *Regulation of the hypoxia-inducible factor 1alpha by the inflammatory mediators nitric oxide and tumor necrosis factor-alpha in contrast to desferroxamine and phenylarsine oxide. J Biol Chem, 2001. 276(43): p. 39805-11.*
 312. Tracey, K.J. and A. Cerami, *Tumor necrosis factor, other cytokines and disease. Annu Rev Cell Biol, 1993. 9: p. 317-43.*
 313. Jung, Y., et al., *Hypoxia-inducible factor induction by tumour necrosis factor in normoxic cells requires receptor-interacting protein-dependent nuclear factor kappa B activation. Biochem J, 2003. 370(Pt 3): p. 1011-7.*
 314. Caldwell, M.C., et al., *Serial analysis of gene expression in renal carcinoma cells reveals VHL-dependent sensitivity to TNFalpha cytotoxicity. Oncogene, 2002. 21(6): p. 929-36.*
 315. Qi, H. and M. Ohh, *The von Hippel-Lindau tumor suppressor protein sensitizes renal cell carcinoma cells to tumor necrosis factor-induced cytotoxicity by suppressing the nuclear factor-kappaB-dependent antiapoptotic pathway. Cancer Res, 2003. 63(21): p. 7076-80.*
 316. Okuda, H., et al., *The von Hippel-Lindau tumor suppressor protein mediates ubiquitination of activated atypical protein kinase C. J Biol Chem, 2001. 276(47): p. 43611-7.*
 317. Lukashev, M.E. and Z. Werb, *ECM signalling: orchestrating cell behaviour and misbehaviour. Trends Cell Biol, 1998. 8(11): p. 437-41.*
 318. Ruoslahti, E., *Fibronectin and its integrin receptors in cancer. Adv Cancer Res, 1999. 76: p. 1-20.*
 319. Giancotti, F.G. and E. Ruoslahti, *Elevated levels of the alpha 5 beta 1 fibronectin receptor suppress the transformed phenotype of Chinese hamster ovary cells. Cell, 1990. 60(5): p. 849-59.*
 320. Lieubeau-Teillet, B., et al., *von Hippel-Lindau gene-mediated growth suppression and induction of differentiation in renal cell carcinoma cells grown as multicellular tumor spheroids. Cancer Res, 1998. 58(21): p. 4957-62.*
 321. Staller, P., et al., *Chemokine receptor CXCR4 downregulated by von Hippel-Lindau tumour suppressor pVHL. Nature, 2003. 425(6955): p. 307-11.*

322. Li, W., et al., *Protein kinase C-delta is an important signaling molecule in insulin-like growth factor I receptor-mediated cell transformation*. Mol Cell Biol, 1998. 18(10): p. 5888-98.
323. Etienne-Manneville, S. and A. Hall, *Cdc42 regulates GSK-3beta and adenomatous polyposis coli to control cell polarity*. Nature, 2003. 421(6924): p. 753-6.
324. Fodde, R., *The APC gene in colorectal cancer*. Eur J Cancer, 2002. 38(7): p. 867-71.
325. Trusolino, L. and P.M. Comoglio, *Scatter-factor and semaphorin receptors: cell signalling for invasive growth*. Nat Rev Cancer, 2002. 2(4): p. 289-300.
326. Stoker, M., et al., *Scatter factor is a fibroblast-derived modulator of epithelial cell mobility*. Nature, 1987. 327(6119): p. 239-42.
327. Nakamura, T., et al., *Molecular cloning and expression of human hepatocyte growth factor*. Nature, 1989. 342(6248): p. 440-3.
328. Montesano, R., et al., *Identification of a fibroblast-derived epithelial morphogen as hepatocyte growth factor*. Cell, 1991. 67(5): p. 901-8.
329. Naldini, L., et al., *Scatter factor and hepatocyte growth factor are indistinguishable ligands for the MET receptor*. Embo J, 1991. 10(10): p. 2867-78.
330. Lafleur, M.A., M.M. Handsley, and D.R. Edwards, *Metalloproteinases and their inhibitors in angiogenesis*. Expert Rev Mol Med, 2003. 5: p. 1-39.
331. Pennacchietti, S., et al., *Hypoxia promotes invasive growth by transcriptional activation of the met protooncogene*. Cancer Cell, 2003. 3(4): p. 347-61.
332. Schioppa, T., et al., *Regulation of the chemokine receptor CXCR4 by hypoxia*. J Exp Med, 2003. 198(9): p. 1391-402.
333. Tachibana, K., et al., *The chemokine receptor CXCR4 is essential for vascularization of the gastrointestinal tract*. Nature, 1998. 393(6685): p. 591-4.
334. Salcedo, R., et al., *Vascular endothelial growth factor and basic fibroblast growth factor induce expression of CXCR4 on human endothelial cells: In vivo neovascularization induced by stromal-derived factor-1alpha*. Am J Pathol, 1999. 154(4): p. 1125-35.
335. Lisztwan, J., et al., *Association of human CUL-1 and ubiquitin-conjugating enzyme CDC34 with the F-box protein p45(SKP2): evidence for evolutionary conservation in the subunit composition of the CDC34-SCF pathway*. Embo J, 1998. 17(2): p. 368-83.
336. Zhao, J., et al., *Expression of NPAT, a novel substrate of cyclin E-CDK2, promotes S-phase entry*. Genes Dev, 1998. 12(4): p. 456-61.
337. Klotzsche, O., et al., *Cytoplasmic retention of mutant tsp53 is dependent on an intermediate filament protein (vimentin) scaffold*. Oncogene, 1998. 16(26): p. 3423-34.
338. Peters, J.M., M.J. Walsh, and W.W. Franke, *An abundant and ubiquitous homooligomeric ring-shaped ATPase particle related to the putative vesicle fusion proteins Sec18p and NSF*. Embo J, 1990. 9(6): p. 1757-67.
339. Moir, D., et al., *Cold-sensitive cell-division-cycle mutants of yeast: isolation, properties, and pseudoreversion studies*. Genetics, 1982. 100(4): p. 547-63.
340. Leon, A. and D. McKearin, *Identification of TER94, an AAA ATPase protein, as a Bam-dependent component of the Drosophila fusome*. Mol Biol Cell, 1999. 10(11): p. 3825-34.
341. Rabouille, C., et al., *Syntaxin 5 is a common component of the NSF- and p97-mediated reassembly pathways of Golgi cisternae from mitotic Golgi fragments in vitro*. Cell, 1998. 92(5): p. 603-10.
342. Roy, L., et al., *Role of p97 and syntaxin 5 in the assembly of transitional endoplasmic reticulum*. Mol Biol Cell, 2000. 11(8): p. 2529-42.

343. Hetzer, M., et al., *Distinct AAA-ATPase p97 complexes function in discrete steps of nuclear assembly*. Nat Cell Biol, 2001. 3(12): p. 1086-91.
344. Madeo, F., E. Frohlich, and K.U. Frohlich, *A yeast mutant showing diagnostic markers of early and late apoptosis*. J Cell Biol, 1997. 139(3): p. 729-34.
345. Madeo, F., et al., *Tyrosine phosphorylation regulates cell cycle-dependent nuclear localization of Cdc48p*. Mol Biol Cell, 1998. 9(1): p. 131-41.
346. Yamada, T., et al., *p97 ATPase, an ATPase involved in membrane fusion, interacts with DNA unwinding factor (DUF) that functions in DNA replication*. FEBS Lett, 2000. 466(2-3): p. 287-91.
347. Ye, Y., H.H. Meyer, and T.A. Rapoport, *The AAA ATPase Cdc48/p97 and its partners transport proteins from the ER into the cytosol*. Nature, 2001. 414(6864): p. 652-6.
348. Braun, S., et al., *Role of the ubiquitin-selective CDC48(UFD1/NPL4) chaperone (segregase) in ERAD of OLE1 and other substrates*. Embo J, 2002. 21(4): p. 615-21.
349. Jarosch, E., et al., *Protein dislocation from the ER requires polyubiquitination and the AAA-ATPase Cdc48*. Nat Cell Biol, 2002. 4(2): p. 134-9.
350. Rabinovich, E., et al., *AAA-ATPase p97/Cdc48p, a cytosolic chaperone required for endoplasmic reticulum-associated protein degradation*. Mol Cell Biol, 2002. 22(2): p. 626-34.
351. Ghislain, M., et al., *Cdc48p interacts with Ufd3p, a WD repeat protein required for ubiquitin-mediated proteolysis in Saccharomyces cerevisiae*. Embo J, 1996. 15(18): p. 4884-99.
352. Dai, R.M., et al., *Involvement of valosin-containing protein, an ATPase Co-purified with I κ B α and 26 S proteasome, in ubiquitin-proteasome-mediated degradation of I κ B α* . J Biol Chem, 1998. 273(6): p. 3562-73.
353. Meyer, H.H., et al., *A complex of mammalian ufd1 and npl4 links the AAA-ATPase, p97, to ubiquitin and nuclear transport pathways*. Embo J, 2000. 19(10): p. 2181-92.
354. Yen, C.H., et al., *Involvement of the ubiquitin-proteasome pathway in the degradation of nontyrosine kinase-type cytokine receptors of IL-9, IL-2, and erythropoietin*. J Immunol, 2000. 165(11): p. 6372-80.
355. Dai, R.M. and C.C. Li, *Valosin-containing protein is a multi-ubiquitin chain-targeting factor required in ubiquitin-proteasome degradation*. Nat Cell Biol, 2001. 3(8): p. 740-4.
356. Kaneko, C., et al., *Characterization of the mouse gene for the U-box-type ubiquitin ligase UFD2a*. Biochem Biophys Res Commun, 2003. 300(2): p. 297-304.
357. Koegl, M., et al., *A novel ubiquitination factor, E4, is involved in multiubiquitin chain assembly*. Cell, 1999. 96(5): p. 635-44.
358. Verma, R., et al., *Proteasomal proteomics: identification of nucleotide-sensitive proteasome-interacting proteins by mass spectrometric analysis of affinity-purified proteasomes*. Mol Biol Cell, 2000. 11(10): p. 3425-39.
359. Kondo, H., et al., *p47 is a cofactor for p97-mediated membrane fusion*. Nature, 1997. 388(6637): p. 75-8.
360. Uchiyama, K., et al., *VCIP135, a novel essential factor for p97/p47-mediated membrane fusion, is required for Golgi and ER assembly in vivo*. J Cell Biol, 2002. 159(5): p. 855-66.
361. Meyer, H.H., Y. Wang, and G. Warren, *Direct binding of ubiquitin conjugates by the mammalian p97 adaptor complexes, p47 and Ufd1-Npl4*. Embo J, 2002. 21(21): p. 5645-52.

362. Tsai, B., Y. Ye, and T.A. Rapoport, *Retro-translocation of proteins from the endoplasmic reticulum into the cytosol*. Nat Rev Mol Cell Biol, 2002. 3(4): p. 246-55.
363. Rape, M., et al., *Mobilization of processed, membrane-tethered SPT23 transcription factor by CDC48(UFD1/NPL4), a ubiquitin-selective chaperone*. Cell, 2001. 107(5): p. 667-77.
364. Hitchcock, A.L., et al., *The conserved npl4 protein complex mediates proteasome-dependent membrane-bound transcription factor activation*. Mol Biol Cell, 2001. 12(10): p. 3226-41.
365. Wang, B., et al., *Structure and ubiquitin interactions of the conserved zinc finger domain of Npl4*. J Biol Chem, 2003. 278(22): p. 20225-34.
366. Ye, Y., H.H. Meyer, and T.A. Rapoport, *Function of the p97-Ufd1-Npl4 complex in retrotranslocation from the ER to the cytosol: dual recognition of nonubiquitinated polypeptide segments and polyubiquitin chains*. J Cell Biol, 2003. 162(1): p. 71-84.
367. Nagahama, M., et al., *SVIP is a novel VCP/p97-interacting protein whose expression causes cell vacuolation*. Mol Biol Cell, 2003. 14(1): p. 262-73.
368. Seigneurin-Berny, D., et al., *Identification of components of the murine histone deacetylase 6 complex: link between acetylation and ubiquitination signaling pathways*. Mol Cell Biol, 2001. 21(23): p. 8035-44.
369. Ayer, D.E., *Histone deacetylases: transcriptional repression with SINers and NuRDs*. Trends Cell Biol, 1999. 9(5): p. 193-8.
370. Jenuwein, T. and C.D. Allis, *Translating the histone code*. Science, 2001. 293(5532): p. 1074-80.
371. Verdin, E., F. Dequiedt, and H.G. Kasler, *Class II histone deacetylases: versatile regulators*. Trends Genet, 2003. 19(5): p. 286-93.
372. Hook, S.S., et al., *Histone deacetylase 6 binds polyubiquitin through its zinc finger (PAZ domain) and copurifies with deubiquitinating enzymes*. Proc Natl Acad Sci U S A, 2002. 99(21): p. 13425-30.
373. Hubbert, C., et al., *HDAC6 is a microtubule-associated deacetylase*. Nature, 2002. 417(6887): p. 455-8.
374. Kopito, R.R., *The missing linker: an unexpected role for a histone deacetylase*. Mol Cell, 2003. 12(6): p. 1349-51.
375. Kawaguchi, Y., et al., *The deacetylase HDAC6 regulates aggresome formation and cell viability in response to misfolded protein stress*. Cell, 2003. 115(6): p. 727-38.
376. Anderson, J., et al., *The essential Gcd10p-Gcd14p nuclear complex is required for 1-methyladenosine modification and maturation of initiator methionyl-tRNA*. Genes Dev, 1998. 12(23): p. 3650-62.
377. Calvo, O., et al., *GCD14p, a repressor of GCN4 translation, cooperates with Gcd10p and Lhp1p in the maturation of initiator methionyl-tRNA in Saccharomyces cerevisiae*. Mol Cell Biol, 1999. 19(6): p. 4167-81.
378. Bjork, G.R., et al., *Transfer RNA modification*. Annu Rev Biochem, 1987. 56: p. 263-87.
379. Astrom, S.U. and A.S. Bystrom, *Rit1, a tRNA backbone-modifying enzyme that mediates initiator and elongator tRNA discrimination*. Cell, 1994. 79(3): p. 535-46.
380. Sprinzl, M., et al., *Compilation of tRNA sequences and sequences of tRNA genes*. Nucleic Acids Res, 1998. 26(1): p. 148-53.
381. Basavappa, R. and P.B. Sigler, *The 3 A crystal structure of yeast initiator tRNA: functional implications in initiator/elongator discrimination*. Embo J, 1991. 10(10): p. 3105-11.

382. Kagan, R.M. and S. Clarke, *Widespread occurrence of three sequence motifs in diverse S-adenosylmethionine-dependent methyltransferases suggests a common structure for these enzymes*. Arch Biochem Biophys, 1994. 310(2): p. 417-27.
383. Garcia-Barrio, M.T., et al., *GCD10, a translational repressor of GCN4, is the RNA-binding subunit of eukaryotic translation initiation factor-3*. Genes Dev, 1995. 9(14): p. 1781-96.
384. Fabbro, M. and B.R. Henderson, *Regulation of tumor suppressors by nuclear-cytoplasmic shuttling*. Exp Cell Res, 2003. 282(2): p. 59-69.
385. Zhang, F., R.L. White, and K.L. Neufeld, *Phosphorylation near nuclear localization signal regulates nuclear import of adenomatous polyposis coli protein*. Proc Natl Acad Sci U S A, 2000. 97(23): p. 12577-82.
386. Woods, D.B. and K.H. Vousden, *Regulation of p53 function*. Exp Cell Res, 2001. 264(1): p. 56-66.
387. Chen, Y., et al., *Aberrant subcellular localization of BRCA1 in breast cancer*. Science, 1995. 270(5237): p. 789-91.
388. Lee, S., et al., *Transcription-dependent nuclear-cytoplasmic trafficking is required for the function of the von Hippel-Lindau tumor suppressor protein*. Mol Cell Biol, 1999. 19(2): p. 1486-97.
389. Groulx, I., M.E. Bonicalzi, and S. Lee, *Ran-mediated nuclear export of the von Hippel-Lindau tumor suppressor protein occurs independently of its assembly with cullin-2*. J Biol Chem, 2000. 275(12): p. 8991-9000.
390. Giannakakou, P., et al., *p53 is associated with cellular microtubules and is transported to the nucleus by dynein*. Nat Cell Biol, 2000. 2(10): p. 709-17.
391. Groulx, I. and S. Lee, *Oxygen-dependent ubiquitination and degradation of hypoxia-inducible factor requires nuclear-cytoplasmic trafficking of the von Hippel-Lindau tumor suppressor protein*. Mol Cell Biol, 2002. 22(15): p. 5319-36.
392. Mabweesh, N.J., et al., *2ME2 inhibits tumor growth and angiogenesis by disrupting microtubules and dysregulating HIF*. Cancer Cell, 2003. 3(4): p. 363-75.
393. Cogoni, C. and G. Macino, *Post-transcriptional gene silencing across kingdoms*. Curr Opin Genet Dev, 2000. 10(6): p. 638-43.
394. Hammond, S.M., A.A. Caudy, and G.J. Hannon, *Post-transcriptional gene silencing by double-stranded RNA*. Nat Rev Genet, 2001. 2(2): p. 110-9.
395. Arber, S., et al., *Regulation of actin dynamics through phosphorylation of cofilin by LIM-kinase*. Nature, 1998. 393(6687): p. 805-9.
396. Mizuno, K., et al., *Identification of a human cDNA encoding a novel protein kinase with two repeats of the LIM/double zinc finger motif*. Oncogene, 1994. 9(6): p. 1605-12.
397. Yang, N., et al., *Cofilin phosphorylation by LIM-kinase 1 and its role in Rac-mediated actin reorganization*. Nature, 1998. 393(6687): p. 809-12.
398. Sumi, T., et al., *Cofilin phosphorylation and actin cytoskeletal dynamics regulated by rho- and Cdc42-activated LIM-kinase 2*. J Cell Biol, 1999. 147(7): p. 1519-32.
399. Takahashi, H., H. Funakoshi, and T. Nakamura, *LIM-kinase as a regulator of actin dynamics in spermatogenesis*. Cytogenet Genome Res, 2003. 103(3-4): p. 290-8.
400. Lonser, R.R., et al., *von Hippel-Lindau disease*. Lancet, 2003. 361(9374): p. 2059-67.
401. Martiny-Baron, G. and D. Marme, *VEGF-mediated tumour angiogenesis: a new target for cancer therapy*. Curr Opin Biotechnol, 1995. 6(6): p. 675-80.
402. Bluysen, H.A., et al., *Fibronectin is a hypoxia-independent target of the tumor suppressor VHL*. FEBS Lett, 2004. 556(1-3): p. 137-42.
403. Xie, Y. and A. Varshavsky, *UFD4 lacking the proteasome-binding region catalyses ubiquitination but is impaired in proteolysis*. Nat Cell Biol, 2002. 4(12): p. 1003-7.

404. Bays, N.W., et al., *HRD4/NPL4 is required for the proteasomal processing of ubiquitinated ER proteins*. Mol Biol Cell, 2001. 12(12): p. 4114-28.
405. Schimmel, P.R. and D. Soll, *Aminoacyl-tRNA synthetases: general features and recognition of transfer RNAs*. Annu Rev Biochem, 1979. 48: p. 601-48.
406. Hershey, J.W., *Translational control in mammalian cells*. Annu Rev Biochem, 1991. 60: p. 717-55.
407. Koumenis, C., et al., *Regulation of protein synthesis by hypoxia via activation of the endoplasmic reticulum kinase PERK and phosphorylation of the translation initiation factor eIF2alpha*. Mol Cell Biol, 2002. 22(21): p. 7405-16.
408. Schraml, P., et al., *Relevance of nuclear and cytoplasmic von hippel lindau protein expression for renal carcinoma progression*. Am J Pathol, 2003. 163(3): p. 1013-20.
409. Hagedorn, M. and A. Bikfalvi, *Target molecules for anti-angiogenic therapy: from basic research to clinical trials*. Crit Rev Oncol Hematol, 2000. 34(2): p. 89-110.
410. Cherrington, J.M., L.M. Strawn, and L.K. Shawver, *New paradigms for the treatment of cancer: the role of anti-angiogenesis agents*. Adv Cancer Res, 2000. 79: p. 1-38.
411. Kim, M., et al., *Recombinant adenovirus expressing Von Hippel-Lindau-mediated cell cycle arrest is associated with the induction of cyclin-dependent kinase inhibitor p27Kip1*. Biochem Biophys Res Commun, 1998. 253(3): p. 672-7.

LEBENS LAUF

Name: Robert Edward Barry

Geburtsdatum: 25/11/73

Staatsangehörigkeit: Irisch

Adresse: *Privat:* Limmattalstrasse 178
CH-8049 Zürich
Tel: 0041-78-7229383
Email: rebarry8@hotmail.com

Geschäftlich: Eidgenössische Technische Hochschule Zürich
Institut für Zellbiologie HPM-F29
CH-8049 Zürich
Tel: 0041-1-6333338
Fax: 0041-1-6331069
Email: robert.barry@cell.biol.ethz.ch

Ausbildung:

Doktorarbeit:
Juni 2003 - Juli 2004 Eidgenössische Technische Hochschule Zürich
CH-8093 Zürich

Okt. 1999 - Juni 2003 Friedrich Miescher Institute for Biomedical Research
CH-4058 Basel
- Suma cum Lauda

Diplomarbeit:
Sep. 1993 - Juni 1999 Trinity College Dublin, Irland
B.A. (mod) in Biochemistry Hons
- Class ranking – 1st

Sekundärschule:
Sep. 1987 - Juni 1993 Holy Faith / de la Salle Secondary School
Skerries, Co.Dublin, Irland
- Ardteistimeireachta – 7 honours

Wissenschaftliche Arbeitserfahrung:

***Okt. 1999 - Juli 2004:* Doktorarbeit**

Projekt: 'Functional analysis of the von Hippel-Lindau tumour suppressor protein and its role in tumourigenesis'

Referenz: Prof.Dr.Wilhelm Krek
FMI, Basel / ETH, Zürich (from June 2003)

***June 1999 – Sep.1999:* Labor Assistent**

Projekt: 'Establishment and development of *in vitro* drug and xenobiotic metabolite analysis assays using HPLC'

Referenz: Dr.Gordon Elliot
National Biotechnology Institute,
Trinity College Dublin, Irland

***Okt. 1998 – Apr.1999:* Diplomarbeit**

Projekt: 'Evaluation of the antiproliferative and/or apoptotic effects of a series of benzodiazepine-like compounds on a human cervix carcinoma cell line'

Referenz: Dr.D.Zisterer
Dept. of Biochemistry
Trinity College Dublin, Irland

Grade: I

***Juni 1998 – Sep.1998:* Labor Assistent**

Projekt: 'Investigation of the role of Raf kinase in the G2/M phase transition in oocytes'

Referenz: Dr.Daniel Fisher
CRBM-CNRS,
Montpellier, Frankreich

Referenten:

1. **Prof.Dr.Wilhelm Krek** – Dissertationsleiter

Eidgenössische Technische Hochschule Zürich
Insitut für Zellbiologie HPM-F42
CH-8093 Zurich
Schweiz

Email: wilhelm.krek@cell.biol.ethz.ch **Telefon:** +41-1-633 34 47

2. **Prof.Dr. Denis Monard** – Fakultätsverantwortlicher

Friedrich Miescher Institute for Biomedical Research
Maulbeerstrasse 66
CH-4058 Basel
Schweiz

Email: denis.monard@fmi.ch **Telefon:** +41-61-697 66 51

3. **Prof.Dr. Holger Moch** – Korreferent

UniversitätsSpital Zürich
Departement Pathologie
Institut für Klinische Pathologie
Schmelzbergstrasse 12
CH-8091 Zurich

Email: holger.moch@usz.ch **Telefon:** +41 1 255 39 30

4. **Prof.D.C.Williams** - Direktor von Biochemie

Department of Biochemistry
Trinity College Dublin
Dublin 2, Ireland

Email: dwillims@tcd.ie **Telefon:** +353-1- 608 10 98

